



UNIVERSITÄT
DES
SAARLANDES

Design and synthesis of MurA enzyme inhibitors and their evaluation as antibacterial agents

PhD thesis

submitted in fulfillment of the requirements for the degree of Doctor of
Philosophy in Pharmaceutical Chemistry at GUC

Dissertation

submitted towards the degree Doctor of Natural Sciences (Dr. rer. nat.)
of the Faculty of Natural Sciences and Technology at UdS

Joint PhD degree

By

Youssef Mohammed Ahmed Aboushady

Supervised by

Prof. Dr. Ashraf Abadi

Professor of Pharmaceutical Chemistry
Head of Pharmaceutical Chemistry
Department
Faculty of Pharmacy and Biotechnology
German University in Cairo

Prof. Dr. Anna K. Hirsch

Head of Department Drug Design and
Optimization
Helmholtz Institute for Pharmaceutical
Research
Saarland University, Germany

Assoc. Prof. Dr. Mohammad Abdel-Halim

Associate professor of Pharmaceutical Chemistry
Department of Pharmaceutical Chemistry
Faculty of Pharmacy and Biotechnology
German University in Cairo

Cairo/Saarbrücken

2023

Tag des Kolloquiums: 17. September 2023

Dekan: Prof. Dr. Ludger Santen

Berichterstatter: Prof. Anna K.H. Hirsch

Prof. Dr. Christian Ducho

Prof. Dr. Ashraf Mostafa Kamal Hassan Abadi

Prof. Dr. Mohammad Abdel-Halim

Weitere Mitglieder: Dr. Matthias Engel

Prof. Dr. Khaled Abouzid

Prof. Dr. Ismail Salama

Vorsitz: Prof. Dr. Ashraf Mostafa Kamal Hassan Abadi

Examination Committee

Supervisors:

Name: **Prof. Dr. Ashraf H. Abadi**
Position Title: Professor of Pharmaceutical Chemistry
Faculty: Pharmacy and Biotechnology
University: German University in Cairo

Name: **Prof. Dr. Anna K. Hirsch**
Position Title: Head of Department Drug Design and Optimization and Full Professor
Faculty: Helmholtz Institute for Pharmaceutical Research
University: University of Saarland, Germany

Name: **Assoc. Prof. Dr. Mohammad Abd El-Halim**
Position Title: Associate Professor of Pharmaceutical Chemistry
Faculty: Pharmacy and Biotechnology
University: German University in Cairo

National Examiners:

Name: **Prof. Dr. Khaled Abouzeid**
Position Title: Dean and Professor of Pharmaceutical Chemistry
Faculty: Faculty of Pharmacy
University: Sadat University

Name: **Prof. Dr. Ismail Salama**
Position Title: Head of Department Pharmaceutical Chemistry
Faculty: Faculty of Pharmacy
University: Suez Canal University

International Examiners:

Name: **Prof. Dr. Christian Ducho**
Position Title: Full Professor of Pharmaceutical Chemistry
Faculty: Pharmacy
University: Saarland University, Germany

Name: **PD Dr. Matthias Engel**
Position Title: Privatdozent of Pharmaceutical Chemistry
Faculty: Pharmacy
University: Saarland University, Germany

Declaration

I, ***Youssef Mohammed Ahmed Aboushady***, declare that this thesis and the work presented in it are my own and has been generated by me as the result of my own original research.

Thesis Title: Design and synthesis of novel MurA enzyme inhibitors and their evaluation as antibacterial agents

Thesis type: M.SC. PhD

I confirm that:

- This work was done wholly or mainly while in candidature for a research degree at the German University in Cairo.
- Where anywhere I have consulted the published work of others, this is always clearly attributed.
- Where I have quoted from the work of others, the source is always given. With the exception of such quotations, this thesis is entirely my own work.
- I have acknowledged all main sources of help.
- Where the thesis is based on work done by myself jointly with others, I have made clear exactly what was done by others and what I have contributed myself.
- Either none of this work has been published before submission, or parts of this work have been published as: *(please list references below)*
- Books, journals and other teaching materials made available to me by the German University in Cairo are for my own studies and copying or using them for other purposes is an infringement of copyright.

Signature: -----

Acknowledgement

Above all else, I offer my deepest praise and gratitude to **God** for granting me the opportunity and the strength, determination, and capability to successfully complete this endeavor. It is through His guidance and support that I have been able to persevere and achieve this accomplishment, and for that, I am eternally grateful. May His blessings be upon me and my loved ones always.

I want to express my sincerest gratitude to my thesis supervisor, **Professor Dr. Ashraf Abadi**, Professor of Pharmaceutical Chemistry and Head of the Pharmaceutical Chemistry Department at the Faculty of Pharmacy and Biotechnology at the German University in Cairo. His excellent leadership and patience, as well as his efforts in revising the thesis, have been invaluable to me. I am deeply grateful for the perfect research atmosphere that he provided, which allowed me to fully immerse myself in my studies and make the most of this opportunity. I am thankful for his guidance and support and feel privileged to have had such a knowledgeable and supportive supervisor.

My cordial thanks to **Prof. Dr. Anna K. Hirsch**, Head of Department of Drug Design and Optimization at the Helmholtz Institute for Pharmaceutical Research at Saarland University in Saarbrücken, Germany, for supervising this project. Your support and assistance during my stay in Germany have been invaluable, and I feel incredibly fortunate to have had your guidance and mentorship throughout my research endeavors. Your generosity in funding my stay allowed me to fully immerse myself in my studies and truly make the most of this opportunity, and I am deeply grateful for your continued support and guidance.

I am deeply thankful to my supervisor, **Assoc. Prof. Mohammad Abdel-Halim**, Lecturer of Pharmaceutical Chemistry at the German University in Cairo, for his endless support and guidance throughout the experimental and theoretical aspects of my research project. I would like to thank him for suggesting this project for me. His suggestions and input were invaluable, and I am highly appreciative of his efforts in revising the text. On both a personal and academic level, Dr. Abdel-Halim has been an irreplaceable mentor and I am grateful for all that he has offered me. Without his continuous help and guidance, this work would not have been possible. I am truly fortunate to have had such a supportive and knowledgeable advisor and could not have imagined a better experience.

I am particularly grateful to **Dr. Mostafa Hamed** (HIPS) and would like to express my deep appreciation for all of his help and support during my time in the lab. His expertise and guidance were invaluable to me, and I feel grateful to have had the opportunity to work with him. In addition to being a fantastic mentor, Dr. Mostafa became an older brother to me, providing support and encouragement throughout my time in the lab. I am deeply thankful for his positive impact on my development as a researcher, and for his generosity in helping me to fully immerse myself in my studies.

Special thanks to **Dr. Matthias Engel** (Saarland University) for his valuable input and suggestions throughout this project.

My sincerest gratitude to my **Dr. Mohammed Salah** for his invaluable guidance and support during my time in the laboratory. His expertise in the field of biology, particularly his skill in obtaining and interpreting results, as well as his ability to optimize assay techniques, were essential to the success of my research project. I am truly grateful for his mentorship and support and feel privileged to have had the opportunity to work with such a knowledgeable and supportive mentor.

I would like to take this opportunity to acknowledge my dear son, **Adam**, whose love and support have been a constant source of inspiration and motivation throughout my PhD journey. From the late nights spent writing and researching, to the moments of doubt and challenge, Adam unwavering has been a beacon of hope and a reminder of why I am pursuing this degree. His presence in my life has brought me joy and purpose, and I am deeply grateful for the love and happiness that he brings to my world. Adam, this thesis is as much a tribute to your impact on my life as it is to my own academic accomplishments. Thank you for being my rock, my guiding light, and my everything. I love you always.

I would like to express my sincere appreciation to my loving and supportive **friends**, who have been with me every step of the way throughout my life. Their continuous guidance and prayers have been a source of strength and encouragement, and I am deeply grateful for their unwavering support. It is to them that I wholeheartedly dedicate this thesis, as a testament to their love and influence on my life and my academic journey. I am thankful for the positive impact they have had on my development and growth and am deeply grateful for their love and encouragement.

Manuscripts Included in This Thesis

This thesis is divided into three manuscripts, to be published, which are referred to in the text by their numbers I–III, respectively.

- I. Inhibiting Bacterial Cell Wall Biosynthesis: Design and Evaluation of Imidazolidinone Compounds Targeting MurA Enzyme**

- II. Discovery of Triaryl Malonamides as a Novel Class of MurA Inhibitors with Potential Antibacterial Activity**

- III. Discovery of MurA Inhibitors Through Screening of the HIPS Library**

Table of Contents

1. INTRODUCTION.....	11
1.1 ANTIBACTERIAL AGENTS.....	11
1.2 ANTIBACTERIAL DRUG DISCOVERY.....	12
1.2.1 <i>The Golden Era of Antibiotics.....</i>	<i>12</i>
1.2.2 <i>Emergence of Resistance.....</i>	<i>13</i>
1.2.3 <i>Reasons of Antimicrobial Resistance.....</i>	<i>13</i>
1.2.4 <i>Mechanisms of Bacterial Resistance.....</i>	<i>14</i>
1.2.4.1 Reduced Permeability.....	15
1.2.4.2 Increased Efflux.....	15
1.2.4.3 Inactivation.....	16
1.2.4.4 Alteration of Target.....	16
1.2.4.5 Overproduction.....	17
1.2.4.6 Bypass.....	17
1.3 RESISTANCE COST.....	17
1.4 CHALLENGES IN ANTIBACTERIAL DRUG DISCOVERY.....	18
1.5 ANTIBIOTICS AND THEIR MAIN TARGETS.....	20
1.5.1 <i>Inhibition of Cell-Wall Synthesis.....</i>	<i>21</i>
1.5.2 <i>Inhibition of Protein Synthesis.....</i>	<i>22</i>
1.5.3 <i>Disruption of Cell Membrane.....</i>	<i>22</i>
1.5.4 <i>Inhibition of Nucleic-Acid Synthesis.....</i>	<i>22</i>
1.5.5 <i>Inhibition of Metabolite Pathways.....</i>	<i>23</i>
1.6 NEED TO DEVELOP NOVEL ANTIBIOTICS: TARGETING PG SYNTHESIS.....	23
1.6.1 <i>Biosynthesis of Peptidoglycan Layer.....</i>	<i>24</i>
1.6.1.1 Historical Perspectives.....	25
1.6.1.2 Pathway for Biosynthesis of Peptidoglycan.....	26
1.6.1.3 Targeting the Cascade of Intracellular Mur enzymes.....	27
1.7 STEPS INVOLVED IN THE ASSEMBLY OF PEPTIDOGLYCAN.....	28
1.7.1.1 MurA Transferase.....	29
1.7.1.1.1 MurA overall structure.....	29
1.7.1.1.2 MurA catalytic site.....	30
1.7.1.2 MurB oxidoreductase.....	30
1.7.2 <i>Step II: Formation of UDP-MurNAc-peptides.....</i>	<i>31</i>
1.7.2.1 MurC ligase.....	31
1.7.2.2 MurD ligase.....	32
1.7.2.3 MurE ligase.....	32
1.7.2.4 MurF ligase.....	33
1.7.3 <i>Step III: Formation of Lipid Intermediates.....</i>	<i>33</i>
1.7.4 <i>: Peptidoglycan Transglycosylation.....</i>	<i>34</i>
1.7.5 <i>: Peptidoglycan Transpeptidation.....</i>	<i>34</i>
1.8 FOSFOMYCIN.....	34
1.8.1 <i>Mechanism of Action.....</i>	<i>34</i>
1.8.2 <i>Clinical Use.....</i>	<i>36</i>
1.8.3 <i>Resistance.....</i>	<i>36</i>
1.8.3.1 Mechanisms of Resistance.....	36
1.8.3.1.1 Inherent Resistance.....	38
1.8.3.1.2 Acquired resistance: fosfomycin transportation.....	39
1.8.3.1.3 Acquired resistance: MurA related.....	40
1.8.3.1.4 Acquired resistance: Antibiotic modification.....	40
1.9 MURA INHIBITORS.....	42
1.9.1 <i>Benzothioxalone derivatives.....</i>	<i>42</i>
1.9.2 <i>Pyrazolopyrimidine, Purine Analogues and Cyclic Disulfide.....</i>	<i>43</i>

1.9.3	<i>Sulfoxyloxy anthranilic acid derivatives</i>	43
1.9.4	<i>Peptidomimetics</i>	44
1.9.5	<i>Imidazole and Diaryl Methane Derivatives</i>	45
1.9.6	<i>Aminotetralone derivatives</i>	46
1.9.7	<i>Sesquiterpene lactone derivatives</i>	46
1.9.8	<i>Miscellaneous</i>	47
1.9.8.1	Thimerosal, Thiram, and Ebselen	47
1.9.8.2	Tulipalines, Tuliposides, and their Derivatives	47
1.9.8.3	Terreic acid.....	48
1.9.8.4	Avenaciolides	48
1.9.8.5	Oxazepene derivatives	49
1.9.8.6	Bromo-cyclobutenaminones.....	50
1.9.8.7	Bromobenzimidazole, benzylidene carboximidamide	50
1.9.8.8	Heterocyclic Electrophiles.....	51
1.9.8.9	Pyrrolidinediones.....	51
1.9.8.10	Chloroacetamides	52
2.	RESEARCH OBJECTIVES	53
2.1	SCIENTIFIC GOAL.....	53
2.2	DEVELOPMENT OF INHIBITORS AGAINST MUR A ENZYME.....	53
2.2.1	<i>Scaffold hopping in Chapter 1</i>	54
2.2.2	<i>Structure simplification in Chapter 2</i>	54
2.2.3	<i>HIPS library screening in Chapter 3</i>	55
3.	RESULTS AND DISCUSSION	56
3.1	CHAPTER 1.....	56
3.1.1	<i>Introduction</i>	56
3.1.2	<i>Results and Discussion</i>	59
3.1.2.1	Compounds' design	59
3.1.3	<i>Chemistry</i>	61
3.1.4	<i>Biological Evaluation</i>	64
3.1.4.1.1	Testing some of carbamate derivatives against MurA(E5-E46).....	75
3.1.4.1.2	Testing some of the cyclized derivatives (with no substituent at position 3). (D5-D46).....	77
3.1.4.1.3	Investigation of the ability of the most potent compounds to inhibit mutant MurA (C115D).	80
3.1.4.1.4	Antibacterial Activity.....	81
3.1.5	<i>Molecular Docking</i>	84
3.1.5.1	Hypothetical binding mode of the nitrothiazolyl derivatives.....	84
3.1.6	<i>Conclusion</i>	85
3.1.7	<i>Experimental</i>	87
3.1.7.1	Chemistry.....	87
3.1.7.1.1	General procedure for the synthesis of the α -aminonitrile derivatives via Strecker reaction of aromatic amines and carbaldehydes. (A5-A46) (Procedure A).....	88
3.1.7.1.2	General procedure for the reduction of the α -aminonitrile derivatives under BOC protection(B5-B46) (Procedure B).....	95
3.1.7.1.3	General procedure for the deprotection of the BOC-protected amino group(C5-C46) (Procedure C) 103	
3.1.7.1.4	General procedure for the synthesis of the imidazolidinone derivatives(D5-D46) (Procedure D) .	110
3.1.7.1.5	General procedure for the synthesis of the carbamate derivatives(E5-E46) (Procedure E)	121
3.1.7.1.6	General procedure for the synthesis of the urea derivatives(F1-F51)(Procedure F)	134
3.1.7.1.7	General procedure for the amide coupling using hydroxylamine(F3) (Procedure G).....	134
3.1.7.2	Biology	152
3.1.7.3	Molecular Docking	154
3.1.8	<i>References</i>	155
3.2	CHAPTER 2.....	157
3.2.1	<i>Introduction</i>	157

3.2.2	<i>Results and Discussion</i>	159
3.2.2.1	Compound design	159
3.2.3	<i>Chemistry</i>	161
3.2.4	<i>Biological Evaluation</i>	163
3.2.4.1.1	Analogues of compound 1c	164
3.2.4.1.2	Analogues of compound 1d	165
3.2.5	<i>Molecular Docking</i>	167
3.2.6	<i>Conclusions</i>	168
3.2.7	<i>Experimental</i>	169
3.2.7.1	Chemistry	169
3.2.7.1.1	General procedure for the synthesis of 3-chloro- <i>N</i> -(3-chlorobenzyl) aniline(1a) and <i>N</i> -([1,1'-biphenyl]-4-ylmethyl) quinolin-3-amine (2a). General Procedure A	170
3.2.7.1.2	General procedure for the synthesis of 3-((3-chlorobenzyl)(3-chlorophenyl)amino)-3-oxopropanoic acid (1b) and 3-((([1,1'-biphenyl]-4-ylmethyl)(quinolin-3-yl)amino)-3-oxopropanoic-acid (2b). General Procedure B. 170	170
3.2.7.1.3	General procedure for the synthesis of malonamide derivatives (1c–10c and 1d–7d). General Procedure C.	171
3.2.7.2	Biology	177
3.2.7.3	Molecular Docking	177
3.2.8	<i>References</i>	177
3.3	CHAPTER 3	180
3.3.1	<i>Screening for Hits</i>	180
3.3.1.1	Introduction	180
3.3.1.2	Terminology	181
3.3.1.3	Primary Screening of HIPS Compounds Against MurA: Identification of Hits	182
3.3.1.4	IC ₅₀ determination for hits	195
3.3.1.5	Similarity search of hits	195
3.3.1.5.1	HIPS015 similarities (Nitrophenylbutylisoindolinediones)	196
3.3.1.5.2	HIPS428 similarities (Benzamidobenzoic acids)	197
3.3.1.5.3	HIPS844 similarities (2-Methylsulfonyl-4-pyrimidinyl tetrazoles)	198
3.3.1.5.4	HIPS1298 similarities (<i>N</i> -Triazolymethylpyridine amines)	199
3.3.1.5.5	HIPS1396 similarities (<i>N</i> -Thiazolymethylpyridine amines)	204
3.3.1.5.6	HIPS1500 similarities (Thiazolymethylamino picolinonitriles)	205
3.3.1.5.7	HIPS5346 similarities (Bithiazole diamines)	210
3.3.1.5.8	HIPS6888 similarities (Thiazolopyridine carboxylates)	211
3.3.2	<i>Conclusions and Future Prospects</i>	211
3.3.3	<i>Experimental</i>	213
3.3.4	<i>References</i>	213
4.	SUMMARY AND FUTURE OUTLOOK	214
5.	REFERENCES	217
	الملخص العربي	225

List of Abbreviations

Ala	<i>Alanine</i>
ATP	Adenosine triphosphate
CC	Column chromatography
CDC	<i>Centers for Disease Control and Prevention</i>
CLSI	Clinical and Laboratory Standards Institute
Cys	Cysteine
DCM	Dichloromethane
DIPEA	Diisopropylethylamine
DMSO	Dimethyl sulfoxide
DNA	Deoxyribonucleic acid
DTT	Dithiothreitol
ESI	Electron-spray ionization
FAD	Flavin adenine dinucleotide
GPA _s	Glycopeptide antibiotics (GPA _s)
HBTU	Hexafluorophosphate benzotriazole tetramethyl uronium
HPLC	High-performance liquid chromatography
HTS	High-throughput screening
Hz	Hertz
IC ₅₀	Half maximal inhibitory concentration
LC/MS	Liquid chromatography/mass spectrometry
m/z	Mass to charge ratio
MIC	Minimum inhibitory concentration
μM	Micromolar
mRNA	Messenger RNA
MRSA	Methicillin-resistant <i>Staphylococcus aureus</i>
MSSA	Methicillin-sensitive <i>Staphylococcus aureus</i>
nM	Nanomolar
NMR	Nuclear magnetic resonance

OEP	Outer membrane efflux protein
PEP	Phosphoenolpyruvate
PG	Peptidoglycan
ppm.	Parts per million
RNA	Ribonucleic acid
Rpm	Rotations per min
RT	Room temperature
SAR	Structure–activity relationship
SLs	Sesquiterpene lactones
STEC	Shiga-like toxin-producing <i>Escherichia coli</i>
TEA	Triethylamine
TLC	Thin layer chromatography
TMP/SMX	Trimethoprim/sulfamethoxazole
tRNA	Transfer ribonucleic acid
UDP	Uridine diphosphate
UDP-GlcNAc/ UNAG	UDP-N-acetylglucosamine
UDPMurNAc	UDP-N-acetylmuramic acid
UMA	UDP-N-acetylmuramoyl-L-alanine
UMAG	UDP-N-acetylmuramoyl-L-alanyl-D-glutamate
UMPP	UDP-N-acetylmuramyl-pentapeptide
UMT	UDP-N-acetylmuramoyl: tripeptide
UNAM	UDP-N-acetylmuramate
UTI	Urinary-tract infection
VRE	Vancomycin-resistant <i>Enterococci</i>

Abstract

Antimicrobial resistance (AMR) is a growing global public health concern, as bacteria are becoming increasingly resistant to drugs used to treat infections. One promising approach to combatting AMR is to target specific enzymes within bacteria that are essential for their survival. One such enzyme is MurA, which plays a key role in the biosynthesis of the bacterial cell wall by being involved in the initial cytoplasmic step of peptidoglycan (PG) synthesis. The focus of this thesis is the identification and optimization of MurA inhibitors as a potential new class of antibacterial agents. Through the synthesis of 167 derivatives, we explored the potential of these compounds as antibacterial agents. Of these, 148 were imidazolidinone derivatives and 19 were triaryl malonamides. Additionally, through the screening of the HIPS library, we identified several hits and leads, demonstrating inhibitory activity against MurA. Our results demonstrate the potential of these compounds as promising candidates for the development of new antibacterial agents to combat AMR by specifically targeting the MurA enzyme.

Zusammenfassung

Die antimikrobielle Resistenz (AMR) ist ein wachsendes globales öffentliches Gesundheitsproblem, da Bakterien zunehmend resistent gegenüber den zur Behandlung von Infektionen verwendeten Medikamenten werden. Ein vielversprechender Ansatz zur Bekämpfung von AMR besteht darin, spezifische Enzyme in Bakterien anzugreifen, die für ihr Überleben unerlässlich sind. Ein solches Enzym ist MurA, das eine Schlüsselrolle in der Biosynthese der bakteriellen Zellwand spielt, indem es an dem initialen zytoplasmatischen Schritt der Peptidoglykansynthese beteiligt ist. Der Schwerpunkt dieser Arbeit liegt auf der Identifizierung und Optimierung von MurA-Inhibitoren als potenziell neue Klasse von antibakteriellen Wirkstoffen. Durch die Synthese von 167 Derivaten haben wir das Potenzial dieser Verbindungen als antibakterielle Wirkstoffe untersucht. Davon waren 148 Imidazolidinon-Derivate und 19 Triaryl-Malonamide. Zusätzlich entdeckten wir durch das Screening der HIPS-Bibliothek mehrere Treffer und vielversprechende Verbindungen, die eine hemmende Aktivität gegenüber MurA aufweisen. Unsere Ergebnisse zeigen das Potenzial dieser Verbindungen als vielversprechende Kandidaten für die Entwicklung neuer antibakterieller Wirkstoffe zur Bekämpfung von AMR, indem sie spezifisch das MurA-Enzym ins Visier nehmen.

1. Introduction

Bacteria are unicellular microorganisms and are one of the three life systems known to exist, alongside Archaea and Eukaryotes¹. They can be found freely in soil and water or living in a mutually beneficial relationship with other living organisms such as plants, animals, and even humans. Within the human body, a large number of bacteria are present on the skin, in the oral cavity, the respiratory tract, the gastro-intestinal tract, and the urogenital tract. It is estimated that more than half of the cells in our bodies are made up of bacteria². This group of bacteria, known as human microbiota, plays a crucial role in maintaining our overall health. Apart from aiding in digestion and stimulating our immune system, our body's bacteria produce many essential compounds, including vitamin K, tryptamine (a neurotransmitter), polysaccharide A (an immunomodulatory compound), deoxycholic acid (a metabomodulatory compound), and numerous antibiotics³. Nevertheless, certain pathogenic bacteria can cause severe illnesses such as tuberculosis, pneumonia, and cholera, either by infecting the human body or when the immune system is compromised due to chemotherapy, leukemia, or HIV infection. These bacterial infections are responsible for millions of deaths worldwide each year.

In ancient times, people utilized antibacterial treatments from molds, plants, or insects for the management of bacterial infections in traditional medicine, although its mechanism was not yet understood then. For instance, tetracycline was discovered in the bones from a tomb in the Dakhleh Oasis, Egypt, which dates back to the late Roman period⁴. In the mid-nineteenth century, Louis Pasteur and Nobel laureate Robert Koch established the link between bacteria and disease. In the early twentieth century, Paul Ehrlich aimed to find a "magic bullet" that would exclusively eliminate the pathogen and not harm the host. After a series of chemical modifications and pharmacological screenings, Ehrlich and his team developed arsphenamine, the first synthetic antibiotic, for the treatment of syphilis. Several years later, sulfa drugs were discovered, and in 1940, penicillin was isolated. Ehrlich's work and Alexander Fleming's discovery marked the beginning of the modern antibiotic era⁵.

1.1 Antibacterial Agents

Antibacterial agents are compounds that are used to inhibit or kill bacterial populations in order to treat bacterial infections. These agents can either inhibit the growth of bacteria (bacteriostatic) or kill them outright (bactericidal)⁶. The efficacy of these drugs is often determined using measures such as MIC (Minimum Inhibitory Concentration), MBC

(Minimum Bactericidal Concentration), and MAC (Minimum Antibiotic Concentration)⁷. To be effective, an antibacterial agent should have a high degree of selectivity for its target and a low level of toxicity to avoid damaging host tissues. This can be achieved by targeting metabolic pathways or enzymes that are specific to bacteria and absent in mammalian cells⁸.

1.2 Antibacterial Drug Discovery

The discovery of the first effective antibacterial agent, penicillin, in 1928 marked the beginning of a new era in medicine. Discovered by Alexander Fleming while studying *Penicillium*, a green and fuzzy substance that is a derivative of bread mold, penicillin was found to inhibit the growth of *Staphylococcus* bacteria on an old petri dish⁹. Following the successful isolation and mass-production of penicillin in the 1940s, the drug revolutionized the treatment of infectious diseases such as pneumonia, scarlet fever, and diphtheria, which were previously often fatal.^{10,11}

1.2.1 The Golden Era of Antibiotics

The period from the 1940s to the 1960s is often referred to as the "Golden Era" of antibiotic use and discovery, during which numerous antimicrobials were identified through the screening of soil-derived microbes. This led to the development and marketing of several classes of antibacterials, including sulphonamides, streptomycin, tetracyclines, macrolides, glycopeptides, and cephalosporins.^{12,13} Cephalosporins, in particular, became widely prescribed antibiotics, leading to the creation of second and third generations in the mid-1980s^{14,15}. The use of antibiotics has contributed to a significant reduction in deaths from infectious diseases in the US, from 7970 deaths per 1,000,000 in 1900 to just 360 deaths per 1,000,000 in 1980¹⁶. In World War II alone, penicillin saved thousands of wounded soldiers and civilians from dying of bacterial infections¹⁷. However, in the early 1980s, the discovery of new antibiotics slowed dramatically¹⁸ with only a few organizations actively engaged in the field. This led to a decrease in the output of novel antibacterials, as many small companies were merged or acquired by larger ones. The class of oxazolidinones was not discovered until 1999–2001 (Figure 1)¹⁹.

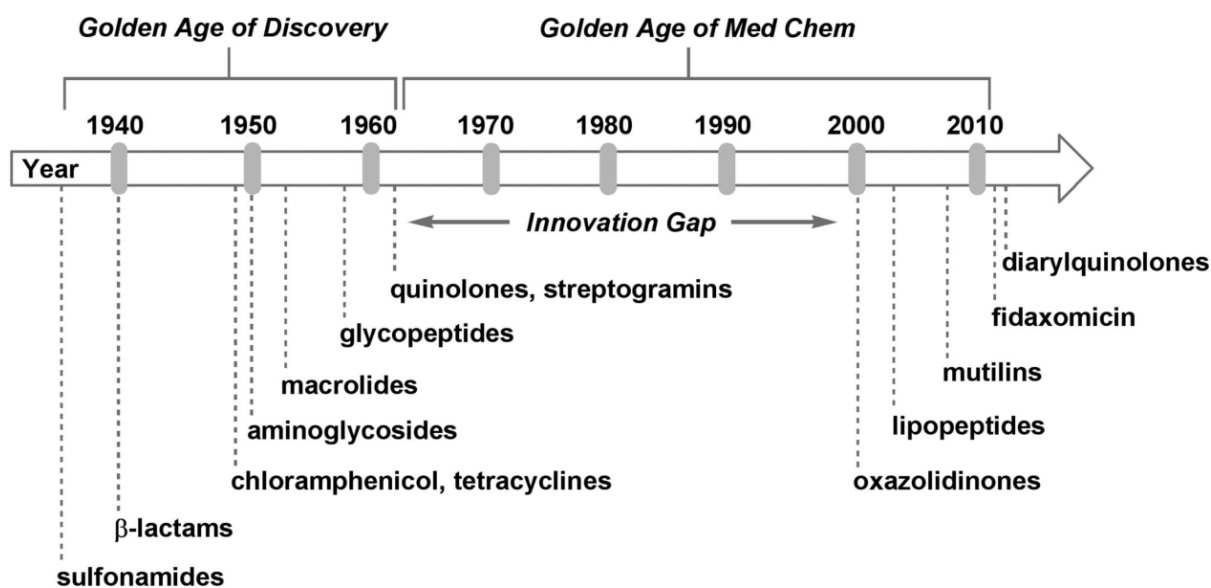


Figure 1: Discovery void in antibacterial drug discovery (Taken from reference 19)¹⁹.

1.2.2 Emergence of Resistance

Antibiotic resistance refers to the ability of microbes to survive in the presence of an antibiotic, reducing the effectiveness of these drugs for treating infections. While some species of bacteria are naturally resistant to certain antibiotics due to evolutionary competition²⁰, acquired resistance in bacterial populations is the primary concern in the field of public health. This type of resistance arises when bacteria that are initially susceptible to an antibiotic become resistant through genetic mutations or the acquisition of resistance genes from other bacteria²¹. Today, resistance to nearly all antibiotics has been observed, and the lack of new antibiotics, coupled with behaviors that promote resistance, have made bacterial infections a significant public health threat once again¹⁷.

1.2.3 Reasons of Antimicrobial Resistance

Undiscriminating antibiotic use in humans, including both inappropriate prescribing and overuse, has contributed to the development of antibiotic resistance²². In addition, the extensive use of antibiotics in agriculture, where approximately 79% of antibiotics sold are used, has also played a significant role in the development of antibiotic resistance²³. In animal agriculture, antibiotics are commonly administered at low, consistent doses to promote weight gain and prevent infections, as well as to treat infections and assist with surgical procedures²⁴. The limited development of new antibiotics since 1970 and the economic and regulatory barriers²⁵ that have hindered pharmaceutical companies from pursuing research in this area have exacerbated the problem of antibiotic resistance^{26,27}. The limited financial incentive for the development of antibiotics, which are used for short periods and are often curative, as well as

the availability, ease of use, and low cost of existing antibiotics²⁸, have led pharmaceutical companies to focus on more profitable drugs for chronic conditions such as psychiatric disorders and diabetes.²⁹

1.2.4 Mechanisms of Bacterial Resistance

Bacteria have the ability to protect themselves from antibiotics, whether they are naturally occurring or developed by humans. This is because bacteria have evolved defense mechanisms to compete for resources and habitat against other species, including antibiotics. There are two types of resistance: intrinsic and acquired. Intrinsic resistance occurs when bacteria have a resistance gene in their chromosomes that allows them to resist the antibiotic. Acquired resistance happens when bacteria mutate or when they receive the resistance gene from other resistant bacteria through plasmids or transposons³⁰. Figure 2 summarizes the various mechanisms of antibiotic resistance.

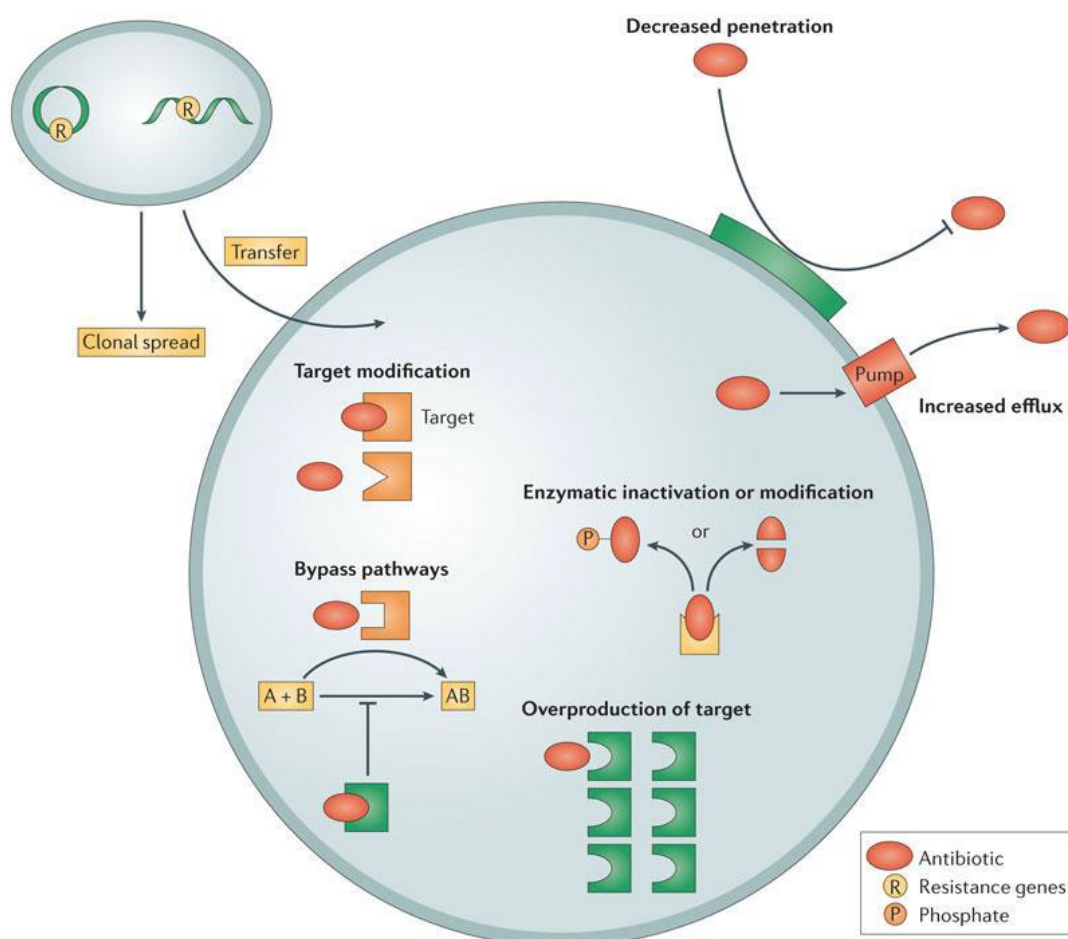


Figure 2: Mechanisms of antibiotic resistance(Taken from reference 12)¹²

1.2.4.1 Reduced Permeability

Gram-negative bacteria, such as Enterobacteriaceae and *Pseudomonas* species, have an outer membrane that serves as a natural defense mechanism against many antibiotics. This membrane is made up of two layers: an inner layer of phospholipids and an outer layer of lipopolysaccharide. Additionally, there are porins or protein channels that cross the outer membrane to facilitate the transport of small hydrophilic nutrients. Antibiotic penetration into Gram-negative bacteria is limited because drugs must either diffuse through the LPS layer or pass through the porins. The outer membrane containing LPS has a lower permeability compared to the cytoplasmic membrane for lipophilic compounds, whereas the number or size of porins affects the entry of hydrophilic antibiotics into the bacterial cell, as porins are selective for the size and charge of the molecules^{31,32}.

1.2.4.2 Increased Efflux

One way that bacteria can naturally resist antibiotics is by using efflux pumps to transport them out of the cell. There are five different groups of efflux pumps, including the major facilitator superfamily (MFS), small multidrug resistance (SMR), resistance-nodulation-cell division (RND), multidrug and toxic compound extrusion (MATE), and ATP binding cassette (ABC) superfamily. Depending on the group, energy for the transport of drugs can come from either ATP (in the case of the ABC superfamily, which are primary transporters), or a proton motive force (PMF) or sodium (for the other families, which are secondary transporters)^{30,33}.

A couple of examples of multidrug efflux pumps include AcrB in *E. coli* and MexB in *P. aeruginosa*, both of which belong to the RND family. These pumps are made up of homotrimers and are located in the inner membrane of the cell. They work together with other proteins - AcrA and TolC for AcrB, and MexA and OprM for MexB - to form a tripartite complex that spans both the inner and outer membranes. Research on the AcrB transporter has shown that it contains two distinct multisite binding pockets - a proximal one and a distal one. These pockets are large and can interact with a wide range of structurally diverse substrates, primarily through hydrophobic and electrostatic interactions³⁴.

The increased expression of efflux pumps is an important factor in antibiotic resistance. The regulation of the genes responsible for efflux pump production is controlled by both local and global regulators, including transcription factors such as MarA, SoxS, and RamA. These transcription factors activate the expression of *acrAB* in Enterobacteriaceae^{31,32,35,36}.

1.2.4.3 Inactivation

Bacteria have enzymes that they can use to modify antibiotics, especially those that are naturally occurring, to make them ineffective. One way they do this is through hydrolysis, which involves breaking down the active part of the antibiotic, such as the β -lactam ring in β -lactams, using enzymes called β -lactamases. β -lactamases bind to the β -lactam using a serine residue at their active site, similar to how transpeptidases (PBPs) bind, to form an intermediate complex. However, unlike PBPs, these intermediate complexes dissociate quickly, leaving behind inactive penicilloic acids with cleaved β -lactam rings³⁷.

Another method of inactivation involves capping the functional groups of an antibiotic, such as OH and NH₂, with masking groups like acetyl, phosphoryl, or nucleotidyl. This prevents the antibiotic from interacting with its target protein, decreasing its binding affinity. Aminoglycosides can be inactivated using three different types of modifying enzymes: acetyltransferases, which add an acetyl group using acetyl-CoA; phosphotransferases, which add a phosphate group using ATP; and adenylyltransferases, which add an AMP moiety from ATP. Chloramphenicol acetyltransferases are responsible for adding an acetyl group to chloramphenicol using acetyl-CoA³⁰. Antibiotics that have been modified in this way have reduced affinity for the RNA components of the ribosome and are unable to inhibit protein synthesis.

1.2.4.4 Alteration of Target

Bacteria have developed mechanisms to modify their antibiotic targets to avoid the detrimental effects of antibiotics. These modifications must not affect the target's function while making it unrecognizable to antibiotics. Target modification can occur through genetic mutation or post-transcriptional modifications mediated by enzymes³⁸.

For example, vancomycin resistance in VRE occurs due to genetic mutations in the vanHAX genes, resulting in the conversion of D-Ala-D-Ala to D-Ala-D-lactate. This modification changes the target's structure and reduces its affinity for vancomycin by 1000-fold, but still enables normal cell wall biosynthesis³⁷. In another example, erythromycin resistance occurs due to N6-methylation of adenine A2058 of 23S rRNA by erythromycin ribosome methylase (Erm), which lowers the target's affinity for erythromycin and leads to cross-resistance to other macrolides, lincosamides, and streptogramin B³⁹.

The qnr gene families encode pentapeptide repeat proteins (PRPs) that bind to DNA gyrase and topoisomerase IV, resulting in the rescue of these enzymes from the effects of fluoroquinolones³². The binding of PRPs to the DNA-topoisomerase-quinolone complex destabilizes the complex and triggers the release of quinolones, thereby restoring the activity of topoisomerase⁴⁰.

1.2.4.5 Overproduction

Bacteria can develop tolerance to antibiotics by increasing the expression of their target genes. When an antibiotic targets a specific function in bacteria, they compensate for the loss of that function by producing an excess of the corresponding target. This leads to a situation where a higher concentration of the antibiotic is needed to completely block the excess target. In clinical isolates of *Mycobacterium tuberculosis* and other *Mycobacterium* species, resistance to isoniazid and ethambutol is believed to be partly due to the overexpression of *inhA* and *emb* genes, respectively⁴¹.

1.2.4.6 Bypass

Bacteria can develop a particular type of resistance to antibiotics that are designed to target metabolic pathways, such as sulfonamides and trimethoprim. In this case, bacteria produce a new protein that is able to perform the same function as the original protein that is inhibited by the antibiotic. This new protein may have a different structure, which makes it less vulnerable to the harmful effects of the antibiotic and sometimes even more efficient in its function. For example, two new dihydrofolate reductases were discovered in *E. coli* that were not susceptible to trimethoprim due to resistance plasmids R388 and R483. These plasmid enzymes had a different molecular weight than the chromosomal enzyme and were less sensitive to trimethoprim, with an IC_{50} 22×10^3 times higher. Interestingly, the R483-carrying *E. coli* had dihydrofolate reductase activity that was 10 times higher than the wild type⁴².

1.3 Resistance Cost

Bacteria can benefit from being resistant to antibiotics when they are under selective pressure, but usually resistant bacteria have a lower fitness level, which means they have a slower growth rate and reduced virulence compared to non-resistant strains when there are no antibiotics present⁴³. This is because resistance mutations target essential components in bacteria, such as antibiotic targets. Even if the resistance is acquired through a plasmid, synthesizing new nucleic

acids and proteins can be energetically taxing and may interfere with the bacteria's physiological processes⁴⁴. To assess fitness costs, the exponential growth rates of wild type and resistant strains can be compared *in vitro* (Figure 3a), or an *in vitro* competition assay (Figure 3b) can be conducted by mixing the two strains in a certain ratio and evaluating the change in ratio over several days. This competition assay can also be done *in vivo* (Figure 3c), using an appropriate animal model that mimics a clinical infection⁴⁵.

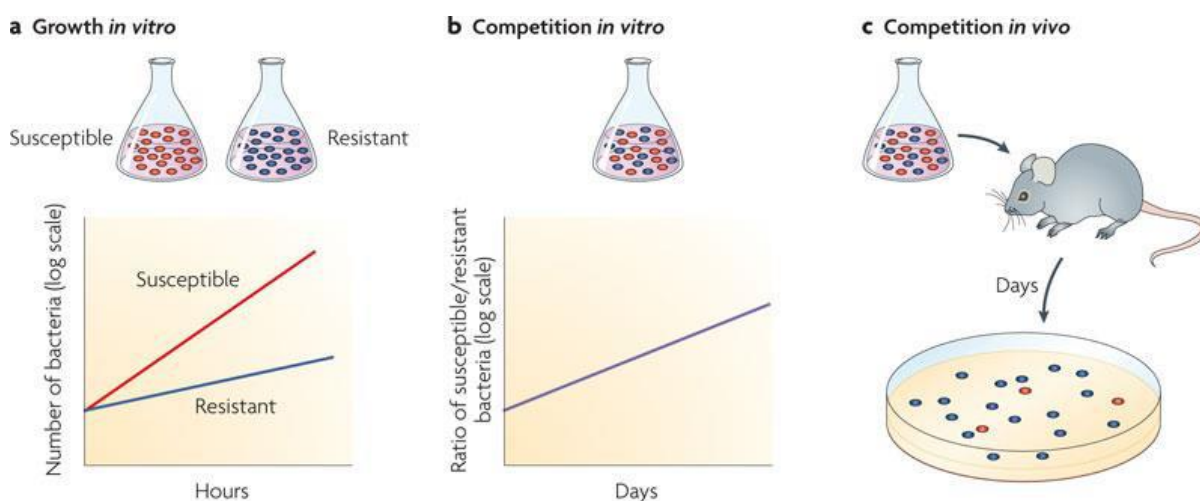


Figure 3: Determination of bacterial fitness(Taken from reference 45)⁴⁵

The cost of resistance can vary depending on various factors, such as the type of antibiotic, the bacterial species, and growth conditions^{45,46}. Some bacteria may have a high cost of resistance, while others may have little to no cost. Although the cost of resistance can provide some hope in fighting antibiotic resistance, the ability of bacteria to adapt to these costs can make it difficult to develop new antibiotics. Bacteria can evolve compensatory or suppressor mutations that reduce the cost of resistance without affecting the resistance itself⁴⁵. For example, *E. coli* mutants resistant to rifampicin had decreased fitness due to impaired transcription efficiency, but after 200 generations, they developed compensatory mutations that increased their fitness without affecting resistance levels⁴⁷. To develop an ideal antibiotic, it is important to understand the costs of resistance and carefully choose targets that severely affect bacterial fitness upon resistance while being difficult to compensate for. This can lead to antibiotics with a lower rate of resistance development⁴⁸.

1.4 Challenges in Antibacterial Drug Discovery

There is a significant gap between the demand for novel antibacterial agents with new mechanisms of action to address the problem of AMR and the current supply of such agents. This is due to the multistep process of discovering and developing new antibacterials as shown

in Figure 4. Several factors contribute to the complexity of this process, including the pressing need to address the flawed business model prevalent in the antibiotic market. The economics of antibiotic development pose significant challenges due to factors like low profitability, limited treatment durations, and the alarming rise of antibiotic resistance hampering progress. Moreover, the development of antibiotics encounters additional technical obstacles. These include the necessity for higher safety margins, given the elevated doses required for effective treatment, as well as the formidable task of penetrating bacteria to deliver the drug precisely to its intended target site. These challenges are further compounded by varying patterns of antibiotic consumption, the presence of secondary infections, stringent approval requirements imposed by regulatory agencies, low productivity within the pharmaceutical industry, the need for multiple clinical trials, and the influence of regulatory agencies on drug pricing and the merging of pharmaceutical companies^{49,50}.

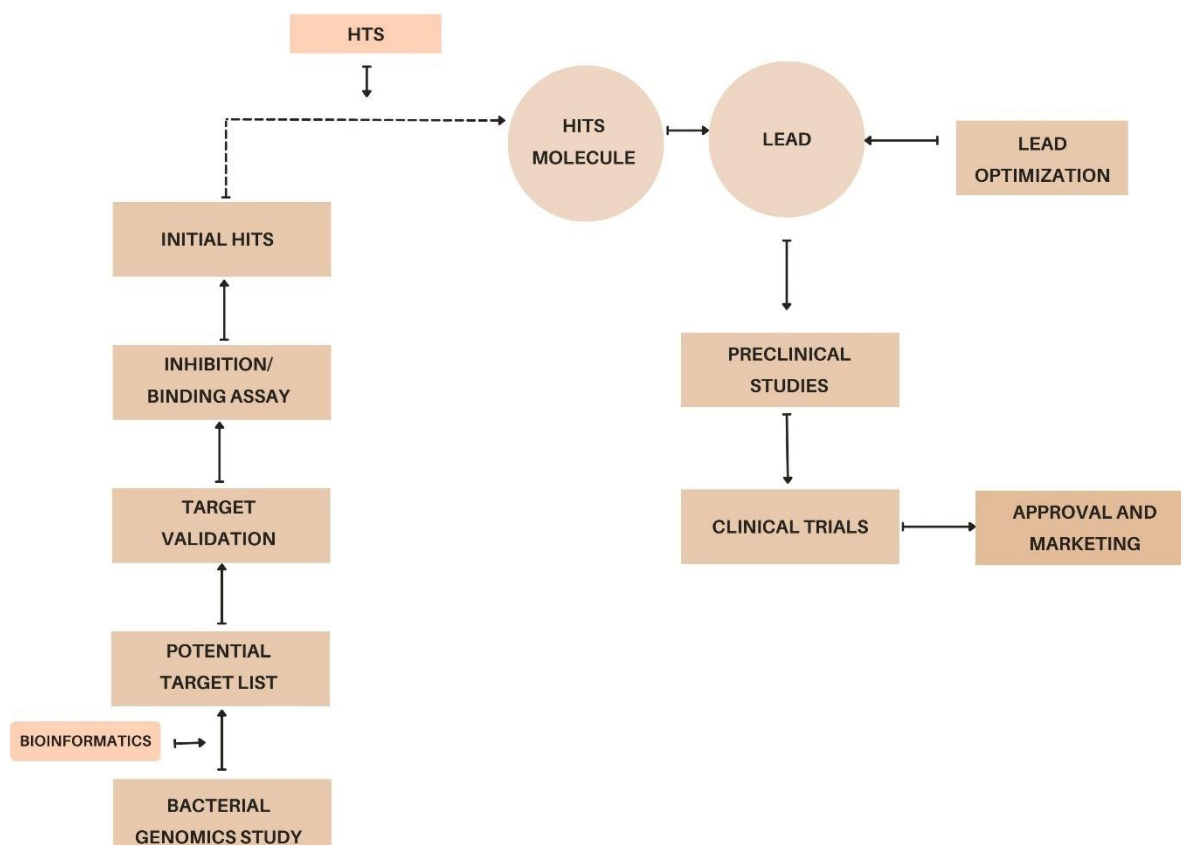


Figure 4: Schematic pathway for discovery and development of antibacterial drugs.

The process of new drug development involves two main approaches. The first approach involves the development of novel molecules for the benefit of society, which can be funded by government agencies. The second approach involves the development of molecules that are

in demand in the market, and requires the initiative and capital investment of a pharmaceutical company⁵¹⁻⁵⁴. Factors that influence a pharmaceutical company's decision to invest in a novel antibacterial drug-discovery program include the need for new molecules in the market, the potential consumer base, the advantages and limitations of the novel agents compared to existing molecules, the presence of competing brands, and the expected return on investment. However, due to these various factors, the number of novel antibacterial drug-discovery programs currently in development is limited, and only a few of them successfully reach the final stage and achieve their goals⁵⁵.

1.5 Antibiotics and their Main Targets

Antibiotics refer to chemical compounds that can either kill or restrict the growth of bacteria. They have multiple crucial applications, including the management of acute bacterial infections, surgical procedures, transplantation, caring for critically ill patients, and cancer chemotherapy. To be considered a suitable antibacterial agent for clinical use, it must meet several requirements beyond the original notion of being a "magic bullet." These requirements include the ability to exhibit selective toxicity towards pathogenic bacteria, be harmless to human cells and normal flora, possess broad-spectrum activity, have a low tendency towards resistance development, and exhibit reasonable pharmacokinetic properties relevant to the site of application, such as solubility, lipophilicity, chemical, and metabolic stability.

The antibiotic mode of action usually is assigned to the intrusion into the function of one or more vital machineries in bacteria: cell-wall, cell-membrane, nucleic-acid (DNA and RNA), protein and metabolites synthesis. The major bacterial targets of antibiotics are described in Figure 5.

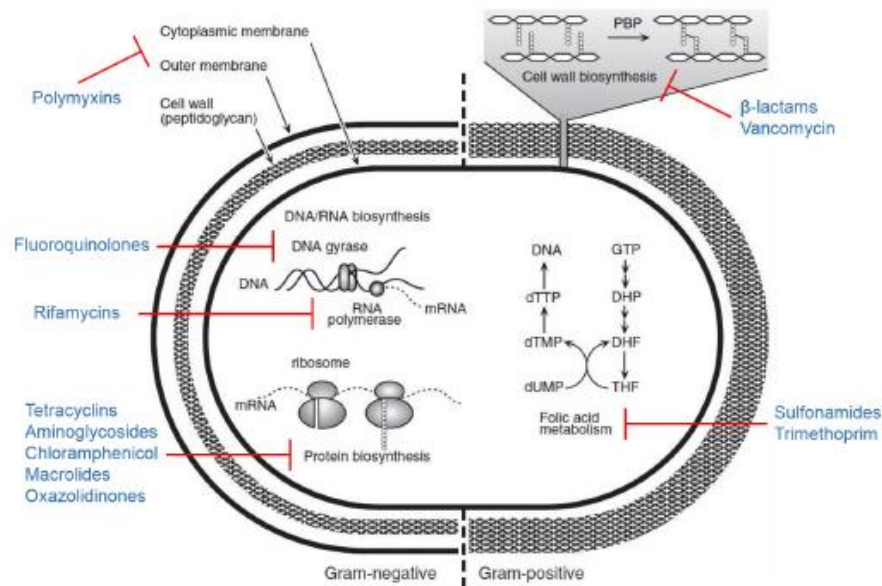


Figure 5: Antibiotic targets in bacteria (Taken from reference 30)³⁰

1.5.1 Inhibition of Cell-Wall Synthesis

The bacterial cell is comprised of various components that are enveloped by a phospholipid bilayer, known as the inner membrane, and a network of peptidoglycan, or murein, which forms the cell wall. In Gram-negative bacteria, an additional layer enclosing LPS encompasses the cell wall, known as the outer membrane. These protective layers are crucial for the bacterial cell's defense against osmolysis. The peptidoglycan network is linked by transglycosylase and transpeptidase, also referred to as penicillin binding protein (PBP).

β -Lactam antibiotics, such as penicillins, cephalosporins, carbapenems, and monobactams, compete with the D-Ala-D-Ala substrate to inhibit peptidoglycan synthesis (see Figure 6)⁵⁶. These antibiotics attach to PBP irreversibly by opening the β -lactam ring and acylating the active site. Another inhibitor of peptidoglycan synthesis is glycopeptides, like vancomycin, which binds to the D-Ala-D-Ala substrate, restricting access to PBP⁵⁷.

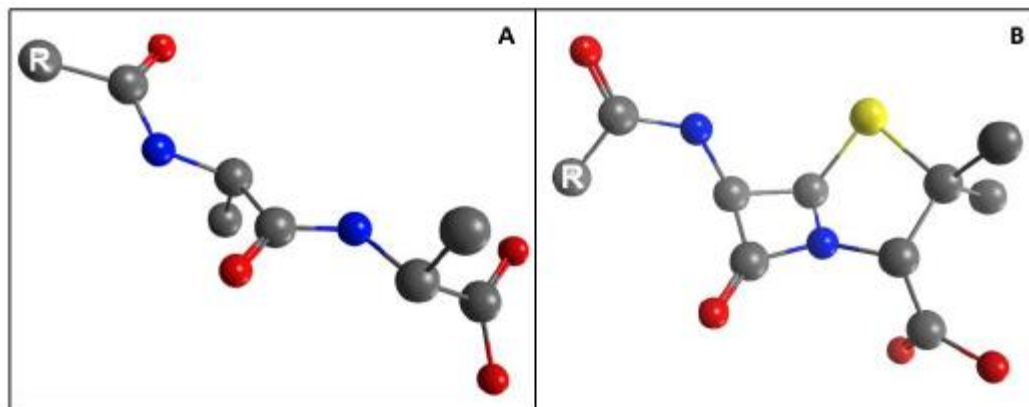


Figure 6: Structural mimicking to the substrate sequence D-Ala-D-Ala (A) by various penicillins (B)⁵⁶.

1.5.2 Inhibition of Protein Synthesis

Translation is the process in which ribosomes decode genetic data carried by mRNA to synthesize proteins, occurring in three stages: initiation, elongation, and termination. The translation process requires ribosomes, tRNAs carrying amino acids, as well as initiation and release factors. Bacterial ribosomes consist of two subunits (30S and 50S) and are essential for protein biosynthesis. Tetracyclines are known to bind to the 30S subunit and prevent tRNAs from interacting with the ribosome. Aminoglycosides like streptomycin and gentamicin irreversibly bind to the 16S rRNA component of the 30S subunit, leading to conformational changes that result in mRNA codon-tRNA mismatching and protein mistranslation. Macrolides such as erythromycin and chloramphenicol interact with the 23S rRNA of the 50S subunit and block peptidyl transferase activity. Oxazolidinones bind to the 50S subunit and prevent the formation of initiation complexes, ultimately inhibiting protein synthesis⁵⁷.

1.5.3 Disruption of Cell Membrane

Maintaining the integrity of the cell membrane is crucial to prevent the leakage of cell components. Polymyxins, which are cationic peptides, can affect both the cytoplasmic and outer membranes of Gram-negative bacteria. They increase the permeability of the membrane, which can result in the death of the cell³⁰.

1.5.4 Inhibition of Nucleic-Acid Synthesis

DNA replication and transcription are crucial processes for bacteria. During DNA replication, topoisomerases are necessary to maintain the topology of the supercoiled DNA strands. Type I topoisomerases cleave one DNA strand temporarily, while type II topoisomerases cleave both strands at once in an ATP-dependent process. Aminocoumarins and fluoroquinolones target

type II topoisomerases, namely DNA gyrase and Topoisomerase IV. Fluoroquinolones such as norfloxacin, ciprofloxacin, and levofloxacin bind to the DNA-bound gyrase forming a ternary complex. This stabilizes the complex in the DNA double-strand cleaved state, preventing DNA religation (topoisomerase poisoning)⁵⁷.

The RNA synthesis process, transcription, is conducted by DNA-dependent RNA polymerase (RNAP) in three stages: initiation, elongation, and termination. RNAP is a multi-subunit enzyme composed of α 2, β , β' , and ω subunits, forming the core enzyme with a molecular weight of ~400 kDa. The core enzyme binds to the initiation factor σ , forming the holoenzyme. Although the core RNAP is the catalytic active motif, binding to the σ factor is a key step for promoter DNA recognition and binding⁵⁸. Rifamycins inhibit transcription by binding to the β subunit of the DNA-bound RNAP adjacent to the active center, causing steric interference with the growing RNA transcript⁵⁹.

1.5.5 Inhibition of Metabolite Pathways

Bacteria require folic acid as a coenzyme for creating nucleotides. The process of folate biosynthesis starts from *p*-aminobenzoic acid and pteridine, which are transformed into dihydropteroic acid by dihydropteroate synthase. Dihydrofolic acid is then produced from dihydropteroic acid by dihydrofolate synthase, and tetrahydrofolic acid is generated from dihydrofolic acid via reduction by dihydrofolate reductase. Sulfonamides and trimethoprim are two classes of antibiotics that target these enzymes. Sulfonamides halt the action of dihydropteroate synthase, while trimethoprim binds competitively to the active site of dihydrofolate reductase, mimicking the shape of the respective substrates PABA and dihydrofolic acid³⁰.

1.6 Need to develop novel antibiotics: Targeting PG synthesis

In light of the growing threat of antibiotic resistance and the urgent need for discovering new antibiotics, research efforts have shifted towards developing novel approaches to combat bacterial infections³⁰. One promising avenue is the synthesis of antibacterial agents targeting the machinery responsible for peptidoglycan biosynthesis⁶⁰. Peptidoglycan, a crucial component of the cell wall in prokaryotic cells, plays a vital role in bacterial survival and is unique to these organisms. This uniqueness presents an attractive opportunity to develop new agents that specifically target the peptidoglycan layer. Such agents are expected to have low initial bacterial resistance, making them potential candidates for combating antibiotic-resistant

strains²⁶. By focusing on peptidoglycan as a target, researchers aim to disrupt the biosynthetic machinery and ultimately hinder bacterial growth and proliferation.

1.6.1 Biosynthesis of Peptidoglycan Layer

Peptidoglycan, also referred to as "murein," is a vital component of the bacterial cell wall^{61,62}. Peptidoglycan, being an essential component of the bacterial cell wall, plays a crucial role in maintaining the structural integrity and survival of bacteria. Without the presence of a peptidoglycan layer, the cells would function as a hypotonic medium, leading to the swelling and bursting of cells. This highlights the importance of the peptidoglycan layer in maintaining the rigidity and shape of cells, as well as facilitating cell division. Thus, the presence of a peptidoglycan layer is essential for bacterial survival⁶³. Peptidoglycan is a particularly promising target for antibacterial drug discovery because it is found exclusively in bacterial cells and not in mammalian cells. It forms a continuous mesh-like structure, referred to as the "Sacculus," through the joining of short strands of glycan. The thickness of the Sacculus layer varies depending on the type of bacteria, with Gram-negative species having a layer that is 3-6 nm thick and Gram-positive species having a layer that is 10–20 nm thick due to multiple layers. Peptidoglycan is composed of short glycan chains of alternating N-acetyl muramoyl-peptides (MurNAc) and N-acetyl glucosamine (GlcNAc), which are crosslinked with each other^{64,65} as shown in Figure 7. A variation in cell's turgor pressure is responsible for expansion & shrinkage of peptidoglycan layer. It is intriguing fact that peptidoglycan layer with its crucial, steadying role is constantly modified⁶⁶. Peptidoglycan layer has a high degree of cross linking and hence must be hydrolyzed by specific enzymes in order to study the structural behavior⁶⁷. Furthermore, the presence of the peptidoglycan layer is an essential criterion for taxonomic classification of bacteria, as the structure of the peptidoglycan layer varies greatly in Gram-positive bacteria and is uniform and unchanging in Gram-negative bacteria⁶⁸. The presence of the peptidoglycan layer in the cell wall of bacteria presents a number of challenges, such as the inhibition of the entry of hydrophilic compounds. A potential solution to this issue is to utilize carrier-mediated transport, which is the normal mechanism used by cells to uptake solutes from the outside to the inside of the cell^{41,69}.

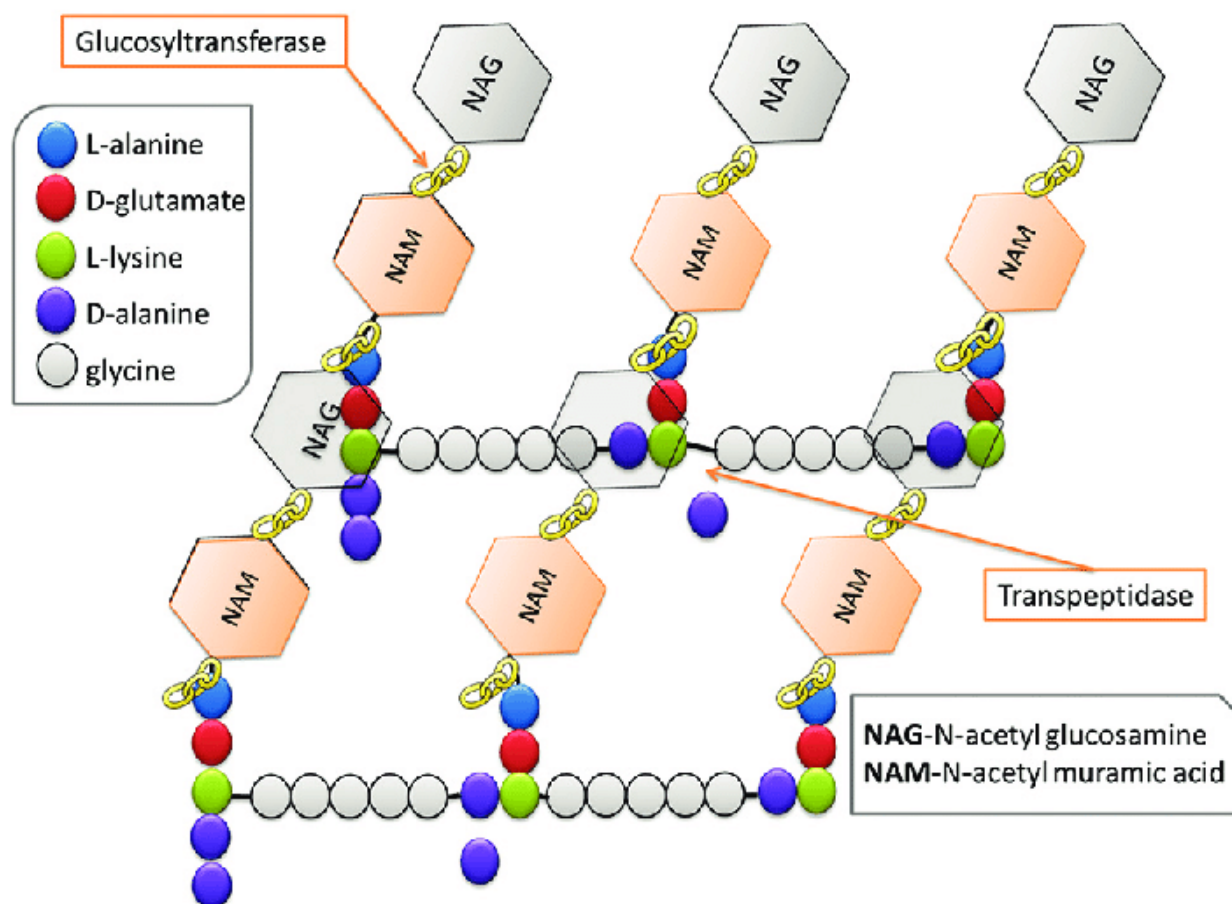


Figure 7: Basic structure of the bacterial cell wall peptidoglycan (Taken from reference 70)⁷⁰.

1.6.1.1 Historical Perspectives

Research on the structure and intermediates involved in the biosynthesis of peptidoglycan is well-established in the field of antibacterial drug discovery. The study of peptidoglycan began with Alexander Fleming's discovery of penicillin, which acts as a specific inhibitor of cell-wall synthesis. With the advancement in techniques for structurally analyzing peptidoglycan, such as determining its assembly and identifying different peptidoglycan precursors like transpeptidase (TPs) and glycosyltransferase (GTase) and their inhibitors. The understanding of the biosynthetic pathway of peptidoglycan was completed by the determination of lipid intermediates, such as Lipid I and Lipid II, by the mid-1960s⁷¹⁻⁷³. Efforts were later directed towards synthesizing peptidoglycan *in vitro*, and some level of success was achieved⁷⁴. The use of more advanced analytical techniques, such as radiolabeling and chromatography, has led to the identification of additional intermediates and an increased understanding of the underlying mechanisms⁶¹.

1.6.1.2 Pathway for Biosynthesis of Peptidoglycan

The biosynthesis of bacterial peptidoglycan has been extensively studied in various species, resulting in a significant amount of knowledge about the biosynthetic pathway. The process can be broken down into two stages: six intracellular cytoplasmic enzymatic steps and three steps that occur outside the plasma membrane.

The first stage involves the formation of the PG complex polymer, which is accomplished by the activity of six essential and structurally related enzymes known as Mur Enzymes shown in Figure 8 (MurA, MurB, MurC, MurD, MurE, and MurF). These enzymes catalyze the assembly of the final cytoplasmic peptidoglycan biosynthesis precursor, known as UDP-MurNAc pentapeptide. Following the activity of the Mur enzymes, a disaccharide-(peptide)-pyrophosphate undecaprenol lipid intermediate is formed by the action of MraY and MraG.

The second stage starts with the translocation of the lipid intermediates outside the cytoplasmic membrane, which then leads to a polymerization reaction. This reaction is driven by two different enzymes, namely glycosyltransferase (GTase) and transpeptidase (TPase). The GTase enzyme is responsible for the polymerization of the glycan strand, while the TPase enzyme performs the formation of peptide cross-linking. (Figure 9)^{60,63,75-77}.

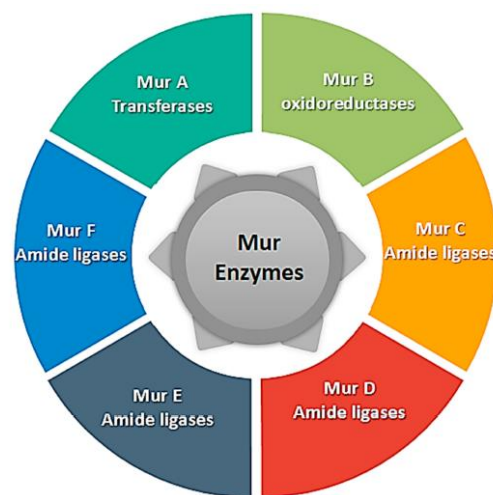
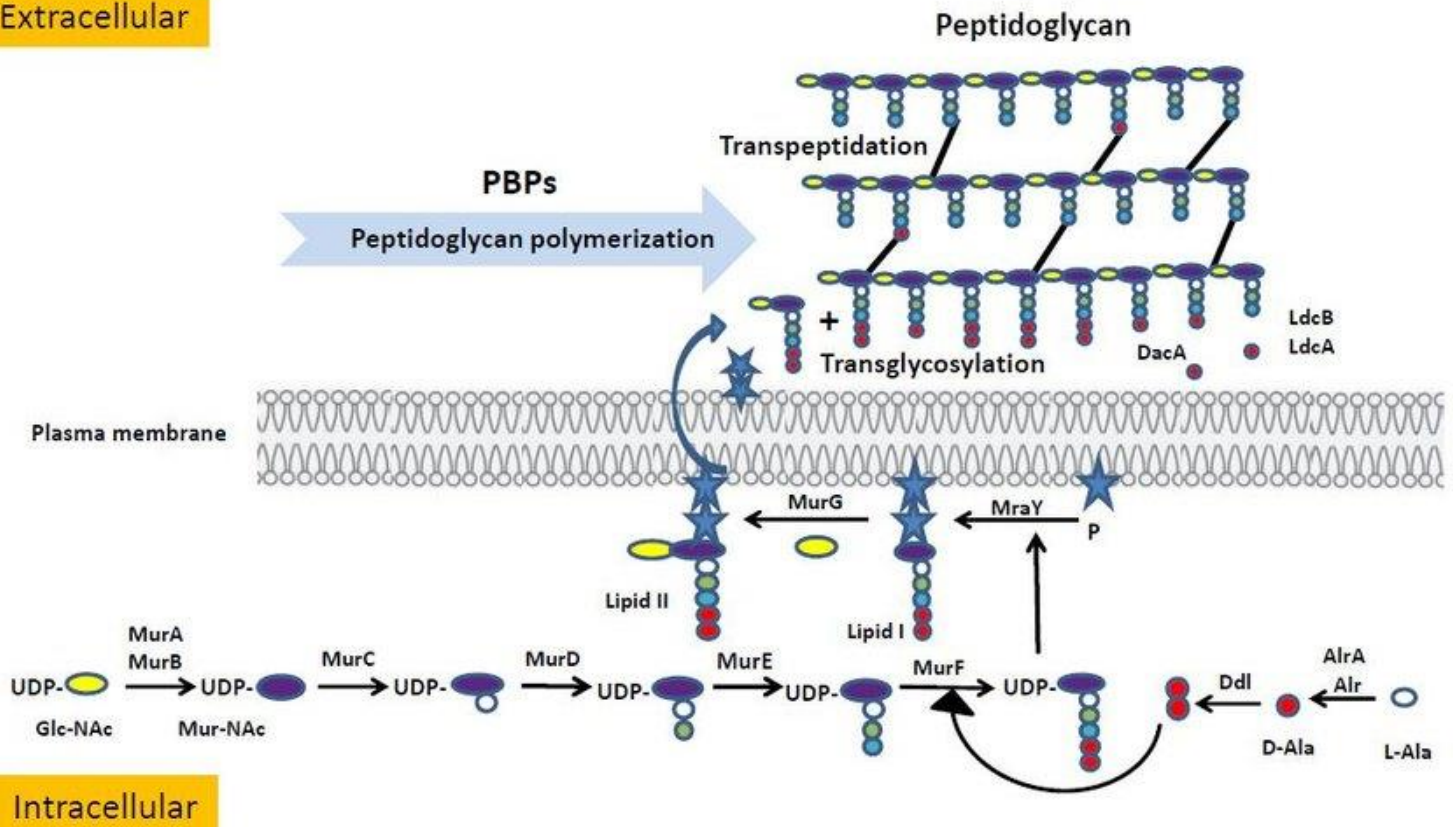


Figure 8: Classification of Mur Enzymes(Taken from reference 78)⁷⁸.

Extracellular



Intracellular

Figure 9: Peptidoglycan Biosynthesis Pathway (Taken from reference 79)⁷⁹.

1.6.1.3 Targeting the Cascade of Intracellular Mur enzymes

The peptidoglycan biosynthesis enzymes remain among the most important antibacterial drug targets. The majority of drugs utilized in targeting peptidoglycan biosynthesis are inhibitors of membrane-bound extracellular enzymes, such as penicillin-binding proteins. On the other hand, the cytoplasmic steps of the peptidoglycan biosynthesis remain underexplored and underutilized in antibacterial drug design, providing an opportunity for the discovery of novel agents. The main cytoplasmic enzymes involved in the peptidoglycan biosynthesis pathway are the Mur enzymes.⁸⁰ Mur enzymes are particularly attractive targets in the design of antibacterial drugs for several reasons. They are essential for bacterial survival, lack structural homology with mammalian enzymes, have available crystal structures which can be used for structure-based drug design, have known substrates and rapid biochemical assays, and are druggable, as demonstrated by the development of the MurA inhibitor fosfomycin. These characteristics of Mur enzymes make them an attractive for the design of new drugs⁸¹.

1.7 Steps involved in the Assembly of Peptidoglycan

Formation of peptidoglycan units is a multistep process and involves three important steps as follows and summarized in Figure 10.

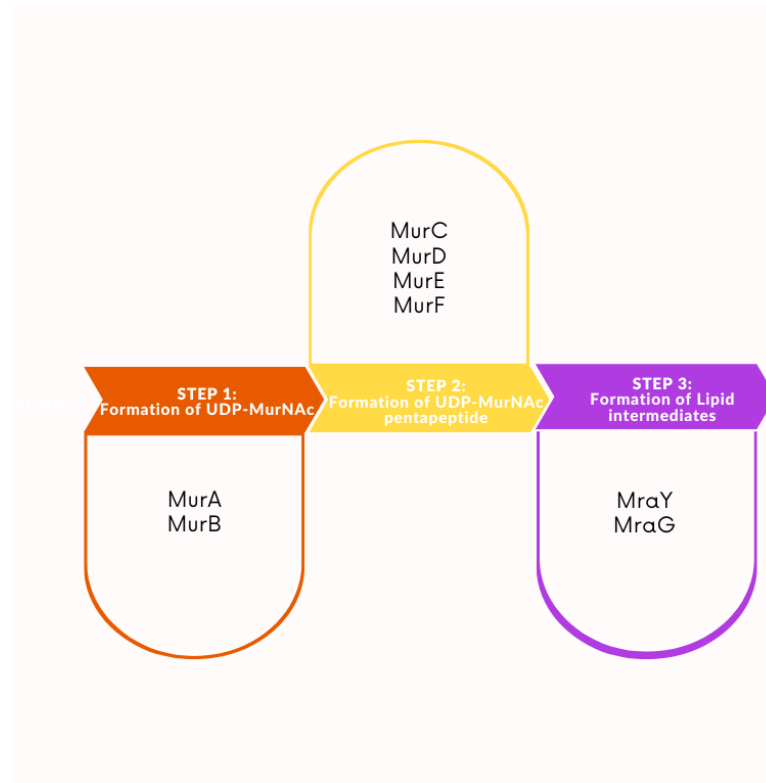


Figure 10: Enzymes involved in assembly of the peptidoglycan.

Step I: Formation of UDP-N-acetyl Muramic acid

The first step in the biosynthesis of peptidoglycan is the formation of UDP-N-acetyl muramic acid, which is a two-step process. The first step is the formation of UDP-Glc-NAc enolpyruvate by the action of the enzyme MurA transferase. In this reaction, the enolpyruvate from phosphoenolpyruvate (PEP) is transferred to the 3rd position of the GlcNAc residue. The second step ends with the formation of UDP-MurNAc by the action of MurB reductase, which reduces the enolpyruvate moiety to D-lactoyl (Figure 11) ⁶³.

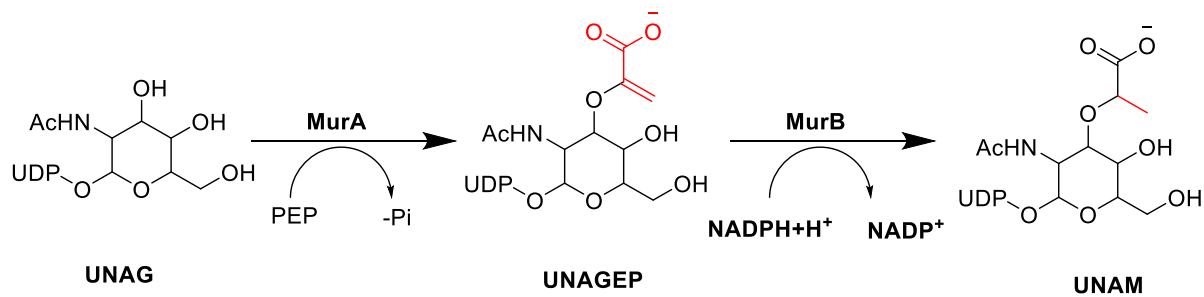


Figure 11: MurA and MurB catalyzed steps of peptidoglycan biosynthesis.

1.7.1.1 MurA Transferase.

The enzyme MurA is responsible for the transfer of the enolpyruvyl moiety of phosphoenolpyruvate (PEP) to UDP-GlcNAc during the first step of peptidoglycan biosynthesis as shown in Figure 11. This enzyme is present in both Gram-positive and Gram-negative bacteria, but its distribution is different between the two groups. Gram-negative bacteria, such as *E. coli*, have a single copy of the MurA gene, while Gram-positive organisms such as *S. pneumoniae* have a second transferase gene. However, it is interesting to note that both copies of the gene perform the same function and can substitute for each other in the biosynthesis process^{82–84}.

1.7.1.1.1 MurA overall structure.

Skarzynski et al. have successfully determined the crystal structure of *Escherichia coli* MurA in complex with UDP-N-acetylglucosamine (UDP-GlcNAc) and fosfomycin at a resolution of 1.8 Å. The structure consists of 418 amino acid residues, UDP-GlcNAc and fosfomycin with two globular domains, domain-I and domain-II, that are connected by a double-stranded linker (Figure 12)⁸⁵. The C-terminal region of the protein is located in domain-I (residues 1 to 21 and 230 to 419), while the N-terminal region is located in domain-II (residues 22 to 229)⁸⁶ which is the domain containing the catalytic Cys115⁸⁷.

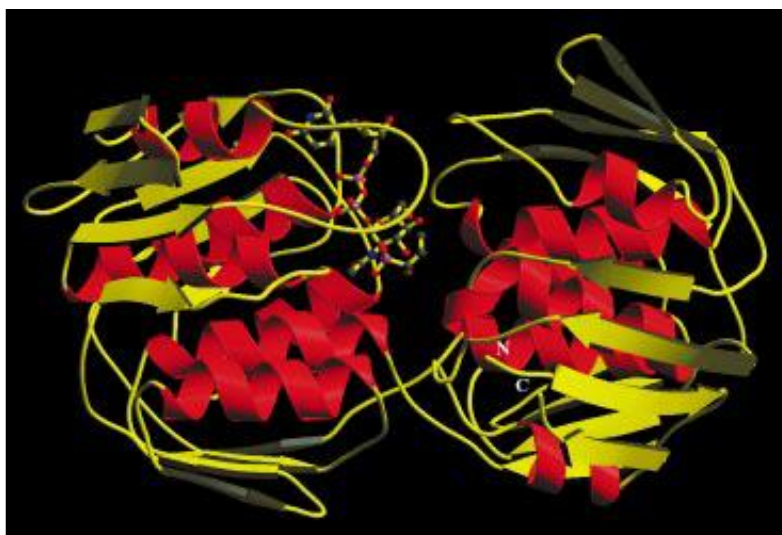


Figure 12: Schematic representation of the overall protein architecture of MurA. It showcases the binding of UDP-GlcNAc and fosfomycin molecules in the active site, visualized using a ball-and-stick model⁸⁷.

1.7.1.1.2 MurA catalytic site.

The catalytic site of MurA enzyme is located within a deep cavity between the two domains (Figure 12). Residues distributed around the catalytic pocket participate in a total of 10 direct interdomain hydrogen bonds. These include four hydrogen bonds between loops 46–49 and 396–400, featuring the Asp49–Arg397 salt bridge. Additionally, there are three hydrogen bonds between loops 116–119 and 329–330, a hydrogen bond between Glu188 and His299, and a salt bridge between Glu190 and Arg232 at the bottom of the active-site cavity. Notably, there are no significant hydrophobic patches between the domains, but a few hydrophobic interactions occur between individual residues in the interface, such as Ile117–Phe328 and Val161–Pro298. These interdomain interactions contribute to stabilizing the closed conformation of the enzyme. Moreover, they may play a specific role in catalysis by controlling access to the active site during different reaction stages. For instance, the Asp49–Arg397 salt bridge, which is conserved in all known MurA sequences, is positioned between the active site and the surrounding solvent, with the arginine residue contributing to the phosphate-binding site⁸⁷.

1.7.1.2 MurB oxidoreductase.

MurB is an NADPH-dependent oxidoreductase that catalyzes its reaction in two steps. The first step involves the formation of a tightly bound flavin by the reduction of FAD using two electrons from NADPH. The second step involves the transfer of these electrons at the C-3 position of the enol ether, which results in the reduction of a vinyl bond, converting the enolpyruvate moiety to D-lactate, and the formation of UDP-MurNAc⁸⁸.

MurB is an enzyme that has been extensively studied for its biochemical, mechanistic, and structural properties in relation to the reduction of an enol ether. It contains a flavin adenine dinucleotide (FAD) cofactor that facilitates hydride transfer between NADPH and the enolpyruvyl substrate during its catalytic process. The structure of MurB has been elucidated, revealing an active site where the flavin molecule is positioned parallel to the enolpyruvyl unsaturated C2-C3 bond, ready for hydride transfer from the flavin to the enolpyruvyl molecule (Figure 13)⁸⁹.

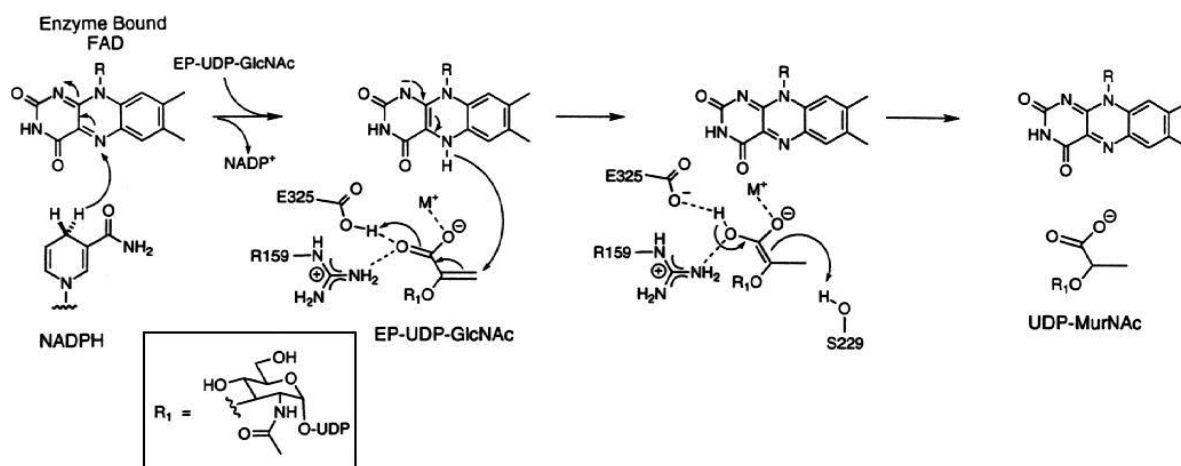


Figure 13: Proposed mechanism of reduction of the enolpyruvyl group of UDP-GlcNAc-EP by MurB. Hydride transfer to C3 is proposed to generate a carbanion equivalent that can be stabilized by protonation from Glu325 and/or Arg159. Quenching of the carbanion is proposed to be mediated by Ser229.⁸⁹

1.7.2 Step II: Formation of UDP-MurNAc-peptides

The formation of monomer units in peptidoglycan biosynthesis involves the stepwise addition of various components to UDP-MurNAc, such as L-alanine, D-glutamic acid, diaminopimelic acid (a diamino acid), and a dipeptide of D-alanine-X (where X is generally D-alanine). This process is carried out by a group of enzymes: MurC, MurD, MurE, and MurF⁷⁵.

1.7.2.1 MurC ligase

UDP-N-acetylmuramate-L-alanine ligase (MurC) is responsible for adding L-alanine (L-Ala) as the first amino acid to form the peptide stem.⁹⁰ This process requires binding of ATP to the enzyme first, followed by binding of UDP-MurNAc, and then L-Ala to form UDP-N-acetylmuramoyl-L-alanine (UMA, Figure 14).

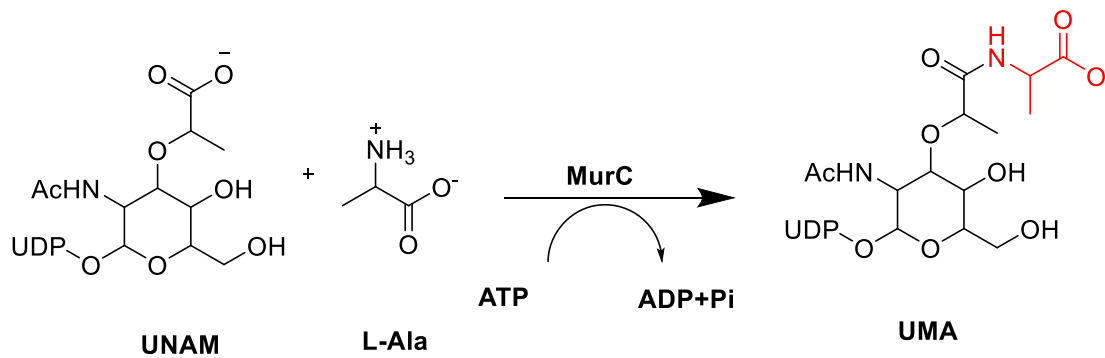


Figure 14: Peptidoglycan precursor biosynthesis catalyzed by ATP-dependent MurC ligase.

1.7.2.2 MurD ligase.

MurD is an enzyme that catalyzes the addition of D-glutamate to the product of the MurC enzyme, UDP-N-acetylmuramoyl-L-alanine to form UDP-N-acetylmuramoyl-L-alanine-D-Glutamate (UMAG, Figure 15)⁹¹.

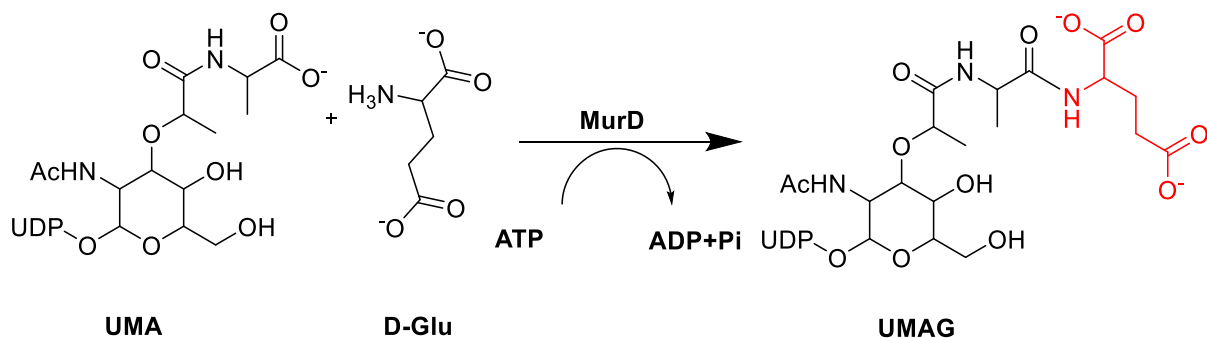


Figure 15: Peptidoglycan precursor biosynthesis catalyzed by ATP-dependent MurD ligase.

1.7.2.3 MurE ligase.

MurE is the third enzyme that adds diaminopimelic acid (DAP) to the growing peptide chain. It is the only Mur ligase that has different substrate specificity among bacteria. Typically, in Gram-negative bacteria and Mycobacteria, the enzyme incorporates meso-diaminopimelic acid at the third position of the growing peptide chain. However, in Gram-positive bacteria, it adds L-lysine instead⁹², forming UDP-N-acetylmuramoyl:tripeptide (UMT, Figure 16). The third residue in the PG is critical for cross-links between the glycan strands, and thus plays a vital role in the maintenance of cell wall integrity⁹³.

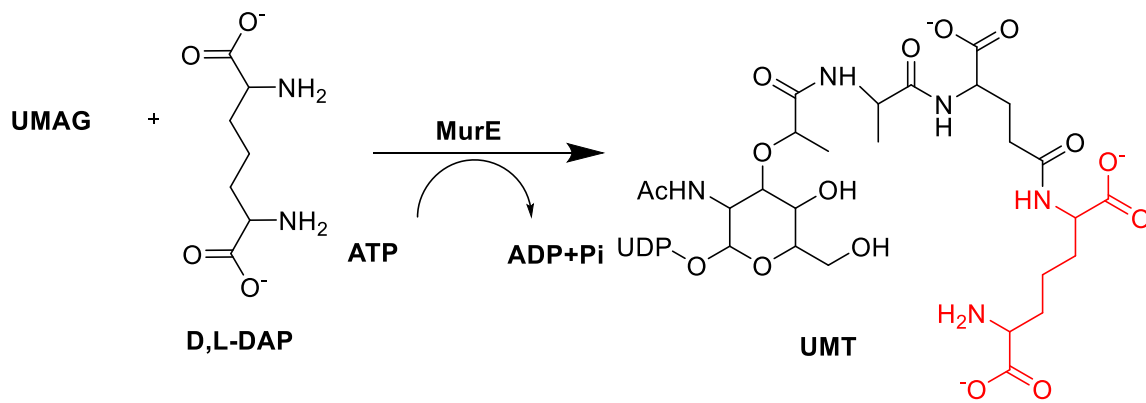


Figure 16: PG precursor biosynthesis catalyzed by ATP–dependent MurE ligase.

1.7.2.4 MurF ligase.

MurF is the final enzyme that adds the dipeptide D-Ala-D-Ala to the UDPMurNAc-tripeptide. This step is essential for the construction of peptidoglycan, as the formation of the peptide bond during this enzymatic reaction provides the energy required for cross-linking between glycan strands in the periplasmic space, where the availability of ATP is limited⁹⁴. Typically, D-Ala-D-Ala is the dipeptide added by MurF (Figure 17). However, MurF from Enterococci strains that showed resistance to vancomycin has been shown to employ alternative dipeptides such as D-Ala-D-Lac and D-Ala-D-Ser as an acquired resistance mechanism against glycopeptide antibiotics⁹⁵.

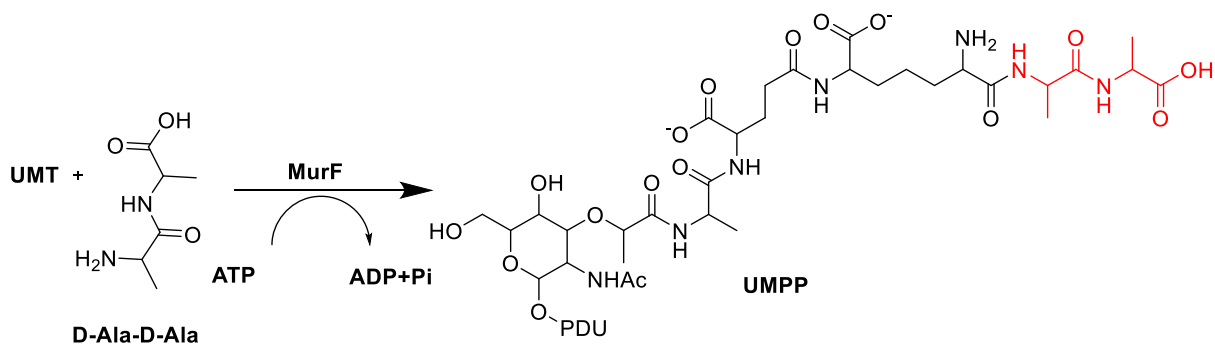


Figure 17: PG precursor biosynthesis catalyzed by ATP–dependent MurE ligase.

1.7.3 Step III: Formation of Lipid Intermediates

The formation of Lipid I and Lipid II is a two-step process. The first step involves the addition of the phospho-MurNAc-pentapeptide group of UDP-MurNAc-pentapeptide (the product of MurF) to undecaprenyl phosphate in the presence of the enzyme MraY, resulting in the formation of MurNAc-(pentapeptide)-pyrophosphoryl undecaprenol (Lipid I). In the second step, the enzyme MraG catalyzes the addition of N-acetylglucosamine to the C4 hydroxyl

MurNAc in Lipid I to produce the lipid-linked β -(1,4) disaccharide, resulting in the formation of GlcNAc-MurNAc-(pentapeptide)-pyrophosphoryl undecaprenol (Lipid II), which will pass through the membrane⁶³.

1.7.4 : Peptidoglycan Transglycosylation

Glycosyltransferase (GTase) is the enzyme that catalyzes the polymerization of glycan strands and is located on the outer surface of the cytoplasmic membrane, thus leading to the occurrence of the transglycosylation process on the outer side of the cytoplasmic membrane^{96,97}.

1.7.5 : Peptidoglycan Transpeptidation

Transpeptidase (TPase) is an enzyme involved in crosslinking glycan strands in a process known as transpeptidation occurs as an essential step in PG layer formation⁹⁸.

1.8 Fosfomicin

Fosfomicin, which was discovered in 1969 from *Streptomyces*, has broad-spectrum activity against both Gram-positive and Gram-negative bacteria⁹⁹. It has been found to be highly effective against extended spectrum beta-lactamase (ESBL)-producing *E. coli*, with (MICs) at 50% (MIC₅₀) and 90% (MIC₉₀) of isolates ranging between 2 and 4 $\mu\text{g}/\text{mL}$ ¹⁰⁰. ESBL-producing bacterial strains are particularly feared because they often resist cephalosporins, all penicillins, aztreonam, quinolones, and trimethoprim/sulfamethoxazole as well¹⁰¹.

1.8.1 Mechanism of Action

Fosfomicin enters the bacterial cell using two different membrane transportation systems: L-alpha glycerol-3-phosphate and the glucose-6-phosphate transporter (GlpT and UhpT, respectively). Interestingly, the chemical structure of fosfomicin resembles both glycerol-3-phosphate and G6P, which are typically transported through GlpT and UhpT and induce their expression (Figure 18)⁴¹.

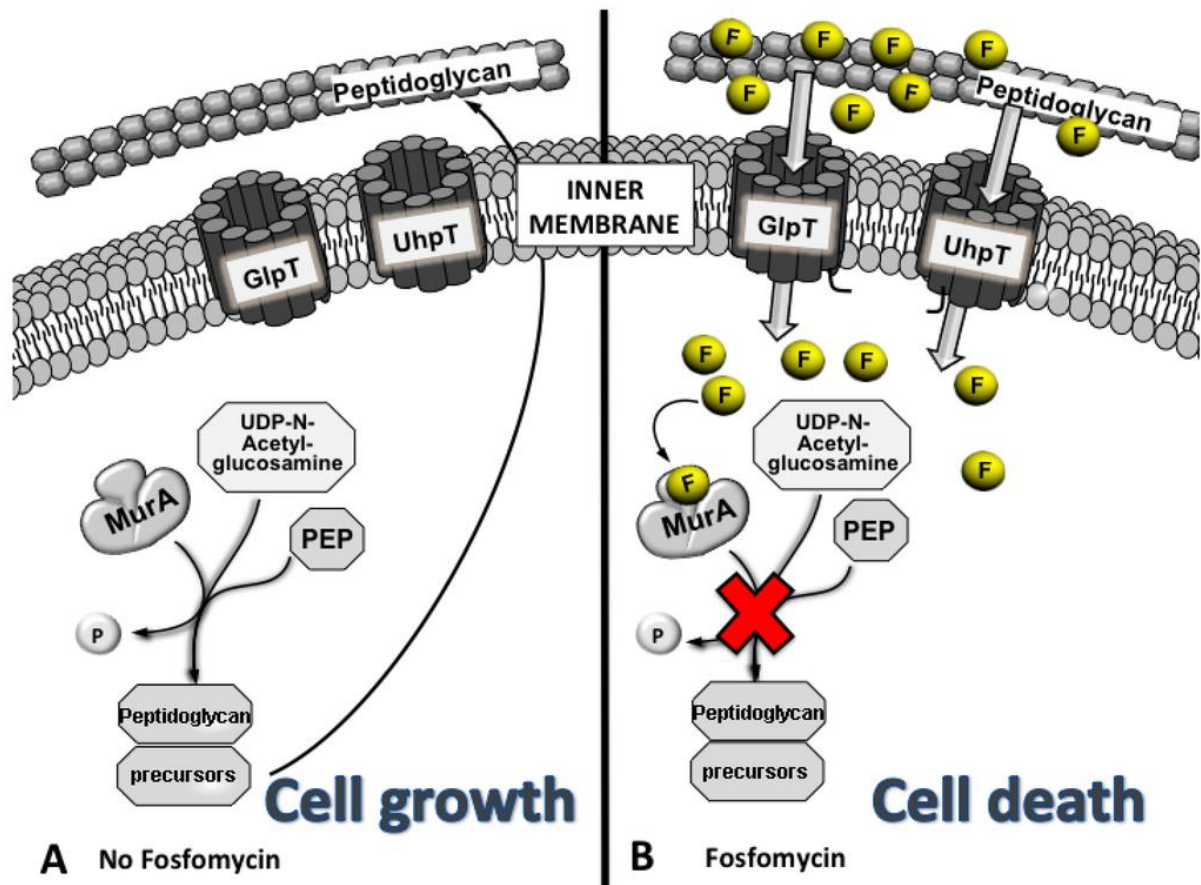


Figure 18: Schematic representation showing: A) MurA normal catalysis when fosfomycin is not present allowing cell growth. B) MurA disrupted catalysis when fosfomycin (F) is present, it is transported inside the cell by GlpT and UhpT, blocking MurA by mimicking the original substrate, PEP, avoiding cell wall synthesis and leading to cell death (Taken from reference 130)

As previously mentioned, MurA is a bacterial enzyme that catalyzes the transfer of enolpyruvate from phosphoenolpyruvate (PEP) to UDP-N-acetylglucosamine (UNAG), which is the initial step in bacterial cell wall synthesis. At present, fosfomycin is the only clinically approved antibiotic that targets MurA, by forming a covalent bond with the Cys115 residue in the active site of the enzyme and thereby inhibiting its normal function which leads to bacterial cell death (Figure 19)¹⁰². Therefore, any species that possess a variant of MurA that lacks the Cys115 residue in the active site are intrinsically resistant to Fosfomycin. Such species include *Borrelia Burgdorferi* and *M. tuberculosis* which have an Asp instead of Cys115 in the MurA active site¹⁰³.

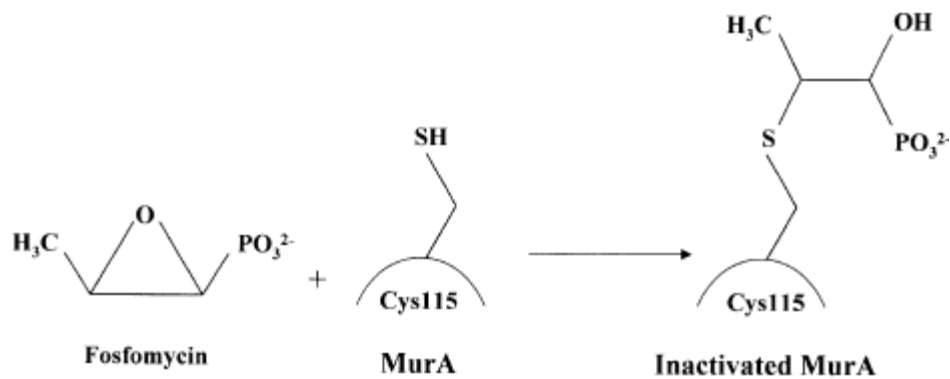


Figure 19: Inactivation of MurA by fosfomycin as a result of the covalent linkage between Cys-115 of MurA and fosfomycin¹⁰⁴.

1.8.2 Clinical Use

Fosfomycin is commonly used as a first-line oral treatment for urinary-tract infections, this is because it functions by inhibiting MurA. Additionally, in some European countries, it is also approved for intravenous administration as a treatment for sepsis and soft-tissue infections¹⁰². Owing to its efficacy against ESBL-producing bacteria, fosfomycin has been used in clinical trials in combination with other antimicrobials for the treatment of nosocomial infections caused by ESBL-producing, carbapenem-resistant *K. pneumoniae*¹⁰⁵.

1.8.3 Resistance

While Fosfomycin is highly effective against ESBL-producing *E. coli*, its efficacy is diminished against other multidrug-resistant bacteria. For example, in ESBL-producing, carbapenem-resistant *K. pneumoniae*, the MIC₅₀ and MIC₉₀ values are significantly higher compared to *E. coli* (~32 mg/L and ~128 mg/L, respectively)^{106,107}.

1.8.3.1 Mechanisms of Resistance

Fosfomycin retains its effectiveness against a significant proportion of both Gram-negative and Gram-positive bacteria. It has shown activity against multidrug-resistant (MDR) pathogens such as methicillin-resistant *S.aureus* (MRSA), vancomycin-resistant *Enterococcus* (VRE), extended-spectrum β -lactamase (ESBL)-producing *Enterobacteriaceae*, and carbapenemase-producing *Enterobacteriaceae* (see Table 1)¹⁰⁸. However, various resistance mechanisms have been identified (Figure 20). Some bacteria possess inherent resistance to fosfomycin, including *Chlamydia spp.*, *Vibrio fischeri*, and *M. tuberculosis*, which can continue to grow even in the presence of high concentrations of the drug¹⁰⁹. Moreover, acquired resistance mechanisms that can potentially be transferred between bacteria are increasingly being reported. The existence of hetero-resistant populations has also been documented.

Table 1. Mechanisms of fosfomycin resistance¹¹⁰.

Mechanism of resistance	Bacterium
Inherent resistance	
Cysteine to Aspartate change in the active site of MurA	<i>Mycobacterium tuberculosis</i> <i>Chlamydia trachomatis</i> <i>Vibrio fischeri</i>
Existence of recycling pathways in peptidoglycan synthesis that MurA does not participate	<i>Pseudomonas putida</i> <i>P. aeruginosa</i> <i>C. trachomatis</i>
Acquired resistance	
Mutations in the structure of glpT and uhpT	<i>Escherichia coli</i>
Modification in the uhpA gene → decreased expression of uhpT	<i>E. coli</i>
Alterations in the ptsI & cyaA genes → reduction of intracellular levels of cAMP	<i>E. coli</i>
New amino acid substitutions in MurA (Asp369Asn & Leu370Ile)	<i>E. coli</i>
Overexpression of MurA & alterations lead to low affinity between enolpyruvyl transferase and fosfomycin	<i>E. coli</i>
FosA, FosA2, FosA3, FosA4, FosA5, FosA6 (Plasmid-borne resistance)	<i>Enterobacteriaceae</i>
FosB (Plasmid-borne resistance)	<i>Staphylococcus spp.</i> <i>Enterococcus spp.</i> <i>Bacillus subtilis</i>
FosX (Plasmid-borne resistance)	<i>Listeria monocytogenes</i>
FosC (Plasmid-borne resistance)	<i>P. syringae</i>
FomA & FomB (kinases)	<i>Streptomyces spp.</i>

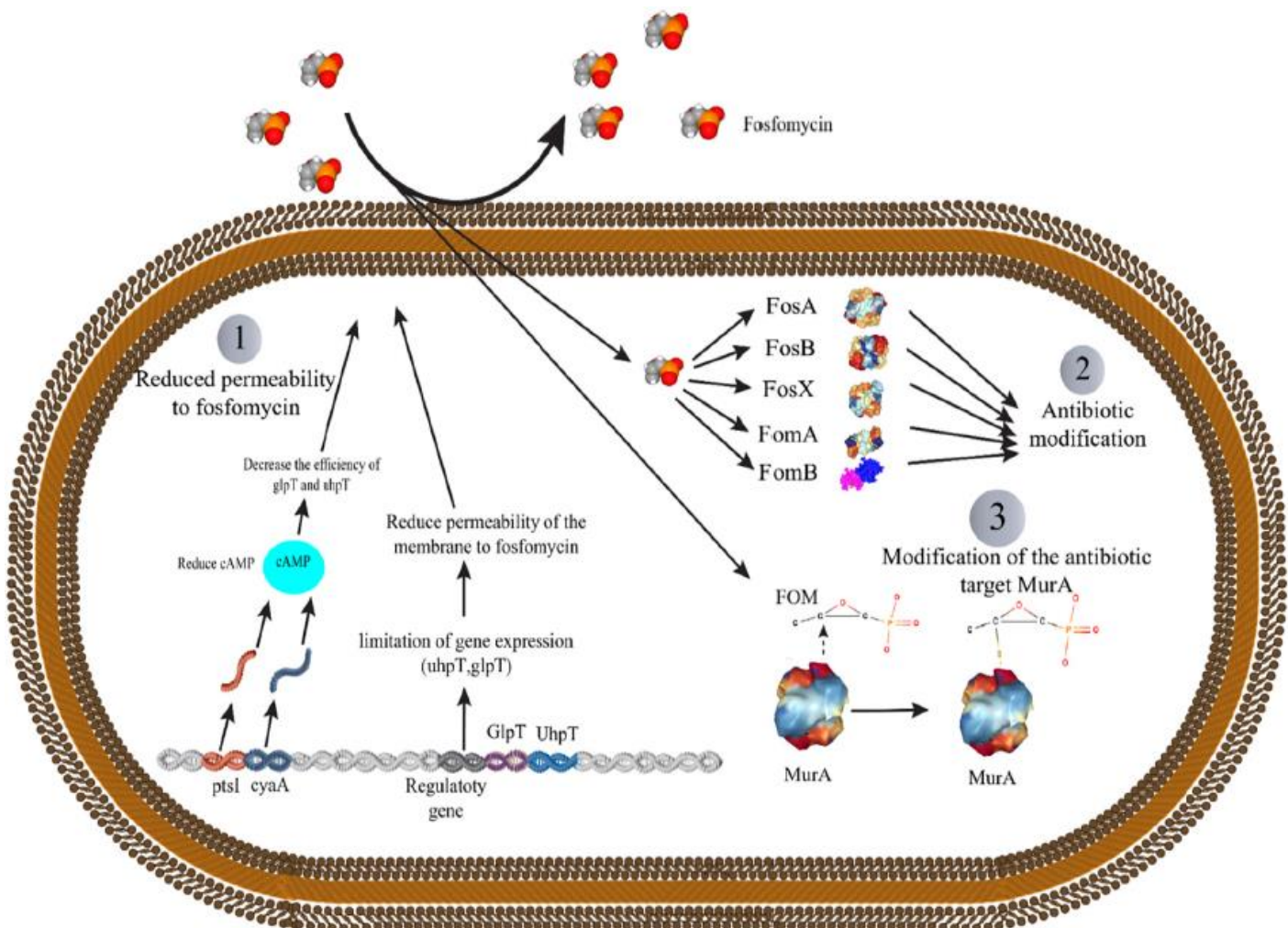


Figure 20: Mechanisms of fosfomycin resistance; 1. Reduced permeability to fosfomycin, 2. fosfomycin- modifying enzymes, and 3. modification of the MurA active site cysteine residue by fosfomycin(Taken from reference 117)¹¹⁷.

1.8.3.1.1 Inherent Resistance

In terms of inherent resistance mechanisms, it has been observed that mutations in the MurA gene can confer resistance to fosfomycin. These mutations led to a structural change in the active site of MurA, replacing cysteine-115 with aspartate, which prevents fosfomycin from binding to MurA.

Regarding chlamydial MurA, it has been suggested that its enzymatic role is limited to specific stages of the chlamydial life cycle, such as the conversion of elementary bodies (EBs) to reticulate bodies (RBs) and early cell differentiation. During these stages, the optimal pH conditions in the inclusion promote MurA activity, which diminishes as the environment changes during cell development ¹⁰⁹.

Recent studies have indicated the presence of recycling pathways for peptidoglycan synthesis in bacteria like *Pseudomonas putida* and *P. aeruginosa*, instead of relying solely on de novo biosynthesis. These pathways involve enzymes such as anomeric cell wall amino-sugar kinase (AmgK) and a uridylyl transferase (MurU), which convert N-acetylMuramic acids (MurNAc) into uridine diphosphate (UDP)-MurNAc by utilizing MurNAc a-1-phosphate. This bypasses the de novo synthesis of UDP-MurNAc, the target of fosfomycin action¹¹¹. Chlamydia has also been proposed to have the ability to recycle peptidoglycan during later stages of their development cycle, reducing the essentiality of chlamydial MurA during their transition into more advanced forms¹⁰⁹.

An interesting phenomenon has been observed in *L.monocytogenes*, where it exhibits resistance to fosfomycin *in vitro* but susceptibility *in vivo*. The bacterium is unable to uptake the antibiotic *in vitro*, but during infection or *in vivo* conditions, it expresses the glucose-6-phosphate permease Hpt, which allows for fosfomycin uptake and renders *L. monocytogenes* susceptible to the drug¹¹².

A newly discovered gene called *abrp* has been found to confer decreased susceptibility to fosfomycin in *A. baumannii*. This gene, located in the chromosome, is also associated with decreased susceptibility to tetracyclines, tigecycline, and chloramphenicol. The *abrp* gene is essential for bacterial growth, and its deletion leads to a 17% reduction in growth rate¹¹³.

1.8.3.1.2 Acquired resistance: fosfomycin transportation.

Bacteria can acquire resistance to fosfomycin through genetic mutations in specific genes, namely GlpT and UhpT, which encode membrane transporters responsible for transporting essential substances like glycerol and carbohydrates. These substances are necessary for bacterial metabolism and virulence, particularly in bacteria such as *E. coli*. Fosfomycin exploits the same transporters to gain access to bacterial cells. Consequently, these mutations impede the penetration of fosfomycin into the bacteria. The absence of certain parts of the *uhp* region, like *uhpA*, is believed to diminish the effectiveness of bacterial transportation systems¹¹⁴. The *uhpA* gene encodes a response regulator protein that plays a crucial role in activating the *uhpT* promoter transcriptionally. Hence, modifications in the *uhpA* gene result in reduced expression of *uhpT*. Additionally, changes in the *ptsI* and *cyaA* genes lead to decreased levels of cAMP within the bacterial cells. This, in turn, causes a decrease in the expression of GlpT and UhpT transporters, resulting in lower uptake of fosfomycin by the bacteria^{115,116}.

Mutations in the *ptsI* and *cyaA* genes can also hinder the biosynthesis of bacterial pili, which are structures that aid in the survival and multiplication of bacteria in the urinary bladder. The reduction in pilus biosynthesis limits the bacteria's ability to adhere to uroepithelial cells. These findings may explain the diminished virulence of fosfomycin-resistant bacteria in urinary-tract infections¹¹⁷.

1.8.3.1.3 Acquired resistance: MurA related.

Originally, a mutation was observed in *E. coli* MurA, where cysteine at position 115 was replaced by aspartate. This mutation rendered susceptible strains highly resistant to fosfomycin¹¹⁸. Additionally, other amino acid substitutions in MurA, such as Asp369Asn and Leu370Ile, have also been linked to fosfomycin resistance¹¹⁴. When specific substances that promote bacterial growth are present, there is an increased transcription of MurA, resulting in fosfomycin resistance with a lower impact on the overall fitness of the bacteria compared to permeability mutants¹¹⁹.

1.8.3.1.4 Acquired resistance: Antibiotic modification.

Resistance to fosfomycin can occur through the acquisition of plasmid-encoded genes that render the antibiotic ineffective. These genes belong to the glyoxalase superfamily and are referred to as plasmid-mediated Fos enzymes¹²⁰. The first described mechanism involves a metalloenzyme called glutathione *S*-transferase, encoded by the *FosA* gene¹²¹. This enzyme utilizes manganese (Mn^{+2}) and potassium (K^{+}) as cofactors. It inactivates fosfomycin by opening the antibiotic's epoxide group and subsequently attaching the sulfhydryl group of cysteine from the tripeptide glutathione (GSH) to the C1 position of the fosfomycin molecule's epoxide ring (Figure 21)¹²². The *FosA* gene is commonly found in Enterobacteriaceae, *Pseudomonas spp.*, and *Acinetobacter spp.*¹²¹. Recent research has identified new subtypes of *FosA*, including *FosA2*, *FosA3*, *FosA5*, and *FosA6*, each sharing similarities with the original *FosA* gene in their structures¹²³.

Another enzyme in the glyoxalase superfamily, called *FosB*, also confers resistance to fosfomycin. While *FosB* shares 38% amino acid identity with *FosA*, it differs from *FosA* in its dependence on magnesium (Mg^{+2}) as a cofactor and its utilization of L-cysteine as the thiol donor. *FosB* catalyzes the addition of either L-cysteine or bacillithiol (BSH) to fosfomycin, resulting in a modified compound that lacks bactericidal properties (Figure 21)¹²⁴. The expression of *FosB* requires the extracytoplasmic sigma factor SigW, which plays a prominent

role in inducible resistance to antimicrobial compounds¹²⁵. FosB is mainly expressed in Gram-positive bacteria and is either plasmid-encoded (in *Staphylococcus spp.* and *Enterococcus spp.*) or chromosomally encoded (in *Bacillus subtilis*)¹²⁶.

Another enzyme, FosX, is a hydrolase that shares sequence similarities of around 30-35% with FosA and FosB¹²⁷. It is a manganese-dependent enzyme encoded by chromosomal genes found in *Listeria monocytogenes*, as well as in other bacteria such as *Mesorhizobium loti*, *Clostridium botulinum*, and *Brucella melitensis*¹²⁸. FosX renders fosfomycin inactive by adding water to the C1 position of the fosfomycin molecule and opening its epoxide ring, similar to other Fos enzymes (Figure 21)¹²⁹.

Finally, in fosfomycin-producing bacteria like *Streptomyces wedmorensis* and *Streptomyces fradiae*, kinases provide protection against the bactericidal effects of fosfomycin¹³⁰. The fomA gene catalyzes the phosphorylation of fosfomycin to fosfomycin monophosphate, while the fomB gene converts fosfomycin monophosphate to fosfomycin diphosphate (Figure 21). Both reactions require ATP and magnesium (Mg^{+}) and occur at binding sites similar to those of eukaryotic kinases¹³¹. Notably, the fomA gene shares 25.8% identity with the fosC gene produced by *Pseudomonas syringae*. FosC exhibits similar activity by converting fosfomycin to fosfomycin monophosphate¹³⁰.

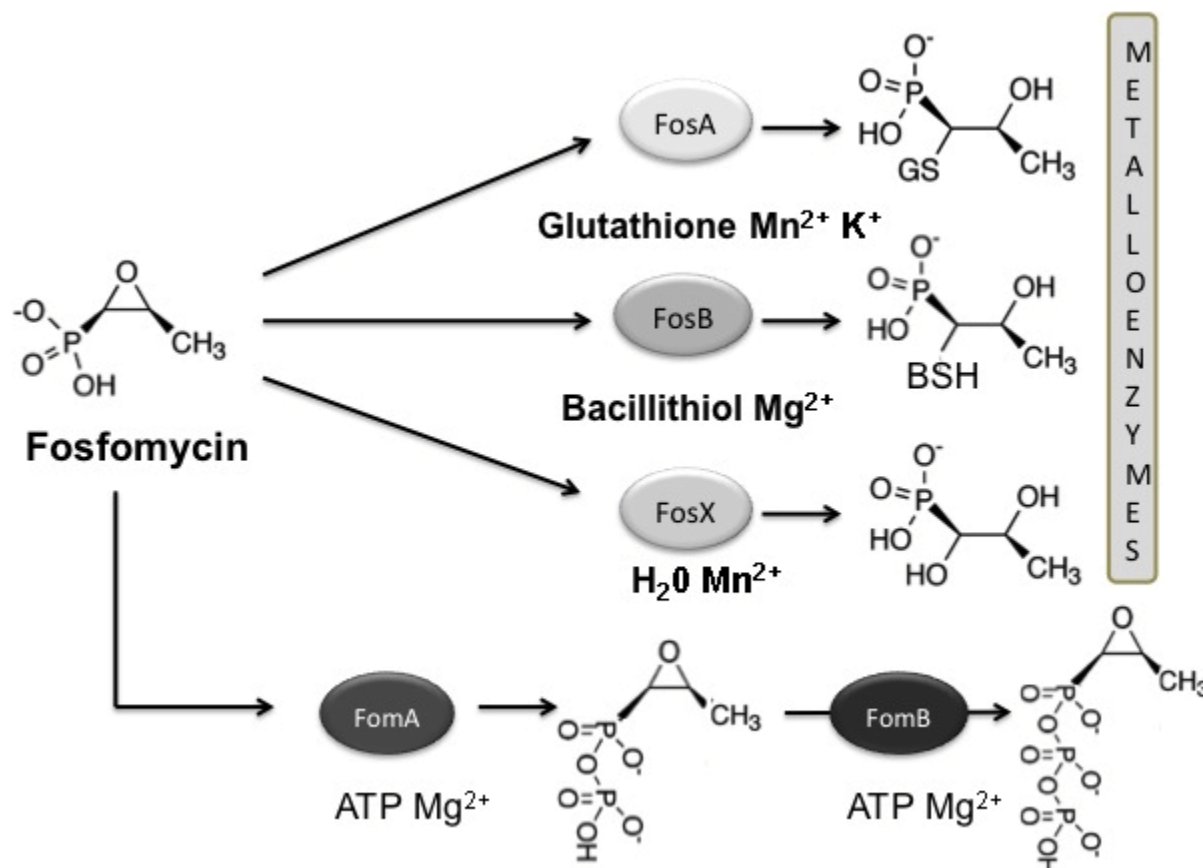


Figure 21: Reactions catalysed by Fos metalloenzymes and fosfomycin kinases. Fosfomycin-inactivating enzymes modify the antibiotic, rendering it inactive by opening the oxirane ring (metalloenzymes) or by phosphorylation (fosfomycin kinases)¹³².

1.9 MurA inhibitors

As discussed earlier, the only approved antibiotic targeting MurA is fosfomycin. However, various research groups have conducted screening campaigns to identify MurA inhibitors. These campaigns have yielded several low micromolar inhibitors, which will be discussed in detail in the following sections. MurA is highly conserved across bacteria and plays a crucial role in cell survival. One of the major benefits of targeting MurA is that it lacks a human homolog, making it an ideal target for drugs¹³³. Therefore, developing a MurA inhibitor that is active against both fosfomycin-susceptible and fosfomycin-resistant variants is a promising area of research.

1.9.1 Benzothioxalone derivatives

New benzothioxalone derivatives **1**, **2** and **3** have been identified as MurA inhibitors by Miller and co-workers using high-throughput screening. Furthermore, by determining the IC_{50} value of MurA from *E. coli*, these hits were validated and they showed high potency with values ranging from 0.25 to 18.54 μM (Figure 22)¹³⁴.

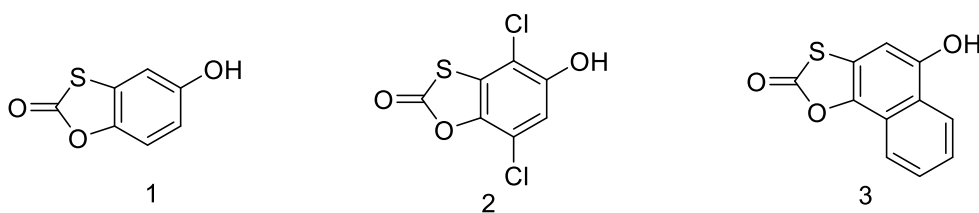


Figure 22: Benzothioxalone derivatives

1.9.2 Pyrazolopyrimidine, Purine Analogues and Cyclic Disulfide

Baum and co-workers have identified three novel inhibitors of MurA from *E. coli* using High throughput screening, a pyrazolopyrimidine (**4**) a purine analogue (**5**) and cyclic disulfide (**6**) with an IC_{50} values ranging from 0.2 to 0.9 μ M (Figure 23). Mass spectrometry and ultrafiltration implied that the compounds do not bind covalently but rather they bind tightly to MurA at or near the active site. Compounds **5** and **6** showed irreversible inhibition while Compound **4** showed reversible pattern of inhibition¹³⁵.

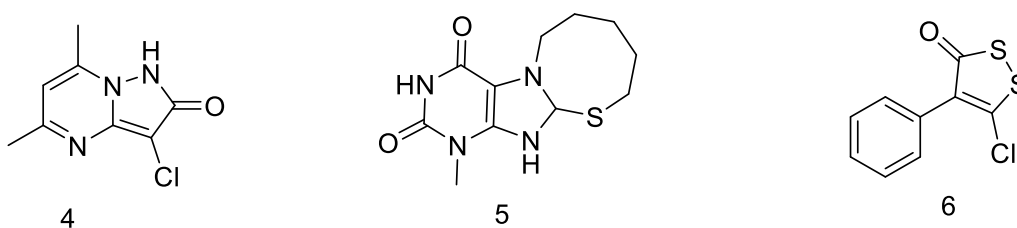


Figure 23: pyrazolopyrimidines, purine derivatives and cyclic disulfide.

1.9.3 Sulfoxyloxy anthranilic acid derivatives

Eschenburg and co-workers have discovered two Sulfoxyloxy anthranilic acid derivatives **T6361** (**7**) and **T6362** (**8**) as MurA inhibitors with IC_{50} values in the sub micromolar range by HTS. It was revealed that both compounds act by competitive pattern of inhibition with UNAG by the steady-state kinetics of MurA. Interactions performed by both compounds from the docking results are shown in Figure 24.

It is demonstrated that compound **7** inhibits MurA transition from the open to the closed form by using the fluorescence data together with the crystal structure of the MurA-T6361 (Figure 25). These two compounds are considered a novel class of MurA inhibitors as they show time dependent inhibition and consequently show reversible mode of action, which is a novel mechanism of action.¹³⁶.

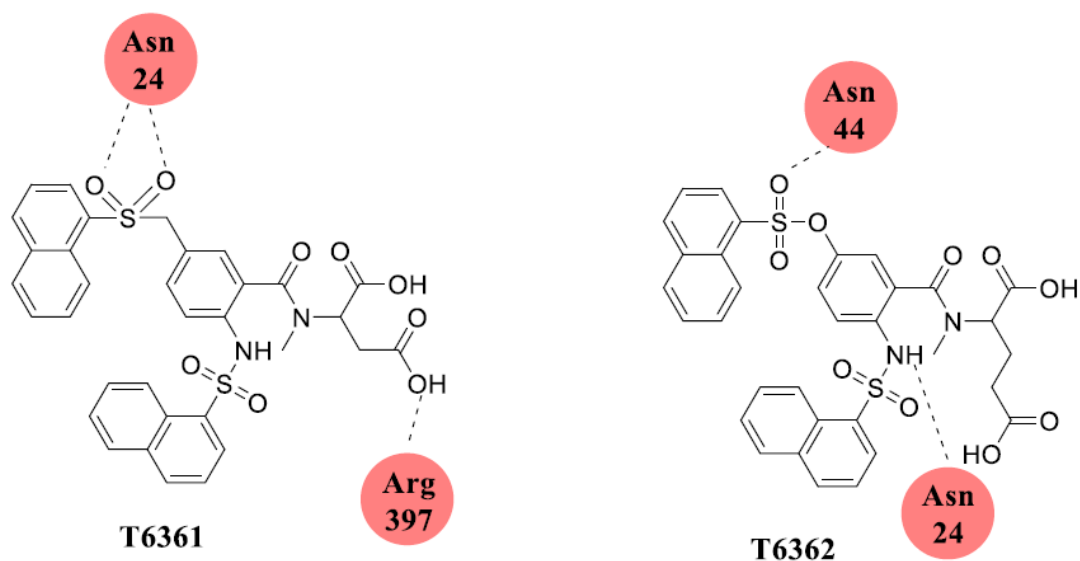


Figure 24: Interaction of 5-sulfonyloxanthranilic acid derivatives T6361 and T6362 with Mtb-MurA enzyme.

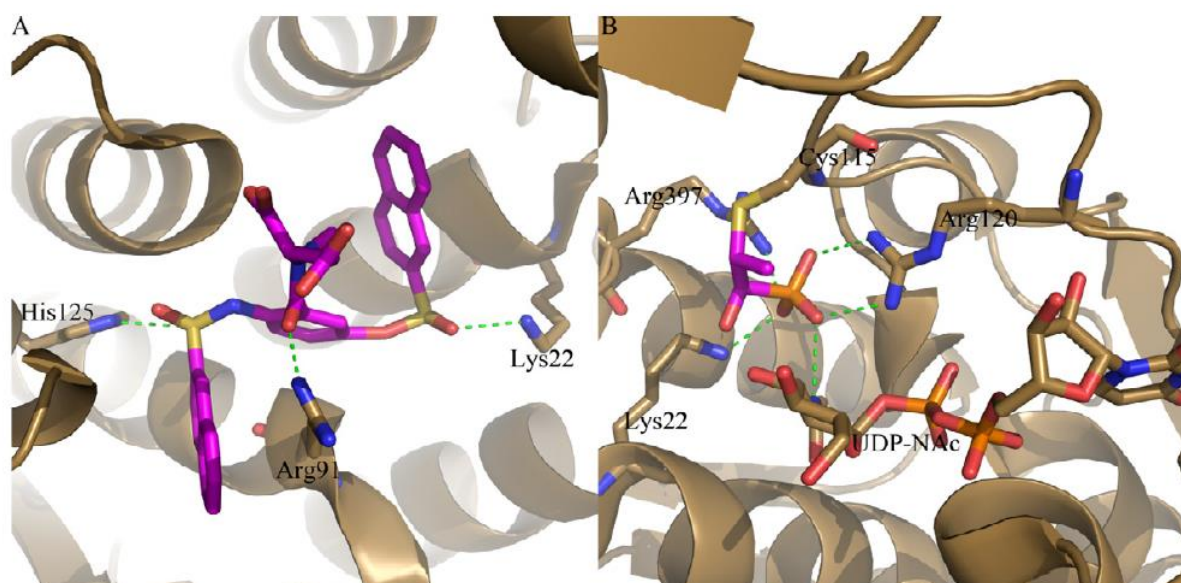


Figure 25: A: Binding mode of compound 4 (the MurA-T6361 complex, pdb code 1YBG) to MurA; B: Binding mode of fosfomycin in the active site of MurA (pdb code 3KR6).

1.9.4 Peptidomimetics

Kumar and co-workers⁸⁵ discovered peptidomimetics compounds as MurA inhibitors. Two peptidomimetics libraries, Asinex containing 11,310 compounds and ChemDiv containing 12,554 compounds were used to conduct virtual screening against Mtb MurA active site residues. The virtual screening was performed based on Lipinski rule of five, HTVS, SP, and XP mode docking, resulting the top 10 hit compounds from each library. From the 20 hits, the top-four compounds (ChemDiv: D675-0217(-8.518 kcal/mol); D675-0102(-8.54 kcal/mol),

Asinex: BDE 26717803 (−9.119 kcal/mol); BDE25373574 (−9.842 kcal/mol)), were selected based on their binding energies, docking scores and interactions with catalytic site amino acid residues (Figure 26).

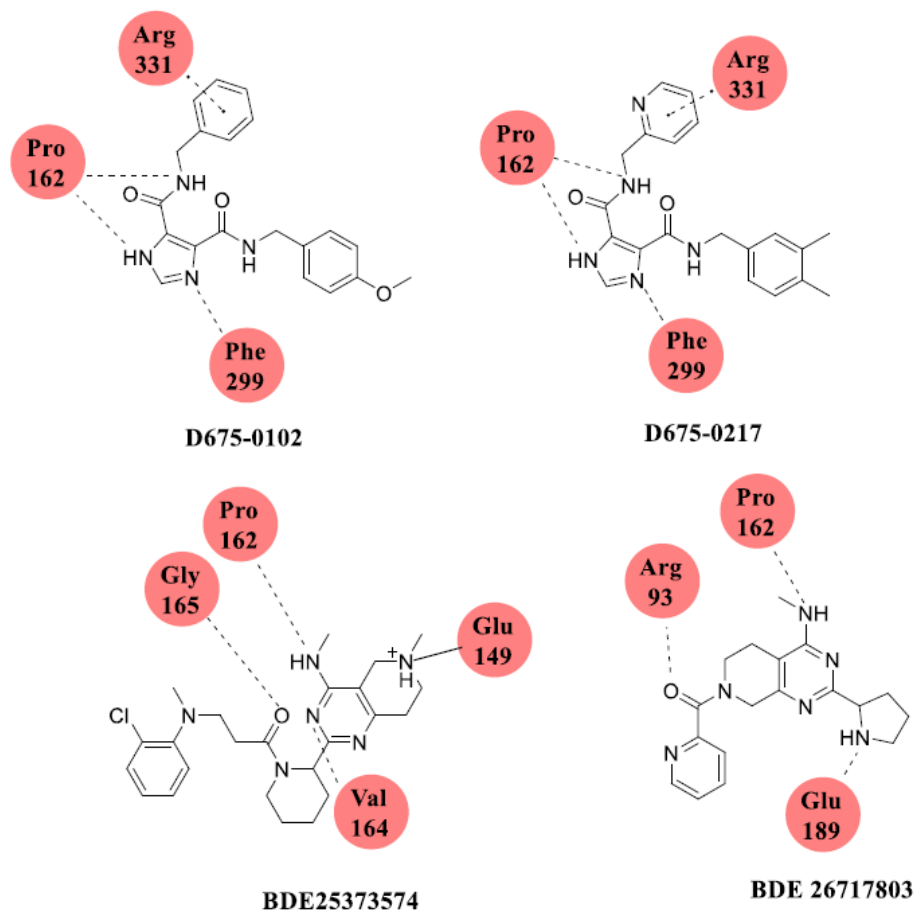


Figure 26: Chemical structure and binding interaction of D675-0102, D675-0217, BDE25373574 and BDE 26717803 with Mtb MurA enzyme.

1.9.5 Imidazole and Diaryl Methane Derivatives

Miller and co-workers have identified two compounds **9** and **10**, as shown in Figure 27, which are derivatives of substituted imidazole and diarylmethane and respectively, were discovered using a whole-cell PG synthesis assay and found to show successful inhibition of PG biosynthesis. Out of these two, only compound **9** was found to be active against MurA (IC₅₀ value of 6 μM). Time-dependent inhibition and antibacterial action was shown by compound **9** but it required pre incubation with UNAG. High concentration of compound **9** (>32.3 μg/mL) was required to show the antibacterial activity, which was the main problem associated with compound **9**. However, this problem is solved by structural modification of the compound **9**¹³⁴.

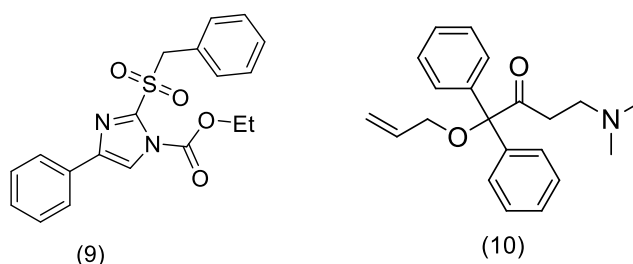


Figure 27: Imidazole and diaryl methane derivatives.

1.9.6 Aminotetralone derivatives

Schönbrunn and co-workers discovered two novel MurA inhibitor compounds **11** & **12** through HTS. The two compounds inhibited *E. coli* MurA with IC_{50} values of 3.1 and 8.5 μ M, respectively. SAR studies reveals that the α - amino ketone moiety is essential for the inhibitory action. Unfortunately, both of the compounds **11** & **12** (Figure 28) were involved in inactivation of two mammalian enzymes, *i.e.*, chymotrypsin and malate dehydrogenase and therefore they are not promiscuous inhibitors.^{137,138}

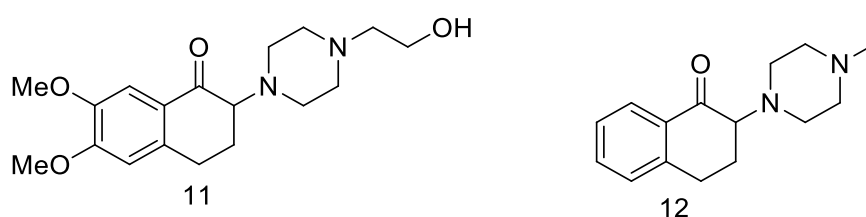


Figure 28: Aminotetralones derivatives.

1.9.7 Sesquiterpene lactone derivatives

Cynaropicrin **13** and Cnicin **14** are two potent natural inhibitors of MurA belonging to class sesquiterpene lactones. The two compounds inhibited *E. coli* MurA with IC_{50} values of 16.7 and 19.5 μ M respectively and *P. aeruginosa* MurA (IC_{50} =of 10.3 and 12.1 μ M, respectively). SAR studies revealed that the ester side chain of Cynaropicrin (**13**) and Cnicin (**14**) is essential for the inhibitory action (Figure 29)¹³⁶.

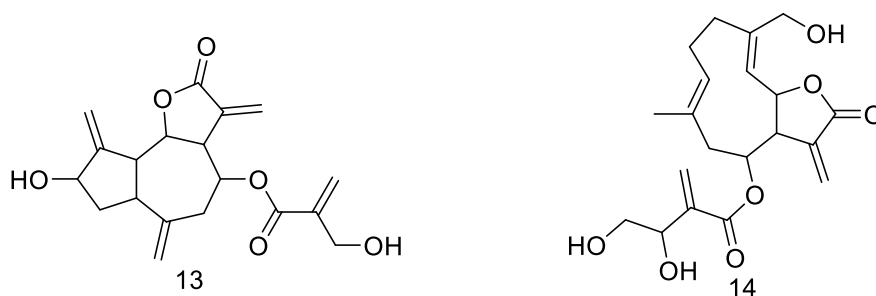


Figure 29: Sesquiterpene lactone derivatives.

1.9.8 Miscellaneous.

1.9.8.1 Thimerosal, Thiram, and Ebselen

Thimerosal (**15**), Thiram (**16**), and Ebselen (**17**) as shown in Figure 30 were reported to show inhibitory action against *H. influenza* MurA (IC₅₀ values, 0.1 to 0.7 μM) during a chemical library screening. Structurally they differ from fosfomycin as Thimerosal is an ethyl(2-mercaptobenzoato-*S*) mercury sodium salt, Thiaram is a 1-(dimethylthiocarbamoyldisulfanyl)-*N,N*-dimethyl-methanethioamide and Ebselen consists of benzoisoselenazolone moiety.¹³⁸

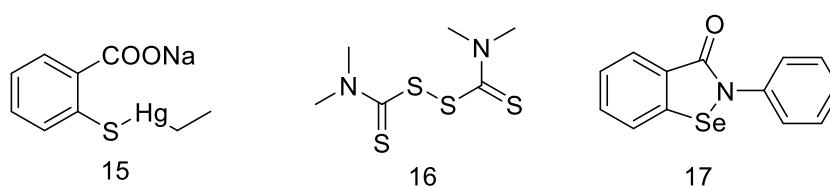


Figure 30: Thimerosal, Thiram and Ebselen.

1.9.8.2 Tulipalines, Tuliposides, and their Derivatives

Ubukata and colleagues synthesized 1-tuliposide B (**18**) and 6-tuliposide B (**19**), in addition to other compounds in the tulip class such as tulipaline A (**20**) and tulipaline B (**21**) as shown in Figure 31. Structure–activity relationship (SAR) studies have indicated that the presence of a 3', 4'-dihydroxy-2' methylenebutanoate (DHMB) moiety is responsible for the inhibitory activity of these compounds. Cnicin (**14**), a potent natural inhibitor of MurA belonging to the class of sesquiterpene lactones, also contains a DHMB moiety and likely acts through a similar mechanism as the tulip derivatives^{139,140}.

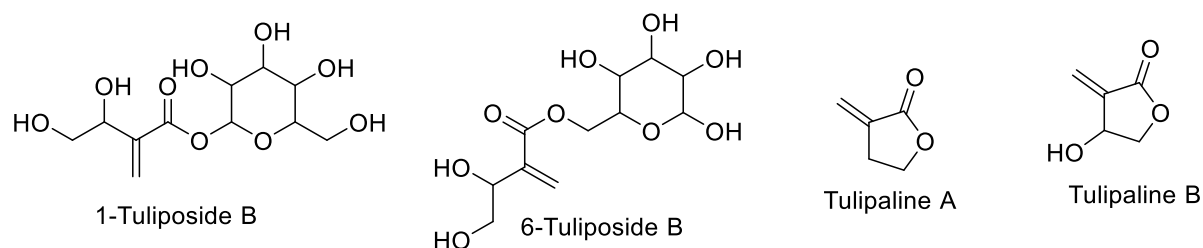


Figure 31: Tulipalines, tuliposides and their derivatives.

1.9.8.3 Terreic acid

Aspergillus terreus is a fungus that produces the metabolite terreic acid (**22**, Figure 32), which has been reported to inhibit both *E. coli* MurA and *E. cloacae* MurA. Structurally, terreic acid exhibits many similarities to fosfomycin, including the presence of an epoxide ring and the requirement for UNAG for activity. Additionally, both compounds covalently bind to the thiol group of Cys115 near the active site of MurA. Despite these similarities, terreic acid is approximately 50 times less potent than fosfomycin as an inhibitor of MurA. One key difference between the two compounds is the conformation of MurA to which they bind: terreic acid binds to the open conformation, while fosfomycin binds to the closed conformation¹⁴¹.

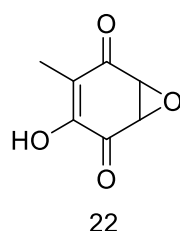


Figure 32: Terreic acid.

1.9.8.4 Avenaciolides

Recently, four avenaciolide derivatives (**23–26**) as shown in Figure 33 were isolated from *Neosartorya fischeri* and demonstrated significant antimicrobial activity against MRSA. SAR studies have indicated that the presence of an alpha, beta-unsaturated carbonyl group is critical for the antibacterial activity of these compounds. These avenaciolide derivatives exhibited high potency against MRSA and fosfomycin-resistant bacteria, suggesting their potential utility in addressing the challenges posed by antibiotic resistance.¹⁴².

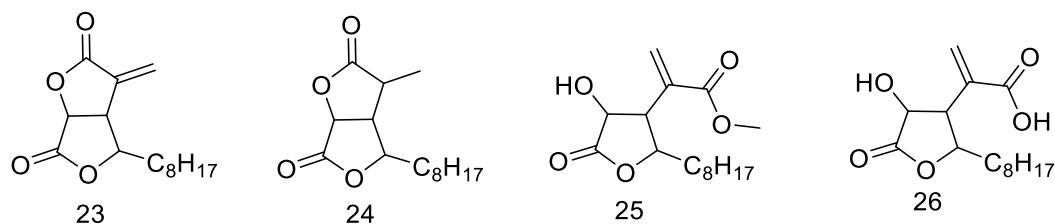


Figure 33: Avenaciolide derivatives.

1.9.8.5 Oxazepene derivatives

Isa et al¹⁴³. utilized a combination of virtual screening and homology modeling to identify potential inhibitors of Mtb-MurA, a protein for which no experimental crystal structure is available in the Protein Data Bank (PDB). To create a 3D model of Mtb-MurA, the team first used the NCBI protein sequence (Accession Number: NP 215831.1) and BLASTp to identify six protein structure templates with high sequence similarity to MurA. Of these, the 3SG1 template was chosen for its high resolution and structural conservation, and Modeller9v16 was used to generate ten models of MurA. The model with the lowest Discrete Optimized Protein (DOPE) value was chosen and subjected to energy minimization through molecular dynamics (MD) simulation. The resulting Mtb-MurA structure consisted of 418 amino acids, with Arg93, Asp305, and Val327 located in the binding site for UNAG and Asp117 participating in direct catalysis and C-3 protonation of phosphoenol pyruvate. Inhibition of these residues can disrupt the normal function of MurA. To identify potential ligands with binding affinity for the enzyme, the team used PyRx 8.0 and the RASPD to perform virtual screening of public databases, yielding 7526 ligands. These compounds were filtered based on pharmacokinetic and physicochemical properties and subjected to a molecular docking analysis. The top four ligands, as determined by binding energy ranging from 10.73 to 8.17 kcal/mol, were ZINC20256175 (10.66 kcal/mol), ZINC12283251 (10.58 kcal/mol), ZINC14538153 (9.90 kcal/mol), and ZINC12217441 (9.73 kcal/mol) (Figure 34).

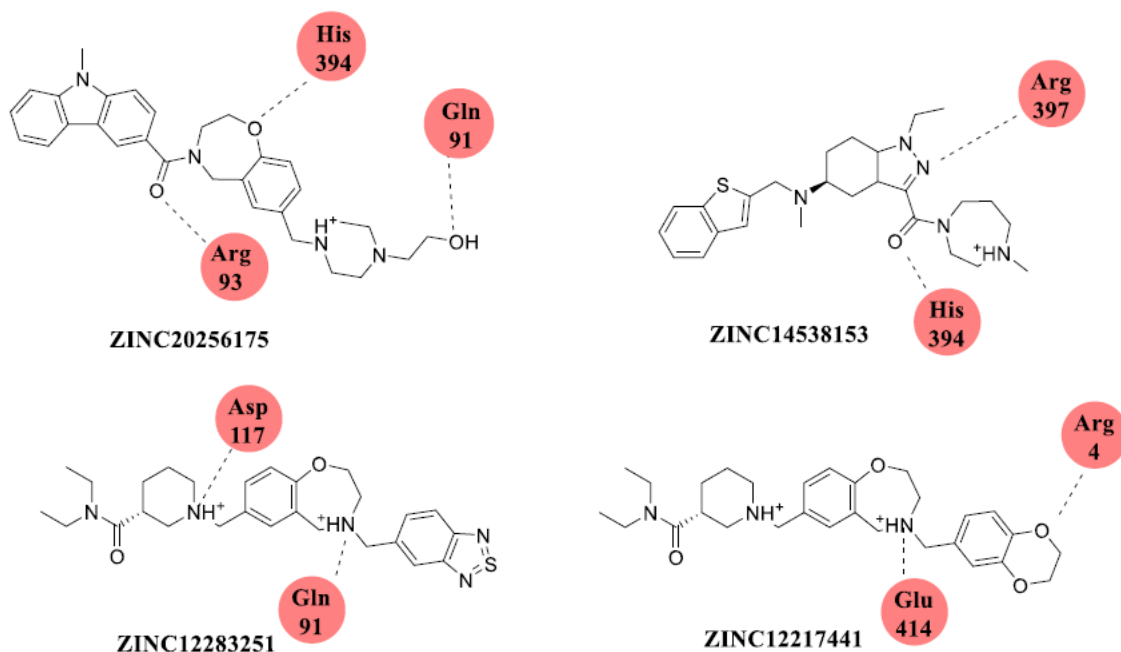


Figure 34: Binding mode of ZINC20256175, ZINC12283251, ZINC14538153 and ZINC12217441 in modeled structure of Mtb-MurA enzyme.

1.9.8.6 Bromo-cyclobutenaminones

In this study, a new family of covalent inhibitors targeting the antibacterial enzyme MurA was developed. The researchers modulated the reactivity of four-membered rings, leading to the identification of bromo-cyclobutenaminones as new electrophilic warheads (**27**, Figure 35). Screening a small library of cyclobutenone derivatives, the researchers found that the bromine atom played a crucial role in the ligand and that covalent labeling of MurA occurred at Cys115 through net nucleophilic substitution ¹⁴⁴.

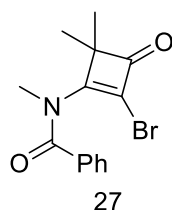


Figure 35: Bromo-cyclobutenaminone derivative.

1.9.8.7 Bromobenzimidazole, benzylidene carboximidamide

Molecular docking-based virtual screening of 1.412 million compounds from three databases was employed to identify potential inhibitors of the essential enzyme MurA, a drug target for antibiotics. Among the top thirty-three compounds, 2-Amino-5-bromobenzimidazole (**28**, Figure 36) showed growth inhibition in both *Listeria innocua* and *Escherichia coli*, with the

same Minimum Inhibitory Concentration (MIC) value of 0.5 mg/mL. Compound 2-[4-(dimethylamino)benzylidene]-n-nitrohydrazinecarboximidamide (**29**, Figure 36) only had growth inhibition in *L. innocua* with a MIC value of 0.5 mg/mL¹⁴⁵.

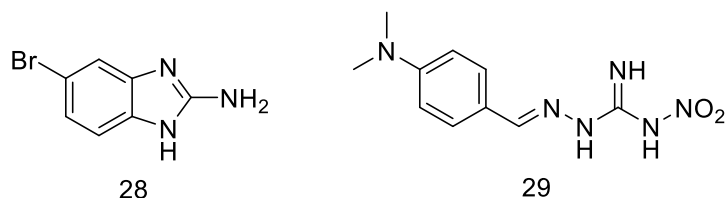


Figure 36: Bromobenzimidazole (**28**) and bezylidine carboximidamide (**29**).

1.9.8.8 Heterocyclic Electrophiles

A new generation of quaternized heterocyclic electrophiles, based on a covalent fragment library, has been developed as potential inhibitors of the antibacterial target MurA (**30** and **31**, Figure 37). The N-methylated heterocycles were found to have improved reactivity and inhibitory potency, as demonstrated through quantum chemical reaction barrier calculations, GSH reactivity assay, and thrombin counter screen¹⁴⁶.

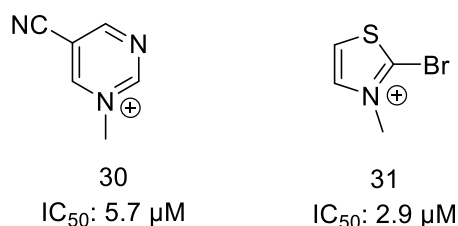


Figure 37: heterocyclic electrophile derivatives.

1.9.8.9 Pyrrolidinediones

A series of reversible pyrrolidinedione-based MurA inhibitors were developed that equally inhibit wild type and fosfomycin-resistant MurA C115D mutant. The most potent inhibitor, compound **32** (IC₅₀ = 4.5 μM), as shown in Figure 38 was analyzed using native mass spectrometry and protein NMR spectroscopy to determine its mode of inhibition. The analysis revealed that it binds to the conformationally open form of MurA when the substrate UNAG is available. Additionally, it was observed that compound **32** can also bind in the absence of UNAG when either fosfomycin or inorganic phosphate is present. This compound class is nontoxic to human cells and stable in human S9 fraction, human plasma, and bacterial cell lysate¹⁴⁷.

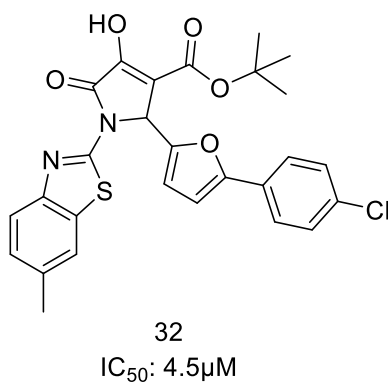


Figure 38: Pyrrolidinedione derivative.

1.9.8.10 Chloroacetamides

The enzyme MurA is a validated target for antibacterial drug discovery, and most inhibitors are small heterocyclic compounds that form a covalent bond with the active site cysteine. A library of 47 fragment-sized chloroacetamide compounds was synthesized, and several *E. coli* MurA inhibitors were identified, with the most potent having an IC₅₀ in the low micromolar range (**33**, Figure 39). The covalent binding of the most potent inhibitor to Cys115 of the digested MurA enzyme was confirmed by LC-MS/MS experiments, and the irreversible and time-dependent mode of action was further investigated by biochemical assays¹⁴⁸.

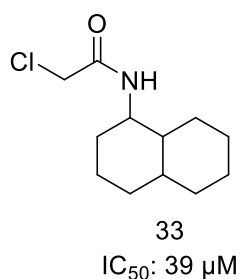


Figure 39: Chloroacetamide derivative.

2. Research Objectives

2.1 Scientific goal

The advent of bacterial resistance to traditional antibiotics has necessitated the identification and development of novel antibacterial agents capable of effectively combating pathogenic microorganisms. Among the various classes of antimicrobials, those that target the biosynthesis of the bacterial cell wall have garnered significant attention due to their ability to disrupt fundamental processes necessary for bacterial survival. In particular, the late stages of peptidoglycan synthesis, including transpeptidation and transglycosylation, have been targeted by drugs such as β lactams¹¹⁸ and vancomycin, respectively. However, the sole clinically utilized agent that targets the early stages of cell-wall synthesis is fosfomycin, which inhibits the enzyme MurA. As the prevalence of antibiotic resistance continues to rise, and the early stages of PG synthesis remain relatively underexplored, the identification of novel targets for antimicrobial drug development is of paramount importance. Mur enzymes present a promising avenue for such investigation, and the successful design and synthesis of MurA inhibitors with potent antimicrobial activity could represent a significant advance in the battle against drug-resistant infections.

2.2 Development of inhibitors against MurA enzyme

MurA enzyme is an interesting target for inhibition, as MurA is the first enzyme in the PG synthetic pathway and by inhibiting this enzyme it will lead to the blockage of the whole cascade and synthetic process. Thus, it is considered as an important target. Throughout our efforts to discover MurA inhibitors to fight bacterial infections, we discovered several Pyrazolidinone derivatives as promising inhibitors of MurA represented by compounds **1** and **2** (Figure 40). This series of pyrazolidinone derivatives could inhibit wild type MurA and the C115D mutant developed by fosfomycin-resistant *E. coli*. Despite the promising activity against MurA, none of the members of this class could reach sub-micromolar inhibition against MurA and no activity was obtained against most Gram-negative bacterial strains. Additionally, these compounds suffer from high logP value as well as synthetic limitations as both rings A and B are obligatory the same, restricting the efforts of structural variations.

2.2.1 Scaffold hopping in Chapter 1

“Scaffold hopping” was employed leading us to imidazolidinone scaffold 3. This scaffold enabled independent modifications of rings A and B which was not possible with the chemistry of compounds 1 and 2. Additionally, the installation of polar hetero-aryls and alicyclic rings simultaneously as rings A and B becomes possible in scaffold 3. Thus, facilitating the process of structure optimization to get more potent compounds against MurA and bacteria. This also aids to improve the logP value of the scaffold.

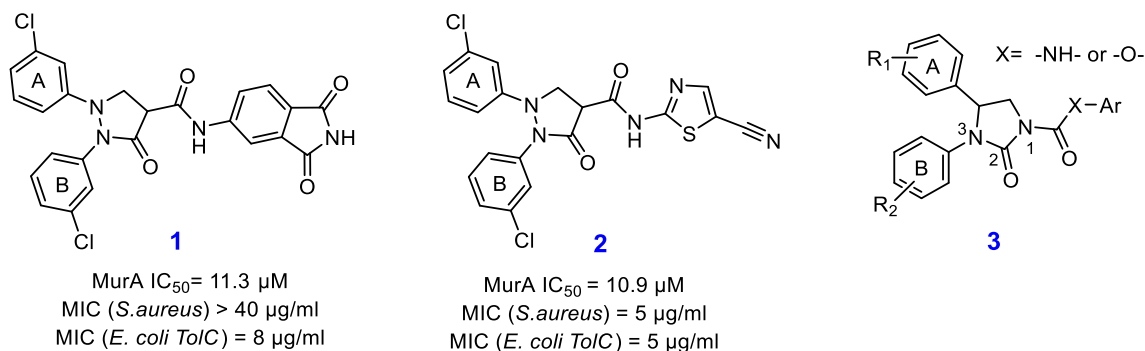


Figure 40: Previously synthesized pyrazolidinone inhibitors (1 and 2) and imidazolidinone scaffold (3)

2.2.2 Structure simplification in Chapter 2

During our investigation into potential inhibitors for MurA, a protein involved in bacterial infections, we identified and developed several imidazolidinone derivatives (Chapter 1), compound 1 and 2 (shown in Figure 41). These derivatives proved to be effective against both the regular MurA protein and a mutated form known as the C115D mutant found in fosfomycin-resistant *E. coli*.

However, the synthesis process for these derivatives was quite complex, requiring a lengthy 6-step procedure outlined in Chapter 1. As a result, we decided to explore the possibility of simplifying the molecular structure while maintaining its effectiveness, in order to expedite the optimization process. In our efforts, we successfully simplified the structure and created new derivatives called triaryl malonamide derivatives 1c and 1d (Figure 41). Moreover, the synthesis of the new derivatives can be accomplished in just three steps, which is more efficient compared to the six-step synthesis required for the imidazolidinone derivatives.

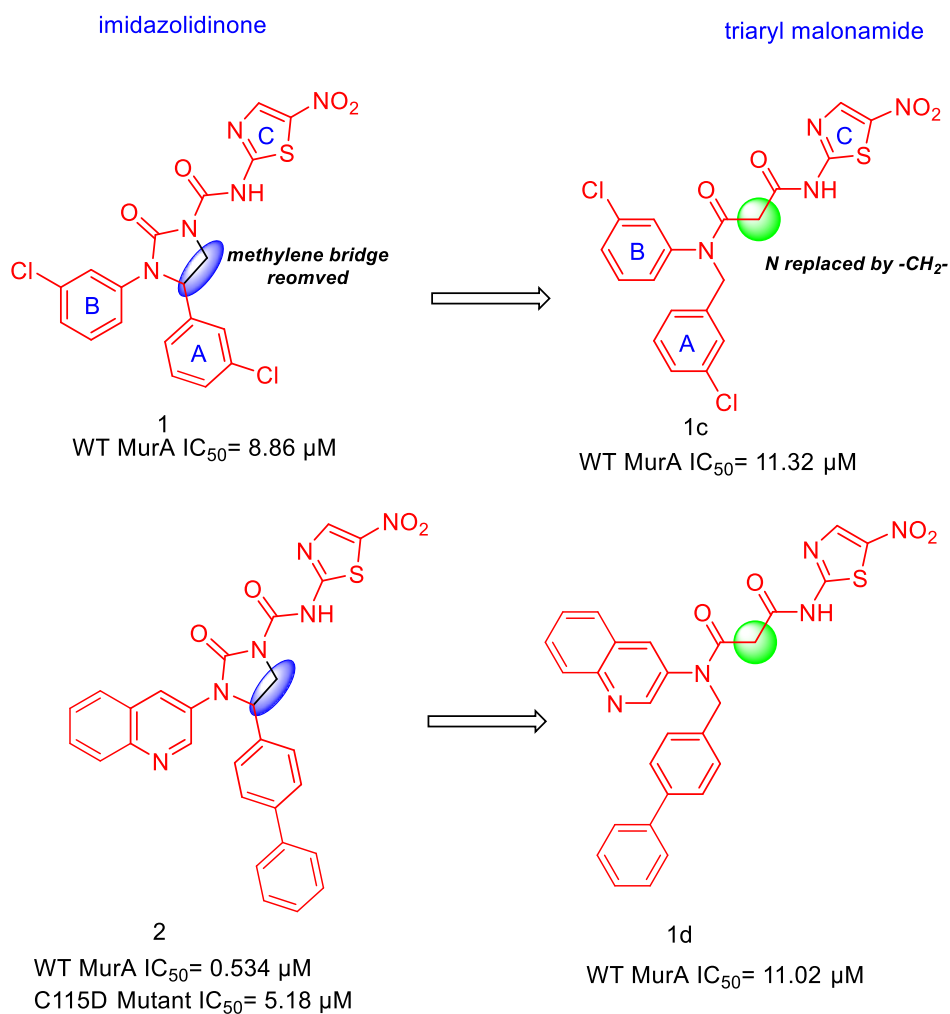


Figure 41: Previously synthesized imidazolidinone inhibitors (1 and 2) and malonamide scaffold (1c and 1d).

In chapter 2, we focused on the 1c and 1d scaffolds, which showed promising activity similar to compounds 1 and 2 as indicated in previous findings (Figure 41). Our choice of these scaffolds was based on the potent effects observed with the ring systems A and B during the investigations outlined in Chapter 1.

2.2.3 HIPS library screening in Chapter 3

The research objectives of this study were to classify HIPS library of 7000 compounds based on their chemical structure, select a subset for screening against MurA, evaluate their drug-likeness and physicochemical properties, apply filtering to minimize false-positive results, and identify promising compounds for further investigation

3. Results and Discussion

3.1 Chapter 1

"Inhibiting Bacterial Cell Wall Biosynthesis: Design and Evaluation of Imidazolidinone Compounds Targeting MurA Enzyme"

Abstract

The development of novel antibiotics targeting early steps of cell-wall PG biosynthesis holds great promise as a strategy for combating bacterial infections. MurA, the first enzyme in this pathway, is typically targeted by the clinically used irreversible inhibitor fosfomycin, but bacterial mutations in its binding site can lead to resistance. The aim of this study is to develop novel antibiotics targeting MurA and evaluate their potential effectiveness. In this study, we report a series of imidazolidinone-based MurA inhibitors that were developed through scaffold hopping from the previous pyrazolidinone scaffold. To optimize the scaffold, we underwent logP-driven optimization and reached various active chemotypes, including imidazolidine-2-one (unsubstituted at position 3), phenyl -2-oxoimidazolidine-1-carboxylate and *N*-imidazolidine-1-carboxamides. The newly developed compounds demonstrated both low logP values and potent inhibition of both wild type (WT) MurA and the fosfomycin-resistant MurA C115D mutant, with IC₅₀ values ranging from 0.534 to 0.881 μM for the most potent compounds. Overall, these findings suggest that the imidazolidinone-based compound class is a promising lead candidate for further development as an effective antibiotic therapy for inhibiting cell-wall synthesis in bacterial infections.

3.1.1 Introduction

The emergence of antibiotic resistance in bacterial populations has led to a need for the discovery of novel classes of antibacterial drugs¹⁻³. One area of focus has been the biosynthesis of peptidoglycan, a structural component of prokaryotic cell walls. Peptidoglycan is a vital component of the cell wall of bacteria, present in both Gram-positive and -negative species. It is the primary target of most antibiotics in clinical use. The bacterial cell wall provides structure and support to the organism, maintains proper osmotic pressure, and protects against lysis, thereby preventing cell death in a hypotonic environment. Therefore, there have been many efforts focused on antibacterial drug discovery by targeting PG biosynthesis. Recently, there has been growing interest in the early cytoplasmic steps of PG biosynthesis as potential targets,

since the established β -lactam antibiotics mainly target the bacterial periplasm, which is more accessible to small molecules and is subject to extensive bacterial resistance⁴. The Mur family of enzymes, which consists of six intracellular enzymes (MurA–F), is responsible for the early steps of PG synthesis. They produce the main cytosolic PG precursor, uridine-5-diphosphate-N-acetylmuramyl-pentapeptide (also known as Park's nucleotide).

MurA, the first enzyme in the cascade, converts UDP-N-acetylglucosamine (UDP-GlcNAc) into UDP-N-acetylglucosamine enolpyruvate (UNAGEP) by adding an enolpyruvate moiety from phosphoenolpyruvate (PEP) as shown in Figure 1.

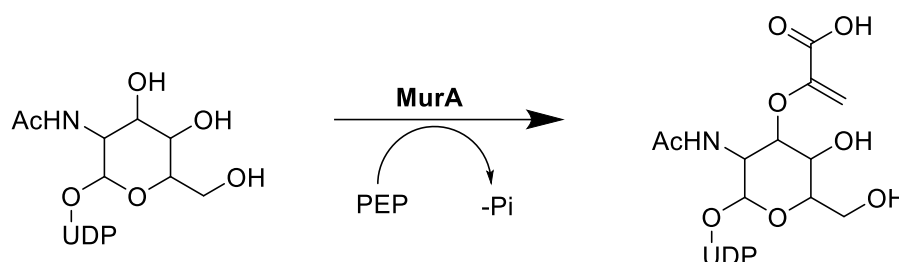


Figure 1: MurA-catalyzed reaction

This enzyme is essential and conserved across both Gram-positive and Gram-negative bacteria, with no mammalian homologue. Therefore, inhibitors directed against bacterial MurA have potential as broad-spectrum antibiotics without affecting human enzymes^{5,6}. Currently, the only approved antibiotic targeting MurA is fosfomycin, which has been used clinically since the early 1970s for the treatment of uncomplicated urinary-tract infections and pediatric gastrointestinal infections caused by Shiga toxin-producing *E. coli* (STEC)⁷. Fosfomycin acts as a PEP analogue and competitively inhibits MurA through covalent alkylation of Cys115, the main catalytic residue involved in PEP binding. However, fosfomycin, like many antibiotics, is not very effective because of multiple mechanisms that led to the development of resistance. These mechanisms include changes in the glycerol-3-phosphate transporter (GlpT) and glucose-6-phosphate transporter (UhpT), modifications to the fosfomycin binding site in MurA, overproduction of the target MurA in bacteria, and the creation of metalloenzymes (FosA, FosB, or FosX) that inactivate fosfomycin. Consequently, it is necessary to develop new inhibitors. This MurA mutant C115D is naturally present in several bacteria, such as *M. tuberculosis*^{8–10}.

The majority of MurA inhibitors that have been published, including fosfomycin, are small heterocyclic compounds that function by creating a covalent connection with the active site

cysteine. Fosfomycin, which is obtained from Actinomyces, is a bactericidal compound that has a reactive epoxide ring and is similar to phosphoenolpyruvate (PEP). RWJ-3981¹¹, cnicin¹², as well as other sesquiterpene lactones¹³, avenaciolides¹⁴, tulipalines¹⁵, benzothioxalone derivatives¹⁶, terreic acid¹⁷ ebselen¹⁸ and more recently, bromocyclobutenaminones¹⁹, all create a covalent link with the thiol group of Cys in the active site of MurA. While targeting the catalytic Cys residue in the active site leads to effective inhibition of MurA, this mechanism also renders most of these compounds inactive against the naturally occurring MurA C115D mutant^{11,13,15,18}.

Therefore, it is of critical importance to identify new scaffolds that specifically inhibit MurA while also demonstrating safety on mammalian cells. In a high-throughput screening campaign, Miller and colleagues identified benzothioxalones as inhibitors of MurA, with IC₅₀ values ranging from 0.25 to 51 μ M. However, these compounds were found to form covalent adducts with Cys115 via a reaction with the cyclic thiocarbonate unit, and consequently binding was not detected with the C115D mutant MurA protein¹⁶. Moreover, the cyclic thiocarbonate motif may also react with other enzymes that have a reactive cysteine in the active site, similar to the aforementioned Michael acceptor-type inhibitors. Another class of reported inhibitors are pyrazolidinediones, which act as dual inhibitors of MurA and MurB (the subsequent enzyme in the peptidoglycan biosynthesis cascade) with MurB as the main target²⁰⁻²². In this study, we report the identification of a di- and tri-arylimidazolidinone scaffold that inhibits MurA without reaction with the key active-site Cys115 residue, resulting in identical inhibitory activities towards the *E. coli* MurA C115D mutant and the wild type MurA enzyme. In addition, the scaffold exhibits improved clogP, which suggests better membrane permeability and potential for oral bioavailability. These findings provide a promising starting point for the development of novel antibacterial agents targeting MurA and highlight the potential of arylimidazolidinone scaffolds as a platform for drug discovery.

3.1.2 Results and Discussion

3.1.2.1 Compounds' design

Throughout our efforts to discover MurA inhibitors to fight bacterial infections, we discovered several pyrazolidinone derivatives as promising inhibitors of MurA presented by compounds **1** and **2** (Figure 2). This series of pyrazolidinone derivatives could equally inhibit wild type MurA and the C115D mutant developed by fosfomycin-resistant *E. coli*. Despite the promising activity against MurA, none of the members of this class could reach submicromolar inhibition against MurA and no activity was obtained against most Gram-negative bacterial strains. Additionally, these compounds suffer from high logP value as well as synthetic limitations as both rings A and B are obligatory the same, restricting the efforts of structural variations²². Thus, “scaffold hopping” was employed leading us to imidazolidinone scaffold **3**. This scaffold enabled independent modifications of rings A and B, which was not possible with the chemistry of compounds **1** and **2**. Additionally, the installation of polar hetero-aryls and alicyclic rings simultaneously as rings A and B becomes possible in scaffold **3**. Thus, facilitating the process of structure optimization to get more potent compounds against MurA and bacteria. This also aids to improve the logP value of the scaffold.

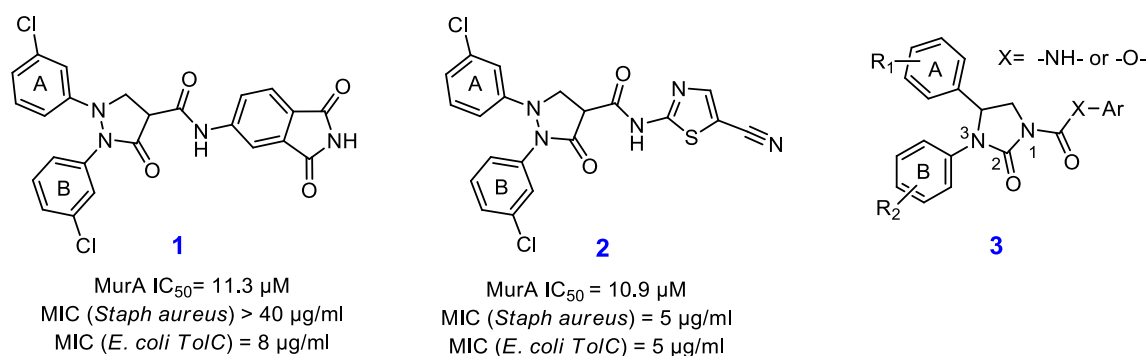


Figure 2: Previously synthesized pyrazolidinone inhibitors (**1** and **2**) and imidazolidinone scaffold (**3**)

Initially, we started the project with the synthesis of imidazolidinone analogues having identical aryl rings to the five most potent compounds from the previously reported pyrazolidinones R1–R5 (Table 1).

Results and Discussion

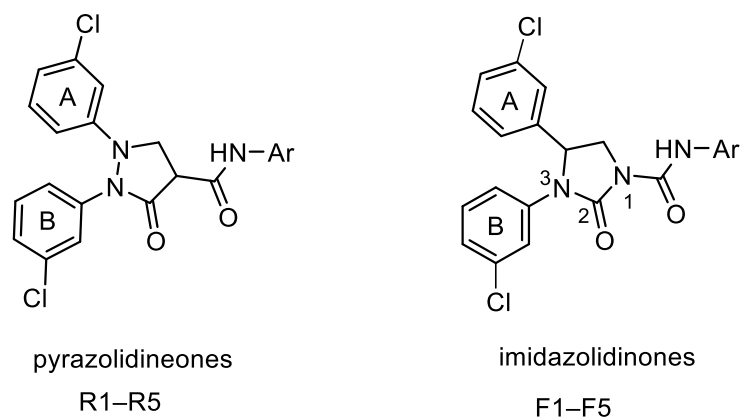
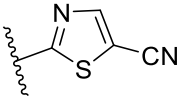
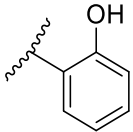
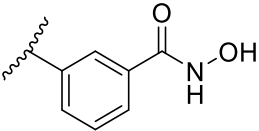
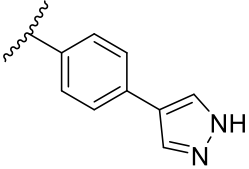
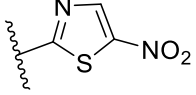


Table 1. MurA inhibition of imidazolidinones versus pyrazolidinones.

Ar	Cpd No.	%inh @50 μM	IC ₅₀ Imidazolidinone	clogP	Cpd No.	IC ₅₀ Pyrazolidinone	clogP
	F1	64.38	21.96	4	R1	10.92	3.4
	F2	67.15	20.22	4.6	R2	12.41	3.92
	F3	81.57	5.67	3.3	R3	4.45	2.21
	F4	90.66	28.34	5.4	R4	12.24	4.50
	F5	78.80	8.86	3.63	R5	9.88	3.90

^aData shown are the mean of at least two independent experiments. clogP values were calculated using ACD Labs software.

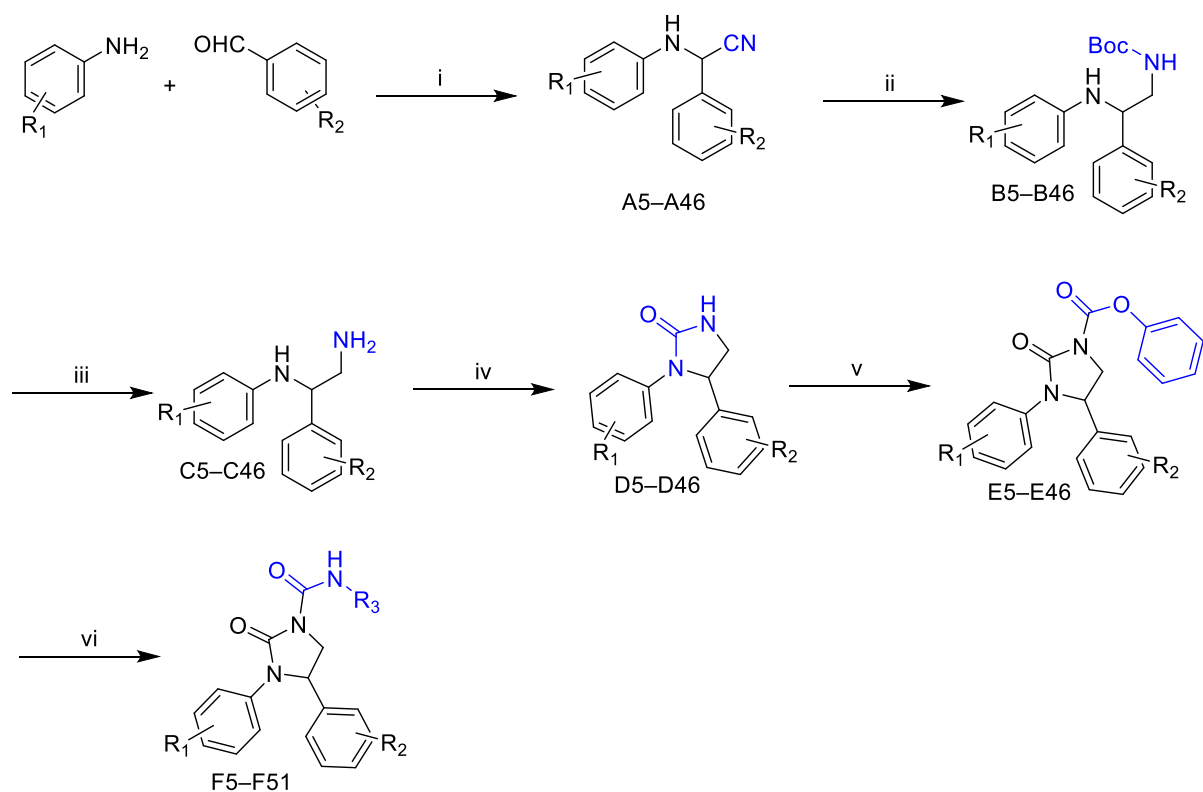
These preliminary results indicate the success of our design concept where all five pilot compounds could show MurA inhibition, with compounds **F3** and **F5** showing comparable

potency to their respective pyrazolidinones. Herein, we report the systematic modification of our newly designed imidazolidinones to optimize their potency against MurA as well as reducing lipophilicity until we reach sub micromolar inhibitors, we also provide evaluation of the antibacterial activity of the most promising MurA inhibitors.

3.1.3 Chemistry

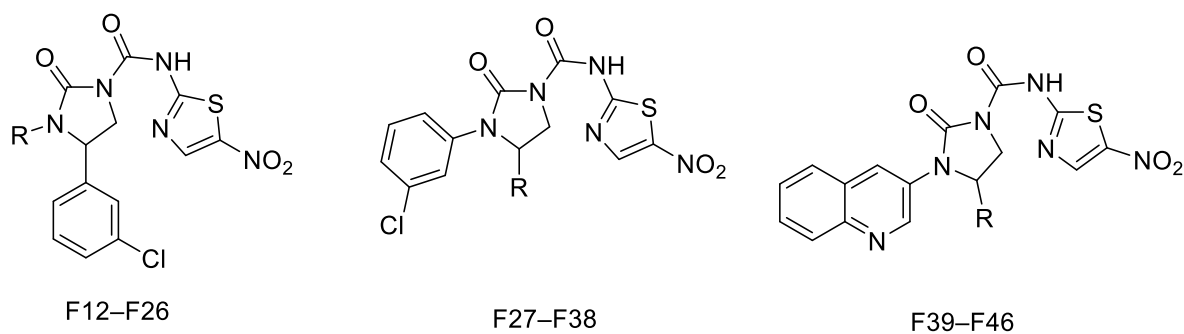
The synthesis of the desired imidazolidinone derivatives (**F1–F51**) was achieved via a six-step sequence as shown in Scheme 1. The procedure started by carrying out a Strecker reaction. The Strecker reaction is a classic organic chemistry reaction that converts an aldehyde or ketone into an α -amino nitrile using aniline, zinc cyanide, and an acid catalyst. The reaction proceeds via the formation of an imine intermediate, which reacts with a cyanide ion to form the α -amino nitrile product²³. A major advantage of this method was that all the aryl amines and aromatic carbaldehydes were usually commercially available in a large variety, which enabled synthesis of diverse analogues. Several amines were reacted with aldehydes in presence of zinc cyanide to furnish the respective aminonitriles (**A5–A46**). Reduction of the α -aminonitriles to the respective amines was done in two steps; first, the α -aminonitrile was reduced under protection using BOC anhydride, NaBH₄ and NiCl₂ anhydrous as a catalyst in methanol at 0 °C then at room temperature overnight to yield the corresponding BOC-protected derivatives (**B5–B46**). The second step was to deprotect the BOC amines to the corresponding ethane-1,2-diamine (**C5–C46**) and this was achieved using HCl in dioxane for 2 h. The cyclization reaction to the corresponding imidazolidinones (**D5–D46**) was accomplished by reacting the ethane-1,2-diamine derivatives with triphosgene in the presence of triethylamine in DCM at room temperature for 30 min. The cyclized product was reacted with phenyl chloroformate using pyridine as a catalyst under reflux in dioxane for 2 h to yield the corresponding carbamate derivatives (**E5–E46**). Finally, the carbamate derivatives were treated with several amines in the presence of triethylamine in DCM at 40°C for 3 h to provide the required urea derivatives (**F1–F51**).

Scheme 1



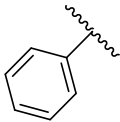
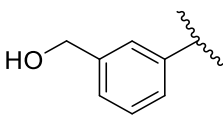
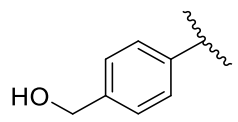
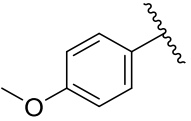
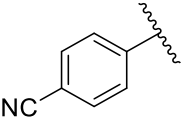
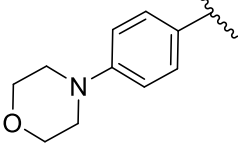
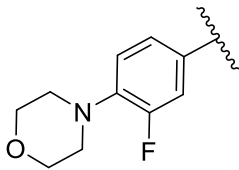
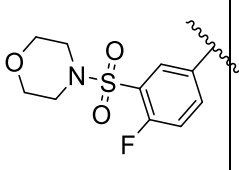
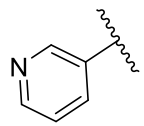
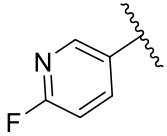
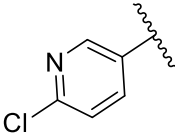
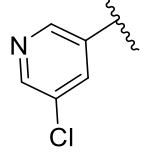
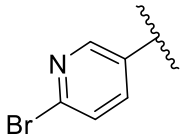
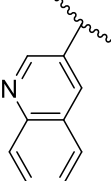
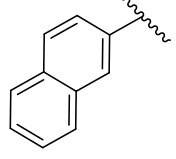
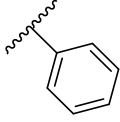
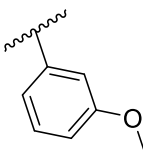
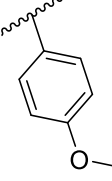
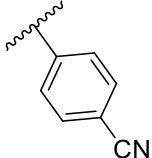
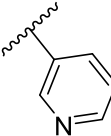
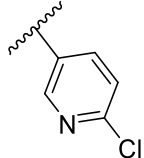
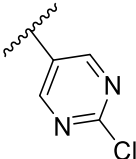
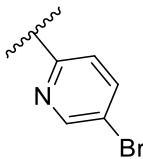
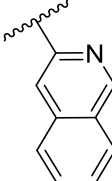
Reagents and conditions i) $\text{Zn}(\text{CN})_2$, EtOH: AcOH (3:1), overnight at RT. ii) Boc anhydride, NaBH_4 , NiCl_2 anhydrous methanol, overnight, RT. iii) HCl, dioxane, 2 h, RT. iv) Triphosgene, TEA, DCM, RT for 30 min. v) Dioxane, Pyridine, phenyl chloroformate, reflux, 2 h. vi) DCM, TEA, corresponding amine at 40 °C 3 h.

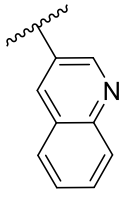
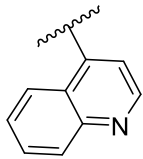
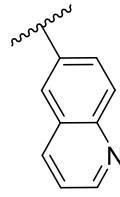
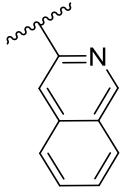
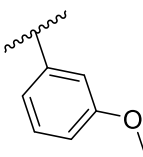
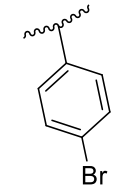
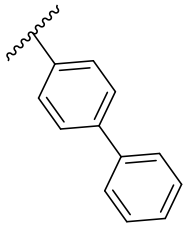
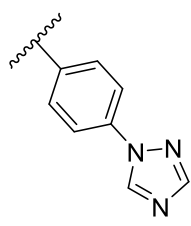
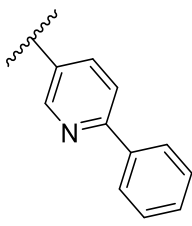
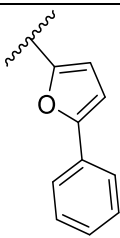
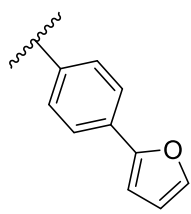
Table 2. Structures and substitution patterns of the synthesized imidazolidinone derivatives (F12–F46)



No.	R	No.	R	No.	R

Results and Discussion

F12		F13		F14	
F15		F16		F17	
F18		F19		F20	
F21		F22		F23	
F24		F25		F26	
F27		F28		F29	
F30		F31		F32	
F33		F34		F35	

F36		F37		F38	
F39		F40		F41	
F42		F43		F44	
F45		F46			

3.1.4 Biological Evaluation

The activity of MurA was evaluated using a standard malachite green assay measuring the amount of released inorganic phosphate using malachite green and sodium molybdate. Together, the phosphate and these reagents form a green complex that is quantified spectrophotometrically.

Given that the 5-ntirothiazolyl group in pilot compound **F5** showed considerable potency against MurA (Table 1, $IC_{50}=8.86 \mu M$), we decided to keep it in most of the synthesized compounds. In the next sections, we describe our iterative cycles of optimization to boost the potency and reduce the clogP of the synthesized compounds.

Compounds were tested for their *in vitro* ability to inhibit MurA *E. coli* enzyme, by first testing the inhibition of the compounds at a screening dose of $20 \mu M$. Fosfomycin was used as positive control and showed an IC_{50} of $6.13 \mu M$. The percentage inhibition recorded for each compound

is an average of at least two independent experiments (Tables 3, 4, 5 and 6). The IC₅₀ values were determined for compounds displaying more than 60% inhibition (Tables 3, 4, 5 and 6). IC₅₀ determination was done through testing a range of 5 concentrations with three replicates per concentration; the IC₅₀ value recorded for each compound is an average of at least two independent experiments. The assay was repeated with an adapted concentration range to allow a more precise evaluation of the IC₅₀ values. Tables 3–6 display the logP values calculated by ACD labs. The purpose of presenting these values is to monitor the advance in reducing clogP of the scaffold.

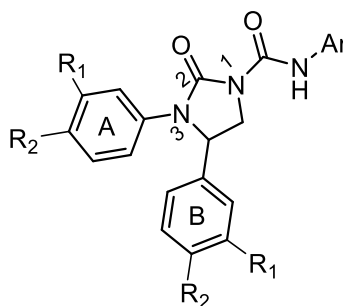
Variation in halogen substitution (F5–F11).

We synthesized seven compounds to investigate the effect of varying the halogen substitution on rings A and B. (rings A and B were kept symmetric) Table 3.

Upon comparing **F5** to **F8**, **F6** to **F9** and **F7** to **F10**, it was concluded that the position of the halogen whether in *meta* or *para* position did not affect the activity. However, the size/lipophilicity of the halogen had a high impact on potency; with fluoro substitution being the least potent in compounds **F6** and **F9**, followed by chloro substitution in compounds **F5** and **F8** and finally the bromo substitution was the most potent in compounds **F7** and **F10** as shown in Table 3, where both bromo compounds could show sub micromolar IC₅₀. However, this increase in potency was accompanied by a significant increase in clogP values, which were 4.3 and 4.2, respectively. The effect of dichloro substitution was also assessed in compound **F11**. As expected, upon comparing **F11** to **F5** and **F8**, a 2- fold improvement in potency was noticed, however, with a huge increase in clogP (Table 3).

Although bromo substitution and multiple halogen substitution showed higher potency, we decided to go to the next round while keeping the 3-Cl (**F5**) substitution to avoid the increase in logP of the synthesized compounds and the related problems like reduced water solubility and increase binding to plasma proteins.

Table 3. Effect of halogens variation on MurA inhibition and clogP.



Cpd No.	R1	R2	IC ₅₀ (μ M)	clogP
F5	Cl	H	8.86 \pm 1.12	3.6
F6	F	H	24.04 \pm 2.31	3
F7	Br	H	0.88 \pm 0.33	4.3
F8	H	Cl	10.24 \pm 0.57	3.9
F9	H	F	25.56 \pm 1.97	2.9
F10	H	Br	0.53 \pm 0.26	4.2
F11	Cl	Cl	5.48 \pm 1.72	5.2

^aData shown are the mean of at least two independent experiments. clogP values were calculated using ACD Labs software.

In the following rounds of optimization, we explored the effect of systematic change of one structural feature of the scaffold while keeping the others (variation of ring A while keeping ring B constant and variation of ring B while keeping ring A constant) to optimize the potency and derive structure activity relationships (SAR). We gave higher focus on installing polar groups and heterocycles (mono and bicycles) to explore polar interactions with the binding pocket and to reduce the clogP of the synthesized compounds. The four rounds (stages) of optimisation applied in work are presented in Figure 3.

Results and Discussion

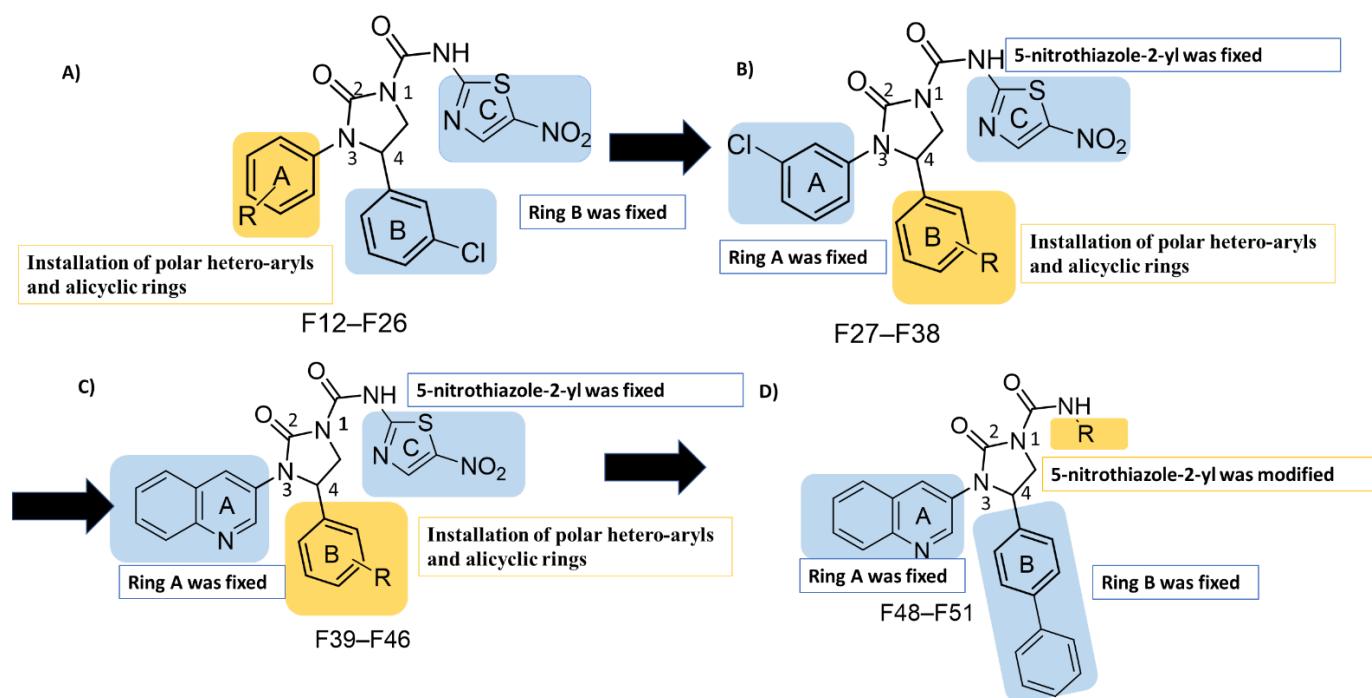
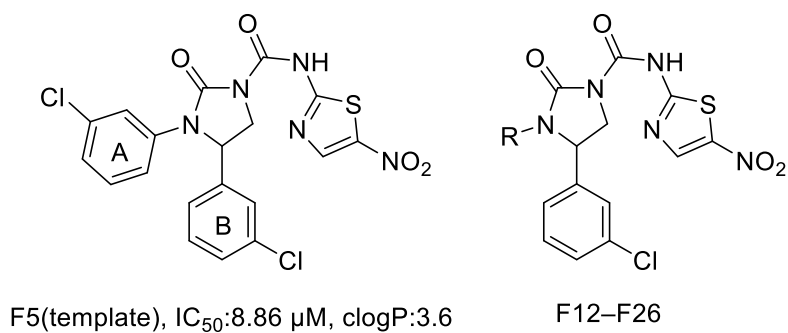


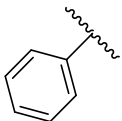
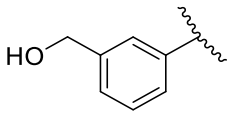
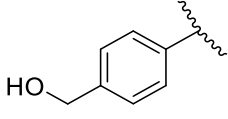
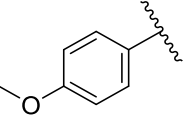
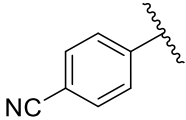
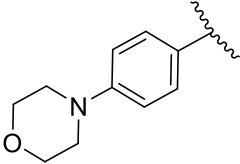
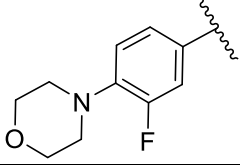
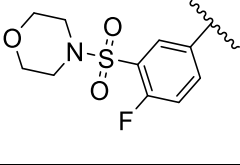
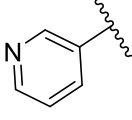
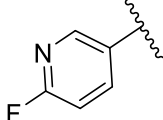
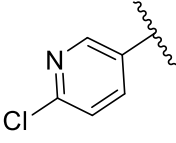
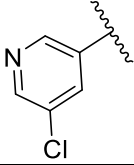
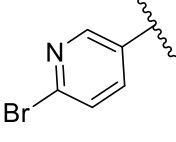
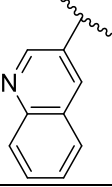
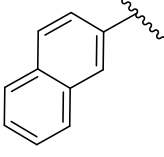
Figure 3: Modifications followed in the stages of optimization.

Stage 1: Variation of ring A (compounds F12–F26)

Table 4. MurA Inhibition of imidazolidinones F12–F26 (Variations in the 1-aryl)



Results and Discussion

Cpd#	R	%inh @20 μ M	IC ₅₀ (μ M)	clogP	Cpd#	R	%inh @20 μ M	IC ₅₀ (μ M)	clogP
F12		18.83 ±1.47	n.d.	3.16	F13		n.i.	n.d.	2.57
F14		72.09 ±1.06	15.12 ±0.33	2.57	F15		58.7 ±3.19	n.d.	3.10
F16		52.04 ±4.83	n.d.	3.26	F17		67.11 ±2.21	17.79 ±1.29	2.80
F18		54.90 ±1.15	n.d.	3.22	F19		54.61 ±3.20	15.99 ±1.73	3.10
F20		44.13 ±4.22	n.d.	2.37	F21		38.11 ±2.21	n.d.	2.50
F22		37.65 ±4.01	n.d.	2.90	F23		15.04 ±2.73	n.d.	2.90
F24		15.36 ±0.97	n.d.	2.95	F25		86.74 ±1.29	6.44 ±1.85	3.40
F26		58.09 ±2.4	21.33 ±1.49	4.30					

^aData shown are the mean of at least two independent experiments ni, no inhibition, n.d., not determined. clogP values were calculated using ACD Labs software.

Taking **F5** as template, deletion of the 3-chloro substitution from ring A (compound **F12**) led to a huge loss of activity showing the importance of the halogen substitution.

Contrastingly, the use of phenyl substituted with different polar groups like 3-hydroxymethyl (**F13**), 4-hydroxymethyl (**F14**), 4-methoxy (**F15**), 4-cyano (**F16**), all resulted in an improvement of activity compared to the unsubstituted phenyl (**F12**) except for **F13**. Compound **F14** showed the highest inhibition with an IC₅₀ of 15.12 μ M. Moreover, several 4-

morpholinyl derivatives **F17–F19** were tried. **F18** and **F19** have an additional fluoro (**F18**) and fluoro and sulfonyl substitutions (**F19**), showed slightly decreased activity when compared to the 4-morphilnyl derivative (**F17**). Overall, none of the used polar groups at the 1-phenyl could reach the potency of the 3-chloro substituents in compound **F5** despite the improvement achieved in clogP values.

Next, we used several heteroaryl analogues. We started with the 3-pyridinyl in **F20** which showed only 44% inhibition of MurA at 20 μM . It is worth mentioning that other positional isomers of pyridine could not be installed due to the reduced reactivity of the starting amino pyridine precursor. Afterwards, halogen substitution was tried at the 3-pyridinyl aiming for enhancing the activity. However, **F21–F24** showed minimal or no activity. Generally, a fluoro, a chloro and a bromo substituent at the 3- or the 4-position of the 3-pyridyl ring did not boost the activity. This suggests that polar atoms/groups at position 3 may have a negative impact, as observed in **F13, F20–F24**.

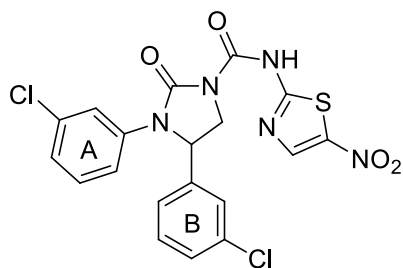
In a last trial to improve potency through variation of ring A, the 3-quinolinyl ring was used (compound **F25**), which intriguingly improved the potency ($\text{IC}_{50} = 6.44 \mu\text{M}$), which is almost equivalent to the 3-chlorophenyl in **F5**, indicating that that the fused phenyl group attached to the pyridine ring might be involved in a π - π interaction with the binding pocket. This interaction potentially restores the potency that was lost in **F20**, which contained a plain pyridine ring. Previous attempts to restore the potency of **F20** using different halogen substitutions, as observed in **F21–F24** were unsuccessful. To investigate the importance of the quinoline nitrogen atom in **F25**, the naphthyl analogue **F26** was prepared, with a more than 3-fold reduction in potency ($\text{IC}_{50} = 21.33 \mu\text{M}$).

The results of this round of optimization yielded compound **F25** (Table 4) with quinoline ring conveyed the strongest MurA inhibition from all of the different aryl moieties as ring A with slight improvement of IC_{50} and clogP when compared to hit compound **F5** (Table 4).

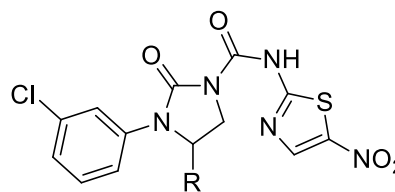
Stage 2: Variation of ring B (compounds **F27–F38**)

Table 5. MurA Inhibition of Imidazolidinones **F27–F38 (Variation of the 5-aryl)**

Results and Discussion



F5 (template), IC₅₀:8.86 μM, cLogP:3.6



F27-F38

Cpd#	R	%inh @20μM	IC ₅₀ (μM)	clogP	Cpd#	R	%inh @20μM	IC ₅₀ (μM)	clogP
F27		61.24 ±2.36	10.52 ±1.72	3.16	F28		68.40 ±2.23	15.4 ±1.31	3.10
F29		58.18 ±4.12	n.d.	3.10	F30		80.90 ±3.09	8.33 ±0.93	3.10
F31		49.11 ±1.39	n.d.	2.40	F32		60.46 ±5.90	6.47 ±2.63	2.60
F33		n. i	n.d.	2.05	F34		45.59 ±2.57	n.d.	3.0
F35		91.20 ±1.21	2.34 ±0.25	3.40	F36		35.90 ±6.43	n.d.	3.40
F37		39.66 ±1.40	n.d.	3.40	F38		19.40 ±5.08	n.d.	3.40

^aData shown are the mean of at least two independent experiments. ni, no inhibition, n.d., not determined. clogP values were calculated using ACD Labs software.

In the second round of optimization, we evaluated the effect of modification of the 5-aryl (ring B). Similar to the first stage, we tested the effect of removing the halogen at the 5-phenyl in **F5** to give **F27**. Interestingly, **F27** maintained activity with almost similar potency (IC₅₀ =

10.52 μM) and reduction of clogP from 3.6 to 3.16. Since this modification did not work when applied to ring A, it is more likely that rings A and B go to different sub-pockets in MurA, also rings A and B are less likely to flip.

The use of a phenyl substituted with different polar groups-maintained activity ranging from 58% to 80% inhibition at 20 μM . **F28** with 3-methoxymethyl showed an IC_{50} of 15.4 μM , and its positional isomer **F29** with 4-methoxymethyl showed 58% inhibition. Compound **F30** with 4-cyano showed an IC_{50} value of 8.33 μM , the three compounds have reduced clogP values when compared to **F5** (3.1).

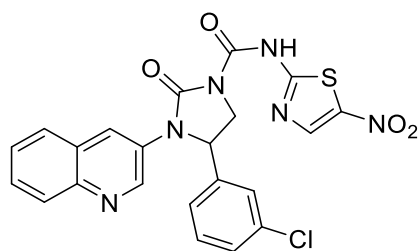
Afterwards, we used several heteroaryl analogues. The 3-pyridyl (**F31**) showed 44% inhibition of MurA at 20 μM . Introducing a 4-chloro to the 3-pyridyl resulted in more than 3-fold increase in potency (**F32**, $\text{IC}_{50} = 6.47 \mu\text{M}$). Compound **F33** was synthesized to test the effect of introducing another N to the pyridine ring. However, compound **F33** with pyrimidine ring lost activity towards MurA at 20 μM . Finally, the use of 5-bromo-2-pyridyl in **F34** showed a decrease in activity with 45% inhibition at 20 μM .

Several (iso)quinoline derivatives **F35** (3-isoquinolinyl), **F36** (3-quinolinyl), **F37** (4-quinolinyl) and **F38**(6-quinolinyl) were synthesized. All the quinoline derivatives showed a huge drop-in activity ranging from 19 to 39% inhibition at 20 μM except the 3-isoquinolinyl analogue (**F35**) showed the highest potency with an IC_{50} of 2.34 μM concluding that not only the N presence is important but also its position is crucial for activity. Furthermore, when comparing **F34** and **F35**, both compounds have the nitrogen atom in the pyridine ring at the same position. However, **F34** has a 5-bromo substitution, while **F35** features a fused phenyl group attached to the pyridine ring. Interestingly, **F35** demonstrated higher potency, implying that the fused phenyl group might be involved in a π - π interaction that contributes to the improved activity. Taken together, these results highlight the significance of both the presence and position of the nitrogen atom, as well as the potential role of aromatic interactions, in modulating the potency of these compounds.

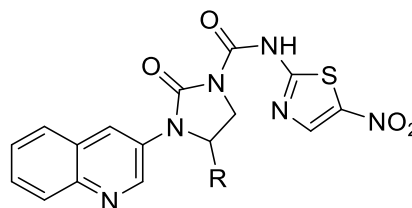
Overall, the 5-aryl modification (ring B) was more tolerant to the deletion of halogen, the use of polar substituents and heteroaryl, yielding compounds with significantly reduced clogP and/or higher potency, like **F30** ($\text{IC}_{50} = 2.34$, clogP = 3.1), **F32** ($\text{IC}_{50} = 6.47$, clogP = 2.8) and **F35** ($\text{IC}_{50} = 2.34$, clogP = 3.4). The LE values for **F30**, **F32**, and **F35** are 0.25, 0.23, and 0.23, respectively.

Stage 3: Further optimization adopting the 3-quinolinyl as ring A (F39–F46)

Table 6. MurA inhibition of imidazolidinones F39–F46



F25(template), IC₅₀:6.44 μM, cLogP:3.4



F39-F46

Cpd#	R	%inh @20μM	IC ₅₀ (μM)	clogP	Cpd#	R	%inh @20μM	IC ₅₀ (μM)	clogP
F39		78.12 ±1.23	17.42 ±0.43	2.70	F40		76.34 ±4.28	3.74 ±0.32	2.90
F41		87.50 ±2.64	6.54 ±0.57	3.50	F42		96.46 ±4.45	0.53 ±0.22	4.20
F43		40.70 ±3.15	n.d.	2.20	F44		88.93 ±1.76	3.21 ±0.51	3.10
F45		80.63 ±0.95	4.72 ±0.62	3.50	F46		89.13 ±3.79	3.47 ±0.87	3.30

^aData shown are the mean of at least two independent experiments. n.d., not determined. clogP values were calculated using ACD Labs software.

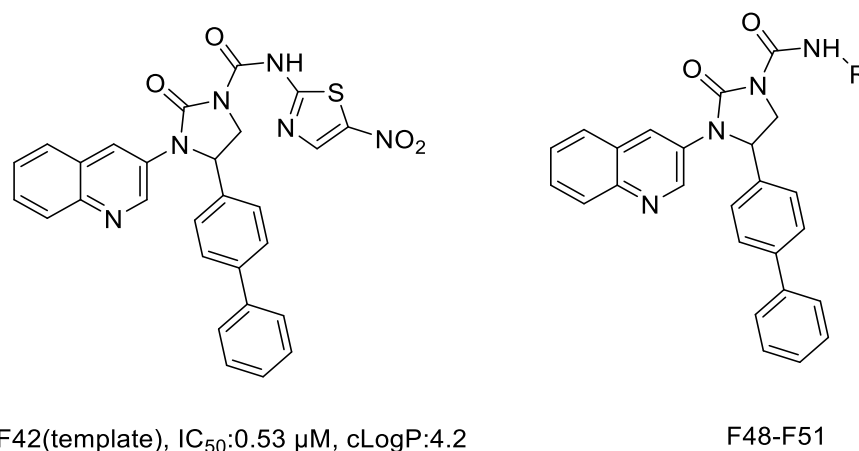
In the next round, **F25** was used as template and more modifications were tested at position 5 (Ring B). The first synthesized (**F39**) combined the best feature from stage 2 (quinoline-3-yl, compound **F25**) and stage 3 (isoquinoline-3-yl, compound **F35**) but the SAR wasn't additive as the compound showed 3–6 times lower potency than **F25** and **F35** (IC₅₀ = 17.42 μM).

Compounds **F40** and **F41** were synthesized employing 3-methoxyphenyl and the 4-bromophenyl respectively. Both compounds showed improved potency with an IC_{50} of 3.74 μ M and 6.54 μ M, respectively. Several biaryl systems were also introduced, including 4-(1,1'-biphenyl) (**F42**), 1-(4-phenyl)-1,2,4-triazole(**F43**), 5-(2-phenylpyridine)(**F44**), 2-(5-phenylfuran)(**F45**) and 2-(4-phenyl)furan(**F46**). Compound **F42** showed the highest potency with an IC_{50} of 0.534 μ M. Changing the outer phenyl with triazole in compound **F43** deteriorated the activity with only 40% inhibition of MurA at 20 μ M. However, substituting the inner phenyl with pyridine in compound **F44** restored activity with an IC_{50} of 3.21 μ M. Moreover, changing the inner and the outer phenyl with a furan in compounds **F45** and **F46** respectively showed high activity with IC_{50} of 4.72 μ M and 3.47 μ M, respectively.

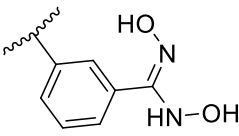
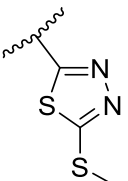
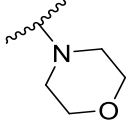
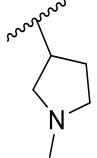
In conclusion, modifications were made to **F25** template in the third stage, resulting in the synthesis of several compounds with varying degrees of potency. While **F39** did not show additive SAR, **F40**, **F41**, **F42**, **F44**, **F45**, and **F46** showed improved potency, with **F42** showing the highest potency with an IC_{50} of 0.534 μ M. The introduction of biaryl systems proved to be a successful modification strategy, with **F44**, **F45**, and **F46** demonstrating particularly high activity. Overall, these findings provide valuable insights for the further optimization of MurA inhibitors.

Stage 4: Further optimisation adopting the 3-quinolinyl as ring A and 4-(1,1'-biphenyl) as ring B (F48–F51)

Table 7. MurA inhibition of imidazolidinones F48–F51



Results and Discussion

Cpd#	R	%inh @20 μ M	IC ₅₀ (μ M)	clogP	Cpd#	R	%inh @20 μ M	IC ₅₀ (μ M)	clogP
F48		78.13 \pm 4.74	14.24 \pm 1.39	3.7	F49		78.31 \pm 5.64	6.13 \pm 2.51	4.7
F50		n. i	n.d.	3.1	F51		54.71 \pm 6.84	n.d.	3.36

^aData shown are the mean of at least two independent experiments. n.d., not determined. clogP values were calculated using ACD Labs software.

In the next round, **F42** was used as template and more modifications were tested at Ring C. While the majority of synthesized compounds retained the 5-nitrothiazolyl group, we decided to synthesize specific derivatives with variations in the nitrothiazole group. This choice was made with the intention of exploring the potential to enhance potency and further reduce clogP values (Table 7).

Compounds **F48** and **F49** were synthesized employing 3-amino-*N,N'*-dihydroxybenzimidamide and 5-(methylthio)-1,3,4-thiadiazol-2-amine, respectively. Unfortunately, both compounds exhibited reduced potency, with an IC₅₀ of 14.24 μ M. and 6.13 μ M, respectively. To explore alternative options, two aliphatic amines, namely morpholin-4-amine (**F50**) and 1-methylpyrrolidin-3-amine (**F51**), were introduced. However, both of the compounds demonstrated reduced activity. This outcome emphasizes the significance of having an aromatic system in that position, as it is likely involved in crucial π - π interactions.

The current work presented a novel series of imidazolidinones as potent MurA inhibitors. Our goal was to understand the SAR toward MurA. The structural modifications on the lead compound **F5** can be summarized in Figure 4:

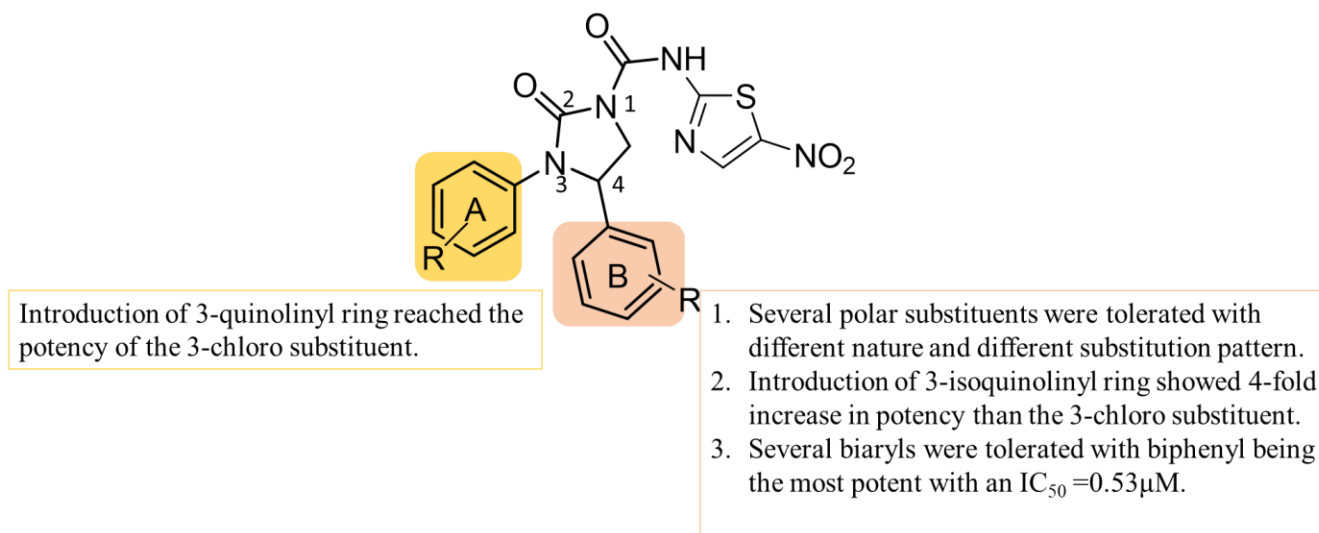
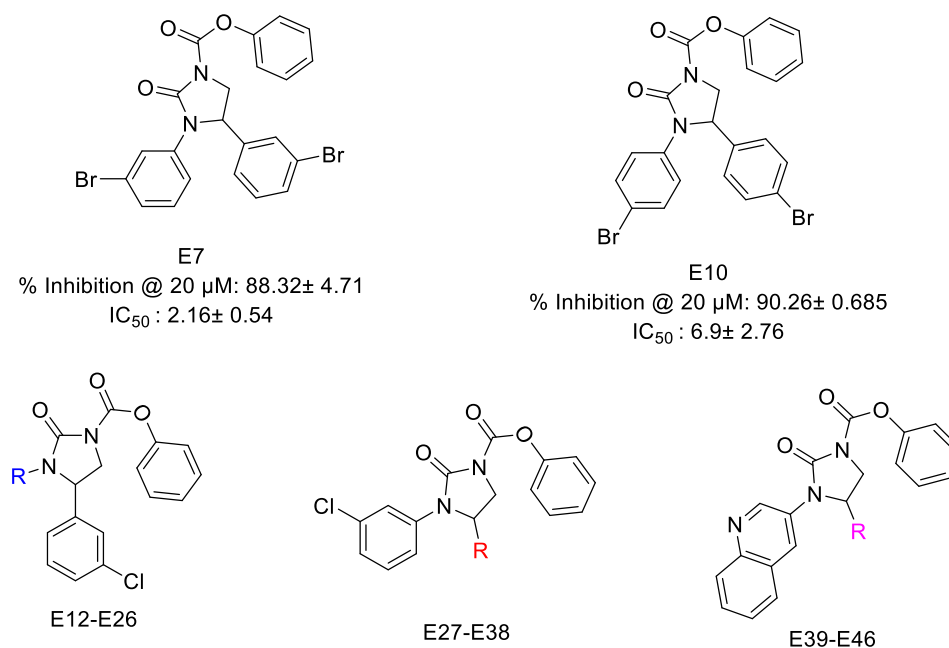


Figure 4: SAR summary.

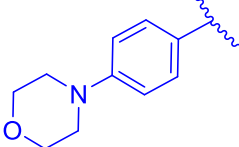
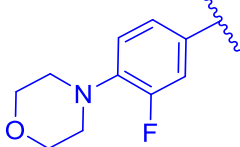
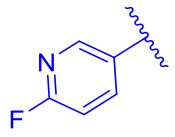
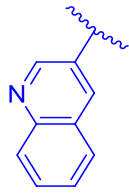
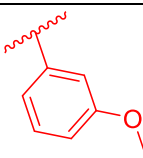
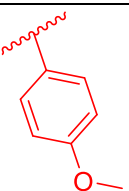
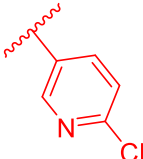
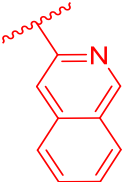
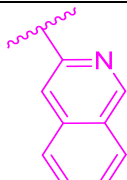
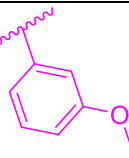
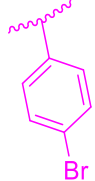
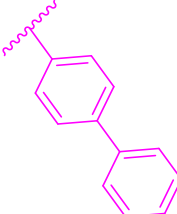
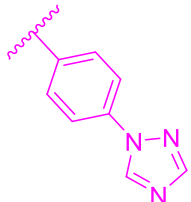
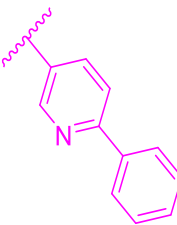
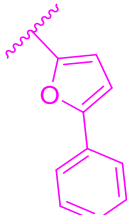
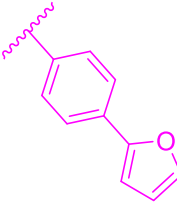
3.1.4.1.1 Testing some of carbamate derivatives against MurA(E5-E46).

Table 8. MurA inhibition of carbamate derivatives.



Cpd#	R	%inh @20 μM	IC_{50} (μM)	Cpd#	R	%inh @20 μM	IC_{50} (μM)
E5		55.77 \pm 2.59	n.d.	E15		18.76 \pm 3.04	n.d.

Results and Discussion

E17		25.40 ±1.32	n.d.	E18		14.28 ±0.64	n.d.
E21		30.65 ±1.74	n.d.	E25		86.67 ±1.44	4.91 ±0.84
E28		21.2 ±1.98	n.d.	E29		28.34 ±1.12	n.d.
E32		33.78 ±3.48	n.d.	E35		81.29 ±2.89	6.28 ±0.95
E39		38.21 ±3.52	n.d.	E40		17.65 ±2.43	n.d.
E41		52.97 ±2.14	n.d.	E42		98.60 ±1.12	1.30 ±0.24
E43		49.85 ±2.15	n.d.	E44		8.93 ±3.15	n.d.
E45		46.66 ±2.15	n.d.	E46		67.23 ±3.15	8.8 ±1.15

^aData shown are the mean of at least two independent experiments. n.d., not determined.

Next, we decided to test some phenyl carbamate precursors and compare them to the respective nitro thiazole urea derivatives, we mainly focused on carbamate precursors of urea compounds that showed high potency. Interestingly, most of the phenyl carbamate derivatives showed significant inhibition of MurA at 20 μM (Table 8). Figure 5 shows a comparison between the tested phenyl carbamates and their respective nitro thiazole urea derivatives. Based on Figure 5, it can be observed that most of the tested phenyl carbamates exhibit a slight decrease in activity when compared to their respective nitro thiazole urea derivatives.

While most phenyl carbamates displayed reduced potency, some quinoline derivatives showed high activity against MurA. Specifically, **E42**, the carbamate derivative of our most potent compound **F42**, demonstrated high potency with an IC_{50} of 1.3 μM . Additionally, **E25** and **E35** also exhibited good potency, with IC_{50} values of 4.91 μM and 6.28 μM , respectively.

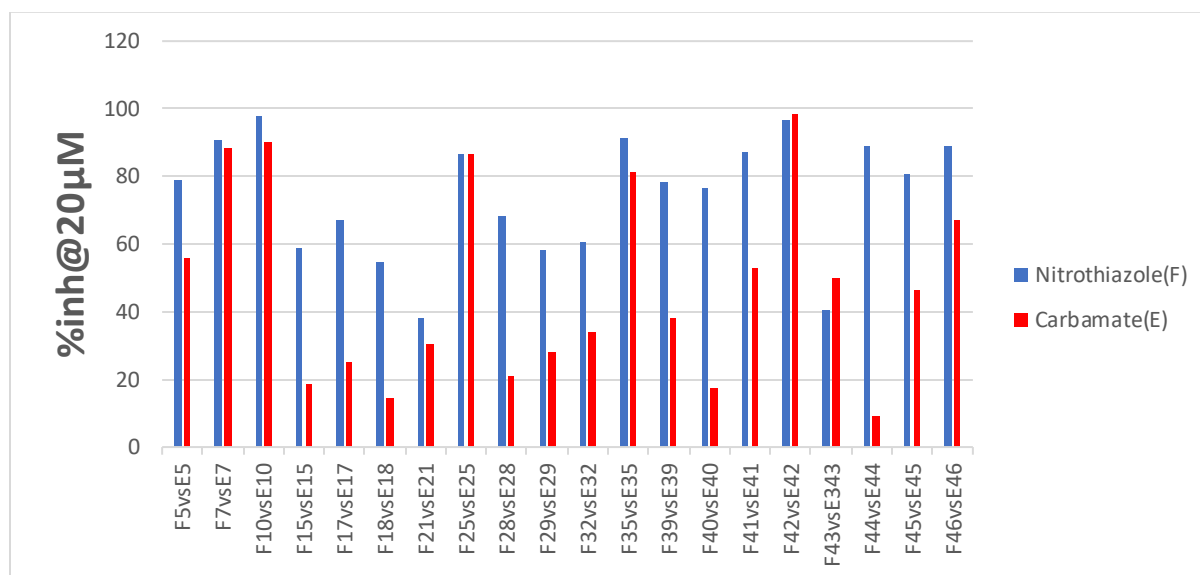
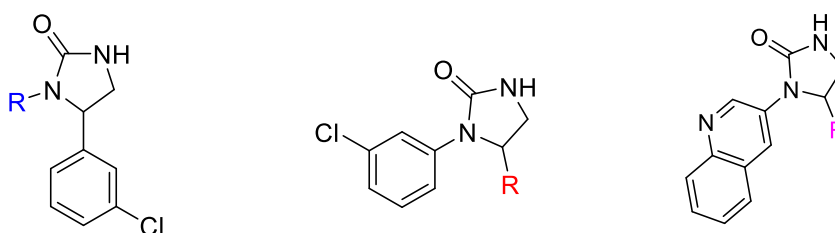


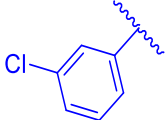
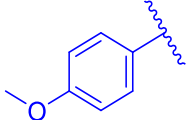
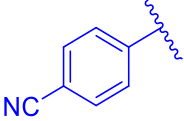
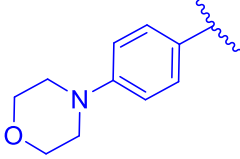
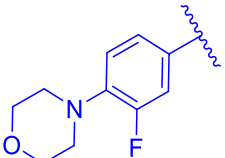
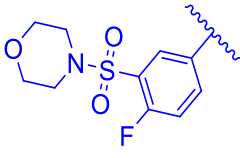
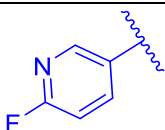
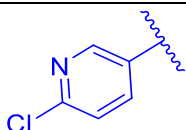
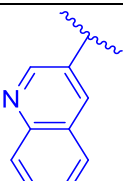
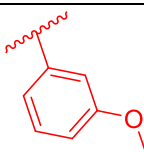
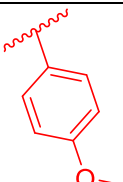
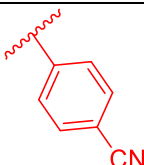
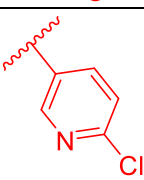
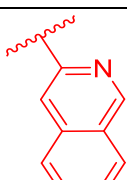
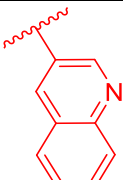
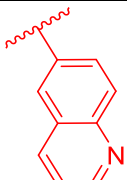
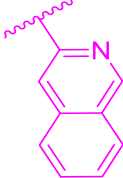
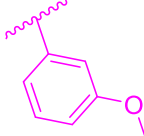
Figure 5: % Inhibition comparison between nitrothiazole urea and phenyl carbamate chemotypes at 20 μM .

3.1.4.1.2 Testing some of the cyclized derivatives (with no substituent at position 3). (D5–D46).

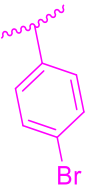
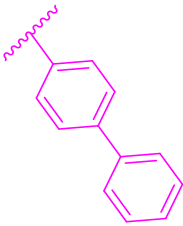
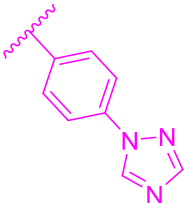
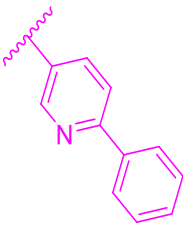
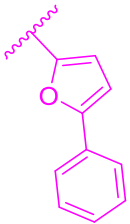
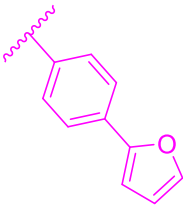
Table 9. MurA Inhibition of cyclized derivatives.



Results and Discussion

Cpd#	R	%inh @20 μ M	IC ₅₀ (μ M)	Cpd#	R	%inh @20 μ M	IC ₅₀ (μ M)
D5		n.i	n.d.	D15		n.i	n.d.
D16		26.36 \pm 0.74	n.d.	D17		24.30 \pm 1.32	n.d.
D18		46.19 \pm 2.42	n.d.	D19		45.92 \pm 1.20	n.d.
D21		30.65 \pm 1.74	n.d.	D22		n.i	n.d.
D25		90.84 \pm 3.74	0.87 \pm 0.84	D28		n.i	n.d.
D29		n.i	n.d.	D30		n.i	n.d.
D32		n.i	n.d.	D35		86.13 \pm 3.96	1.75 \pm 0.84
D36		83.53 \pm 5.06	4.58 \pm 0.59	D38		18.76 \pm 4.35	n.d.
D39		25.22 \pm 2.52	n.d.	D40		n.i	n.d.

Results and Discussion

D41		16.77 ±1.94	n.d.	D42		56.12 ±1.34	n.d.
D43		87.51 ±4.83	2.29 ±0.67	D44		n.i	n.d.
D45		49.73 ±3.43	n.d.	D46		n.i	n.d.

^aData shown are the mean of at least two independent experiments. ni, no inhibition, n.d., not determined.

To have a broader picture about the SAR and intrigued by the high potency of some phenyl carbamate derivatives, we thought of testing some of the cyclized derivatives before inserting the substituent at position 3, especially the precursors of derivatives that showed high potency. Surprisingly, some of the cyclized compounds showed very high potency (Table 9), although most of them were much less active than their respective phenyl carbamate and nitro thiazole urea derivatives.

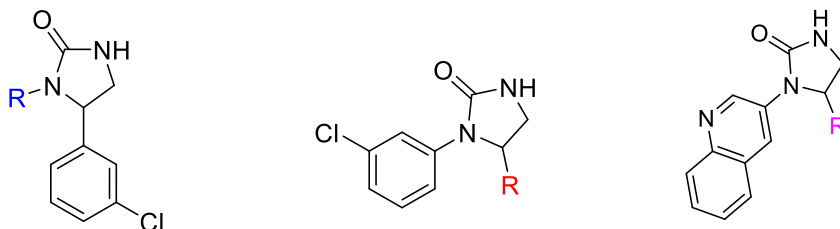
Interestingly, **D25**, which is a cyclized quinoline derivative, showed a significant increase in potency compared to its analogue **F25**. **D35**, **D36** and **D42**, which are also quinoline derivatives, similarly showed high potency against MurA. This may suggest that the quinoline moiety is important for the activity of this chemotype.

Finally, **D43** showed high potency against MurA, which is surprising as neither the corresponding carbamate derivative **E43** nor the corresponding nitro thiazole derivative **F43** showed any activity. This suggests that the cyclized derivatives have a different pharmacophore that is responsible for activity with the quinoline ring playing a major role in this chemotype.

It is worth mentioning that **D25**, **D35**, **D36**, and **D43** have a relatively low clogP values (1.9–3.2) with a remarkable potency against MurA, where they show potency despite lacking the 3rd aryl. We calculated Ligand Efficiency (LE) and Ligand Lipophilicity Efficiency (LLE) for those analogues (Table 10). It can be seen that all of these derivatives possess acceptable LE

(>0.3), however, the LLE is still hampered by the micromolar potency of the scaffold. Notably, **D43**, the compound with the lowest clogP showed the most promising LLE (3.8).

Table 10. clogP, LE and LLE of the most potent cyclized derivatives.



Cpd#	R	% inh @20 μ M	IC ₅₀ (μ M)	clogP	HAC	LE	LLE
D25		90.84 \pm 3.74	0.87 \pm 0.84	3.1	23	0.37	3
D35		86.13 \pm 3.96	\pm 1.75 \pm 0.91	3.2	23	0.35	2.6
D36		83.53 \pm 5.06	4.58 \pm 0.54	3.2	23	0.33	2.1
D43		87.51 \pm 4.83	2.29 \pm 0.67	1.9	27	0.29	3.8

^aData shown are the mean of at least two independent experiments. clogP values were calculated using ACD Labs software. The formula for calculating Ligand Efficiency (LE) and (LLE) are²⁴: $LE = (1.37/HAC) \times pIC_{50}$, $LLE = pIC_{50} - clogP$

3.1.4.1.3 Investigation of the ability of the most potent compounds to inhibit mutant MurA (C115D).

Next, four of the most potent compounds against MurA (**F42**, **F44**, **F45** and **F46**) along with Fosfomycin were chosen to explore their ability to inhibit mutant MurA C115D developed by resistant *E. coli* towards fosfomycin (Table 11).

Table11: Testing the inhibition of the most potent compounds against mutant MurA.

Cpd #	% Inhibition at 20 μ M of Mutant MurA C115D ^a	Mutant IC ₅₀ (μ M) ^a	WT IC ₅₀ (μ M) ^a
F42	90.29	5.18 \pm 0.43	0.53 \pm 0.22
F44	100	1.28 \pm 0.67	3.21 \pm 0.51
F45	72.15	4.54 \pm 0.35	4.72 \pm 0.62
F46	89.35	3.41 \pm 0.14	3.47 \pm 0.87
Fosfomycin	No inhibition	n.d.	6.13

^aData shown are the mean of at least two independent experiments, SD \leq 10%. ni, no inhibition, n.d., not determined.

Compound **F44** demonstrated significantly higher inhibitory activity against the mutant MurA. Both **F45** and **F46** displayed similar levels of inhibitory activity against the WT and the mutant MurA, while only **F42** showed lower inhibitory activity against the mutant MurA than the WT. Fosfomycin was inactive towards this mutant since it exerts its mode of action via covalent binding with C115. Thus, our chemotype has an advantage over fosfomycin to affect bacteria harbouring this fosfomycin-resistant MurA. Additionally, this excludes any critical binding between these compounds with the sulfhydryl of C115.

3.1.4.1.4 Antibacterial Activity

Table 12. Antibacterial activity of nitrothiazole urea derivatives against *S. aureus*, *E. coli* acrB and D22.

Cpd #	<i>S.aureus</i> % inh@ 50 μ M	<i>Ec acrB</i> % inh @50 μ M	<i>Ec D22</i> % inh @50 μ M	Cpd #	<i>S.aureus</i> % inh@5 0 μ M	<i>Ec acrB</i> % inh @50 μ M	<i>Ec D22</i> % inh @50 μ M
F13	10	n.i	n.i	F15	n.i	60	n.i
F16	MIC: 8.5 μ g/mL	n.i	n.d.	F17	5.4	15	10
F25	n.i	n.i	n.d.	F28	n.i	26	15.8

Results and Discussion

F29	n.i	33	13	F30	n.i	21	n.i
F32	63.46	19.2	n.d.	F39	10	8	n.i
F40	19	37	n.i	F41	n.i	11	n.i
F42	12.7	n.i	n.i	F43	n.i	42	12
F44	n.i	10.9	n.i	F45	n.i	16	n.i
F46	n.i	10	3.5	Fosfomycin	MIC 8.2±3.3 µg/mL	MIC 3.1±0.9 µg/mL	n.d.

^aData shown are the mean of at least two independent experiments, SD ≤ 10%. ni, no inhibition, n.d., not determined.

Table 13. Antibacterial activity of phenyl carbamate derivatives against *E. coli* TolC, D22 and *S. aureus*.

Cpd #	<i>S. aureus</i> % inh @ 50 µM	<i>Ec acrB</i> % inh @ 50 µM	<i>Ec D22</i> % inh @ 50 µM	Cpd #	<i>S. aureus</i> % inh @ 50 µM	<i>Ec acrB</i> % inh @ 50 µM	<i>Ec D22</i> % inh @ 50 µM
E28	n.i	10	10	E29	n.i	12	12
E41	n.i	10	13.4	E42	20	99	n.i
E43	n.i	n.i	7.5	E44	n.i	31	13
E46	n.i	8.6	n.i	Fosfomycin	MIC 8.2±3.3 µg/mL	MIC 3.1±0.9 µg/mL	n.d.

^aData shown are the mean of at least two independent experiments, SD ≤ 10%. ni, no inhibition, n.d., not determined.

Table 14. Antibacterial activity of cyclized derivatives (with no substituent at position 3) against *E. coli* TolC, D22 and *S. aureus*.

Results and Discussion

Cpd #	<i>S. aureus</i> % inh @ 50 μ M	<i>Ec acrB</i> % inh @ 50 μ M	<i>Ec D22</i> % inh @ 50 μ M	Cpd #	<i>S. aureus</i> % inh @ 50 μ M	<i>Ec acrB</i> % inh @ 50 μ M	<i>Ec D22</i> % inh @ 50 μ M
D17	6	64	28	D19	17.1	50.3	17.2
D25	59.7 @ 25 μ M	86.7 @ 25 μ M	n.d.	D28	n.i	27	7
D29	n.i	13.3	n.i	D30	7.4	n.i	n.i
D35	17.3	18.4	n.d.	D41	n.i	29	11.1
D42	n.i	42	n.i	D43	n.i	20	n.i
D44	n.i	10	1.4	D45	n.i	n.i	n.i
D46	n.i	8.4	6.6	Fosfomycin	MIC 8.2 \pm 3.3 μ g/mL	MIC 3.1 \pm 0.9 μ g/mL	n.d.

^aData shown are the mean of at least two independent experiments, SD \leq 10%. ni, no inhibition, n.d., not determined.

The antibacterial activity of three different chemotypes, including nitrothiazole urea derivatives, phenyl carbamate derivatives, and cyclized derivatives (with no substituent at position 3), against both Gram-negative mutant *E. coli* strains (*acrB* and *D22*) and Gram-positive wild-type *S. aureus*. was tested at a concentration of 50 micromolar (Table 12, 13 and 14). It was observed that most of the compounds did not exhibit significant activity at this concentration, and further testing with higher concentrations and permeation enhancers is necessary to evaluate their antibacterial potential.

It was noted that the LPS permeation could have affected the activity of some compounds, and thus, permeation enhancers may be required to improve their activity. The remaining compounds are still being tested, and it is possible that they may exhibit higher activity at different concentrations or in combination with permeation enhancers.

Among the nitrothiazole urea derivatives, only **F16** and **F25** showed some activity against *S. aureus*, with MIC values of 26.2 and 8.5, respectively. The other compounds in this chemotype did not exhibit significant activity at this concentration.

For the phenyl carbamate derivatives, only **E42** exhibited some activity, with 99% inhibition against *E. coli* acrB at 50 micromolar concentration.

In the cyclized derivatives (with no substituent at position 3) chemotype, only **D25** showed some activity against both *S. aureus* and *E. coli* acrB at a concentration of 25 micromolar, with 60% inhibition against *S. aureus* and 86.7% inhibition against *E. coli* acrB.

Overall, the tested compounds showed limited activity against the selected bacteria at 50 micromolar concentration, and further testing with higher concentrations and permeation enhancers may be needed to fully evaluate their potential as antibacterial agents.

3.1.5 Molecular Docking

3.1.5.1 Hypothetical binding mode of the nitrothiazolyl derivatives

In an attempt to get a better insight about the binding mode of our most potent inhibitor from the nitrothiazole series, F42 ($IC_{50} = 0.53 \mu\text{M}$), molecular docking was performed at MurA binding pocket (PDB code: 1UAE)²⁵ using MOE. As depicted in Figure 6, the hypothetical binding model revealed anchoring of compound F42 between K22 and L124 via performing cation- π interactions and hydrogen bond interactions with the outer phenyl of biphenyl and nitro oxygen, respectively. In addition, four CH- π interactions were found with T304, V163, L124 and P121 and one cation- π interaction with R120. Two additional important hydrogen bond interactions are also encountered between the oxygen of the 2-oxo imidazolidine and V163 and between the carbonyl of the urea with R91, which can interpret the improved potency of F42.

Results and Discussion

Specifically, for the *N*-imidazolidine-1-carboxamide chemotype, we achieved a logP of 2.6, and for the imidazolidine-2-one, unsubstituted at position 3, we achieved a logP of 1.9.

Furthermore, compounds **D25** and **D43**(imidazolidine-2-one, unsubstituted at position 3, chemotype) exhibited high potency with IC₅₀ values of 0.87 and 2.29 μM, respectively, and **D25** also showed a good ligand efficiency (LE) value of 0.37. This approach not only led to the identification of potent inhibitors of MurA but also demonstrates the potential of this scaffold for further optimization and development of novel antibiotics to combat bacterial infections, including those caused by fosfomycin-resistant strains.

A potential future direction for this research is to investigate the mechanism of action of the substituted imidazolidinones and their interaction with MurA. This could involve structural studies, such as X-ray crystallography or NMR spectroscopy, to determine the precise binding mode of these compounds to the enzyme and the basis for their potency.

Furthermore, discovering further targets for these compounds, such as MurB or MurC enzymes of these compounds could broaden their utility as antimicrobial agents and expand their potential as lead compounds for drug discovery.

Additionally, it is also crucial to conduct toxicity, pharmacokinetics and pharmacodynamics studies. Conducting toxicity studies will help identify any potential harmful effects of these compounds on both bacterial cells and host cells, which is essential for determining their safety for human use. Additionally, pharmacokinetic studies can provide insights into the absorption, distribution, metabolism, and excretion of the compounds *in vivo*, which can guide optimal dosing regimens. Finally, pharmacodynamic studies can reveal the relationship between the dose of the compound and its impact on bacterial cells, as well as the time-course of its activity, providing valuable information on its efficacy. It is important to note that these studies can also aid in the selection of lead compounds for further optimization and development.

Finally, investigating combination therapy with other antibiotics that have different modes of action has been shown to be an effective strategy for reducing the risk of resistance development. Investigating potential synergistic interactions between substituted imidazolidinones and other antibiotics could lead to the development of more effective treatments for bacterial infections. Such studies could involve testing the compounds in combination with other antibiotics against bacterial strains *in vitro* and *in vivo*.

3.1.7 Experimental

3.1.7.1 Chemistry

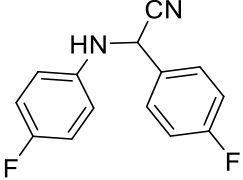
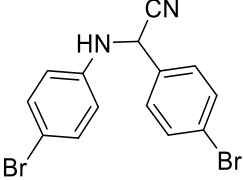
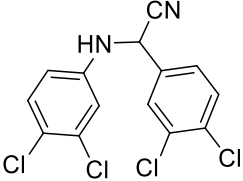
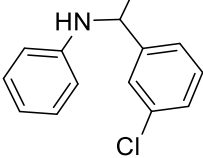
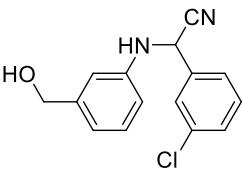
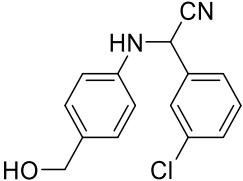
All air- or moisture-sensitive reactions were carried out in dried glassware (>100 °C) under an atmosphere of nitrogen or argon. Dried solvents were distilled before use. Analytical TLC was performed on precoated silica gel plates (Macherey-Nagel, Polygram SIL G/UV254). Visualization was accomplished with UV-light, KMnO₄, or a ceric ammonium molybdate chamber. The products were purified by flash chromatography on silica gel columns (Macherey-Nagel 60, 0.04–0.063 mm). Preparative high-performance liquid chromatography (HPLC) was performed on a Waters Autopurifier System (APS) with a Phenomenex Gemini C18 column (250 × 4.6 mm, particle size 5 μm) as an analytical column for method development and a Phenomenex Gemini C18 column (250 × 19 mm, particle size 5 μm) for preparative separation. Detection was performed using a mass trigger. ¹H and ¹³C spectra were recorded with a Bruker Fourier Spectrometer [300 MHz (¹H), 75 MHz (¹³C)] or a Bruker AV 500 [500 MHz (¹H), 126 MHz (¹³C)] spectrometer in CDCl₃, acetone-d₆, DMSO-d₆, or MeOH-d₄ unless otherwise specified. Chemical shifts are given in parts per million (ppm) and referenced against the residual proton or carbon resonances of the >99% deuterated solvents as internal standard. Coupling constants (*J*) are given in hertz (Hz). Data are reported as follows: chemical shift, multiplicity (s = singlet, d = doublet, t = triplet, q = quartet, m = multiplet, dd = doublet of doublets, dt = doublet of triplets, br = broad, and combinations of these) coupling constants, and integration. NMR spectra were evaluated using Mnova. Liquid chromatography–mass spectrometry (LC–MS) was performed on a LC–MS system consisting of a Dionex UltiMate 3000 pump, autosampler, column compartment, detector (Thermo Fisher Scientific, Dreieich, Germany), and ESI quadrupole MS (MSQ Plus or ISQ EC, Thermo Fisher Scientific, Dreieich, Germany). High-resolution mass was determined by LC–MS/MS using the Thermo Scientific Q Exactive Focus Orbitrap LC–MS/MS system. The purity of the final compounds was determined by LC–MS using a gradient with (A) H₂O + 0.1% FA to (B) ACN + 0.1% FA at a flow rate of 600 μL/min and 45 °C. The gradient was initiated by a 1 min isocratic step at 5% B followed by an increase to 99% B in 15 min to end up with a 5 min step at 99% B before re-equilibration under the initial conditions. The purity of the final compounds was determined by using the area percentage method on the UV trace recorded at a wavelength of 254 nm and found to be >95%.

3.1.7.1.1 General procedure for the synthesis of the α -aminonitrile derivatives via Strecker reaction of aromatic amines and carbaldehydes. (A5–A46) (Procedure A)

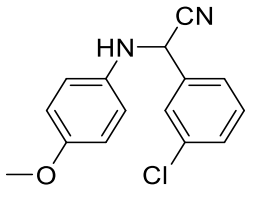
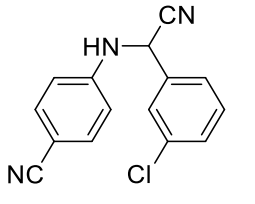
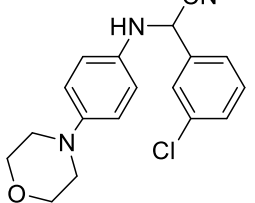
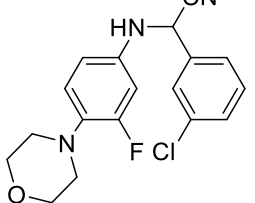
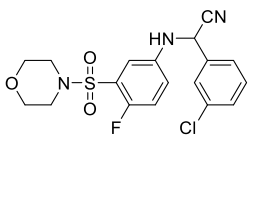
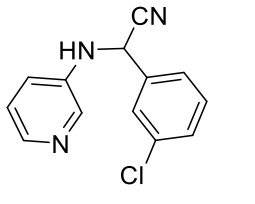
In a 250 mL round-bottomed flask, the aromatic amine derivative (10 mmol, 1.0 equiv) and the carbaldehyde derivative (10 mmol, 1.0 equiv) were dissolved in EtOH: AcOH (100 mL, 3:1), and zinc cyanide (1.17g, 10 mmol, 1.0 equiv) was subsequently added. The reaction mixture was heated to reflux for 24 h. After completion of the reaction (monitored by TLC), the mixture was partitioned between dichloromethane (150 mL) and H₂O (50 mL) and then the aqueous layer was re-extracted using dichloromethane (3 x 150 mL). Organic layers were then collected and dried over anhydrous magnesium sulfate and evaporated under vacuum. The product was confirmed using mass spectrometry and used in the next step without further purification.

Cpd	Structure	IUPAC name	Preparation Method	<i>m/z</i> : (M+H) ⁺ .
A5		2-(3-chlorophenyl)-2-((3-chlorophenyl)amino)acetonitrile	The title compound was synthesized according to the procedure A using 3-chloroaniline and 3-chlorobenzaldehyde	277.02
A6		2-(3-fluorophenyl)-2-((3-fluorophenyl)amino)acetonitrile	The title compound was synthesized according to the procedure A using 3-fluoroaniline and 3-fluorobenzaldehyde	245.09
A7		2-(3-bromophenyl)-2-((3-bromophenyl)amino)acetonitrile	The title compound was synthesized according to the procedure A using 3-bromoaniline and 3-bromoobenzaldehyde	364.92
A8		2-(4-chlorophenyl)-2-((4-chlorophenyl)amino)acetonitrile	The title compound was synthesized according to the procedure A using 4-chloroaniline and 4-chlorobenzaldehyde	277.02

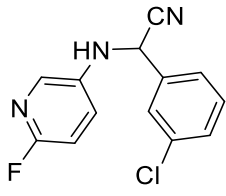
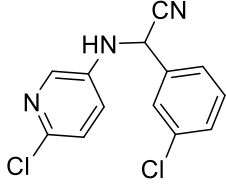
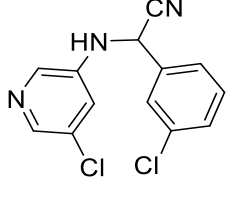
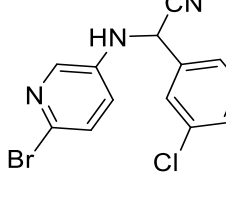
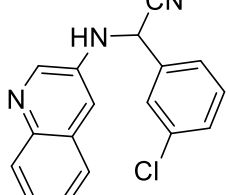
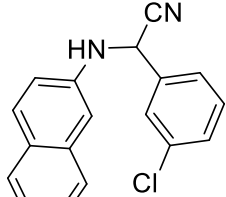
Results and Discussion

A9		2-(4-fluorophenyl)-2-((4-fluorophenyl)amino)acetonitrile	The title compound was synthesized according to the procedure A using 4-fluoroaniline and 4-fluorobenzaldehyde	245.09
A10		2-(4-bromophenyl)-2-((4-bromophenyl)amino)acetonitrile	The title compound was synthesized according to the procedure A using 4-bromoaniline and 4-bromoobenzaldehyde	364.92
A11		2-(3,4-dichlorophenyl)-2-((3,4-dichlorophenyl)amino)acetonitrile	The title compound was synthesized according to the procedure A using 3,4-dichloroaniline and 3,4-dichlorobenzaldehyde	344.94
A12		2-(3-chlorophenyl)-2-(phenylamino)acetonitrile	The title compound was synthesized according to the procedure A using aniline and 3-chlorobenzaldehyde	243.06
A13		2-(3-chlorophenyl)-2-((3-(hydroxymethyl)phenyl)amino)acetonitrile	The title compound was synthesized according to the procedure A using (3-aminophenyl) methanol and 3-chlorobenzaldehyde	273.07
A14		2-(3-chlorophenyl)-2-((4-(hydroxymethyl)phenyl)amino)acetonitrile	The title compound was synthesized according to the procedure A using (4-aminophenyl)methanol and 3-chlorobenzaldehyde	273.07

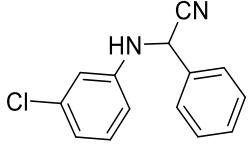
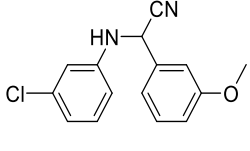
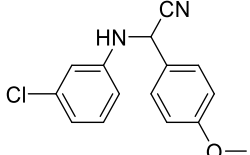
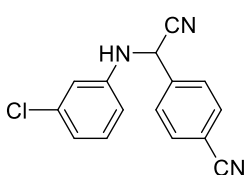
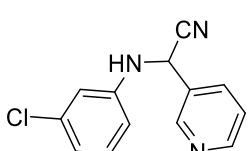
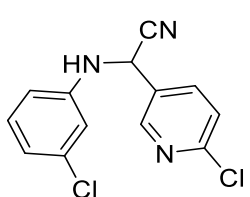
Results and Discussion

A15		2-(3-chlorophenyl)-2-((4-methoxyphenyl)amino)acetonitrile	The title compound was synthesized according to the procedure A using 4-methoxyaniline and 3-chlorobenzaldehyde	273.07
A16		4-(((3-chlorophenyl)(cyano)methyl)amino)benzonitrile	The title compound was synthesized according to the procedure A using 4-aminobenzonitrile and 3-chlorobenzaldehyde	268.06
A17		2-(3-chlorophenyl)-2-((4-morpholinophenyl)amino)acetonitrile	The title compound was synthesized according to the procedure A using 4-morpholinoaniline and 3-chlorobenzaldehyde	328.11
A18		2-(3-chlorophenyl)-2-((3-fluoro-4-morpholinophenyl)amino)acetonitrile	The title compound was synthesized according to the procedure A using 3-fluoro-4-morpholinoaniline and 3-chlorobenzaldehyde	346.10
A19		2-(3-chlorophenyl)-2-((4-fluoro-3-(morpholinosulfonyl)phenyl)amino)acetonitrile	The title compound was synthesized according to the procedure A using 4-fluoro-3-(morpholinosulfonyl)aniline and 3-chlorobenzaldehyde	410.07
A20		2-(3-chlorophenyl)-2-(pyridin-3-ylamino)acetonitrile	The title compound was synthesized according to the procedure A using 3-aminopyridine and 3-chlorobenzaldehyde	244.06

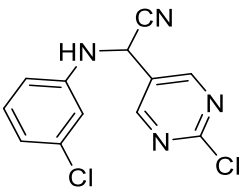
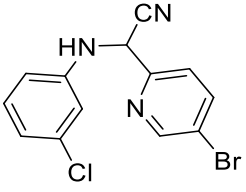
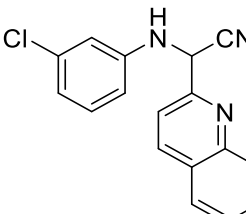
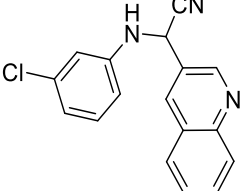
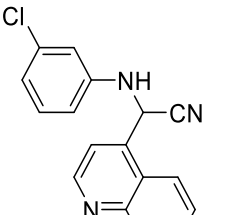
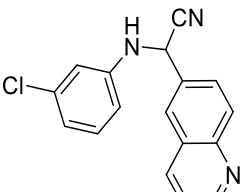
Results and Discussion

A21		2-((6-fluoropyridin-3-yl)amino)-2-(3-chlorophenyl)acetonitrile	The title compound was synthesized according to the procedure A using 6-fluoropyridin-3-amine and 3-chlorobenzaldehyde	262.05
A22		2-((6-chloropyridin-3-yl)amino)-2-(3-chlorophenyl)acetonitrile	The title compound was synthesized according to the procedure A using 6-chloropyridin-3-amine and 3-chlorobenzaldehyde	278.02
A23		2-((5-chloropyridin-3-yl)amino)-2-(3-chlorophenyl)acetonitrile	The title compound was synthesized according to the procedure A using 5-chloropyridin-3-amine and 3-chlorobenzaldehyde	278.02
A24		2-((6-bromopyridin-3-yl)amino)-2-(3-chlorophenyl)acetonitrile	The title compound was synthesized according to the procedure A using 6-bromopyridin-3-amine and 3-chlorobenzaldehyde	323.96
A25		2-((quinolin-3-yl)amino)-2-(3-chlorophenyl)acetonitrile	The title compound was synthesized according to the procedure A using quinolin-3-amine and 3-chlorobenzaldehyde	294.07
A26		2-((naphthalen-2-yl)amino)-2-(3-chlorophenyl)acetonitrile	The title compound was synthesized according to the procedure A using naphthalen-2-amine and 3-chlorobenzaldehyde	293.08

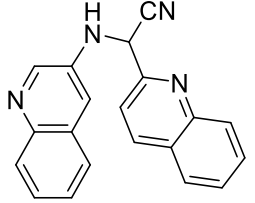
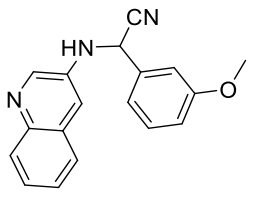
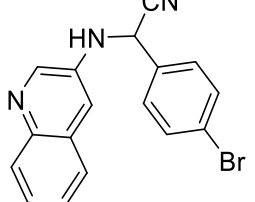
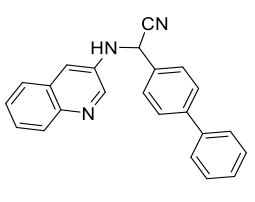
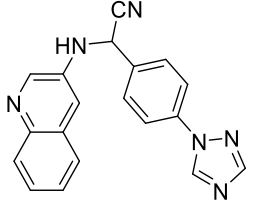
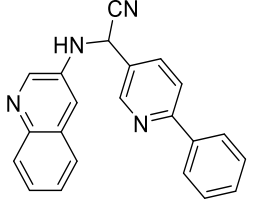
Results and Discussion

A27		2-((3-chlorophenyl)amino)-2-phenylacetonitrile	The title compound was synthesized according to the procedure A using 3-chloroaniline and benzaldehyde	243.06
A28		2-((3-chlorophenyl)amino)-2-(3-methoxyphenyl)acetonitrile	The title compound was synthesized according to the procedure A using 3-chloroaniline and 3-methoxybenzaldehyde	273.07
A29		2-((3-chlorophenyl)amino)-2-(4-methoxyphenyl)acetonitrile	The title compound was synthesized according to the procedure A using 3-chloroaniline and 4-methoxybenzaldehyde	273.07
A30		4-(((3-chlorophenyl)amino)(cyano)methyl)benzonitrile	The title compound was synthesized according to the procedure A using 3-chloroaniline and 4-cyanobenzaldehyde	268.06
A31		2-((3-chlorophenyl)amino)-2-(pyridin-3-yl)acetonitrile	The title compound was synthesized according to the procedure A using 3-chloroaniline and nicotinaldehyde	244.06
A32		2-((3-chlorophenyl)amino)-2-(6-chloropyridin-3-yl)acetonitrile	The title compound was synthesized according to the procedure A using 3-chloroaniline and 6-chloronicotinaldehyde	278.02

Results and Discussion

A33		2-((3-chlorophenyl)amino)-2-(2-chloropyrimidin-5-yl)acetonitrile	The title compound was synthesized according to the procedure A using 3-chloroaniline and 2-chloropyrimidine-5-carbaldehyde	279.01
A34		2-((3-chlorophenyl)amino)-2-(5-bromopyridin-2-yl)acetonitrile	The title compound was synthesized according to the procedure A using 3-chloroaniline and 5-bromopicolinaldehyde	323.96
A35		2-((3-chlorophenyl)amino)-2-(quinolin-2-yl)acetonitrile	The title compound was synthesized according to the procedure A using 3-chloroaniline and quinoline-2-carbaldehyde	294.07
A36		2-((3-chlorophenyl)amino)-2-(quinolin-3-yl)acetonitrile	The title compound was synthesized according to the procedure A using 3-chloroaniline and quinoline-3-carbaldehyde	294.07
A37		2-((3-chlorophenyl)amino)-2-(quinolin-4-yl)acetonitrile	The title compound was synthesized according to the procedure A using 3-chloroaniline and quinoline-4-carbaldehyde	294.07
A38		2-((3-chlorophenyl)amino)-2-(quinolin-6-yl)acetonitrile	The title compound was synthesized according to the procedure A using 3-chloroaniline and quinoline-6-carbaldehyde	294.07

Results and Discussion

A39		2-(quinolin-2-yl)-2-(quinolin-3-ylamino)acetonitrile	The title compound was synthesized according to the procedure A using quinolin-3-amine and quinoline-2-carbaldehyde	311.12
A40		2-(3-methoxyphenyl)-2-(quinolin-3-ylamino)acetonitrile	The title compound was synthesized according to the procedure A using quinolin-3-amine and 3-methoxybenzaldehyde	290.12
A41		2-(4-bromophenyl)-2-(quinolin-3-ylamino)acetonitrile	The title compound was synthesized according to the procedure A using quinolin-3-amine and 4-bromobenzaldehyde	338.02
A42		2-([1,1'-biphenyl]-4-yl)-2-(quinolin-3-ylamino)acetonitrile	The title compound was synthesized according to the procedure A using quinolin-3-amine and [1,1'-biphenyl]-4-carbaldehyde	336.14
A43		2-(4-(1H-1,2,4-triazol-1-yl)phenyl)-2-(quinolin-3-ylamino)acetonitrile	The title compound was synthesized according to the procedure A using quinolin-3-amine and 4-(1H-1,2,4-triazol-1-yl)benzaldehyde	327.13
A44		2-(6-phenylpyridin-3-yl)-2-(quinolin-3-ylamino)acetonitrile	The title compound was synthesized according to the procedure A using quinolin-3-amine and 6-phenylnicotinaldehyde	337.14

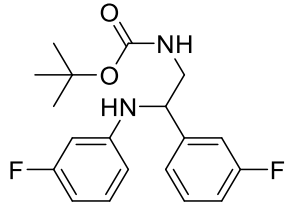
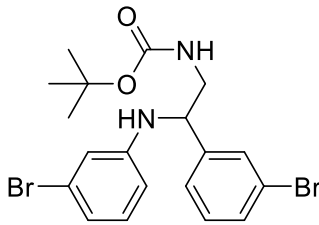
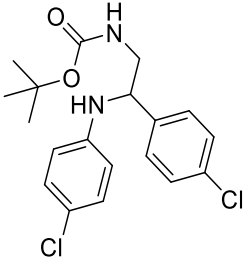
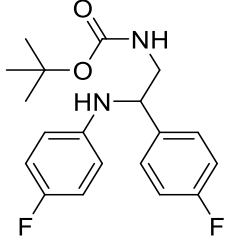
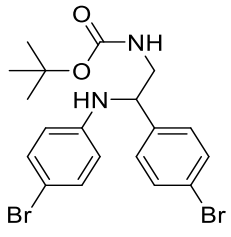
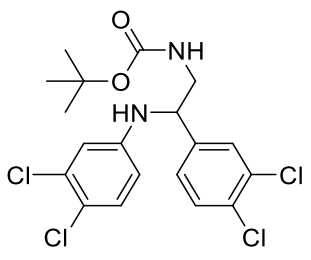
A45		2-(5-phenylfuran-2-yl)-2-(quinolin-3-ylamino)acetonitrile	The title compound was synthesized according to the procedure A using quinolin-3-amine and 5-phenylfuran-2-carbaldehyde	326.12
A46		2-(4-(furan-2-yl)phenyl)-2-(quinolin-3-ylamino)acetonitrile	The title compound was synthesized according to the procedure A using quinolin-3-amine and 4-(furan-2-yl)benzaldehyde	326.12

3.1.7.1.2 General procedure for the reduction of the α -aminonitrile derivatives under BOC protection(B5–B46) (Procedure B)

In a 500 mL round-bottomed flask the α -aminonitrile derivative (10 mmol) was dissolved in methanol(100 mL), BOC anhydride (6.5g, 30 mmol, 3.0 equiv) and a catalytic amount of NiCl₂ anhydrous (0.39gm, 3 mmol, 0.3 equiv) were added and left to stir at 0 °C. NaBH₄ (1.5g, 40 mmol, 4.0 equiv) was then cautiously added to the mixture, and then the reaction was left to stir for 24 h. After completion of the reaction (monitored by TLC), the mixture was evaporated till complete dryness under vacuum. The residue was partitioned between ethyl acetate (150 mL) and saturated NH₄Cl (50 mL) and then the aqueous layer was re-extracted using 3 portions of Ethyl acetate(150 mL) Organic layers were then collected and dried over anhydrous magnesium sulfate and evaporated under vacuum. The product was confirmed using mass spectrometry and used in the next step without further purification.

Cpd	Structure	IUPAC name	Preparation Method	<i>m/z</i> : (<i>M+H</i>) ⁺ .
B5		tert-butyl ((3-chlorophenyl)((3-chlorophenyl)amino)ethyl)carbamate	The title compound was synthesized according to the procedure B using A5	381.11

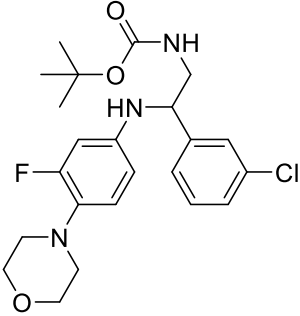
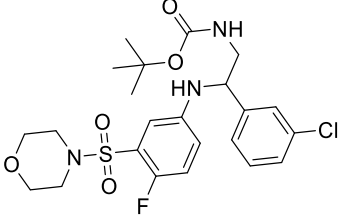
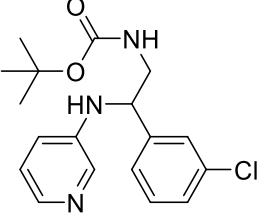
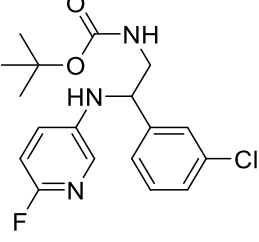
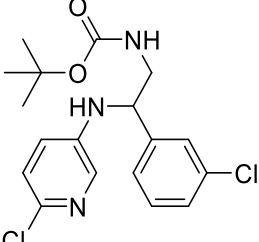
Results and Discussion

B6		tert-butyl ((3-fluorophenyl)((3-fluorophenyl)amino)ethyl)carbamate	The title compound was synthesized according to the procedure B using A6	349.16
B7		tert-butyl ((3-bromophenyl)((3-bromophenyl)amino)ethyl)carbamate	The title compound was synthesized according to the procedure B using A7	469.00
B8		tert-butyl ((4-chlorophenyl)((4-chlorophenyl)amino)ethyl)carbamate	The title compound was synthesized according to the procedure B using A8	381.11
B9		tert-butyl ((4-fluorophenyl)((4-fluorophenyl)amino)ethyl)carbamate	The title compound was synthesized according to the procedure B using A9	349.16
B10		tert-butyl ((4-bromophenyl)((4-bromophenyl)amino)ethyl)carbamate	The title compound was synthesized according to the procedure B using A10	469.00
B11		tert-butyl ((3,4-dichlorophenyl)((3,4-dichlorophenyl)amino)ethyl)carbamate	The title compound was synthesized according to the procedure B using A11	449.02

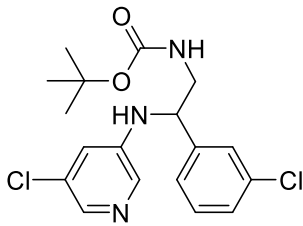
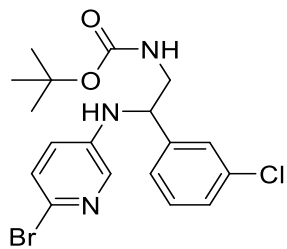
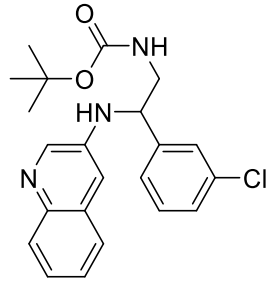
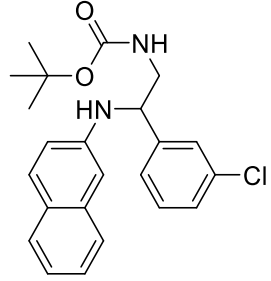
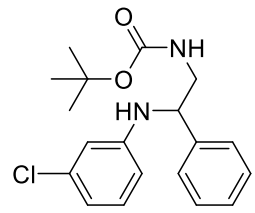
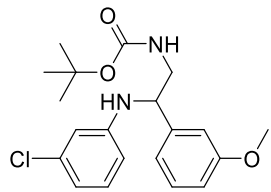
Results and Discussion

B12		tert-butyl ((3-chlorophenyl)(phenylamino)ethyl)carbamate	The title compound was synthesized according to the procedure B using A12	347.14
B13		tert-butyl ((3-chlorophenyl)((3-(hydroxymethyl)phenyl)amino)ethyl)carbamate	The title compound was synthesized according to the procedure B using A13	377.16
B14		tert-butyl ((3-chlorophenyl)((4-(hydroxymethyl)phenyl)amino)ethyl)carbamate	The title compound was synthesized according to the procedure B using A14	377.16
B15		tert-butyl ((3-chlorophenyl)((4-methoxyphenyl)amino)ethyl)carbamate	The title compound was synthesized according to the procedure B using A15	377.16
B16		tert-butyl ((3-chlorophenyl)((4-cyanophenyl)amino)ethyl)carbamate	The title compound was synthesized according to the procedure B using A16	372.14
B17		tert-butyl ((3-chlorophenyl)((4-morpholinophenyl)amino)ethyl)carbamate	The title compound was synthesized according to the procedure B using A17	432.20

Results and Discussion

B18		tert-butyl ((3-chlorophenyl)((3-fluoro-4-morpholinophenyl)amino)ethyl)carbamate	The title compound was synthesized according to the procedure B using A18	450.19
B19		tert-butyl ((3-chlorophenyl)((4-fluoro-3-(morpholinylsulfonyl)phenyl)amino)ethyl)carbamate	The title compound was synthesized according to the procedure B using A19	514.15
B20		tert-butyl (2-(3-chlorophenyl)-2-(pyridin-3-ylamino)ethyl)carbamate	The title compound was synthesized according to the procedure B using A20	348.14
B21		tert-butyl ((3-chlorophenyl)((6-fluoropyridin-3-yl)amino)ethyl)carbamate	The title compound was synthesized according to the procedure B using A21	366.13
B22		tert-butyl ((3-chlorophenyl)((6-chloropyridin-3-yl)amino)ethyl)carbamate	The title compound was synthesized according to the procedure B using A22	382.10

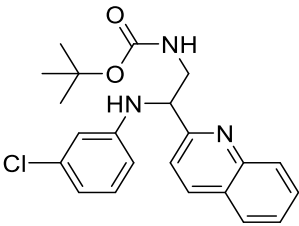
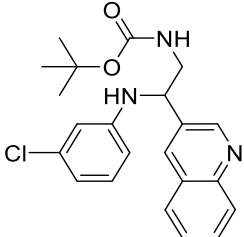
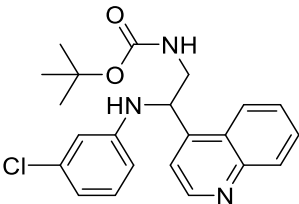
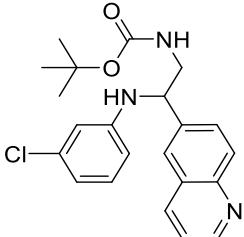
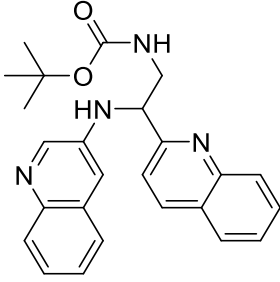
Results and Discussion

B23		tert-butyl ((3-chlorophenyl)((5-chloropyridin-3-yl)amino)ethyl)carbamate	The title compound was synthesized according to the procedure B using A23	382.10
B24		tert-butyl (((6-bromopyridin-3-yl) amino)(3-chlorophenyl)ethyl)carbamate	The title compound was synthesized according to the procedure B using A24	428.05
B25		tert-butyl ((3-chlorophenyl)(quinolin-3-ylamino)ethyl)carbamate	The title compound was synthesized according to the procedure B using A25	398.16
B26		tert-butyl ((3-chlorophenyl)(naphthalen-2-ylamino)ethyl)carbamate	The title compound was synthesized according to the procedure B using A26	397.16
B27		tert-butyl (((3-chlorophenyl) amino)(phenyl)ethyl)carbamate	The title compound was synthesized according to the procedure B using A27	347.14
B28		tert-butyl (((3-chlorophenyl) amino)(3-methoxyphenyl)ethyl)carbamate	The title compound was synthesized according to the procedure B using A28	377.16

Results and Discussion

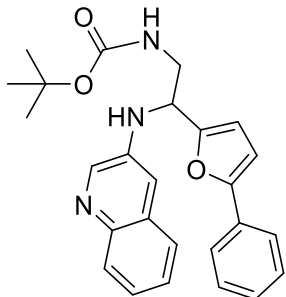
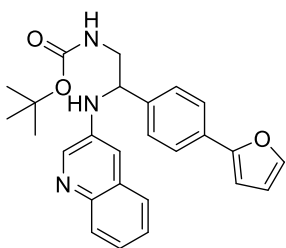
B29		tert-butyl ((3-chlorophenyl)amino)(4-methoxyphenyl)ethylcarbamate	The title compound was synthesized according to the procedure B using A29	377.16
B30		tert-butyl ((3-chlorophenyl)amino)(4-cyanophenyl)ethylcarbamate	The title compound was synthesized according to the procedure B using A30	372.14
B31		tert-butyl ((3-chlorophenyl)amino)(pyridin-3-yl)ethylcarbamate	The title compound was synthesized according to the procedure B using A31	348.14
B32		tert-butyl ((3-chlorophenyl)amino)(6-chloropyridin-3-yl)ethylcarbamate	The title compound was synthesized according to the procedure B using A32	382.10
B33		tert-butyl ((3-chlorophenyl)amino)(2-chloropyrimidin-5-yl)ethylcarbamate	The title compound was synthesized according to the procedure B using A33	383.10
B34		tert-butyl ((5-bromopyridin-2-yl)((3-chlorophenyl)amino)ethylcarbamate	The title compound was synthesized according to the procedure B using A34	428.05

Results and Discussion

		no)ethyl)carbamat e		
B35		tert-butyl (((3-chlorophenyl)amino)(quinolin-2-yl)ethyl)carbamat e	The title compound was synthesized according to the procedure B using A35	398.16
B36		tert-butyl (((3-chlorophenyl)amino)(quinolin-3-yl)ethyl)carbamat e	The title compound was synthesized according to the procedure B using A36	398.16
B37		tert-butyl (((3-chlorophenyl)amino)(quinolin-4-yl)methyl)carbamat ate	The title compound was synthesized according to the procedure B using A37	398.16
B38		tert-butyl (((3-chlorophenyl)amino)(quinolin-6-yl)ethyl)carbamat e	The title compound was synthesized according to the procedure B using A38	398.16
B39		tert-butyl ((quinolin-2-yl)(quinolin-3-ylamino)ethyl)carbamate	The title compound was synthesized according to the procedure B using A39	415.21

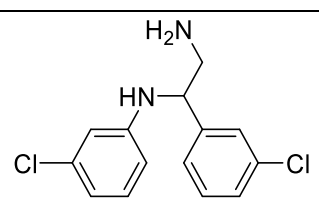
Results and Discussion

B40		tert-butyl (2-(3-methoxyphenyl)-2-(quinolin-3-ylamino)ethyl)carbamate	The title compound was synthesized according to the procedure B using A40	394.21
B41		tert-butyl (2-(4-bromophenyl)-2-(quinolin-3-ylamino)ethyl)carbamate	The title compound was synthesized according to the procedure B using A41	442.11
B42		tert-butyl (2-([1,1'-biphenyl]-4-yl)-2-(quinolin-3-ylamino)ethyl)carbamate	The title compound was synthesized according to the procedure B using A42	440.23
B43		tert-butyl (2-(4-(1H-1,2,4-triazol-1-yl)phenyl)-2-(quinolin-3-ylamino)ethyl)carbamate	The title compound was synthesized according to the procedure B using A43	431.21
B44		tert-butyl (2-(6-phenylpyridin-3-yl)-2-(quinolin-3-ylamino)ethyl)carbamate	The title compound was synthesized according to the procedure B using A44	441.22

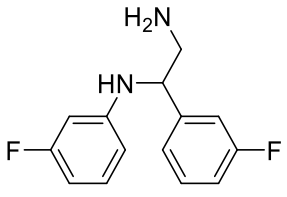
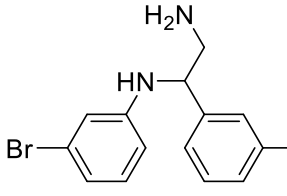
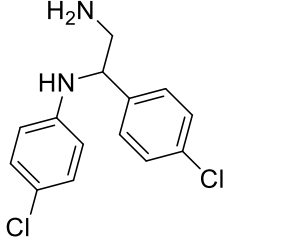
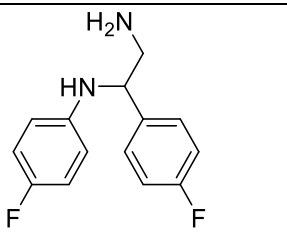
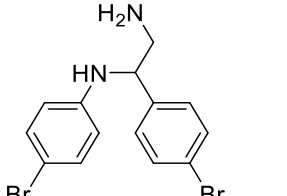
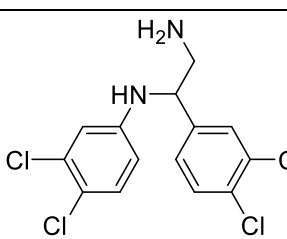
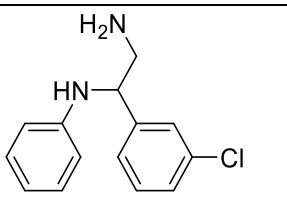
B45		tert-butyl (2-(5-phenylfuran-2-yl)-2-(quinolin-3-ylamino)ethyl)carbamate	The title compound was synthesized according to the procedure B using A45	430.21
B46		tert-butyl (2-(4-(furan-2-yl)phenyl)-2-(quinolin-3-ylamino)ethyl)carbamate	The title compound was synthesized according to the procedure B using A46	430.21

3.1.7.1.3 General procedure for the deprotection of the BOC-protected amino group(C5–C46) (Procedure C)

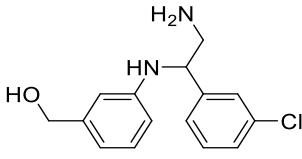
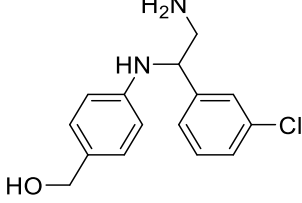
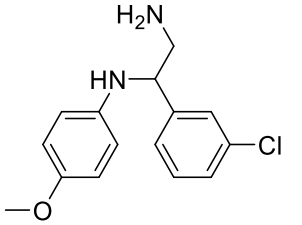
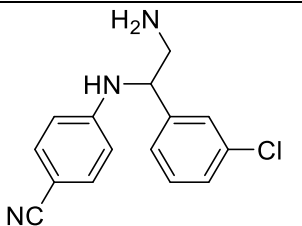
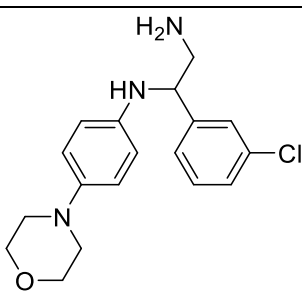
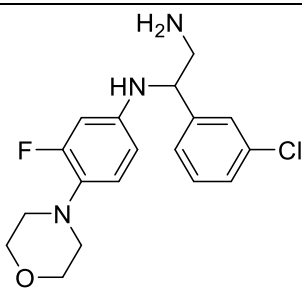
In a 250 mL round-bottomed flask, the BOC-protected derivative (10 mmol) was dissolved in dioxane(10 mL), and then conc. HCl was subsequently added(4 mL). The reaction mixture was left to stir for 2 h. After completion of the reaction (monitored by TLC), the mixture was evaporated till complete dryness under vacuum. The residue was partitioned between dichloromethane (150 mL) and 4M NaOH(50 mL), and then the aqueous layer was re-extracted using 3 portions of dichloromethane(150 mL). Organic layers were then collected and dried over anhydrous magnesium sulfate and evaporated under vacuum. The residue was then purified using preparative high-performance liquid chromatography (H₂O:acetonitrile + 0.05% formic acid, gradient 5% to 100% acetonitrile).

Cpd	Structure	IUPAC Name	Preparation Method	<i>m/z</i> : (<i>M</i> + <i>H</i>) ⁺ .
C5		<i>N</i> ',1-bis(3-chlorophenyl)ethane-1,2-diamine	The title compound was synthesized according to the procedure C using B5	281.11

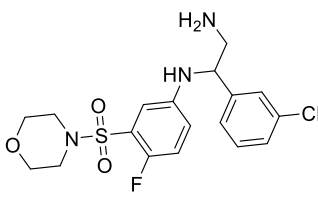
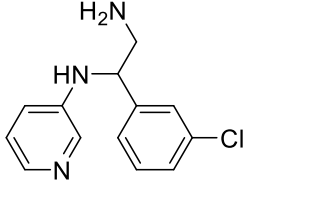
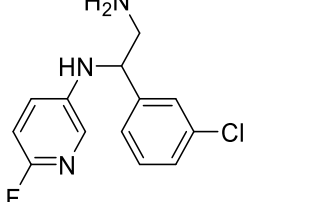
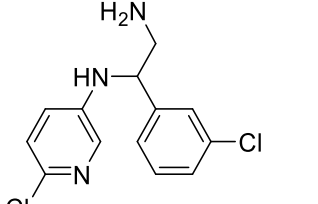
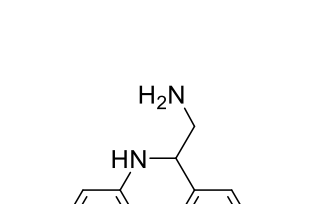
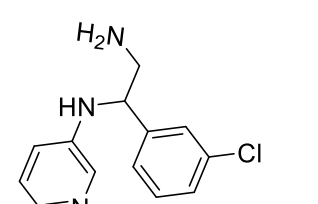
Results and Discussion

C6		<i>N</i> ¹ ,1-bis(3-fluorophenyl)ethane-1,2-diamine	The title compound was synthesized according to the procedure C using B6	249.16
C7		<i>N</i> ¹ ,1-bis(3-bromophenyl)ethane-1,2-diamine	The title compound was synthesized according to the procedure C using B7	371.00
C8		<i>N</i> ¹ ,1-bis(4-chlorophenyl)ethane-1,2-diamine	The title compound was synthesized according to the procedure C using B8	281.11
C9		<i>N</i> ¹ ,1-bis(4-fluorophenyl)ethane-1,2-diamine	The title compound was synthesized according to the procedure C using B9	249.16
C10		<i>N</i> ¹ ,1-bis(4-bromophenyl)ethane-1,2-diamine	The title compound was synthesized according to the procedure C using B10	371.00
C11		<i>N</i> ¹ ,1-bis(3,4-dichlorophenyl)ethane-1,2-diamine	The title compound was synthesized according to the procedure C using B11	351.02
C12		1-(3-chlorophenyl)- <i>N</i> ¹ -phenylethane-1,2-diamine	The title compound was synthesized according to the procedure C using B12	247.14

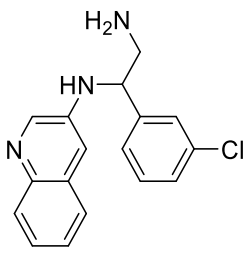
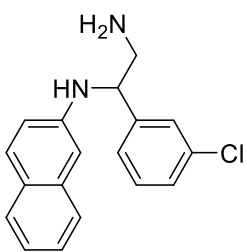
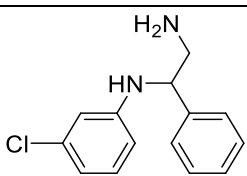
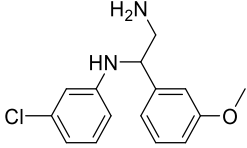
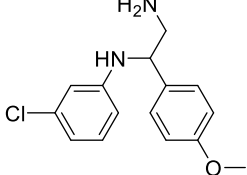
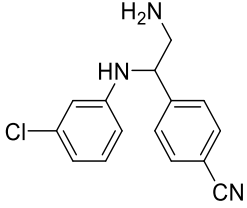
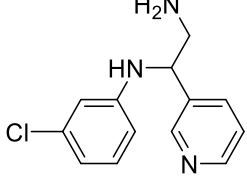
Results and Discussion

C13		(3-((2-amino-1-(3-chlorophenyl)ethyl)amino)phenyl)methanol	The title compound was synthesized according to the procedure C using B13	277.16
C14		(4-((2-amino-1-(3-chlorophenyl)ethyl)amino)phenyl)methanol	The title compound was synthesized according to the procedure C using B14	277.16
C15		1-(3-chlorophenyl)- <i>N</i> ¹ -(4-methoxyphenyl)ethane-1,2-diamine	The title compound was synthesized according to the procedure C using B15	277.16
C16		4-((2-amino-1-(3-chlorophenyl)ethyl)amino)benzonitrile	The title compound was synthesized according to the procedure C using B16	272.14
C17		1-(3-chlorophenyl)- <i>N</i> ¹ -(4-morpholinophenyl)ethane-1,2-diamine	The title compound was synthesized according to the procedure C using B17	332.20
C18		1-(3-chlorophenyl)- <i>N</i> ¹ -(3-fluoro-4-morpholinophenyl)ethane-1,2-diamine	The title compound was synthesized according to the procedure C using B18	350.19

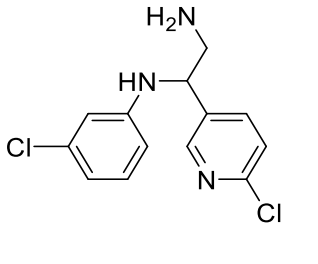
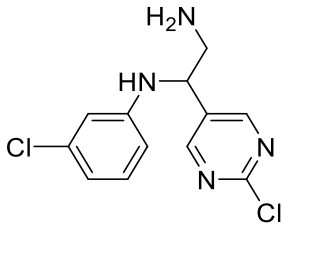
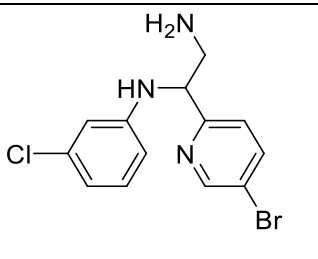
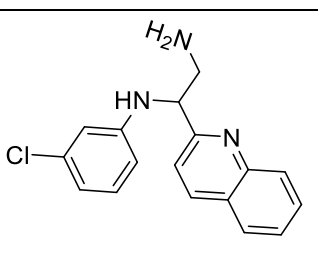
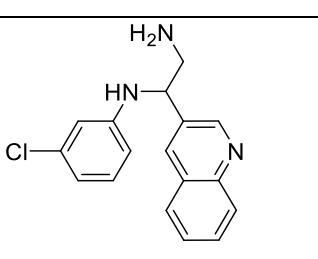
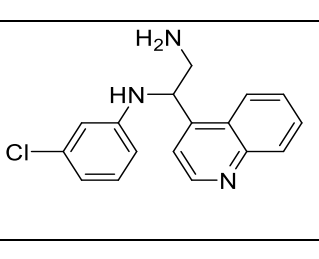
Results and Discussion

C19		1-(3-chlorophenyl)- <i>N</i> ¹ - (4-fluoro-3- (morpholinosulfonyl) phenyl)ethane-1,2- diamine	The title compound was synthesized according to the procedure C using B19	414.15
C20		1-(3-chlorophenyl)- <i>N</i> ¹ - (pyridin-3-yl) ethane- 1,2-diamine	The title compound was synthesized according to the procedure C using B20	248.14
C21		1-(3-chlorophenyl)- <i>N</i> ¹ - (6-fluoropyridin-3-yl) ethane-1,2-diamine	The title compound was synthesized according to the procedure C using B21	266.13
C22		1-(3-chlorophenyl)- <i>N</i> ¹ - (6-chloropyridin-3-yl) ethane-1,2-diamine	The title compound was synthesized according to the procedure C using B22	282.10
C23		1-(3-chlorophenyl)- <i>N</i> ¹ - (5-chloropyridin-3-yl) ethane-1,2-diamine	The title compound was synthesized according to the procedure C using B23	282.10
C24		<i>N</i> ¹ -(6-bromopyridin-3- yl)-1-(3-chlorophenyl) ethane-1,2-diamine	The title compound was synthesized according to the procedure C using B24	328.05

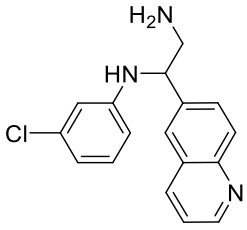
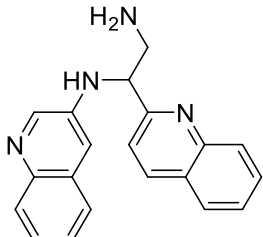
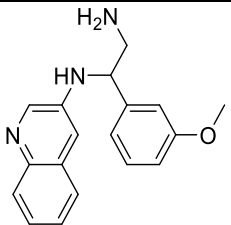
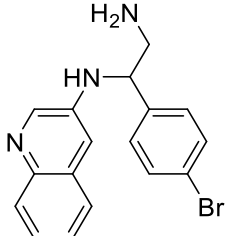
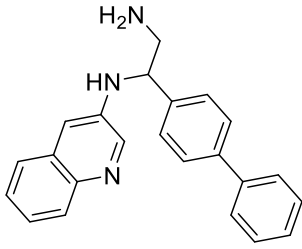
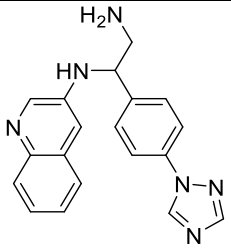
Results and Discussion

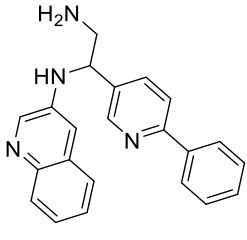
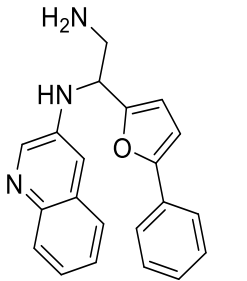
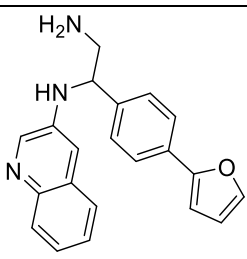
C25		1-(3-chlorophenyl)- <i>N</i> ¹ -(quinolin-3-yl) ethane-1,2-diamine	The title compound was synthesized according to the procedure C using B25	298.16
C26		1-(3-chlorophenyl)- <i>N</i> ¹ -(naphthalen-2-yl) ethane-1,2-diamine	The title compound was synthesized according to the procedure C using B26	297.16
C27		<i>N</i> ¹ -(3-chlorophenyl)-1-phenylethane-1,2-diamine	The title compound was synthesized according to the procedure C using B27	247.14
C28		<i>N</i> ¹ -(3-chlorophenyl)-1-(3-methoxyphenyl) ethane-1,2-diamine	The title compound was synthesized according to the procedure C using B28	277.16
C29		<i>N</i> ¹ -(3-chlorophenyl)-1-(4-methoxyphenyl) ethane-1,2-diamine	The title compound was synthesized according to the procedure C using B29	277.16
C30		4-(2-amino-1-((3-chlorophenyl)amino)ethyl)benzonitrile	The title compound was synthesized according to the procedure C using B30	272.14
C31		<i>N</i> ¹ -(3-chlorophenyl)-1-(pyridin-3-yl) ethane-1,2-diamine	The title compound was synthesized according to the procedure C using B31	248.14

Results and Discussion

C32		<i>N</i> ¹ -(3-chlorophenyl)-1-(6-chloropyridin-3-yl)ethane-1,2-diamine	The title compound was synthesized according to the procedure C using B32	282.10
C33		<i>N</i> ¹ -(3-chlorophenyl)-1-(2-chloropyrimidin-5-yl)ethane-1,2-diamine	The title compound was synthesized according to the procedure C using B33	283.10
C34		1-(5-bromopyridin-2-yl)- <i>N</i> ¹ -(3-chlorophenyl)ethane-1,2-diamine	The title compound was synthesized according to the procedure C using B34	328.05
C35		<i>N</i> ¹ -(3-chlorophenyl)-1-(quinolin-2-yl)ethane-1,2-diamine	The title compound was synthesized according to the procedure C using B35	298.16
C36		<i>N</i> ¹ -(3-chlorophenyl)-1-(quinolin-3-yl)ethane-1,2-diamine	The title compound was synthesized according to the procedure C using B36	298.16
C37		<i>N</i> ¹ -(3-chlorophenyl)-1-(quinolin-4-yl)ethane-1,2-diamine	The title compound was synthesized according to the procedure C using B37	298.16

Results and Discussion

C38		N^1 -(3-chlorophenyl)-1-(quinolin-6-yl) ethane-1,2-diamine	The title compound was synthesized according to the procedure C using B38	298.16
C39		1-(quinolin-2-yl)- N^1 -(quinolin-3-yl) ethane-1,2-diamine	The title compound was synthesized according to the procedure C using B39	315.21
C40		1-(3-methoxyphenyl)- N^1 -(quinolin-3-yl) ethane-1,2-diamine	The title compound was synthesized according to the procedure C using B40	294.21
C41		1-(4-bromophenyl)- N^1 -(quinolin-3-yl) ethane-1,2-diamine	The title compound was synthesized according to the procedure C using B41	342.11
C42		1-([1,1'-biphenyl]-4-yl)- N^1 -(quinolin-3-yl) ethane-1,2-diamine	The title compound was synthesized according to the procedure C using B42	340.23
C43		1-(4-(1H-1,2,4-triazol-1-yl)phenyl)- N^1 -(quinolin-3-yl) ethane-1,2-diamine	The title compound was synthesized according to the procedure C using B43	331.21

C44		1-(6-phenylpyridin-3-yl)- <i>N</i> ¹ -(quinolin-3-yl)ethane-1,2-diamine	The title compound was synthesized according to the procedure C using B44	341.22
C45		1-(5-phenylfuran-2-yl)- <i>N</i> ¹ -(quinolin-3-yl)ethane-1,2-diamine	The title compound was synthesized according to the procedure C using B45	330.21
C46		1-(4-(furan-2-yl)phenyl)- <i>N</i> ¹ -(quinolin-3-yl)ethane-1,2-diamine	The title compound was synthesized according to the procedure C using B46	330.21

3.1.7.1.4 General procedure for the synthesis of the imidazolidinone derivatives(D5–D46) (Procedure D)

In a 250 mL round-bottomed flask, ethane-1,2-di-amine derivative (10 mmol) was dissolved in dichloromethane(50 mL), and then triphosgene (1.18g, 4 mmol, 0.4 equiv) was added along with triethylamine(12 drops). The reaction mixture was left to stir for 1 h. After completion of the reaction (monitored by TLC), the mixture was partitioned between dichloromethane (150 mL) and H₂O (50 mL), and then the aqueous layer was re-extracted using 3 portions of dichloromethane (150 mL). Organic layers were then collected and dried over anhydrous magnesium sulfate and evaporated under vacuum. The residue was then purified using preparative high-performance liquid chromatography (H₂O:acetonitrile + 0.05% formic acid, gradient 5% to 100% acetonitrile).

1,5-Bis(3-chlorophenyl)imidazolidin-2-one (D5): The title compound was synthesized according to the procedure D using **C5**, yield: 82%, white solid. ¹H NMR (500 MHz, acetone) δ 7.83 (d, *J* = 2.2 Hz, 1H), 7.46 (d, *J* = 2.0 Hz, 1H), 7.43 – 7.34 (m, 2H), 7.34 – 7.26 (m, 2H), 7.19 (t, *J* = 8.1 Hz, 1H), 6.95 (dd, *J* = 8.0, 2.0 Hz, 1H), 6.31 (s, 1H), 5.57 (dd, *J* = 9.2, 4.7 Hz,

1H), 4.05 (t, $J = 9.1$ Hz, 1H), 3.29 (dd, $J = 9.0, 4.8$ Hz, 1H). ^{13}C NMR (126 MHz, acetone) δ 159.67, 144.53, 141.98, 135.19, 134.53, 131.64, 130.62, 128.92, 127.12, 125.56, 122.85, 119.95, 117.90, 59.50, 47.23. HRMS (ESI): calculated for ($\text{C}_{15}\text{H}_{12}\text{Cl}_2\text{N}_2\text{O}$) 307.03949, found 307.03888 (M+H)⁺

1,5-Bis(3-fluorophenyl) imidazolidin-2-one (D6): The title compound was synthesized according to the procedure D using **C6**, yield: 88%, white solid. ^1H NMR (500 MHz, acetone) δ 7.75 (d, $J = 2.2$ Hz, 1H), 7.49 (d, $J = 2.0$ Hz, 1H), 7.40 – 7.36 (m, 2H), 7.09 – 7.13 (m, 2H), 7.02 (t, $J = 8.1$ Hz, 1H), 6.97 (dd, $J = 8.0, 2.0$ Hz, 1H), 6.94 (s, 1H), 5.50 (dd, $J = 9.2, 4.7$ Hz, 1H), 3.83 (t, $J = 9.1$ Hz, 1H), 3.58 (dd, $J = 9.0, 4.8$ Hz, 1H). ^{13}C NMR (126 MHz, acetone) δ 163.01 (d, $J = 245.4$ Hz) 162.70 (d, $J = 243.6$ Hz), 158.76, 140.77 (d, $J = 7.5$ Hz), 130.55 (d, $J = 10.4$ Hz), 130.11 (d, $J = 8.3$ Hz), 123.10 (d, $J = 9.3$ Hz), 122.57 (d, $J = 2.7$ Hz), 116.17 (d, $J = 2.9$ Hz), 113.95 (d, $J = 21.3$ Hz), 113.59 (d, $J = 22.8$ Hz), 113.02 (d, $J = 21.2$ Hz), 110.17 (d, $J = 26.0$ Hz), 57.39, 48.82. HRMS (ESI): calculated for ($\text{C}_{15}\text{H}_{12}\text{F}_2\text{N}_2\text{O}$) 275.09777, found 275.09821 (M+H)⁺

1,5-Bis(3-bromophenyl)imidazolidin-2-one (D7): The title compound was synthesized according to the procedure D using **C7**, yield: 91%, white solid. ^1H NMR (500 MHz, DMSO) δ 7.89 (t, $J = 2.0$ Hz, 1H), 7.55 (t, $J = 1.8$ Hz, 1H), 7.46 (dt, $J = 6.9, 2.1$ Hz, 1H), 7.31 (dd, $J = 9.6, 7.6$ Hz, 3H), 7.25 – 7.21 (m, 1H), 7.14 (t, $J = 8.0$ Hz, 1H), 7.10 (dt, $J = 8.0, 1.5$ Hz, 1H), 5.53 (dd, $J = 9.2, 4.8$ Hz, 1H), 3.87 (t, $J = 9.2$ Hz, 1H), 3.10 (dd, $J = 9.2, 4.8$ Hz, 1H). ^{13}C NMR (126 MHz, DMSO) δ 158.64, 143.59, 140.73, 131.16, 130.79, 130.33, 128.98, 125.03, 124.79, 122.11, 121.64, 121.53, 117.50, 57.61, 45.96. HRMS (ESI): calculated for ($\text{C}_{15}\text{H}_{12}\text{Br}_2\text{N}_2\text{O}$) 396.93464, found 396.93579 (M+H)⁺

1,5-Bis(4-chlorophenyl)imidazolidin-2-one(D8): The title compound was synthesized according to the procedure D using **C8**, yield: 94%, white solid. ^1H NMR (500 MHz, acetone) δ 7.59 – 7.54 (m, 2H), 7.43 – 7.41 (m, 2H), 7.39 – 7.35 (m, 4H), 6.24 (s, 1H), 5.52 (dd, $J = 9.1, 5.1$ Hz, 1H), 4.01 (t, $J = 9.0$ Hz, 1H), 3.24 (dd, $J = 8.9, 5.1$ Hz, 1H). ^{13}C NMR (126 MHz, acetone) δ 158.73, 142.31, 136.82, 132.82, 132.14, 128.55, 122.08, 122.02, 114.24, 58.53, 46.27. HRMS (ESI): calculated for ($\text{C}_{15}\text{H}_{12}\text{Cl}_2\text{N}_2\text{O}$) 307.03949, found 307.03878 (M+H)⁺

1,5-Bis(4-fluorophenyl)imidazolidin-2-one(D9): The title compound was synthesized according to the procedure D using **C9**, yield: 90%, white solid. ^1H NMR (500 MHz, DMSO) δ 7.42 – 7.34 (m, 4H), 7.18 – 7.13 (m, 2H), 7.11 (s, 1H), 7.07 – 7.01 (m, 2H), 5.48 (dd, $J = 9.0, 5.8$ Hz, 1H), 3.83 (t, $J = 9.0$ Hz, 1H), 3.08 (ddd, $J = 9.1, 5.9, 1.1$ Hz, 1H). ^{13}C NMR (126 MHz,

DMSO) δ 161.56 (d, $J = 243.6$ Hz), 159.14, 157.68 (d, $J = 239.5$ Hz), 136.97 (d, $J = 3.2$ Hz), 135.47 (d, $J = 2.8$ Hz), 128.43 (d, $J = 8.3$ Hz), 121.75 (d, $J = 7.8$ Hz), 115.62 (d, $J = 21.6$ Hz), 114.96 (d, $J = 22.1$ Hz), 58.23, 46.31. HRMS (ESI): calculated for (C₁₅H₁₂F₂N₂O) 275.09777, found 275.09805 (M+H)⁺

1,5-Bis(4-bromophenyl)imidazolidin-2-one(D10): The title compound was synthesized according to the procedure D using **C10**, yield: 92%, white solid. ¹H NMR (500 MHz, acetone) δ 7.55 – 7.51 (m, 2H), 7.49 – 7.44 (m, 2H), 7.38 – 7.32 (m, 4H), 6.28 (s, 1H), 5.51 (dd, $J = 9.1$, 5.1 Hz, 1H), 4.02 (t, $J = 9.0$ Hz, 1H), 3.26 (dd, $J = 8.9$, 5.1 Hz, 1H). ¹³C NMR (126 MHz, acetone) δ 159.79, 141.32, 139.84, 132.83, 132.04, 129.25, 122.09, 122.04, 115.24, 59.57, 47.26. HRMS (ESI): calculated for (C₁₅H₁₂Br₂N₂O) 396.93464, found 396.93579 (M+H)⁺

1,5-Bis(3,4-dichlorophenyl)imidazolidin-2-one(D11): The title compound was synthesized according to the procedure D using **C11**, yield: 89%, white solid. ¹H NMR (500 MHz, acetone) δ 7.49 (d, $J = 1.5$ Hz, 4H), 7.33 (d, $J = 8.8$ Hz, 2H), 7.28 (dd, $J = 8.8$, 2.5 Hz, 1H), 5.61 (dd, $J = 9.8$, 6.1 Hz, 1H), 4.37 (t, $J = 10.3$ Hz, 1H), 3.91 (dd, $J = 10.7$, 6.1 Hz, 1H). ¹³C NMR (126 MHz, acetone) 154.31, 142.27, 141.80, 140.42, 136.67, 134.19, 133.26, 131.29, 130.52, 128.52, 127.27, 125.13, 121.07, 55.78, 47.19. HRMS (ESI): calculated for (C₁₅H₁₀Cl₄N₂O) 376.95914, found 376.95792 (M+H)⁺

5-(3-Chlorophenyl)-1-phenylimidazolidin-2-one(D12): The title compound was synthesized according to the procedure D using **C12**, yield: 91%, white solid. ¹H NMR (500 MHz, acetone) δ 7.59 – 7.54 (m, 2H), 7.43 – 7.27 (m, 5H), 7.28 – 7.15 (m, 2H), 6.23 (s, 1H), 5.51 (dd, $J = 9.1$, 5.1 Hz, 1H), 4.01 (t, $J = 9.0$ Hz, 1H), 3.22 (dd, $J = 8.9$, 5.1 Hz, 1H). ¹³C NMR (126 MHz, DMSO) δ 158.64, 143.59, 140.73, 131.16, 130.79, 128.98, 125.03, 124.79, 122.11, 121.53, 117.50, 57.61, 45.96. HRMS (ESI): calculated for (C₁₅H₁₃ClN₂O) 273.07947, found 273.07864 (M+H)⁺

5-(3-Chlorophenyl)-1-(3-(hydroxymethyl)phenyl)imidazolidin-2-one(D13): The title compound was synthesized according to the procedure D using **C13**, yield: 84%, white solid. ¹H NMR (500 MHz, acetone) δ 12.91 (s, 1H), 7.83 (d, $J = 2.2$ Hz, 1H), 7.46 (d, $J = 2.0$ Hz, 1H), 7.43 – 7.34 (m, 2H), 7.34 – 7.26 (m, 2H), 7.19 (t, $J = 8.1$ Hz, 1H), 6.95 (dd, $J = 8.0$, 2.0 Hz, 1H), 6.31 (s, 1H), 5.57 (dd, $J = 9.2$, 4.7 Hz, 1H), 5.20 (d, $J = 1.6$ Hz, 2H), 4.05 (t, $J = 9.1$ Hz, 1H), 3.29 (dd, $J = 9.0$, 4.8 Hz, 1H). ¹³C NMR (126 MHz, acetone) δ 159.67, 144.53, 141.98, 135.19, 134.53, 131.64, 130.62, 128.92, 127.12, 125.56, 122.85, 119.95, 117.90, 68.93, 59.50, 47.23. HRMS (ESI): calculated for (C₁₆H₁₅ClN₂O₂) 303.09003, found 303.09248 (M+H)⁺

5-(3-Chlorophenyl)-1-(4-(hydroxymethyl)phenyl)imidazolidin-2-one(D14): The title compound was synthesized according to the procedure D using **C14**, yield: 88%, white solid. ¹H NMR (500 MHz, DMSO) δ 12.89 (s, 1H), 7.66 (t, *J* = 2.0 Hz, 1H), 7.27 – 7.16 (m, 4H), 6.97 – 6.93 (m, 1H), 6.91 – 6.87 (m, 2H), 5.57 (dd, *J* = 9.2, 4.7 Hz, 1H), 5.20 (d, *J* = 1.6 Hz, 2H), 4.05 (t, *J* = 9.1 Hz, 1H), 3.29 (dd, *J* = 9.0, 4.8 Hz, 1H). ¹³C NMR (126 MHz, DMSO) δ 159.43, 154.98, 143.78, 133.30, 132.08, 130.72, 127.73, 126.39, 125.10, 121.87, 119.89, 113.97, 113.45, 68.60, 55.06, 46.16. HRMS (ESI): calculated for (C₁₆H₁₅ClN₂O₂) 303.09003, found 303.09248 (M+H)⁺

5-(3-Chlorophenyl)-1-(4-methoxyphenyl)imidazolidin-2-one(D15): The title compound was synthesized according to the procedure D using **C15**, yield: 92%, white solid. ¹H NMR (500 MHz, DMSO) δ 6.55 – 6.42 (m, 6H), 6.14 (s, 1H), 5.98 – 5.92 (m, 2H), 4.60 (dd, *J* = 9.0, 6.0 Hz, 1H), 3.01 – 2.95 (m, 1H), 2.81 (s, 3H), 2.24 (ddd, *J* = 9.2, 6.0, 1.1 Hz, 1H). ¹³C NMR (126 MHz, DMSO) δ 159.43, 154.98, 143.78, 133.30, 132.08, 130.72, 127.73, 126.39, 125.10, 121.87, 119.89, 113.97, 113.45, 58.60, 55.06, 46.16. HRMS (ESI): calculated for (C₁₆H₁₅ClN₂O₂) 303.09003, found 303.08868 (M+H)⁺

4-(5-(3-Chlorophenyl)-2-oxoimidazolidin-1-yl)benzotrile(D16): The title compound was synthesized according to the procedure D using **C16**, yield: 92%, white solid. ¹H NMR (500 MHz, acetone) δ 7.85 – 7.69 (m, 2H), 7.66 – 7.51 (m, 2H), 7.51 – 7.27 (m, 4H), 6.52 (d, *J* = 6.9 Hz, 1H), 5.62 (dt, *J* = 8.7, 4.2 Hz, 1H), 4.09 (q, *J* = 8.8 Hz, 1H), 3.32 (dt, *J* = 8.6, 4.1 Hz, 1H). ¹³C NMR (126 MHz, acetone) δ 154.42, 151.26, 144.23, 140.65, 137.21, 135.81, 132.83, 129.11, 125.54, 117.49, 110.10, 57.01, 49.06. HRMS (ESI): calculated for (C₁₆H₁₂ClN₃O) 298.07471, found 298.07327 (M+H)⁺

5-(3-Chlorophenyl)-1-(4-morpholinophenyl)imidazolidin-2-one(D17): The title compound was synthesized according to the procedure D using **C17**, yield: 85%, white solid. ¹H NMR (500 MHz, DMSO) δ 7.39 – 7.33 (m, 2H), 7.29 (t, *J* = 8.7 Hz, 2H), 7.24 (d, *J* = 8.8 Hz, 2H), 6.94 (s, 1H), 6.80 (d, *J* = 8.7 Hz, 2H), 5.42 (dd, *J* = 9.1, 5.9 Hz, 1H), 3.81 (t, *J* = 9.1 Hz, 1H), 3.68 (t, *J* = 4.8 Hz, 4H), 3.06 (dd, *J* = 6.1, 2.9 Hz, 1H), 2.97 (t, *J* = 4.8 Hz, 4H). ¹³C NMR (126 MHz, DMSO) δ 159.52, 146.78, 143.98, 133.33, 131.25, 130.74, 127.72, 126.37, 125.10, 121.40, 115.32, 66.11, 58.56, 48.80, 46.22. HRMS (ESI): calculated for (C₁₉H₂₀ClN₃O₂) 358.13223, found 358.13089 (M+H)⁺

5-(3-Chlorophenyl)-1-(3-fluoro-4-morpholinophenyl)imidazolidin-2-one(D18): The title compound was synthesized according to the procedure D using **C18**, yield: 89%, white solid.

^1H NMR (500 MHz, acetone) δ 7.53-7.48 (m, 3H), 7.44 – 7.33 (m, 3H), 7.23 – 7.15 (m, 1H), 6.96 (t, $J = 9.2$ Hz, 1H), 5.76 (dd, $J = 9.8, 6.0$ Hz, 1H), 4.62 (t, $J = 10.2$ Hz, 1H), 3.90 (dd, $J = 10.7, 6.0$ Hz, 1H), 3.79 – 3.70 (m, 4H), 3.03 – 2.99 (m, 4H). ^{13}C NMR (126 MHz, acetone) δ 156.71 (d, $J = 245.4$ Hz), 154.74, 150.66, 143.78, 139.91 (d, $J = 8.5$ Hz), 134.22, 132.11 (d, $J = 10.2$ Hz), 131.69, 129.70, 128.12, 119.78 (d, $J = 3.2$ Hz), 118.62 (d, $J = 4.1$ Hz), 113.97 (d, $J = 25.0$ Hz), 67.27, 57.60, 51.58, 48.77. HRMS (ESI): calculated for ($\text{C}_{19}\text{H}_{19}\text{ClFN}_3\text{O}_2$) 376.12281, found 376.12397 (M+H)⁺

5-(3-Chlorophenyl)-1-(4-fluoro-3-(morpholin sulfonyl)phenyl)imidazolidin-2-one(D19):

The title compound was synthesized according to the procedure D using **C19**, yield: 81%, white solid. ^1H NMR (500 MHz, acetone) δ 7.81 (dd, $J = 5.8, 2.8$ Hz, 1H), 7.74 (t, $J = 1.9$ Hz, 1H), 7.68 (dt, $J = 7.6, 1.6$ Hz, 1H), 7.49 – 7.37 (m, 5H), 5.90 (dd, $J = 9.7, 6.8$ Hz, 1H), 4.70 (t, $J = 10.2$ Hz, 1H), 3.97 (dd, $J = 10.7, 6.8$ Hz, 1H), 3.68 – 3.56 (m, 4H), 2.98 – 2.85 (m, 4H). ^{13}C NMR (126 MHz, acetone) δ 156.87 (d, $J = 254.6$ Hz), 154.32, 145.98, 142.54, 138.92, 135.23 (d, $J = 3.0$ Hz), 132.55, 130.17 (d, $J = 8.5$ Hz), 128.93, 128.50, 125.90, 124.01 (d, $J = 16.3$ Hz), 119.17 (d, $J = 23.9$ Hz), 66.62, 57.78, 48.80, 46.63. HRMS (ESI): calculated for ($\text{C}_{19}\text{H}_{19}\text{ClFN}_3\text{O}_4\text{S}$) 440.08471, found 440.08646 (M+H)⁺

1-(3-Chlorophenyl)-5-(pyridin-3-yl)imidazolidin-2-one(D20): The title compound was synthesized according to the procedure D using **C20**, yield: 88%, white solid. ^1H NMR (500 MHz, DMSO) δ 8.59 (q, $J = 6.7$ Hz, 1H), 7.93 – 7.79 (m, 3H), 7.61 (t, $J = 8.4$ Hz, 1H), 7.42 (d, $J = 8.2$ Hz, 1H), 7.35 – 7.26 (m, 2H), 7.14 – 6.99 (m, 1H), 5.74 (dd, $J = 12.0, 5.9$ Hz, 1H), 3.88 (q, $J = 9.0$ Hz, 1H), 3.29 (td, $J = 9.1, 4.9$ Hz, 1H). ^{13}C NMR (126 MHz, DMSO) δ 158.61, 152.22, 150.42, 145.29, 139.22, 137.24, 135.13, 133.19, 129.83, 127.61, 119.28, 118.28, 55.89, 48.33. HRMS (ESI): calculated for ($\text{C}_{15}\text{H}_{13}\text{ClN}_2\text{O}$) 273.07947, found 273.07882 (M+H)⁺

5-(3-Chlorophenyl)-1-(6-fluoropyridin-3-yl)imidazolidin-2-one(D21): The title compound was synthesized according to the procedure D using **C21**, yield: 89%, white solid. ^1H NMR (500 MHz, acetone) δ 8.24 (ddd, $J = 9.2, 6.9, 2.9$ Hz, 1H), 7.47 (d, $J = 2.0$ Hz, 1H), 7.27 (dt, $J = 7.4, 1.5$ Hz, 1H), 7.20 – 7.09 (m, 4H), 7.01 (dd, $J = 8.9, 3.3$ Hz, 1H), 5.84 (dd, $J = 9.7, 6.5$ Hz, 1H), 4.72 (t, $J = 10.2$ Hz, 1H), 3.95 (dd, $J = 10.7, 6.5$ Hz, 1H). ^{13}C NMR (126 MHz, acetone) δ 160.41 (d, $J = 236.2$ Hz), 151.74, 143.28, 142.93 (d, $J = 16.0$ Hz), 140.25, 139.18 (d, $J = 8.3$ Hz), 137.54, 135.51 (d, $J = 4.7$ Hz), 132.90, 129.09, 124.07, 111.67 (d, $J = 39.5$ Hz), 58.65, 47.18. HRMS (ESI): calculated for ($\text{C}_{14}\text{H}_{11}\text{FCIN}_3\text{O}$) 292.06529, found 292.06721 (M+H)⁺

5-(3-Chlorophenyl)-1-(6-chloropyridin-3-yl)imidazolidin-2-one(D22): The title compound was synthesized according to the procedure D using **C22**, yield: 81%, white solid. ¹H NMR (500 MHz, DMSO) δ 8.41 (q, *J* = 6.7 Hz, 1H), 7.81 – 7.62 (m, 2H), 7.52 (t, *J* = 8.4 Hz, 1H), 7.39 (d, *J* = 8.2 Hz, 1H), 7.29 – 7.19 (m, 2H), 7.05 – 6.91 (m, 1H), 5.69 (dd, *J* = 12.0, 5.9 Hz, 1H), 3.85 (q, *J* = 9.0 Hz, 1H), 3.19 (td, *J* = 9.1, 4.9 Hz, 1H). ¹³C NMR (126 MHz, DMSO) δ 157.57, 150.17, 149.88, 141.25, 136.66, 134.77, 134.03, 132.13, 126.75, 124.59, 118.13, 117.40, 54.68, 46.17. HRMS (ESI): calculated for (C₁₄H₁₁Cl₂N₃O) 308.03574, found 308.03430 (M+H)⁺

5-(3-Chlorophenyl)-1-(5-chloropyridin-3-yl)imidazolidin-2-one(D23): The title compound was synthesized according to the procedure D using **C23**, yield: 89%, white solid. ¹H NMR (500 MHz, DMSO) δ 8.44 (q, *J* = 6.7 Hz, 1H), 7.89 – 7.81 (m, 2H), 7.62 (t, *J* = 8.4 Hz, 1H), 7.59 (d, *J* = 8.2 Hz, 1H), 7.39 – 7.31 (m, 2H), 7.01 – 6.95 (m, 1H), 5.59 (dd, *J* = 12.0, 5.9 Hz, 1H), 3.79 (q, *J* = 9.0 Hz, 1H), 3.27 (td, *J* = 9.1, 4.9 Hz, 1H). ¹³C NMR (126 MHz, DMSO) δ 157.57, 150.17, 149.88, 141.25, 136.66, 134.77, 134.03, 132.13, 126.75, 124.59, 118.13, 117.40, 54.68, 46.17. HRMS (ESI): calculated for (C₁₄H₁₁Cl₂N₃O) 308.03574, found 308.03430 (M+H)⁺

1-(6-Bromopyridin-3-yl)-5-(3-chlorophenyl)imidazolidin-2-one(D24): The title compound was synthesized according to the procedure D using **C24** yield: 82%, white solid. ¹H NMR (500 MHz, DMSO) δ 8.58 (q, *J* = 3.0 Hz, 1H), 8.22 (dt, *J* = 7.8, 4.2 Hz, 1H), 7.95 (dt, *J* = 4.3, 2.1 Hz, 1H), 7.53 (dq, *J* = 7.8, 3.6 Hz, 2H), 7.43 – 7.31 (m, 2H), 7.06 (ddt, *J* = 8.1, 4.6, 2.0 Hz, 1H), 5.40 (dq, *J* = 8.1, 4.1 Hz, 1H), 3.72 – 3.65 (m, 1H), 3.33 (dq, *J* = 8.2, 4.1 Hz, 1H). ¹³C NMR (126 MHz, DMSO) δ 156.49, 152.56, 144.31, 138.19, 135.03, 133.14, 132.18, 128.70, 125.42, 121.32, 119.26, 118.54, 58.51, 47.12. HRMS (ESI): calculated for (C₁₄H₁₁BrClN₃O) 353.98040, found 353.98148 (M+H)⁺

5-(3-Chlorophenyl)-1-(quinolin-3-yl)imidazolidin-2-one(D25): The title compound was synthesized according to the procedure D using **C25**, yield: 90%, white solid. ¹H NMR (500 MHz, DMSO) δ 9.14 (d, *J* = 2.5 Hz, 1H), 8.16 (d, *J* = 2.5 Hz, 1H), 7.88 (d, *J* = 8.5 Hz, 1H), 7.79 (d, *J* = 8.1 Hz, 1H), 7.55 (dt, *J* = 40.3, 7.1 Hz, 3H), 7.44 (s, 1H), 7.40 – 7.28 (m, 3H), 5.75 (dd, *J* = 9.3, 5.6 Hz, 1H), 3.96 (t, *J* = 9.2 Hz, 1H), 3.22 (dd, *J* = 8.9, 5.5 Hz, 1H). ¹³C NMR (126 MHz, DMSO) δ 158.92, 144.84, 143.51, 142.97, 133.51, 132.98, 130.95, 128.47, 128.06, 127.82, 127.59, 127.36, 127.02, 126.55, 125.07, 122.45, 57.69, 46.26. HRMS (ESI): calculated for (C₁₈H₁₄ClN₃O) 324.08674, found 324.08850 (M+H)⁺

5-(3-Chlorophenyl)-1-(naphthalen-2-yl)imidazolidin-2-one(D26): The title compound was synthesized according to the procedure D using **C26**, yield: 78%, white solid. ^1H NMR (500 MHz, DMSO) δ 7.81 (t, $J = 7.5$ Hz, 2H), 7.79 – 7.68 (m, 4H), 7.59 – 7.45 (m, 3H), 7.38 – 7.29 (m, 3H), 5.84 (dd, $J = 9.7, 6.1$ Hz, 1H), 4.59 (t, $J = 10.1$ Hz, 1H), 3.81 – 3.69 (m, 1H). ^{13}C NMR (126 MHz, DMSO) δ 158.15, 148.19, 147.09, 145.08, 142.25, 134.43, 133.13, 132.51, 131.11, 129.19, 128.02, 127.01, 126.36, 126.07, 124.19, 122.69, 121.84, 56.82, 48.08. HRMS (ESI): calculated for ($\text{C}_{19}\text{H}_{15}\text{ClN}_2\text{O}$) 323.09512, found 323.09619 (M+H) $^+$

1-(3-Chlorophenyl)-5-phenylimidazolidin-2-one(D27): The title compound was synthesized according to the procedure D using **C27**, yield: 92%, white solid. ^1H NMR (500 MHz, acetone) δ 7.51 – 7.44 (m, 2H), 7.41 – 7.30 (m, 5H), 7.28 – 7.17 (m, 2H), 6.28 (s, 1H), 5.51 (dd, $J = 9.1, 5.1$ Hz, 1H), 4.01 (t, $J = 9.0$ Hz, 1H), 3.22 (dd, $J = 8.9, 5.1$ Hz, 1H). ^{13}C NMR (126 MHz, DMSO) δ 157.54, 144.69, 141.72, 132.16, 131.74, 126.97, 125.33, 123.59, 122.11, 121.63, 116.50, 57.61, 45.96. HRMS (ESI): calculated for ($\text{C}_{15}\text{H}_{13}\text{ClN}_2\text{O}$) 273.07947, found 273.07857 (M+H) $^+$

1-(3-Chlorophenyl)-5-(3-methoxyphenyl)imidazolidin-2-one(D28): The title compound was synthesized according to the procedure D using **C28**, yield: 91%, white solid. ^1H NMR (500 MHz, DMSO) δ 7.70 (d, $J = 2.2$ Hz, 1H), 7.30 – 7.17 (m, 4H), 6.96 (dt, $J = 6.9, 1.7$ Hz, 1H), 6.89 – 6.80 (m, 3H), 5.46 (dd, $J = 9.2, 4.9$ Hz, 1H), 3.85 (t, $J = 9.1$ Hz, 1H), 3.71 (s, 3H), 3.08 (dd, $J = 9.1, 4.9$ Hz, 1H). ^{13}C NMR (126 MHz, acetone) δ 159.67, 144.53, 141.98, 135.19, 134.53, 131.64, 130.62, 128.92, 127.12, 125.56, 122.85, 119.95, 117.90, 59.93, 58.50, 47.23. HRMS (ESI): calculated for ($\text{C}_{16}\text{H}_{15}\text{ClN}_2\text{O}_2$) 303.09003, found 303.08862 (M+H) $^+$

1-(3-Chlorophenyl)-5-(4-methoxyphenyl)imidazolidin-2-one(D29): The title compound was synthesized according to the procedure D using **C29**, yield: 94%, white solid. ^1H NMR (500 MHz, DMSO) δ 7.66 (t, $J = 2.0$ Hz, 1H), 7.27 – 7.16 (m, 5H), 6.97 – 6.93 (m, 1H), 6.91 – 6.87 (m, 2H), 5.50 – 5.36 (m, 1H), 3.82 (t, $J = 9.1$ Hz, 1H), 3.71 (s, 3H), 3.05 (dd, $J = 8.9, 5.3$ Hz, 1H). ^{13}C NMR (126 MHz, DMSO) δ 159.43, 154.98, 143.78, 133.30, 132.08, 130.72, 127.73, 126.39, 125.10, 121.87, 119.89, 113.97, 113.45, 58.60, 55.06, 46.16. HRMS (ESI): calculated for ($\text{C}_{16}\text{H}_{15}\text{ClN}_2\text{O}_2$) 303.09003, found 303.08862 (M+H) $^+$

4-(3-(3-Chlorophenyl)-2-oxoimidazolidin-4-yl)benzotrile(D30): The title compound was synthesized according to the procedure D using **C30**, yield: 94%, white solid. ^1H NMR (500 MHz, DMSO) δ 7.66 (t, $J = 2.0$ Hz, 1H), 7.27 – 7.16 (m, 4H), 6.97 – 6.93 (m, 1H), 6.91 – 6.87 (m, 2H), 5.57 (dd, $J = 9.2, 4.7$ Hz, 1H), 4.05 (t, $J = 9.1$ Hz, 1H), 3.29 (dd, $J = 9.0, 4.8$ Hz, 1H).

^{13}C NMR (126 MHz, acetone) δ 155.41, 153.16, 149.13, 147.61, 139.21, 137.21, 135.23, 129.61, 127.14, 119.89, 111.12, 57.01, 49.06. HRMS (ESI): calculated for ($\text{C}_{16}\text{H}_{12}\text{ClN}_3\text{O}$) 358.13223, found 358.13089 ($\text{M}+\text{H}$)⁺

1-(3-Chlorophenyl)-5-(pyridin-3-yl)imidazolidin-2-one(D31): The title compound was synthesized according to the procedure D using **C31**, yield: 83%, white solid. ^1H NMR (500 MHz, DMSO) δ 8.41 (q, $J = 6.7$ Hz, 1H), 7.82 – 7.61 (m, 3H), 7.50 (t, $J = 8.4$ Hz, 1H), 7.35 (d, $J = 8.2$ Hz, 1H), 7.29 – 7.19 (m, 2H), 7.05 – 6.91 (m, 1H), 5.69 (dd, $J = 12.0, 5.9$ Hz, 1H), 3.85 (q, $J = 9.0$ Hz, 1H), 3.19 (td, $J = 9.1, 4.9$ Hz, 1H). ^{13}C NMR (126 MHz, DMSO) δ 157.53, 150.19, 149.84, 141.21, 136.62, 134.74, 134.33, 132.23, 126.95, 124.59, 118.13, 117.40, 54.68, 47.07. HRMS (ESI): calculated for ($\text{C}_{15}\text{H}_{13}\text{ClN}_2\text{O}$) 273.07947, found 273.07857 ($\text{M}+\text{H}$)⁺

1-(3-Chlorophenyl)-5-(6-chloropyridin-3-yl)imidazolidin-2-one(D32): The title compound was synthesized according to the procedure D using **C32**, yield: 92%, white solid. ^1H NMR (500 MHz, DMSO) δ 8.44 (q, $J = 6.7$ Hz, 1H), 7.85 – 7.66 (m, 2H), 7.50 (t, $J = 8.4$ Hz, 1H), 7.37 (d, $J = 8.2$ Hz, 1H), 7.25 – 7.16 (m, 2H), 7.06 – 6.90 (m, 1H), 5.64 (dd, $J = 12.0, 5.9$ Hz, 1H), 3.89 (q, $J = 9.0$ Hz, 1H), 3.17 (td, $J = 9.1, 4.9$ Hz, 1H). ^{13}C NMR (126 MHz, DMSO) δ 158.54, 149.77, 148.48, 140.24, 137.66, 135.77, 133.03, 130.13, 124.70, 122.19, 119.23, 117.50, 55.48, 45.57. HRMS (ESI): calculated for ($\text{C}_{14}\text{H}_{11}\text{Cl}_2\text{N}_3\text{O}$) 308.03574, found 308.03424 ($\text{M}+\text{H}$)⁺

1-(3-Chlorophenyl)-5-(2-chloropyrimidin-5-yl)imidazolidin-2-one(D33): The title compound was synthesized according to the procedure D using **C33**, yield: 82%, white solid. ^1H NMR (500 MHz, acetone) δ 7.75 – 7.70 (m, 3H), 7.48 (dd, $J = 8.2, 2.0$ Hz, 1H), 7.40 (t, $J = 8.1$ Hz, 1H), 7.24 (dd, $J = 7.9, 2.0$ Hz, 1H), 7.01 – 6.95 (m, 1H), 5.29 (dd, $J = 9.9, 6.1$ Hz, 1H), 4.79 (t, $J = 10.4$ Hz, 1H), 4.51 (dd, $J = 10.8, 6.1$ Hz, 1H). ^{13}C NMR (126 MHz, acetone) δ 158.26, 156.20, 154.63, 149.10, 145.74, 139.21, 137.63, 135.14, 133.21, 129.87, 126.12, 54.28, 47.29. HRMS (ESI): calculated for ($\text{C}_{13}\text{H}_{10}\text{Cl}_2\text{N}_4\text{O}$) 309.03099, found 309.03241 ($\text{M}+\text{H}$)⁺

5-(5-Bromopyridin-2-yl)-1-(3-chlorophenyl)imidazolidin-2-one(D34): The title compound was synthesized according to the procedure D using **C34**, yield: 92%, white solid. ^1H NMR (500 MHz, DMSO) δ 8.68 (q, $J = 3.0$ Hz, 1H), 8.02 (dt, $J = 7.8, 4.2$ Hz, 1H), 7.75 (dt, $J = 4.3, 2.1$ Hz, 1H), 7.32 (dq, $J = 7.8, 3.6$ Hz, 2H), 7.23 – 7.16 (m, 2H), 6.96 (ddt, $J = 8.1, 4.6, 2.0$ Hz, 1H), 5.56 (dq, $J = 8.1, 4.1$ Hz, 1H), 3.92 – 3.80 (m, 1H), 3.20 (dq, $J = 8.2, 4.1$ Hz, 1H). ^{13}C NMR (126 MHz, DMSO) δ 158.59, 150.50, 140.91, 139.99, 133.06, 130.15, 122.88, 121.70,

121.42, 119.42, 118.26, 116.59, 59.11, 44.19. HRMS (ESI): calculated for (C₁₄H₁₁BrClN₃O) 353.98040, found 353.98148 (M+H)⁺

1-(3-Chlorophenyl)-5-(quinolin-2-yl)imidazolidin-2-one(D35): The title compound was synthesized according to the procedure D using **C35**, yield: 94%, white solid. ¹H NMR (500 MHz, DMSO) δ 8.85 (d, *J* = 2.5 Hz, 1H), 8.33 (d, *J* = 2.5 Hz, 1H), 7.90 (d, *J* = 8.5 Hz, 1H), 7.61 (d, *J* = 8.1 Hz, 1H), 7.32 (dt, *J* = 40.3, 7.1 Hz, 3H), 7.21 (s, 1H), 7.16 – 7.06 (m, 3H), 5.54 (dd, *J* = 9.3, 5.6 Hz, 1H), 3.78 (t, *J* = 9.2 Hz, 1H), 3.05 (dd, *J* = 8.9, 5.5 Hz, 1H). ¹³C NMR (126 MHz, DMSO) δ 159.52, 152.56, 148.71, 146.37, 145.47, 144.18, 143.76, 141.37, 138.66, 134.78, 129.79, 128.49, 128.02, 126.25, 125.67, 121.52, 55.47, 46.41. HRMS (ESI): calculated for (C₁₈H₁₄ClN₃O) 324.08654, found 324.08878 (M+H)⁺

1-(3-Chlorophenyl)-5-(quinolin-3-yl)imidazolidin-2-one(D36): The title compound was synthesized according to the procedure D using **C36**, yield: 92%, white solid. ¹H NMR (500 MHz, DMSO) δ 8.99 (d, *J* = 2.5 Hz, 1H), 8.23 (d, *J* = 2.5 Hz, 1H), 7.85 (d, *J* = 8.5 Hz, 1H), 7.66 (d, *J* = 8.1 Hz, 1H), 7.49 (dt, *J* = 40.3, 7.1 Hz, 3H), 7.42 (s, 1H), 7.36 – 7.20 (m, 3H), 5.69 (dd, *J* = 9.3, 5.6 Hz, 1H), 3.82 (t, *J* = 9.2 Hz, 1H), 3.11 (dd, *J* = 8.9, 5.5 Hz, 1H). ¹³C NMR (126 MHz, DMSO) δ 157.42, 148.25, 144.61, 145.77, 142.41, 135.28, 133.76, 131.37, 130.66, 129.78, 128.79, 128.19, 127.82, 127.25, 124.67, 122.42, 58.49, 49.73. HRMS (ESI): calculated for (C₁₈H₁₄ClN₃O) 324.08654, found 324.08744 (M+H)⁺

1-(3-Chlorophenyl)-5-(quinolin-4-yl)imidazolidin-2-one(D37): The title compound was synthesized according to the procedure D using **C37**, yield: 88%, white solid. ¹H NMR (500 MHz, acetone) δ 8.45 (dd, *J* = 8.4, 1.2 Hz, 1H), 8.23 (d, *J* = 8.5 Hz, 1H), 7.78 – 7.72 (m, 3H), 7.69 – 7.63 (m, 1H), 7.58 – 7.52 (m, 3H), 7.42 (t, *J* = 8.2 Hz, 1H), 7.21 (dd, *J* = 8.0, 2.1 Hz, 1H), 5.63 (s, 1H), 4.51 (t, *J* = 10.2 Hz, 1H), 3.88 (dd, *J* = 10.5, 4.9 Hz, 1H). ¹³C NMR (126 MHz, DMSO) δ 158.12, 155.26, 149.75, 148.37, 146.77, 14.18, 143.76, 141.37, 138.66, 134.78, 129.79, 128.49, 127.12, 126.85, 125.71, 123.62, 57.47, 48.11. HRMS (ESI): calculated for (C₁₈H₁₄ClN₃O) 324.08654, found 324.08878 (M+H)⁺

1-(3-Chlorophenyl)-5-(quinolin-6-yl)imidazolidin-2-one(D38): The title compound was synthesized according to the procedure D using **C38**, yield: 90%, white solid. ¹H NMR (500 MHz, DMSO) δ 9.04 (d, *J* = 2.5 Hz, 1H), 8.11 (d, *J* = 2.5 Hz, 1H), 7.81 (d, *J* = 8.5 Hz, 1H), 7.76 (d, *J* = 8.1 Hz, 1H), 7.51 (dt, *J* = 40.3, 7.1 Hz, 3H), 7.42 (s, 1H), 7.40 – 7.25 (m, 3H), 5.76 (dd, *J* = 9.3, 5.6 Hz, 1H), 3.98 (t, *J* = 9.2 Hz, 1H), 3.21 (dd, *J* = 8.9, 5.5 Hz, 1H). ¹³C NMR (126 MHz, DMSO) δ 156.62, 145.94, 143.51, 141.67, 135.61, 131.48, 130.75, 129.77, 129.36,

128.72, 127.69, 127.16, 127.02, 126.85, 125.17, 123.46, 56.69, 45.76. HRMS (ESI): calculated for (C₁₈H₁₄ClN₃O) 324.08654, found 324.08750 (M+H)⁺

5-(Quinolin-2-yl)-1-(quinolin-3-yl)imidazolidin-2-one(D39): The title compound was synthesized according to the procedure D using **C39**, yield: 92%, white solid. ¹H NMR (500 MHz, DMSO) δ 8.44 (d, *J* = 2.6 Hz, 1H), 8.39 (d, *J* = 8.6 Hz, 1H), 7.98 (d, *J* = 8.5 Hz, 1H), 7.94 – 7.86 (m, 5H), 7.80 (d, *J* = 8.5 Hz, 1H), 7.74 (ddd, *J* = 8.4, 6.7, 1.4 Hz, 1H), 7.67 (ddd, *J* = 8.5, 6.7, 1.5 Hz, 1H), 7.57 (dt, *J* = 12.0, 7.5 Hz, 2H), 6.15 (dd, *J* = 9.8, 5.1 Hz, 1H), 4.63 (t, *J* = 10.2 Hz, 1H), 4.09 (dd, *J* = 10.6, 5.1 Hz, 1H). ¹³C NMR (126 MHz, DMSO) δ 157.96, 154.38, 146.99, 145.74, 144.79, 138.09, 130.93, 129.33, 128.74, 128.04, 127.88, 127.50, 127.43, 127.20, 126.90, 125.88, 119.79, 115.43, 57.93, 45.66. HRMS (ESI): calculated for (C₂₅H₁₇N₇O₄S) 341.14024, found 341.13989 (M+H)⁺

5-(3-Methoxyphenyl)-1-(quinolin-3-yl)imidazolidin-2-one(D40): The title compound was synthesized according to the procedure D using **C40**, yield: 91%, white solid. ¹H NMR (500 MHz, DMSO) δ 9.14 (d, *J* = 2.5 Hz, 1H), 8.16 (d, *J* = 2.5 Hz, 1H), 7.88 (d, *J* = 8.5 Hz, 1H), 7.79 (d, *J* = 8.1 Hz, 1H), 7.55 (dt, *J* = 40.3, 7.1 Hz, 3H), 7.44 (s, 1H), 7.40 – 7.28 (m, 3H), 5.75 (dd, *J* = 9.3, 5.6 Hz, 1H), 3.96 (t, *J* = 9.2 Hz, 1H), 3.71 (s, 3H), 3.22 (dd, *J* = 8.9, 5.5 Hz, 1H). ¹³C NMR (126 MHz, DMSO) δ 158.92, 144.84, 143.51, 142.97, 133.51, 132.98, 130.95, 128.47, 128.06, 127.82, 127.59, 127.36, 127.02, 126.55, 125.07, 122.45, 57.69, 55.81, 46.26. HRMS (ESI): calculated for (C₁₉H₁₇N₃O₂) 320.13990, found 320.13840 (M+H)⁺

5-(4-Bromophenyl)-1-(quinolin-3-yl)imidazolidin-2-one(D41): The title compound was synthesized according to the procedure D using **C41**, yield: 91%, white solid. ¹H NMR (500 MHz, DMSO) δ 8.33 (d, *J* = 2.5 Hz, 1H), 7.94-7.85 (m, 4H), 7.69 (t, *J* = 7.7 Hz, 1H), 7.55 (t, *J* = 7.5 Hz, 1H), 7.54 (t, *J* = 7.1 Hz, 4H), 5.81 (dd, *J* = 9.6, 6.4 Hz, 1H), 4.52 (t, *J* = 10.1 Hz, 1H), 3.82 (dd, *J* = 10.5, 6.4 Hz, 1H). ¹³C NMR (126 MHz, acetone) δ 154.29, 141.70, 139.33, 137.01, 135.25, 133.62, 129.11, 129.48, 128.51, 127.92, 125.11, 123.33, 122.05, 114.07, 57.01, 47.09. HRMS (ESI): calculated for (C₁₈H₁₄BrN₃O) 368.03985, found 368.03991 (M+H)⁺

5-([1,1'-Biphenyl]-4-yl)-1-(quinolin-3-yl)imidazolidin-2-one(D42): The title compound was synthesized according to the procedure D using **C42**, yield: 91%, white solid. ¹H NMR (500 MHz, DMSO) δ 8.49 (d, *J* = 2.5 Hz, 1H), 7.95 – 7.89 (m, 4H), 7.75 – 7.59 (m, 8H), 7.42 (t, *J* = 7.6 Hz, 2H), 7.32 (t, *J* = 7.3 Hz, 1H), 5.96 (dd, *J* = 9.6, 6.4 Hz, 1H), 4.60 (t, *J* = 10.0 Hz, 1H), 3.87 (dd, *J* = 10.4, 6.4 Hz, 1H). ¹³C NMR (126 MHz, DMSO) δ 155.26, 148.12, 144.09, 143.91, 142.17, 141.23, 139.26, 138.37, 130.21, 128.41, 127.89, 127.14, 126.85, 126.67, 126.47,

126.24, 125.17, 125.68, 57.56, 48.09. HRMS (ESI): calculated for (C₂₄H₁₉N₃O) 366.16064, found 366.15930 (M+H)⁺

5-(4-(1*H*-1,2,4-Triazol-1-yl)phenyl)-1-(quinolin-3-yl)imidazolidin-2-one(D43): The title compound was synthesized according to the procedure D using **C43**, yield: 90%, white solid. ¹H NMR (500 MHz, DMSO) δ 9.20 (s, 1H), 9.18 (d, *J* = 2.6 Hz, 1H), 8.20 – 8.15 (m, 2H), 7.88 (d, *J* = 8.4 Hz, 1H), 7.83 – 7.77 (m, 3H), 7.62 (d, *J* = 8.4 Hz, 2H), 7.57 (ddd, *J* = 8.5, 6.7, 1.5 Hz, 1H), 7.51 – 7.45 (m, 2H), 5.81 (dd, *J* = 9.2, 5.9 Hz, 1H), 4.00 (t, *J* = 9.1 Hz, 1H), 3.27 (dd, *J* = 9.1, 5.9 Hz, 1H). ¹³C NMR (126 MHz, DMSO) δ 159.00, 152.43, 145.06, 143.52, 142.36, 139.93, 136.34, 133.05, 128.47, 128.04, 127.80, 127.60, 127.34, 126.98, 122.65, 120.04, 57.84, 46.40. HRMS (ESI): calculated for (C₂₀H₁₆N₆O) 357.14638, found 357.14484 (M+H)⁺

5-(6-Phenylpyridin-3-yl)-1-(quinolin-3-yl)imidazolidin-2-one(D44): The title compound was synthesized according to the procedure D using **C44**, yield: 88%, white solid. ¹H NMR (500 MHz, DMSO) δ 9.20 (d, *J* = 2.5 Hz, 1H), 8.77 (s, 1H), 8.19 (d, *J* = 2.5 Hz, 1H), 8.00 (d, *J* = 7.3 Hz, 2H), 7.89 (dt, *J* = 8.4, 6.2 Hz, 3H), 7.81 (d, *J* = 8.1 Hz, 1H), 7.60 – 7.56 (m, 1H), 7.53 – 7.47 (m, 2H), 7.47 – 7.36 (m, 3H), 5.85 (dd, *J* = 9.1, 6.0 Hz, 1H), 4.02 (t, *J* = 9.2 Hz, 1H), 3.33 – 3.30 (m, 1H). ¹³C NMR (126 MHz, DMSO) δ 158.95, 155.84, 148.46, 145.18, 143.57, 138.07, 135.37, 134.41, 132.87, 129.23, 128.78, 128.47, 127.89, 127.60, 127.37, 127.03, 126.52, 122.80, 120.45, 56.06, 46.17. HRMS (ESI): calculated for (C₂₃H₁₈N₄O) 367.15589, found 367.15454 (M+H)⁺

5-(5-Phenylfuran-2-yl)-1-(quinolin-3-yl)imidazolidin-2-one(D45): The title compound was synthesized according to the procedure D using **C45**, yield: 82%, white solid. ¹H NMR (500 MHz, acetone) δ 9.32 (d, *J* = 2.6 Hz, 1H), 8.30 (t, *J* = 7.1 Hz, 1H), 7.90 (dd, *J* = 21.2, 11.7 Hz, 1H), 7.81 (d, *J* = 8.0 Hz, 1H), 7.64 (d, *J* = 7.4 Hz, 2H), 7.59 – 7.56 (m, 1H), 7.52 – 7.46 (m, 1H), 7.40 – 7.32 (m, 2H), 7.25 (dd, *J* = 15.4, 7.9 Hz, 1H), 6.73 (d, *J* = 3.4 Hz, 1H), 6.64 – 6.58 (m, 1H), 5.90 (dd, *J* = 9.1, 5.6 Hz, 1H), 4.13 – 4.01 (m, 1H), 3.81 – 3.77 (m, 1H). ¹³C NMR (126 MHz, acetone) δ 162.49, 159.48, 154.83, 152.62, 146.25, 145.33, 134.42, 131.32, 129.76, 129.62, 128.92, 128.46, 128.22, 127.59, 124.45, 123.83, 121.98, 120.41, 54.33, 44.45. HRMS (ESI): calculated for (C₂₂H₁₇N₃O₂) 356.13990, found 356.13812 (M+H)⁺

5-(4-(Furan-2-yl)phenyl)-1-(quinolin-3-yl)imidazolidin-2-one(D46): The title compound was synthesized according to the procedure D using **C46**, yield: 84%, white solid. ¹H NMR (500 MHz, acetone) δ 9.29 (d, *J* = 2.6 Hz, 1H), 8.14 (d, *J* = 2.7 Hz, 1H), 7.88 (d, *J* = 8.3 Hz, 1H), 7.78 – 7.68 (m, 3H), 7.62 – 7.50 (m, 4H), 7.50 – 7.41 (m, 1H), 6.81 (d, *J* = 3.4 Hz, 1H),

6.51 (dd, $J = 3.5, 1.8$ Hz, 1H), 6.38 (s, 1H), 5.76 (dd, $J = 9.1, 5.7$ Hz, 1H), 4.21 – 4.05 (m, 1H), 3.43 (dt, $J = 9.0, 5.9$ Hz, 1H). ^{13}C NMR (126 MHz, acetone) δ 160.02, 154.14, 145.87, 145.07, 143.50, 140.58, 134.57, 131.63, 129.76, 128.89, 128.22, 128.10, 127.94, 127.54, 125.08, 123.03, 122.33, 121.84, 59.90, 47.77. HRMS (ESI): calculated for ($\text{C}_{22}\text{H}_{17}\text{N}_3\text{O}_2$) 356.13990, found 356.13899 ($\text{M}+\text{H}$)⁺

3.1.7.1.5 General procedure for the synthesis of the carbamate derivatives(E5–E46) (Procedure E)

In a 250 mL round-bottomed flask, imidazolidinone derivative (10 mmol) was dissolved in dioxane(50 mL) and then phenyl chloroformate (2.3g, 15 mmol, 1.5 equiv) was subsequently added along with pyridine(12 drops). The reaction mixture was left to reflux at 100°C for 2 h. After completion of the reaction (monitored by TLC), the mixture was the mixture was evaporated till complete dryness under vacuum. The residue was partitioned between dichloromethane (150 mL) and H₂O (50 mL), and then the aqueous layer was re-extracted using 3 portions of dichloromethane(150 mL). Organic layers were then collected and dried over anhydrous magnesium sulfate and evaporated under vacuum. The residue was then purified using preparative high-performance liquid chromatography.

Phenyl 3,4-bis(3-chlorophenyl)-2-oxoimidazolidine-1-carboxylate(E5)

The title compound was synthesized according to the procedure E using **D5**, yield: 86%, white solid. ^1H NMR (500 MHz, acetone) δ 7.75 (dq, $J = 4.2, 2.1$ Hz, 1H), 7.60 (dq, $J = 4.1, 1.9$ Hz, 1H), 7.47 – 7.33 (m, 6H), 7.34 – 7.19 (m, 5H), 5.74 (ddd, $J = 8.9, 7.0, 5.2$ Hz, 1H), 4.64 (td, $J = 10.4, 4.5$ Hz, 1H), 3.91 (ddd, $J = 10.2, 7.0, 5.2$ Hz, 1H). ^{13}C NMR (126 MHz, acetone) δ 152.11, 151.71, 150.57, 143.02, 140.31, 135.35, 134.68, 131.76, 130.93, 130.26, 129.45, 127.75, 126.74, 126.09, 125.19, 122.54, 122.40, 120.50, 56.48, 50.17. HRMS (ESI): calculated for ($\text{C}_{22}\text{H}_{16}\text{Cl}_2\text{N}_2\text{O}_3$) 427.06162, found 427.05988 ($\text{M}+\text{H}$)⁺

Phenyl 3,4-bis(3-fluorophenyl)-2-oxoimidazolidine-1-carboxylate(E6)

The title compound was synthesized according to the procedure E using **D6**, yield: 83%, white solid. ^1H NMR (500 MHz, acetone) δ 7.78 (dq, $J = 4.2, 2.1$ Hz, 1H), 7.62 (dq, $J = 4.1, 1.9$ Hz, 1H), 7.45 – 7.38 (m, 6H), 7.34 – 7.16 (m, 5H), 5.75 (ddd, $J = 8.9, 7.0, 5.2$ Hz, 1H), 4.60 (td, $J = 10.4, 4.5$ Hz, 1H), 3.90 (ddd, $J = 10.2, 7.0, 5.2$ Hz, 1H). ^{13}C NMR (126 MHz, acetone) δ 163.11 (d, $J = 245.4$ Hz) 161.50 (d, $J = 243.6$ Hz), 158.56, 152.14, 151.11, 150.66, 148.14, 145.66, 141.07 (d, $J = 7.5$ Hz), 139.25 (d, $J = 10.4$ Hz), 137.11 (d, $J = 8.3$ Hz), 132.40 (d, $J =$

9.3 Hz), 128.57 (d, $J = 2.7$ Hz), 119.57 (d, $J = 2.9$ Hz), 118.05 (d, $J = 21.3$ Hz), 115.39 (d, $J = 22.8$ Hz), 114.22 (d, $J = 21.2$ Hz), 111.17 (d, $J = 26.0$ Hz), 57.39, 48.82. HRMS (ESI): calculated for (C₂₂H₁₆F₂N₂O₃) 395.12072, found 395.11905 (M+H)⁺

Phenyl 3,4-bis(3-bromophenyl)-2-oxoimidazolidine-1-carboxylate(E7)

The title compound was synthesized according to the procedure E using **D7**, yield: 85%, white solid. ¹H NMR (500 MHz, DMSO) δ 7.83 (t, $J = 2.0$ Hz, 1H), 7.74 (t, $J = 1.8$ Hz, 1H), 7.49 – 7.41 (m, 4H), 7.38 (dt, $J = 7.6, 1.9$ Hz, 1H), 7.33 – 7.21 (m, 6H), 5.67 (dd, $J = 9.5, 5.9$ Hz, 1H), 4.50 (t, $J = 9.9$ Hz, 1H), 3.77 (dd, $J = 10.3, 5.9$ Hz, 1H). ¹³C NMR (126 MHz, DMSO) δ 151.20, 150.18, 149.48, 141.90, 138.85, 131.33, 131.14, 130.58, 129.86, 129.53, 127.41, 126.05, 125.85, 124.53, 122.22, 121.74, 121.53, 120.50, 54.80, 48.98. HRMS (ESI): calculated for (C₂₂H₁₆Br₂N₂O₃) 516.95559, found 516.95673 (M+H)⁺

Phenyl 3,4-bis(4-chlorophenyl)-2-oxoimidazolidine-1-carboxylate(E8)

The title compound was synthesized according to the procedure E using **D8**, yield: 89%, white solid. ¹H NMR (500 MHz, DMSO) δ 7.59 – 7.51 (m, 2H), 7.49 – 7.44 (m, 2H), 7.43 (t, $J = 7.9$ Hz, 2H), 7.41 – 7.37 (m, 4H), 7.30 (t, $J = 7.4$ Hz, 1H), 7.28 – 7.23 (m, 2H), 5.64 (dd, $J = 9.4, 5.9$ Hz, 1H), 4.47 (t, $J = 9.8$ Hz, 1H), 3.75 (dd, $J = 10.3, 5.9$ Hz, 1H). ¹³C NMR (126 MHz, DMSO) δ 152.16, 151.39, 148.32, 139.61, 138.57, 134.20, 133.50, 131.56, 129.16, 125.17, 123.47, 122.07, 121.25, 117.56, 55.07, 47.35. HRMS (ESI): calculated for (C₂₂H₁₆Cl₂N₂O₃) 427.06162, found 427.06004 (M+H)⁺

Phenyl 3,4-bis(4-fluorophenyl)-2-oxoimidazolidine-1-carboxylate(E9)

The title compound was synthesized according to the procedure E using **D9**, yield: 87%, white solid. ¹H NMR (500 MHz, DMSO) δ 7.53 – 7.48 (m, 2H), 7.48 – 7.42 (m, 4H), 7.27 (dd, $J = 18.1, 7.6$ Hz, 3H), 7.15 (dt, $J = 12.7, 8.7$ Hz, 4H), 5.60 (dd, $J = 9.3, 6.4$ Hz, 1H), 4.50 (t, $J = 9.8$ Hz, 1H), 3.77 (dd, $J = 10.3, 6.4$ Hz, 1H). ¹³C NMR (126 MHz, DMSO) δ 161.47 (d, $J = 346.5$ Hz), 159.53 (d, $J = 343.8$ Hz), 151.43, 150.25, 149.61, 135.34 (d, $J = 3.2$ Hz), 133.55 (d, $J = 2.8$ Hz), 129.53, 129.28 (d, $J = 8.7$ Hz), 126.00, 124.85 (d, $J = 8.3$ Hz), 121.77, 115.73 (d, $J = 21.6$ Hz), 115.44 (d, $J = 22.5$ Hz), 55.49, 49.21. HRMS (ESI): calculated for (C₂₂H₁₆F₂N₂O₃) 395.12072, found 395.11893 (M+H)⁺

Phenyl 3,4-bis(4-bromophenyl)-2-oxoimidazolidine-1-carboxylate(E10)

The title compound was synthesized according to the procedure E using **D10**, yield: 84%, white solid. ^1H NMR (500 MHz, DMSO) δ 7.57 – 7.52 (m, 2H), 7.51 – 7.47 (m, 2H), 7.44 (t, $J = 7.9$ Hz, 2H), 7.42 – 7.36 (m, 4H), 7.29 (t, $J = 7.4$ Hz, 1H), 7.25 – 7.21 (m, 2H), 5.61 (dd, $J = 9.4$, 5.9 Hz, 1H), 4.49 (t, $J = 9.8$ Hz, 1H), 3.73 (dd, $J = 10.3$, 5.9 Hz, 1H). ^{13}C NMR (126 MHz, DMSO) δ 151.16, 150.19, 149.52, 138.61, 136.67, 131.90, 131.59, 129.56, 129.19, 126.07, 123.97, 121.77, 121.55, 116.96, 54.97, 48.95. HRMS (ESI): calculated for ($\text{C}_{22}\text{H}_{16}\text{Br}_2\text{N}_2\text{O}_3$) 516.95559, found 516.95703 ($\text{M}+\text{H}$)⁺

Phenyl 3,4-bis(3,4-dichlorophenyl)-2-oxoimidazolidine-1-carboxylate(E11)

The title compound was synthesized according to the procedure E using **D11**, yield: 84%, white solid. ^1H NMR (500 MHz, acetone) δ 7.92 (d, $J = 2.5$ Hz, 1H), 7.81 (d, $J = 2.1$ Hz, 1H), 7.60 (d, $J = 8.3$ Hz, 1H), 7.53 (dd, $J = 8.4$, 2.1 Hz, 1H), 7.48 (d, $J = 8.8$ Hz, 1H), 7.46 – 7.41 (m, 3H), 7.30 – 7.26 (m, 1H), 7.25 – 7.22 (m, 2H), 5.77 (dd, $J = 9.5$, 5.7 Hz, 1H), 4.65 (t, $J = 10.0$ Hz, 1H), 3.94 (dd, $J = 10.5$, 5.6 Hz, 1H). ^{13}C NMR (126 MHz, acetone) δ 151.98, 151.65, 150.45, 141.22, 138.71, 133.44, 132.81, 132.75, 132.21, 131.32, 130.28, 130.13, 128.05, 127.71, 126.80, 124.13, 122.49, 121.98, 55.94, 49.97. HRMS (ESI): calculated for ($\text{C}_{22}\text{H}_{14}\text{Cl}_4\text{N}_2\text{O}_3$) 496.97968, found 496.97881 ($\text{M}+\text{H}$)⁺

Phenyl 4-(3-chlorophenyl)-2-oxo-3-phenylimidazolidine-1-carboxylate(E12)

The title compound was synthesized according to the procedure E using **D12**, yield: 91%, white solid. ^1H NMR (500 MHz, DMSO) δ 8.65 (d, $J = 2.2$ Hz, 1H), 8.59 (dd, $J = 4.8$, 1.5 Hz, 1H), 7.84 (dt, $J = 8.1$, 2.0 Hz, 1H), 7.69 (d, $J = 2.2$ Hz, 1H), 7.44 (t, $J = 7.9$ Hz, 2H), 7.39 (dd, $J = 7.9$, 4.7 Hz, 1H), 7.35 – 7.26 (m, 4H), 7.21 (d, $J = 8.0$ Hz, 2H), 7.13 (dt, $J = 6.9$, 2.2 Hz, 1H), 5.70 (dd, $J = 9.4$, 6.2 Hz, 1H), 4.51 (t, $J = 9.9$ Hz, 1H), 3.83 (dd, $J = 10.3$, 6.2 Hz, 1H). ^{13}C NMR (126 MHz, DMSO) δ 152.20, 151.21, 149.99, 149.42, 148.81, 147.14, 139.17, 138.76, 134.65, 133.90, 131.84, 129.31, 127.19, 126.62, 124.44, 123.14, 122.79, 121.17, 54.28, 47.55. HRMS (ESI): calculated for ($\text{C}_{15}\text{H}_{13}\text{ClN}_2\text{O}$) 393.10060, found 393.10156 ($\text{M}+\text{H}$)⁺

Phenyl 4-(3-chlorophenyl)-3-(3-(hydroxymethyl)phenyl)-2-oxoimidazolidine-1-carboxylate(E13)

The title compound was synthesized according to the procedure E using **D13**, yield: 84%, white solid. ^1H NMR (500 MHz, acetone) δ 12.91 (s, 1H), 7.83 (t, $J = 2.0$ Hz, 1H), 7.74 (t, $J = 1.8$

Hz, 1H), 7.49 – 7.41 (m, 4H), 7.38 (dt, $J = 7.6, 1.9$ Hz, 1H), 7.33 – 7.21 (m, 6H), 5.67 (dd, $J = 9.5, 5.9$ Hz, 1H), 5.20 (d, $J = 1.6$ Hz, 2H), 4.50 (t, $J = 9.9$ Hz, 1H), 3.77 (dd, $J = 10.3, 5.9$ Hz, 1H). ^{13}C NMR (126 MHz, acetone) δ 158.97, 158.22, 157.95, 154.93, 150.11, 146.28, 142.23, 140.01, 137.29, 136.53, 134.44, 132.11, 129.91, 128.46, 126.16, 125.53, 119.91, 118.03, 67.34, 59.11, 47.48. HRMS (ESI): calculated for $(\text{C}_{23}\text{H}_{19}\text{ClN}_2\text{O}_4)$ 423.11116, found 423.11248 (M+H)⁺

Phenyl 4-(3-chlorophenyl)-3-(4-(hydroxymethyl)phenyl)-2-oxoimidazolidine-1-carboxylate(E14)

The title compound was synthesized according to the procedure E using **D14**, yield: 88%, white solid. ^1H NMR (500 MHz, DMSO) δ 12.74 (s, 1H), 7.66 (t, $J = 2.0$ Hz, 1H), 7.48 – 7.40 (m, 5H), 7.41 – 7.34 (m, 3H), 7.31 – 7.26 (m, 4H), 7.19 (s, 1H), 5.54 (dd, $J = 9.1, 5.1$ Hz, 1H), 5.20 (d, $J = 1.6$ Hz, 2H), 3.86 (t, $J = 9.2$ Hz, 1H), 3.09 (dd, $J = 9.2, 5.1$ Hz, 1H). ^{13}C NMR (126 MHz, DMSO) δ 159.43, 154.98, 151.92, 150.62, 148.33, 143.78, 133.30, 132.08, 130.72, 127.73, 126.39, 125.10, 121.87, 119.89, 113.97, 113.45, 68.60, 55.06, 46.16. HRMS (ESI): calculated for $(\text{C}_{23}\text{H}_{19}\text{ClN}_2\text{O}_4)$ 423.11116, found 423.11258 (M+H)⁺

Phenyl 4-(3-chlorophenyl)-3-(4-methoxyphenyl)-2-oxoimidazolidine-1-carboxylate(E15)

The title compound was synthesized according to the procedure E using **D15**, yield: 94%, white solid. ^1H NMR (500 MHz, acetone) δ 7.55 (t, $J = 1.7$ Hz, 1H), 7.48 – 7.37 (m, 6H), 7.35 – 7.32 (m, 1H), 7.30 – 7.21 (m, 3H), 6.87 – 6.83 (m, 2H), 5.64 – 5.56 (m, 1H), 4.59 (dd, $J = 10.3, 9.6$ Hz, 1H), 3.88 (dd, $J = 10.5, 6.1$ Hz, 1H), 3.73 (s, 3H). ^{13}C NMR (126 MHz, acetone) δ 157.98, 152.38, 151.81, 150.73, 143.48, 135.16, 131.57, 131.53, 130.22, 129.28, 128.00, 126.63, 126.42, 125.18, 122.60, 114.72, 57.32, 55.59, 50.16. HRMS (ESI): calculated for $(\text{C}_{23}\text{H}_{19}\text{ClN}_2\text{O}_4)$ 423.10821, found 423.10974 (M+H)⁺

Phenyl 4-(3-chlorophenyl)-3-(4-cyanophenyl)-2-oxoimidazolidine-1-carboxylate(E16)

The title compound was synthesized according to the procedure E using **D16**, yield: 91%, white solid. ^1H NMR (500 MHz, acetone) δ 7.55 (t, $J = 1.7$ Hz, 1H), 7.48 – 7.37 (m, 6H), 7.35 – 7.32 (m, 1H), 7.30 – 7.21 (m, 3H), 6.87 – 6.83 (m, 2H), 5.64 – 5.56 (m, 1H), 4.59 (dd, $J = 10.3, 9.6$ Hz, 1H), 3.88 (dd, $J = 10.5, 6.1$ Hz, 1H). ^{13}C NMR (126 MHz, acetone) δ 157.98, 152.38, 151.81, 150.73, 143.48, 135.16, 131.57, 131.53, 130.22, 129.28, 128.00, 126.63, 126.42, 125.18, 122.60, 114.72, 55.59, 50.16. HRMS (ESI): calculated for $(\text{C}_{23}\text{H}_{16}\text{ClN}_3\text{O}_3)$ 418.09711, found 418.09584 (M+H)⁺

Phenyl 4-(3-chlorophenyl)-3-(4-morpholinophenyl)-2-oxoimidazolidine-1-carboxylate(E17)

The title compound was synthesized according to the procedure E using **D17**, yield: 93%, white solid. ¹H NMR (500 MHz, DMSO) δ 7.53 (s, 1H), 7.44 (t, *J* = 7.9 Hz, 2H), 7.41 – 7.31 (m, 3H), 7.26 (ddd, *J* = 20.5, 13.1, 7.6 Hz, 5H), 6.87 (d, *J* = 9.1 Hz, 2H), 5.52 (dd, *J* = 9.4, 6.2 Hz, 1H), 4.47 (t, *J* = 9.9 Hz, 1H), 3.73 (dt, *J* = 13.6, 6.8 Hz, 1H), 3.71 – 3.63 (m, 4H), 3.10 – 2.97 (m, 4H). ¹³C NMR (126 MHz, DMSO) δ 151.46, 150.28, 149.63, 148.37, 142.33, 133.43, 130.78, 129.53, 128.70, 128.27, 127.11, 125.98, 125.79, 123.97, 121.83, 114.99, 66.06, 55.64, 48.94, 48.20. HRMS (ESI): calculated for (C₂₆H₂₄ClN₃O₄) 478.15336, found 478.15219 (M+H)⁺

Phenyl 4-(3-chlorophenyl)-3-(3-fluoro-4-morpholinophenyl)-2-oxoimidazolidine-1-carboxylate(E18)

The title compound was synthesized according to the procedure E using **D18**, yield: 91%, white solid. ¹H NMR (500 MHz, acetone) δ 7.57 (d, *J* = 2.0 Hz, 1H), 7.50 – 7.40 (m, 5H), 7.36 (dt, *J* = 8.0, 1.7 Hz, 1H), 7.30 – 7.21 (m, 3H), 7.16 (dd, *J* = 8.8, 2.5 Hz, 1H), 6.93 (t, *J* = 9.3 Hz, 1H), 5.70 – 5.56 (m, 1H), 4.60 (t, *J* = 10.0 Hz, 1H), 3.88 (dd, *J* = 10.5, 5.6 Hz, 1H), 3.76 – 3.69 (m, 4H), 3.01 – 2.94 (m, 4H). ¹³C NMR (126 MHz, acetone) δ 155.83 (d, *J* = 244.5 Hz), 152.15, 151.74, 150.61, 143.35, 137.81, 135.29, 133.48 (d, *J* = 10.6 Hz), 131.72, 130.24, 129.39, 127.78, 126.70, 126.14, 122.56, 119.44 (d, *J* = 4.1 Hz), 118.67 (d, *J* = 3.7 Hz), 111.25 (d, *J* = 25.3 Hz), 67.39, 56.73, 51.70, 50.14. HRMS (ESI): calculated for (C₂₆H₂₃ClFN₃O₄) 496.14394, found 496.14255 (M+H)⁺

Phenyl 4-(3-chlorophenyl)-3-(4-fluoro-3-(morpholinosulfonyl)phenyl)-2-oxoimidazolidine-1-carboxylate(E19)

The title compound was synthesized according to the procedure E using **D19**, yield: 84%, white solid. ¹H NMR (500 MHz, acetone) δ 8.17 (d, *J* = 2.0 Hz, 1H), 7.89 – 7.74 (m, 4H), 7.54 (dt, *J* = 8.0, 1.7 Hz, 1H), 7.51 – 7.42 (m, 3H), 7.36 (dd, *J* = 8.8, 2.5 Hz, 1H), 6.99 (t, *J* = 9.3 Hz, 1H), 5.84 – 5.79 (m, 1H), 4.69 (t, *J* = 10.0 Hz, 1H), 3.85 (dd, *J* = 10.5, 5.6 Hz, 1H), 3.72 – 3.61 (m, 4H), 3.04 – 2.99 (m, 4H). ¹³C NMR (126 MHz, acetone) δ 161.18, 158.21 (d, *J* = 255.8 Hz), 157.11, 152.611, 150.32, 148.22, 147.66, 144.31, 139.21, 137.28 (d, *J* = 3.1 Hz), 135.29, 130.68 (d, *J* = 8.3 Hz), 129.84, 128.03, 127.92, 125.17, 125.43 (d, *J* = 16.0 Hz), 118.22 (d, *J* =

23.8 Hz), 65.13, 58.22, 49.84, 47.21. HRMS (ESI): calculated for (C₂₃H₂₀ClFN₆O₇S₂) 560.10584, found 560.10646 (M+H)⁺

Phenyl 4-(3-chlorophenyl)-2-oxo-3-(pyridin-3-yl)imidazolidine-1-carboxylate(E20)

The title compound was synthesized according to the procedure E using **D20**, yield: 80%, white solid. ¹H NMR (500 MHz, DMSO) δ 8.72 (d, *J* = 2.2 Hz, 1H), 8.55 (dd, *J* = 4.8, 1.5 Hz, 1H), 7.99 (dt, *J* = 8.1, 2.0 Hz, 1H), 7.77 (d, *J* = 2.2 Hz, 1H), 7.58 (t, *J* = 7.9 Hz, 2H), 7.42 (dd, *J* = 7.9, 4.7 Hz, 1H), 7.39 – 7.30 (m, 3H), 7.21 (d, *J* = 8.0 Hz, 2H), 7.16 (dt, *J* = 6.9, 2.2 Hz, 1H), 5.74 (dd, *J* = 9.4, 6.2 Hz, 1H), 4.49 (t, *J* = 9.9 Hz, 1H), 3.87 (dd, *J* = 10.3, 6.2 Hz, 1H). ¹³C NMR (126 MHz, DMSO) δ 151.10, 150.03, 148.79, 148.42, 147.46, 145.22, 139.18, 137.96, 135.23, 134.98, 132.64, 129.10, 12.19, 125.59, 124.04, 123.98, 122.72, 120.28, 54.38, 47.29. HRMS (ESI): calculated for (C₁₅H₁₃ClN₂O) 394.09663, found 394.09437 (M+H)⁺

Phenyl 4-(3-chlorophenyl)-3-(6-fluoropyridin-3-yl)-2-oxoimidazolidine-1-carboxylate(E21)

The title compound was synthesized according to the procedure E using **D21**, yield: 80%, white solid. ¹H NMR (500 MHz, DMSO) δ 8.65 (d, *J* = 2.2 Hz, 1H), 8.59 (dd, *J* = 4.8, 1.5 Hz, 1H), 7.84 (dt, *J* = 8.1, 2.0 Hz, 1H), 7.69 (d, *J* = 2.2 Hz, 1H), 7.44 (t, *J* = 7.9 Hz, 2H), 7.39 (dd, *J* = 7.9, 4.7 Hz, 1H), 7.35 – 7.26 (m, 4H), 7.21 (d, *J* = 8.0 Hz, 2H), 7.13 (dt, *J* = 6.9, 2.2 Hz, 1H), 5.70 (dd, *J* = 9.4, 6.2 Hz, 1H), 4.51 (t, *J* = 9.9 Hz, 1H), 3.83 (dd, *J* = 10.3, 6.2 Hz, 1H). ¹³C NMR (126 MHz, acetone) δ 161.61 (d, *J* = 236.2 Hz), 155.71, 150.74, 149.14, 147.49, 144.28, 143.00, 142.93 (d, *J* = 16.0 Hz), 141.55, 137.15 (d, *J* = 8.3 Hz), 135.59, 132.53 (d, *J* = 4.7 Hz), 131.90, 130.07, 128.49, 126.97, 110.61 (d, *J* = 39.5 Hz), 57.75, 49.11. HRMS (ESI): calculated for (C₂₁H₁₅ClFN₃O₃) 412.08642, found 412.08721 (M+H)⁺

Phenyl 4-(3-chlorophenyl)-3-(6-chloropyridin-3-yl)-2-oxoimidazolidine-1-carboxylate(E22)

The title compound was synthesized according to the procedure E using **D22**, yield: 84%, white solid. ¹H NMR (500 MHz, DMSO) δ 8.58 (d, *J* = 2.4 Hz, 1H), 8.00 (dd, *J* = 8.2, 2.4 Hz, 1H), 7.65 (t, *J* = 2.0 Hz, 1H), 7.51 (d, *J* = 8.2 Hz, 1H), 7.41 (t, *J* = 7.8 Hz, 2H), 7.39 – 7.28 (m, 3H), 7.22 (d, *J* = 8.0 Hz, 2H), 7.11 (dt, *J* = 7.3, 1.8 Hz, 1H), 5.70 (dd, *J* = 9.5, 6.3 Hz, 1H), 4.51 (t, *J* = 10.0 Hz, 1H), 3.85 (dd, *J* = 10.4, 6.2 Hz, 1H). ¹³C NMR (126 MHz, DMSO) δ 152.23, 151.31, 150.08, 149.97, 149.14, 139.21, 138.07, 135.87, 133.09, 131.67, 128.48, 127.29,

125.01, 124.54, 123.56, 122.83, 121.39, 53.04, 49.39. HRMS (ESI): calculated for (C₂₁H₁₅Cl₂N₃O₃) 428.05687, found 428.05527 (M+H)⁺

Phenyl 4-(3-chlorophenyl)-3-(5-chloropyridin-3-yl)-2-oxoimidazolidine-1-carboxylate(E23)

The title compound was synthesized according to the procedure E using **D23**, yield: 81%, white solid. ¹H NMR (500 MHz, DMSO) δ 8.51 (d, *J* = 2.2 Hz, 1H), 8.03 (dd, *J* = 8.4, 2.2 Hz, 1H), 7.68 (t, *J* = 2.0 Hz, 1H), 7.54 (d, *J* = 8.4 Hz, 1H), 7.44 (t, *J* = 7.5 Hz, 2H), 7.38 – 7.29 (m, 3H), 7.22 (d, *J* = 8.0 Hz, 2H), 7.19 (dt, *J* = 7.3, 1.8 Hz, 1H), 5.74 (dd, *J* = 9.5, 6.3 Hz, 1H), 4.53 (t, *J* = 10.0 Hz, 1H), 3.88 (dd, *J* = 10.4, 6.2 Hz, 1H). ¹³C NMR (126 MHz, DMSO) δ 153.13, 152.01, 151.34, 150.97, 149.44, 144.21, 139.07, 138.46, 135.42, 133.27, 129.48, 127.29, 125.31, 124.26, 123.17, 122.29, 121.16, 53.66, 49.38. HRMS (ESI): calculated for (C₂₁H₁₅Cl₂N₃O₃) 428.05687, found 428.05534 (M+H)⁺

Phenyl 3-(6-bromopyridin-3-yl)-4-(3-chlorophenyl)-2-oxoimidazolidine-1-carboxylate(E24)

The title compound was synthesized according to the procedure E using **D24**, yield: 85%, white solid. ¹H NMR (500 MHz, DMSO) δ 8.52 (d, *J* = 2.2 Hz, 1H), 8.17 (dd, *J* = 8.1, 2.4 Hz, 1H), 7.62 (t, *J* = 2.1 Hz, 1H), 7.52 (d, *J* = 8.1 Hz, 1H), 7.48 (t, *J* = 7.9 Hz, 2H), 7.39 – 7.28 (m, 3H), 7.25 – 7.18 (m, 2H), 7.11 (dt, *J* = 7.8, 1.5 Hz, 1H), 5.79 (dd, *J* = 9.6, 4.1 Hz, 1H), 4.43 (t, *J* = 9.9 Hz, 1H), 3.86 (dd, *J* = 10.3, 4.1 Hz, 1H). ¹³C NMR (126 MHz, DMSO) δ 153.21, 152.11, 151.18, 149.24, 149.04, 139.11, 138.64, 137.47, 134.43, 132.14, 129.21, 128.17, 127.16, 125.16, 124.37, 123.72, 122.26, 52.14, 48.22. HRMS (ESI): calculated for (C₂₁H₁₅Br₂N₃O₃) 474.00436, found 474.00234 (M+H)⁺

Phenyl 4-(3-chlorophenyl)-2-oxo-3-(quinolin-3-yl)imidazolidine-1-carboxylate(E25)

The title compound was synthesized according to the procedure E using **D25**, yield: 80%, white solid. ¹H NMR (500 MHz, DMSO) δ 9.09 (d, *J* = 2.6 Hz, 1H), 8.34 (d, *J* = 2.5 Hz, 1H), 8.01 – 7.85 (m, 2H), 7.73 – 7.63 (m, 2H), 7.54 – 7.47 (m, 3H), 7.39 – 7.26 (m, 6H), 5.85 (dd, *J* = 9.4, 6.5 Hz, 1H), 4.61 (t, *J* = 9.9 Hz, 1H), 3.87 (dd, *J* = 10.3, 6.5 Hz, 1H). ¹³C NMR (126 MHz, DMSO) δ 151.55, 150.68, 150.21, 149.51, 146.10, 144.57, 141.35, 133.57, 131.08, 130.86, 129.73, 129.58, 128.98, 128.53, 127.71, 127.28, 126.50, 126.09, 125.93, 121.76, 121.26, 54.90, 49.16. HRMS (ESI): calculated for (C₂₅H₁₈ClN₃O₃) 444.11149, found 444.10985 (M+H)⁺

Phenyl 4-(3-chlorophenyl)-3-(naphthalen-2-yl)-2-oxoimidazolidine-1-carboxylate(E26)

The title compound was synthesized according to the procedure E using **D26**, yield: 80%, white solid. ¹H NMR (500 MHz, DMSO) δ 8.79 (d, *J* = 2.6 Hz, 1H), 8.41 (d, *J* = 2.5 Hz, 1H), 8.04 – 7.89 (m, 3H), 7.75 – 7.69 (m, 2H), 7.58 – 7.49 (m, 3H), 7.38 – 7.29 (m, 6H), 5.84 (dd, *J* = 9.4, 6.5 Hz, 1H), 4.63 (t, *J* = 9.9 Hz, 1H), 3.88 (dd, *J* = 10.3, 6.5 Hz, 1H). ¹³C NMR (126 MHz, DMSO) δ 151.55, 150.68, 149.51, 146.10, 144.57, 143.21, 142.34, 141.35, 133.57, 131.08, 130.86, 129.58, 128.98, 128.53, 127.71, 127.28, 126.50, 126.09, 125.93, 121.76, 121.26, 54.90, 49.16. HRMS (ESI): calculated for (C₂₆H₁₉ClN₂O₃) 443.11625, found 443.11885 (M+H)⁺

Phenyl 3-(3-chlorophenyl)-2-oxo-4-phenylimidazolidine-1-carboxylate(E27)

The title compound was synthesized according to the procedure E using **D27**, yield: 83%, white solid. ¹H NMR (500 MHz, DMSO) δ 8.61 (d, *J* = 2.5 Hz, 1H), 8.55 (dd, *J* = 4.8, 1.5 Hz, 1H), 7.81 (dt, *J* = 8.1, 2.0 Hz, 1H), 7.62 (d, *J* = 2.5 Hz, 1H), 7.48 (t, *J* = 7.78 Hz, 2H), 7.41 (dd, *J* = 7.78, 4.7 Hz, 1H), 7.38 – 7.30 (m, 4H), 7.21 (d, *J* = 8.1 Hz, 2H), 7.12 (dt, *J* = 6.9, 2.2 Hz, 1H), 5.78 (dd, *J* = 9.4, 6.1 Hz, 1H), 4.48 (t, *J* = 9.5 Hz, 1H), 3.81 (dd, *J* = 10.3, 6.1 Hz, 1H). ¹³C NMR (126 MHz, DMSO) δ 153.10, 152.25, 150.19, 149.01, 148.83, 147.52, 144.21, 139.74, 137.49, 136.92, 132.44, 129.18, 128.64, 126.52, 124.24, 123.84, 122.09, 120.88, 55.15, 48.22. HRMS (ESI): calculated for (C₂₂H₁₇ClN₂O₃) 393.10060, found 393.10169 (M+H)⁺

Phenyl 3-(3-chlorophenyl)-4-(3-methoxyphenyl)-2-oxoimidazolidine-1-carboxylate(E28)

The title compound was synthesized according to the procedure E using **D28**, yield: 96%, white solid. ¹H NMR (500 MHz, acetone) δ ¹H NMR (500 MHz, DMSO) δ 7.65 (d, *J* = 2.0 Hz, 1H), 7.45 (t, *J* = 7.9 Hz, 2H), 7.36 – 7.26 (m, 4H), 7.24 (d, *J* = 7.7 Hz, 2H), 7.14 (dt, *J* = 7.2, 1.7 Hz, 1H), 7.02 (d, *J* = 1.9 Hz, 1H), 6.98 (d, *J* = 7.7 Hz, 1H), 6.86 (dd, *J* = 8.2, 2.4 Hz, 1H), 5.61 (dd, *J* = 9.3, 5.8 Hz, 1H), 4.48 (t, *J* = 9.8 Hz, 1H), 3.77 – 3.71 (m, 4H). ¹³C NMR (126 MHz, DMSO) δ 154.22, 153.11, 152.45, 151.92, 149.05, 147.37, 146.25, 139.38, 138.08, 137.21, 135.11, 131.84, 129.92, 128.62, 126.95, 125.181, 123.75, 122.88, 54.61, 48.29, 45.61. HRMS (ESI): calculated for (C₂₃H₁₉ClN₂O₄) 423.10821, found 423.10977 (M+H)⁺

Phenyl 3-(3-chlorophenyl)-4-(4-methoxyphenyl)-2-oxoimidazolidine-1-carboxylate(E29)

The title compound was synthesized according to the procedure E using **D29**, yield: 93%, white solid. ¹H NMR (500 MHz, DMSO) δ 7.62 (t, *J* = 2.0 Hz, 1H), 7.49 – 7.20 (m, 9H), 7.13 (dt, *J* = 7.4, 1.8 Hz, 1H), 6.94 – 6.84 (m, 2H), 5.64 – 5.46 (m, 1H), 4.46 (t, *J* = 9.9 Hz, 1H), 3.77 –

3.62 (m, 4H). ^{13}C NMR (126 MHz, DMSO) δ 159.12, 151.21, 150.16, 149.55, 138.95, 132.93, 130.85, 130.20, 129.54, 128.79, 128.65, 128.16, 126.04, 124.33, 122.99, 121.77, 120.38, 114.33, 55.06, 49.45, 45.65. HRMS (ESI): calculated for ($\text{C}_{23}\text{H}_{19}\text{ClN}_2\text{O}_4$) 423.10821, found 423.10971 ($\text{M}+\text{H}$)⁺

Phenyl 3-(3-chlorophenyl)-4-(4-cyanophenyl)-2-oxoimidazolidine-1-carboxylate(E30)

The title compound was synthesized according to the procedure E using **D30**, yield: 83%, white solid. ^1H NMR (500 MHz, acetone) δ 7.71 (t, $J = 1.7$ Hz, 1H), 7.54 – 7.44 (m, 6H), 7.41 – 7.38 (m, 1H), 7.35 – 7.24 (m, 3H), 6.88 – 6.81 (m, 2H), 5.61 – 5.57 (m, 1H), 4.71 (dd, $J = 10.3, 9.6$ Hz, 1H), 3.82 (dd, $J = 10.5, 6.1$ Hz, 1H). ^{13}C NMR (126 MHz, acetone) δ 158.04, 154.29, 153.29, 152.11, 148.92, 139.15, 138.11, 134.93, 131.15, 129.05, 128.08, 127.96, 126.81, 125.70, 124.72, 119.04, 54.11, 49.18. HRMS (ESI): calculated for ($\text{C}_{23}\text{H}_{16}\text{ClN}_3\text{O}_3$) 418.09584, found 418.09721 ($\text{M}+\text{H}$)⁺

Phenyl 3-(3-chlorophenyl)-2-oxo-4-(pyridin-3-yl)imidazolidine-1-carboxylate(E31)

The title compound was synthesized according to the procedure E using **D31**, yield: 83%, white solid. ^1H NMR (500 MHz, DMSO) δ 8.68 (d, $J = 2.2$ Hz, 1H), 8.49 (dd, $J = 4.8, 1.5$ Hz, 1H), 7.90 (dt, $J = 8.1, 2.0$ Hz, 1H), 7.64 (d, $J = 2.2$ Hz, 1H), 7.45 (t, $J = 7.9$ Hz, 2H), 7.38 (dd, $J = 7.9, 4.7$ Hz, 1H), 7.36 – 7.27 (m, 3H), 7.24 (d, $J = 8.0$ Hz, 2H), 7.15 (dt, $J = 6.9, 2.2$ Hz, 1H), 5.73 (dd, $J = 9.4, 6.2$ Hz, 1H), 4.53 (t, $J = 9.9$ Hz, 1H), 3.81 (dd, $J = 10.3, 6.2$ Hz, 1H). ^{13}C NMR (126 MHz, DMSO) δ 151.22, 150.20, 149.69, 149.52, 148.85, 138.57, 134.76, 134.64, 133.10, 130.40, 129.61, 126.12, 124.72, 124.10, 122.14, 121.79, 120.60, 53.48, 48.85. HRMS (ESI): calculated for ($\text{C}_{21}\text{H}_{17}\text{ClN}_3\text{O}_3$) 394.09663, found 394.09424 ($\text{M}+\text{H}$)⁺

Phenyl 3-(3-chlorophenyl)-4-(6-chloropyridin-3-yl)-2-oxoimidazolidine-1-carboxylate(E32)

The title compound was synthesized according to the procedure E using **D32**, yield: 83%, white solid. ^1H NMR (500 MHz, DMSO) δ 8.56 (d, $J = 2.5$ Hz, 1H), 8.00 (dd, $J = 8.3, 2.5$ Hz, 1H), 7.67 (t, $J = 2.0$ Hz, 1H), 7.50 (d, $J = 8.3$ Hz, 1H), 7.45 (t, $J = 7.8$ Hz, 2H), 7.36 – 7.26 (m, 3H), 7.24 (d, $J = 8.0$ Hz, 2H), 7.15 (dt, $J = 7.3, 1.8$ Hz, 1H), 5.76 (dd, $J = 9.5, 6.3$ Hz, 1H), 4.53 (t, $J = 10.0$ Hz, 1H), 3.83 (dd, $J = 10.4, 6.2$ Hz, 1H). ^{13}C NMR (126 MHz, DMSO) δ 151.13, 150.30, 150.18, 149.47, 149.31, 138.51, 138.37, 134.27, 133.19, 130.40, 129.58, 126.09, 124.81, 124.72, 122.19, 120.57, 52.78, 48.57. HRMS (ESI): calculated for ($\text{C}_{21}\text{H}_{15}\text{Cl}_2\text{N}_3\text{O}_3$) 428.05687, found 428.05527 ($\text{M}+\text{H}$)⁺

Phenyl 3-(3-chlorophenyl)-4-(2-chloropyrimidin-5-yl)-2-oxoimidazolidine-1-carboxylate(E33)

The title compound was synthesized according to the procedure E using **D33**, yield: 79%, white solid. ¹H NMR (500 MHz, DMSO) δ 8.54 (d, *J* = 2.5 Hz, 1H), 8.21 (dd, *J* = 8.3, 2.5 Hz, 1H), 7.97 (t, *J* = 2.0 Hz, 1H), 7.84 (d, *J* = 8.3 Hz, 1H), 7.55 (t, *J* = 7.8 Hz, 2H), 7.49 – 7.36 (m, 2H), 7.29 (d, *J* = 8.0 Hz, 2H), 7.09 (dt, *J* = 7.3, 1.8 Hz, 1H), 5.78 (dd, *J* = 9.5, 6.3 Hz, 1H), 4.59 (t, *J* = 10.0 Hz, 1H), 3.79 (dd, *J* = 10.4, 6.2 Hz, 1H). ¹³C NMR (126 MHz, DMSO) δ 154.13, 152.10, 151.09, 150.18, 149.93, 148.18, 139.58, 137.66, 136.48, 135.23, 133.63, 129.15, 127.83, 125.63, 124.81, 122.03, 121.84, 54.81, 49.05. HRMS (ESI): calculated for (C₂₀H₁₄Cl₂N₄O₃) 429.05212, found 429.05395 (M+H)⁺

Phenyl 4-(5-bromopyridin-2-yl)-3-(3-chlorophenyl)-2-oxoimidazolidine-1-carboxylate(E34)

The title compound was synthesized according to the procedure E using **D34**, yield: 82%, white solid. ¹H NMR (500 MHz, DMSO) δ 8.72 (d, *J* = 2.2 Hz, 1H), 8.07 (dd, *J* = 8.3, 2.4 Hz, 1H), 7.72 (t, *J* = 2.1 Hz, 1H), 7.54 (d, *J* = 8.3 Hz, 1H), 7.44 (t, *J* = 7.9 Hz, 2H), 7.38 – 7.26 (m, 3H), 7.26 – 7.17 (m, 2H), 7.14 (dt, *J* = 7.8, 1.5 Hz, 1H), 5.74 (dd, *J* = 9.6, 4.1 Hz, 1H), 4.47 (t, *J* = 9.9 Hz, 1H), 3.88 (dd, *J* = 10.3, 4.1 Hz, 1H). ¹³C NMR (126 MHz, DMSO) δ 156.84, 151.18, 150.82, 150.16, 149.52, 140.04, 139.12, 133.22, 130.48, 129.61, 126.14, 124.31, 124.24, 121.79, 120.82, 120.03, 119.35, 55.84, 47.22. HRMS (ESI): calculated for (C₂₁H₁₅BrClN₃O₃) 474.00436, found 474.00223 (M+H)⁺

Phenyl 3-(3-chlorophenyl)-2-oxo-4-(quinolin-2-yl)imidazolidine-1-carboxylate(E35)

The title compound was synthesized according to the procedure E using **D35**, yield: 88%, white solid. ¹H NMR (500 MHz, acetone) δ 8.39 (d, *J* = 8.5 Hz, 1H), 8.05 (d, *J* = 8.5 Hz, 1H), 7.96 (dd, *J* = 8.1, 1.4 Hz, 1H), 7.87 (t, *J* = 2.1 Hz, 1H), 7.82 – 7.74 (m, 2H), 7.70 (d, *J* = 8.5 Hz, 1H), 7.62 (ddd, *J* = 8.1, 6.8, 1.2 Hz, 1H), 7.48 – 7.40 (m, 4H), 7.26 (dt, *J* = 9.5, 7.9 Hz, 4H), 7.06 (dd, *J* = 8.0, 2.0 Hz, 1H), 5.90 (dd, *J* = 9.6, 4.6 Hz, 1H), 4.69 (t, *J* = 10.0 Hz, 1H), 4.14 (dd, *J* = 10.5, 4.6 Hz, 1H). ¹³C NMR (126 MHz, acetone) δ 160.02, 152.29, 151.80, 150.73, 148.81, 141.00, 138.91, 134.75, 130.94, 130.33, 130.10, 128.90, 128.79, 127.95, 126.81, 124.95, 122.87, 122.64, 121.89, 119.94, 119.74, 59.00, 48.56. HRMS (ESI): calculated for (C₂₅H₁₈ClN₃O₃) 444.11149, found 444.10980 (M+H)⁺

Phenyl 3-(3-chlorophenyl)-2-oxo-4-(quinolin-3-yl)imidazolidine-1-carboxylate(E36)

The title compound was synthesized according to the procedure E using **D36**, yield: 81%, white solid. ^1H NMR (500 MHz, acetone) δ 8.39 (d, $J = 8.5$ Hz, 1H), 8.05 (d, $J = 8.5$ Hz, 1H), 7.96 (dd, $J = 8.1, 1.4$ Hz, 1H), 7.87 (t, $J = 2.1$ Hz, 1H), 7.82 – 7.74 (m, 2H), 7.70 (d, $J = 8.5$ Hz, 1H), 7.62 (ddd, $J = 8.1, 6.8, 1.2$ Hz, 1H), 7.48 – 7.40 (m, 4H), 7.26 (dt, $J = 9.5, 7.9$ Hz, 4H), 7.06 (dd, $J = 8.0, 2.0$ Hz, 1H), 5.90 (dd, $J = 9.6, 4.6$ Hz, 1H), 4.69 (t, $J = 10.0$ Hz, 1H), 4.14 (dd, $J = 10.5, 4.6$ Hz, 1H). ^{13}C NMR (126 MHz, acetone) δ 159.11, 155.17, 154.37, 152.31, 149.18, 145.00, 141.73, 139.71, 138.91, 135.21, 131.57, 128.81, 127.79, 126.95, 125.81, 124.22, 122.91, 121.03, 120.93, 119.01, 118.16, 59.05, 48.59. HRMS (ESI): calculated for ($\text{C}_{25}\text{H}_{18}\text{ClN}_3\text{O}_3$) 444.11149, found 444.10981 (M+H)⁺

Phenyl 3-(3-chlorophenyl)-2-oxo-4-(quinolin-4-yl)imidazolidine-1-carboxylate(E37)

The title compound was synthesized according to the procedure E using **D37**, yield: 72%, white solid. ^1H NMR (500 MHz, acetone) δ 8.35 (dd, $J = 8.4, 1.2$ Hz, 1H), 8.24 (d, $J = 8.5$ Hz, 1H), 7.91 – 7.84 (m, 4H), 7.81 – 7.72 (m, 2H), 7.54 – 7.45 (m, 4H), 7.33 (t, $J = 8.2$ Hz, 1H), 7.19 (dd, $J = 8.0, 2.1$ Hz, 1H), 6.73 (s, 1H), 5.92 (d, $J = 4.9$ Hz, 1H), 4.92 (t, $J = 10.2$ Hz, 1H), 3.99 (dd, $J = 10.5, 4.9$ Hz, 1H). ^{13}C NMR (126 MHz, acetone) δ 158.28, 152.24, 151.52, 149.22, 148.13, 146.18, 145.74, 144.23, 139.38, 135.05, 132.24, 131.71, 131.21, 129.28, 127.11, 126.18, 125.19, 123.16, 121.33, 119.32, 118.21, 54.09, 47.88. HRMS (ESI): calculated for ($\text{C}_{25}\text{H}_{18}\text{ClN}_3\text{O}_3$) 444.11149, found 444.10988 (M+H)⁺

Phenyl 3-(3-chlorophenyl)-2-oxo-4-(quinolin-6-yl)imidazolidine-1-carboxylate(E38)

The title compound was synthesized according to the procedure E using **D38**, yield: 77%, white solid. ^1H NMR (500 MHz, acetone) δ 8.33 (dd, $J = 8.2, 1.7$ Hz, 1H), 8.27 – 8.19 (m, 3H), 8.14 (d, $J = 8.5$ Hz, 1H), 7.98 (dd, $J = 8.5, 2.1$ Hz, 1H), 7.74 (t, $J = 2.1$ Hz, 1H), 7.64 – 7.54 (m, 4H), 7.50 (ddd, $J = 13.5, 8.2, 3.2$ Hz, 2H), 7.32 (t, $J = 8.2$ Hz, 1H), 7.21 (dd, $J = 8.1, 2.0$ Hz, 1H), 6.01 (dd, $J = 9.8, 5.7$ Hz, 1H), 4.72 (t, $J = 10.2$ Hz, 1H), 4.01 (dd, $J = 10.7, 5.7$ Hz, 1H). ^{13}C NMR (126 MHz, acetone) δ 158.21, 156.33, 155.16, 154.28, 148.26, 147.38, 145.22, 144.61, 139.01, 138.73, 137.18, 136.05, 135.74, 134.28, 129.04, 128.26, 127.07, 125.28, 124.32, 123.21, 122.17, 58.05, 47.99. HRMS (ESI): calculated for ($\text{C}_{25}\text{H}_{18}\text{ClN}_3\text{O}_3$) 444.11149, found 444.10982 (M+H)⁺

Phenyl 2-oxo-4-(quinolin-2-yl)-3-(quinolin-3-yl)imidazolidine-1-carboxylate(E39)

The title compound was synthesized according to the procedure E using **D39**, yield: 85%, white solid. ^1H NMR (500 MHz, DMSO) δ 8.42 (d, $J = 2.6$ Hz, 2H), 8.36 (d, $J = 8.6$ Hz, 2H), 7.91

(d, $J = 8.2$ Hz, 2H), 7.84 – 7.73 (m, 5H), 7.70 (d, $J = 8.2$ Hz, 2H), 7.61 (ddd, $J = 8.4, 6.7, 1.4$ Hz, 1H), 7.52 (ddd, $J = 8.2, 6.7, 1.5$ Hz, 1H), 7.29 (dt, $J = 12.0, 7.5$ Hz, 2H), 6.01 (dd, $J = 9.8, 4.9$ Hz, 1H), 4.55 (t, $J = 10.2$ Hz, 1H), 3.98 (dd, $J = 10.6, 4.9$ Hz, 1H). ^{13}C NMR (126 MHz, acetone) δ 158.04, 157.94, 156.83, 155.04, 154.29, 153.29, 152.11, 151.91, 149.01, 148.92, 147.55, 146.61, 139.15, 138.11, 134.93, 131.15, 129.05, 128.08, 127.96, 126.81, 125.70, 124.72, 121.82, 119.04, 54.11, 49.18. HRMS (ESI): calculated for ($\text{C}_{28}\text{H}_{20}\text{N}_4\text{O}_3$) 461.16394, found 461.16204 ($\text{M}+\text{H}$)⁺

Phenyl 4-(3-methoxyphenyl)-2-oxo-3-(quinolin-3-yl)imidazolidine-1-carboxylate(E40)

The title compound was synthesized according to the procedure E using **D40**, yield: 81%, white solid. ^1H NMR (500 MHz, DMSO) δ 8.51 (t, $J = 3.3$ Hz, 1H), 7.81 (dd, $J = 12.0, 8.2$ Hz, 2H), 7.71 – 7.62 (m, 4H), 7.59 – 7.48 (m, 4H), 7.11 (d, $J = 7.8$ Hz, 1H), 7.11 (s, 1H), 7.01 (d, $J = 7.6$ Hz, 1H), 6.71 (dd, $J = 8.1, 2.4$ Hz, 1H), 5.81 (dd, $J = 9.4, 6.5$ Hz, 1H), 4.41 (t, $J = 9.0$ Hz, 1H), 3.79 (dd, $J = 9.3, 6.5$ Hz, 1H), 3.69 (s, 3H). ^{13}C NMR (126 MHz, DMSO) δ 160.21, 158.23, 157.19, 155.82, 151.38, 149.71, 148.34, 147.79, 144.61, 141.88, 139.51, 138.61, 135.37, 129.53, 128.84, 127.39, 126.82, 125.95, 121.11, 119.51, 118.84, 57.41, 55.09, 48.76. HRMS (ESI): calculated for ($\text{C}_{26}\text{H}_{21}\text{N}_3\text{O}_4$) 440.16103, found 440.16329 ($\text{M}+\text{H}$)⁺

Phenyl 4-(4-bromophenyl)-2-oxo-3-(quinolin-3-yl)imidazolidine-1-carboxylate(E41)

The title compound was synthesized according to the procedure E using **D41**, yield: 84%, white solid. ^1H NMR (500 MHz, DMSO) δ 9.18 (d, $J = 2.5$ Hz, 1H), 8.45 (d, $J = 2.5$ Hz, 1H), 8.02 (d, $J = 8.4$ Hz, 1H), 7.96 (d, $J = 8.3$ Hz, 1H), 7.76 (ddd, $J = 8.3, 6.7, 1.4$ Hz, 1H), 7.64 (t, $J = 7.5$ Hz, 1H), 7.54 (m, 4H), 7.47 (t, $J = 7.9$ Hz, 2H), 7.34 – 7.24 (m, 3H), 5.86 (dd, $J = 9.5, 6.3$ Hz, 1H), 4.62 (t, $J = 9.8$ Hz, 1H), 3.06 (qd, $J = 7.3, 4.8$ Hz, 1H). ^{13}C NMR (126 MHz, DMSO) δ 158.45, 154.24, 151.55, 150.18, 149.48, 144.94, 142.72, 138.03, 131.93, 131.28, 129.85, 129.56, 129.03, 128.83, 127.47, 127.10, 126.50, 126.15, 121.75, 54.90, 49.21. HRMS (ESI): calculated for ($\text{C}_{25}\text{H}_{18}\text{BrN}_3\text{O}_3$) 488.06098, found 488.05936 ($\text{M}+\text{H}$)⁺

Phenyl 4-([1,1'-biphenyl]-4-yl)-2-oxo-3-(quinolin-3-yl)imidazolidine-1-carboxylate(E42)

The title compound was synthesized according to the procedure E using **D42**, yield: 88%, white solid. ^1H NMR (500 MHz, DMSO) δ 8.28 (d, $J = 2.5$ Hz, 1H), 7.55 (d, $J = 2.5$ Hz, 1H), 7.08 (dd, $J = 17.2, 8.3$ Hz, 2H), 6.86 – 6.78 (m, 5H), 6.78 – 6.71 (m, 3H), 6.63 (t, $J = 7.8$ Hz, 2H), 6.57 (t, $J = 7.6$ Hz, 2H), 6.51 – 6.41 (m, 4H), 5.06 (dd, $J = 9.4, 6.3$ Hz, 1H), 3.79 (t, $J = 9.8$ Hz, 1H), 3.12 – 3.01 (m, 1H). ^{13}C NMR (126 MHz, DMSO) δ 151.66, 150.23, 149.57, 146.04,

144.53, 140.22, 139.33, 137.98, 131.33, 129.59, 128.91, 128.56, 127.77, 127.72, 127.63, 127.39, 127.32, 127.28, 126.66, 126.54, 126.09, 122.55, 121.78, 55.19, 49.45. HRMS (ESI): calculated for (C₃₁H₂₃N₃O₃) 486.18177, found 486.18030 (M+H)⁺

Phenyl4-(4-(1H-1,2,4-triazol-1-yl)phenyl)-2-oxo-3-(quinolin-3-yl)imidazolidine-1-carboxylate(E43)

The title compound was synthesized according to the procedure E using **D43**, yield: 91%, white solid. ¹H NMR (500 MHz, DMSO) δ 9.21 (s, 1H), 9.10 (d, *J* = 2.5 Hz, 1H), 8.34 (d, *J* = 2.4 Hz, 1H), 8.18 (s, 1H), 7.93 (d, *J* = 8.4 Hz, 1H), 7.89 (d, *J* = 7.8 Hz, 1H), 7.82 (d, *J* = 8.7 Hz, 2H), 7.76 (d, *J* = 8.7 Hz, 2H), 7.70 – 7.65 (m, 1H), 7.57 (t, *J* = 7.5 Hz, 1H), 7.47 (dd, *J* = 10.9, 4.9 Hz, 2H), 7.33 – 7.25 (m, 3H), 5.91 (dd, *J* = 9.3, 6.6 Hz, 1H), 4.69 – 4.60 (m, 1H), 3.91 (dd, *J* = 10.2, 6.6 Hz, 1H). ¹³C NMR (126 MHz, DMSO) δ 163.10, 152.45, 151.60, 150.23, 149.57, 146.27, 144.58, 142.41, 138.27, 136.64, 131.15, 129.61, 129.00, 128.87, 128.57, 127.72, 127.29, 126.81, 126.12, 121.78, 119.91, 55.06, 49.29. HRMS (ESI): calculated for (C₂₇H₂₀N₆O₃) 477.16751, found 477.16583 (M+H)⁺

Phenyl 2-oxo-4-(6-phenylpyridin-3-yl)-3-(quinolin-3-yl)imidazolidine-1-carboxylate(E44)

The title compound was synthesized according to the procedure E using **D44**, yield: 97%, white solid. ¹H NMR (500 MHz, acetone) δ 9.21 (d, *J* = 2.6 Hz, 1H), 8.92 (d, *J* = 2.4 Hz, 1H), 8.36 (d, *J* = 2.6 Hz, 1H), 8.12 (dd, *J* = 8.4, 2.4 Hz, 1H), 8.08 – 8.02 (m, 2H), 7.94 (t, *J* = 8.5 Hz, 2H), 7.86 (dd, *J* = 8.3, 1.5 Hz, 1H), 7.65 (ddd, *J* = 8.4, 6.9, 1.5 Hz, 1H), 7.53 (ddd, *J* = 8.2, 6.8, 1.3 Hz, 1H), 7.48 – 7.37 (m, 5H), 7.32 – 7.25 (m, 3H), 6.05 (dd, *J* = 9.3, 6.3 Hz, 1H), 4.80 (dd, *J* = 10.5, 9.4 Hz, 1H), 4.12 (dd, *J* = 10.5, 6.4 Hz, 1H). ¹³C NMR (126 MHz, acetone) δ 157.94, 152.54, 151.74, 150.61, 149.95, 147.03, 146.19, 139.38, 136.48, 134.13, 132.52, 130.30, 130.07, 129.89, 129.52, 128.85, 128.62, 128.50, 127.98, 127.55, 127.20, 126.79, 122.56, 121.20, 54.90, 50.37. HRMS (ESI): calculated for (C₃₀H₂₂N₄O₃) 487.17702, found 487.17572 (M+H)⁺

Phenyl 2-oxo-4-(5-phenylfuran-2-yl)-3-(quinolin-3-yl)imidazolidine-1-carboxylate(E45)

The title compound was synthesized according to the procedure E using **D45**, yield: 93%, white solid. ¹H NMR (500 MHz, acetone) δ 9.11 (d, *J* = 2.5 Hz, 1H), 8.79 (d, *J* = 2.4 Hz, 1H), 7.99 (d, *J* = 8.1 Hz, 1H), 7.81 (d, *J* = 6.6 Hz, 1H), 7.70 (d, *J* = 8.3 Hz, 2H), 7.64 – 7.61 (m, 2H), 7.55 (d, *J* = 1.5 Hz, 1H), 7.41 (dd, *J* = 8.3, 5.3 Hz, 3H), 7.28 – 7.26 (m, 4H), 6.91 (d, *J* = 3.3

Hz, 1H), 6.78 (dd, $J = 3.3, 1.7$ Hz, 1H), 5.95 (dd, $J = 9.2, 6.1$ Hz, 1H), 4.78 (dd, $J = 12.7, 6.8$ Hz, 1H), 4.28 (dd, $J = 9.2, 5.0$ Hz, 1H). ^{13}C NMR (126 MHz, acetone) δ 161.41, 160.06, 159.92, 158.72, 157.81, 156.91, 155.51, 149.28, 148.83, 147.71, 146.04, 139.88, 138.71, 133.11, 131.55, 129.14, 128.61, 127.82, 126.15, 125.77, 124.81, 123.63, 119.51, 59.90, 47.77. HRMS (ESI): calculated for ($\text{C}_{29}\text{H}_{21}\text{N}_3\text{O}_4$) 476.16003, found 476.15939 ($\text{M}+\text{H}$)⁺

Phenyl 4-(4-(furan-2-yl)phenyl)-2-oxo-3-(quinolin-3-yl)imidazolidine-1-carboxylate(E46)

The title compound was synthesized according to the procedure E using **D46**, yield: 90%, white solid. ^1H NMR (500 MHz, acetone) δ 9.17 (d, $J = 2.6$ Hz, 1H), 8.32 (d, $J = 2.5$ Hz, 1H), 7.94 (d, $J = 8.2$ Hz, 1H), 7.84 (d, $J = 6.7$ Hz, 1H), 7.72 (d, $J = 8.4$ Hz, 2H), 7.67 – 7.65 (m, 2H), 7.59 (d, $J = 1.6$ Hz, 1H), 7.45 (dd, $J = 8.4, 5.4$ Hz, 3H), 7.29 – 7.23 (m, 4H), 6.83 (d, $J = 3.4$ Hz, 1H), 6.51 (dd, $J = 3.4, 1.8$ Hz, 1H), 5.91 (dd, $J = 9.3, 6.2$ Hz, 1H), 4.73 (dd, $J = 12.8, 6.9$ Hz, 1H), 4.02 (dd, $J = 9.3, 5.1$ Hz, 1H). ^{13}C NMR (126 MHz, acetone) δ 160.02, 159.31, 158.61, 157.01, 156.22, 155.97, 154.14, 145.87, 145.07, 143.50, 140.58, 134.57, 131.63, 129.76, 128.89, 128.22, 128.10, 127.94, 127.54, 125.08, 123.03, 119.62, 119.51, 58.77, 49.28. HRMS (ESI): calculated for ($\text{C}_{29}\text{H}_{21}\text{N}_3\text{O}_4$) 476.16003, found 476.15958 ($\text{M}+\text{H}$)⁺

3.1.7.1.6 General procedure for the synthesis of the urea derivatives(F1-F51)(Procedure F)

In a 250 mL round-bottomed flask, carbamate derivative (10 mmol) was dissolved in 100 mL dichloromethane and then the corresponding amine (15 mmol) was subsequently added along with 20 drops of triethylamine. The reaction mixture was left to reflux at 40 °C for 24 h. After completion of the reaction (monitored by TLC), the mixture was partitioned between 150 mL dichloromethane and 100 mL H_2O and then the aqueous layer was re-extracted using 3 portions of 150 mL dichloromethane. Organic layers were then collected and dried over anhydrous magnesium sulfate, filtered and evaporated under vacuum. The residue was then purified using preparative high-performance liquid chromatography (H_2O : acetonitrile + 0.05% formic acid, gradient 5% to 100% acetonitrile).

3.1.7.1.7 General procedure for the amide coupling using hydroxylamine(F3) (Procedure G)

A solution of the carboxylic acid derivative F47 (0.34 mmol) dissolved in 20 mL dichloromethane was treated with 0.5 mL triethylamine followed by the addition of HBTU (0.3 g, 0.8 mmol). The reaction mixture was left to stir for 15 min at room temperature. Following

this, hydroxylamine (2 equiv) was added drop-wise, and the reaction mixture was stirred at room temperature for 2 h. The flask content was then evaporated under vacuum till dryness. The residue was partitioned between 100 mL of dichloromethane and 100 mL of brine, and then the aqueous layer was extracted with three 50 mL portions of dichloromethane. The combined organic extracts were filtered over anhydrous MgSO₄, filtered, the solvent was removed under reduced pressure, and the product was purified by preparative high-performance liquid chromatography to give the carboxylic acid amide derivative **F3**.

3,4-Bis(3-chlorophenyl)-N-(5-cyanothiazol-2-yl)-2-oxoimidazolidine-1-carboxamide(F1)

The title compound was synthesized according to the procedure F using **E5** and 2-amino-5-cyanothiazole, yield: 83%, white solid. ¹H NMR (500 MHz, acetone) δ 8.19 (s, 1H), 7.70 (t, *J* = 2.1 Hz, 1H), 7.66 (t, *J* = 1.9 Hz, 1H), 7.54 (dt, *J* = 7.8, 1.5 Hz, 1H), 7.47 – 7.38 (m, 2H), 7.38 – 7.32 (m, 2H), 7.19 (dd, *J* = 8.0, 2.0 Hz, 1H), 5.86 (dd, *J* = 9.8, 6.0 Hz, 1H), 4.65 (t, *J* = 10.2 Hz, 1H), 3.91 (dd, *J* = 10.7, 6.1 Hz, 1H). ¹³C NMR (126 MHz, acetone) δ 162.93, 155.47, 150.46, 142.20, 139.07, 135.37, 134.83, 131.73, 131.19, 129.71, 128.10, 126.57, 126.31, 124.86, 123.28, 121.49, 113.32, 99.92, 57.28, 48.91. HRMS (ESI): calculated for (C₂₀H₁₃Cl₂N₅O₂S) 458.02453 found 458.02249 (M+H)⁺

3,4-Bis(3-chlorophenyl)-N-(2-hydroxyphenyl)-2-oxoimidazolidine-1-carboxamide(F2)

The title compound was synthesized according to the procedure F using **E5** and 2-amino phenol, yield: 78%, white solid. ¹H NMR (500 MHz, acetone) δ 10.73 (s, 1H), 9.01 (s, 1H), 8.15 (dd, *J* = 8.0, 1.5 Hz, 1H), 7.75 (t, *J* = 2.1 Hz, 1H), 7.64 (t, *J* = 1.9 Hz, 1H), 7.52 (d, *J* = 7.7 Hz, 1H), 7.41 (ddd, *J* = 7.9, 4.8, 2.6 Hz, 2H), 7.37 – 7.28 (m, 2H), 7.13 (dd, *J* = 8.0, 2.0 Hz, 1H), 6.97 – 6.86 (m, 2H), 6.83 (td, *J* = 7.7, 1.6 Hz, 1H), 5.74 (dd, *J* = 9.7, 6.0 Hz, 1H), 4.54 (t, *J* = 10.1 Hz, 1H), 3.81 (dd, *J* = 10.6, 6.0 Hz, 1H). ¹³C NMR (126 MHz, acetone) δ 155.88, 151.07, 147.19, 143.08, 140.08, 135.42, 134.77, 131.82, 131.07, 129.53, 127.95, 127.91, 126.30, 125.47, 124.24, 122.70, 120.77, 120.73, 120.66, 115.81, 56.79, 49.24. HRMS (ESI): calculated for (C₂₂H₁₇Cl₂N₃O₃) 442.07252 found 442.07063 (M+H)⁺

3,4-Bis(3-chlorophenyl)-N-(3-(hydroxycarbonyl)phenyl)-2-oxoimidazolidine-1-carboxamide(F3)

The title compound was synthesized according to the procedure G using **F49** and hydroxylamine, yield: 85%, white solid. ¹H NMR (500 MHz, DMSO) δ 11.33 (s, 1H), 10.97 (s, 1H), 8.67 (s, 1H), 8.48 (t, *J* = 1.9 Hz, 1H), 8.27 (dd, *J* = 8.0, 2.2 Hz, 1H), 8.20 (d, *J* = 2.2

Hz, 1H), 8.08 (t, $J = 1.9$ Hz, 1H), 7.99 (dd, $J = 20.4, 7.7$ Hz, 2H), 7.91 – 7.83 (m, 3H), 7.82 – 7.75 (m, 2H), 7.60 (dd, $J = 7.8, 2.0$ Hz, 1H), 6.21 (dd, $J = 9.7, 6.1$ Hz, 1H), 5.00 (t, $J = 10.1$ Hz, 1H), 4.26 (dd, $J = 10.6, 6.0$ Hz, 1H). ^{13}C NMR (126 MHz, DMSO) δ 164.87, 155.65, 150.50, 142.35, 139.31, 139.04, 134.91, 134.30, 133.70, 132.01, 131.30, 130.61, 129.64, 129.09, 127.48, 125.88, 125.22, 122.40, 122.26, 120.38, 118.03, 56.32, 48.67. HRMS (ESI): calculated for ($\text{C}_{23}\text{H}_{18}\text{Cl}_2\text{N}_4\text{O}_4$) 485.07834 found 485.07645 (M+H)⁺

***N*-(4-(1*H*-Pyrazol-4-yl)phenyl)-3,4-bis(3-chlorophenyl)-2-oxoimidazolidine-1-carboxamide(F4)**

The title compound was synthesized according to the procedure F using **E2** and 4-(1*H*-pyrazol-4-yl)aniline, yield: 89%, white solid. ^1H NMR (500 MHz, acetone) δ 10.38 (s, 1H), 7.99 (s, 2H), 7.76 (t, $J = 2.1$ Hz, 1H), 7.65 – 7.56 (m, 5H), 7.55 – 7.49 (m, 1H), 7.41 (dd, $J = 8.9, 6.8$ Hz, 2H), 7.36 – 7.29 (m, 2H), 7.15 (dd, $J = 7.8, 2.0$ Hz, 1H), 5.75 (dd, $J = 9.7, 6.0$ Hz, 1H), 4.54 (t, $J = 10.1$ Hz, 1H), 3.80 (dd, $J = 10.5, 6.1$ Hz, 1H). ^{13}C NMR (126 MHz, acetone) δ 156.18, 150.91, 142.96, 139.93, 137.34, 136.45, 135.44, 134.82, 131.82, 131.11, 129.59, 128.00, 126.85, 126.64, 126.37, 125.66, 123.38, 122.87, 122.56, 120.88, 120.55, 56.83, 49.23. HRMS (ESI): calculated for ($\text{C}_{25}\text{H}_{19}\text{Cl}_2\text{N}_5\text{O}_2$) 492.09941 found 492.09756 (M+H)⁺

3,4-Bis(3-chlorophenyl)-*N*-(5-nitrothiazol-2-yl)-2-oxoimidazolidine-1-carboxamide(F5)

The title compound was synthesized according to the procedure F using **E5** and 2-amino-5-nitrothiazole, yield: 82%, yellowish white solid. ^1H NMR (500 MHz, acetone) δ 11.97 (s, 1H), 8.45 (s, 1H), 7.70 (t, $J = 2.1$ Hz, 1H), 7.67 (t, $J = 1.9$ Hz, 1H), 7.56 (dt, $J = 7.7, 1.4$ Hz, 1H), 7.48 – 7.39 (m, 2H), 7.39 – 7.33 (m, 2H), 7.20 (dd, $J = 8.0, 2.0$ Hz, 1H), 5.88 (dd, $J = 9.8, 6.1$ Hz, 1H), 4.67 (t, $J = 10.2$ Hz, 1H), 3.92 (dd, $J = 10.6, 6.1$ Hz, 1H). ^{13}C NMR (126 MHz, acetone) δ 162.23, 155.42, 150.69, 144.11, 142.76, 142.10, 138.94, 135.32, 134.80, 131.71, 131.22, 129.73, 128.12, 126.62, 126.41, 123.31, 121.56, 57.26, 48.82. HRMS (ESI): calculated for ($\text{C}_{19}\text{H}_{13}\text{Cl}_2\text{N}_5\text{O}_4\text{S}$) 478.01436, found 478.01285 (M+H)⁺

3,4-Bis(3-fluorophenyl)-*N*-(5-nitrothiazol-2-yl)-2-oxoimidazolidine-1-carboxamide(F6)

The title compound was synthesized according to the procedure F using **E6** and 2-amino-5-nitrothiazole, yield: 84%, yellowish white solid. ^1H NMR (500 MHz, acetone) δ 8.47 (s, 1H), 7.48 – 7.30 (m, 6H), 7.09 (ddt, $J = 9.3, 7.1, 2.3$ Hz, 1H), 6.98 – 6.89 (m, 1H), 5.87 (dd, $J = 9.8, 5.8$ Hz, 1H), 4.65 (t, $J = 10.2$ Hz, 1H), 3.92 (dd, $J = 10.6, 5.9$ Hz, 1H). ^{13}C NMR (126 MHz, acetone) δ 164.01 (d, $J = 245.4$ Hz) 163.50 (d, $J = 243.6$ Hz), 155.36, 150.66, 142.67 (d, $J =$

7.5 Hz), 139.35 (d, $J = 10.4$ Hz), 132.01 (d, $J = 8.3$ Hz), 131.30 (d, $J = 9.3$ Hz), 123.97 (d, $J = 2.7$ Hz), 118.77 (d, $J = 2.9$ Hz), 116.45 (d, $J = 21.3$ Hz), 114.79 (d, $J = 22.8$ Hz), 113.02 (d, $J = 21.2$ Hz), 110.37 (d, $J = 26.0$ Hz), 57.39, 48.82. HRMS (ESI): calculated for (C₁₉H₁₃F₂N₅O₄S) 446.07346, found 446.07184 (M+H)⁺

3,4-Bis(3-bromophenyl)-N-(5-nitrothiazol-2-yl)-2-oxoimidazolidine-1-carboxamide(F7)

The title compound was synthesized according to the procedure F using **E7** and 2-amino-5-nitrothiazole, yield: 88%, yellowish white solid. ¹H NMR (500 MHz, DMSO) δ 11.90 (s, 1H), 8.64 (s, 1H), 7.79 (d, $J = 1.9$ Hz, 1H), 7.76 (t, $J = 2.0$ Hz, 1H), 7.51 (d, $J = 7.7$ Hz, 1H), 7.48 (dd, $J = 7.9, 2.0$ Hz, 1H), 7.39 (dt, $J = 8.0, 1.5$ Hz, 1H), 7.35 – 7.26 (m, 3H), 5.73 (dd, $J = 9.7, 6.1$ Hz, 1H), 4.46 (t, $J = 10.1$ Hz, 1H), 3.71 (dd, $J = 10.5, 6.1$ Hz, 1H). ¹³C NMR (126 MHz, DMSO) δ 161.22, 153.93, 149.65, 142.88, 142.49, 141.26, 137.71, 131.59, 131.10, 130.83, 130.18, 128.40, 126.42, 125.12, 122.22, 121.58, 121.24, 55.48, 47.74. HRMS (ESI): calculated for (C₁₉H₁₃Br₂N₅O₄S) 567.91128, found 567.90936 (M+H)⁺

3,4-Bis(4-chlorophenyl)-N-(5-nitrothiazol-2-yl)-2-oxoimidazolidine-1-carboxamide(F8)

The title compound was synthesized according to the procedure F using **E8** and 2-amino-5-nitrothiazole, yield: 84%, yellowish white solid. ¹H NMR (500 MHz, acetone) δ 11.99 (s, 1H), 8.45 (s, 1H), 7.63 – 7.50 (m, 4H), 7.43 – 7.31 (m, 4H), 5.83 (dd, $J = 9.7, 6.2$ Hz, 1H), 4.64 (dd, $J = 10.7, 9.7$ Hz, 1H), 3.90 (dd, $J = 10.6, 6.2$ Hz, 1H). ¹³C NMR (126 MHz, acetone) δ 162.29, 155.46, 150.82, 144.11, 142.80, 138.61, 136.39, 134.93, 131.35, 130.02, 129.98, 129.78, 125.18, 57.43, 48.88. HRMS (ESI): calculated for (C₁₉H₁₃Cl₂N₅O₄S) 478.01436, found 478.01289 (M+H)⁺

3,4-Bis(4-fluorophenyl)-N-(5-nitrothiazol-2-yl)-2-oxoimidazolidine-1-carboxamide(F9)

The title compound was synthesized according to the procedure F using **E9** and 2-amino-5-nitrothiazole, yield: 88%, yellowish white solid. ¹H NMR (500 MHz, DMSO) δ 11.97 (s, 1H), 8.62 (s, 1H), 7.59 – 7.51 (m, 2H), 7.47 – 7.39 (m, 2H), 7.16 (td, $J = 8.7, 5.5$ Hz, 4H), 5.66 (dd, $J = 9.6, 6.5$ Hz, 1H), 4.47 (t, $J = 10.1$ Hz, 1H), 3.73 (dd, $J = 10.5, 6.5$ Hz, 1H). ¹³C NMR (126 MHz, DMSO) δ 161.82 (d, $J = 299.7$ Hz), 161.28, 159.88 (d, $J = 298.7$ Hz), 154.11, 149.71, 142.88, 142.46, 134.71 (d, $J = 3.7$ Hz), 132.37 (d, $J = 2.8$ Hz), 129.72 (d, $J = 9.2$ Hz), 125.43 (d, $J = 8.3$ Hz), 115.83 (d, $J = 4.6$ Hz), 115.66 (d, $J = 4.6$ Hz), 56.22, 47.88. HRMS (ESI): calculated for (C₁₉H₁₃F₂N₅O₄S) 446.07346, found 446.07153 (M+H)⁺

3,4-Bis(4-bromophenyl)-N-(5-nitrothiazol-2-yl)-2-oxoimidazolidine-1-carboxamide(F10)

The title compound was synthesized according to the procedure F using **E10** and 2-amino-5-nitrothiazole, yield: 83%, yellowish white solid. ¹H NMR (500 MHz, acetone) δ 11.97 (s, 1H), 8.44 (s, 1H), 7.52 (dq, *J* = 19.9, 8.7 Hz, 8H), 5.81 (dd, *J* = 9.8, 6.1 Hz, 1H), 4.64 (t, *J* = 10.2 Hz, 1H), 3.90 (dd, *J* = 10.6, 6.1 Hz, 1H). ¹³C NMR (126 MHz, acetone) δ 162.36, 155.49, 150.84, 144.20, 142.80, 139.13, 136.97, 133.11, 132.83, 130.27, 125.46, 123.16, 119.23, 57.41, 48.88. HRMS (ESI): calculated for (C₁₉H₁₃Br₂N₅O₄S) 567.91128, found 567.90955 (M+H)⁺

3,4-Bis(3,4-dichlorophenyl)-N-(5-nitrothiazol-2-yl)-2-oxoimidazolidine-1-carboxamide(F11)

The title compound was synthesized according to the procedure F using **E11** and 2-amino-5-nitrothiazole, yield: 83%, yellowish white solid. ¹H NMR (500 MHz, acetone) δ 11.84 (s, 1H), 8.43 (s, 1H), 7.86 (dd, *J* = 5.1, 2.0 Hz, 2H), 7.59 (d, *J* = 1.5 Hz, 2H), 7.53 (d, *J* = 8.8 Hz, 1H), 7.48 (dd, *J* = 8.8, 2.5 Hz, 1H), 5.91 (dd, *J* = 9.8, 6.1 Hz, 1H), 4.67 (t, *J* = 10.3 Hz, 1H), 3.96 (dd, *J* = 10.7, 6.1 Hz, 1H). ¹³C NMR (126 MHz, acetone) δ 162.30, 155.41, 150.74, 144.27, 142.80, 140.42, 137.47, 133.59, 133.26, 133.10, 132.29, 131.72, 130.52, 129.52, 128.27, 125.13, 123.07, 56.88, 48.79. HRMS (ESI): calculated for (C₂₃H₂₀Cl₂N₅O₇S₂) 547.93341, found 547.93158 (M+H)⁺

4-(3-Chlorophenyl)-N-(5-nitrothiazol-2-yl)-2-oxo-3-phenylimidazolidine-1-carboxamide(F12)

The title compound was synthesized according to the procedure F using **E12** and 2-amino-5-nitrothiazole, yield: 83%, yellowish white solid. ¹H NMR (500 MHz, acetone) δ 12.07 (s, 1H), 8.43 (s, 1H), 7.63 (d, *J* = 2.0 Hz, 1H), 7.52 (dd, *J* = 8.3, 3.0 Hz, 3H), 7.41 – 7.30 (m, 4H), 7.16 (t, *J* = 7.4 Hz, 1H), 5.83 (dd, *J* = 9.8, 6.1 Hz, 1H), 4.65 (t, *J* = 10.2 Hz, 1H), 3.92 (dd, *J* = 10.7, 6.1 Hz, 1H). ¹³C NMR (126 MHz, DMSO) δ 161.45, 154.07, 149.89, 143.03, 142.35, 141.47, 136.16, 133.55, 130.78, 128.98, 128.58, 127.33, 126.14, 125.77, 122.75, 55.77, 47.74. HRMS (ESI): calculated for (C₁₉H₁₄ClN₅O₄S) 444.05333, found 444.05170 (M+H)⁺

4-(3-Chlorophenyl)-3-(3-(hydroxymethyl)phenyl)-N-(5-nitrothiazol-2-yl)-2-oxoimidazolidine-1-carboxamide(F13)

The title compound was synthesized according to the procedure F using **E13** and 2-amino-5-nitrothiazole, yield: 87%, yellowish white solid. ¹H NMR (500 MHz, DMSO) δ 12.93 (s, 1H),

8.56 (s, 1H), 7.64 (t, $J = 1.9$ Hz, 1H), 7.38 (t, $J = 1.8$ Hz, 1H), 7.36 – 7.22 (m, 5H), 7.19 (s, 1H), 7.02 (d, $J = 7.5$ Hz, 1H), 5.51 (dd, $J = 9.1, 5.0$ Hz, 1H), 5.20 (d, $J = 1.6$ Hz, 2H), 3.86 (t, $J = 9.1$ Hz, 1H), 3.09 (dd, $J = 9.1, 5.0$ Hz, 1H). ^{13}C NMR (126 MHz, DMSO) δ 164.29, 158.93, 153.71, 143.62, 143.24, 141.98, 139.38, 135.55, 133.39, 130.76, 128.73, 127.77, 126.09, 124.83, 122.32, 119.26, 119.21, 67.95, 57.93, 46.03. HRMS (ESI): calculated for ($\text{C}_{20}\text{H}_{16}\text{ClN}_5\text{O}_5\text{S}$) 474.06389, found 474.06232 ($\text{M}+\text{H}$)⁺

4-(3-Chlorophenyl)-3-(4-(hydroxymethyl)phenyl)-N-(5-nitrothiazol-2-yl)-2-oxoimidazolidine-1-carboxamide(F14)

The title compound was synthesized according to the procedure F using **E14** and 2-amino-5-nitrothiazole, yield: 82%, yellowish white solid. ^1H NMR (500 MHz, DMSO) δ 12.85 (s, 1H), 8.54 (s, 1H), 7.48 – 7.42 (m, 2H), 7.41 – 7.34 (m, 2H), 7.34 – 7.26 (m, 4H), 7.19 (s, 1H), 5.54 (dd, $J = 9.1, 5.1$ Hz, 1H), 5.20 (d, $J = 1.6$ Hz, 2H), 3.86 (t, $J = 9.2$ Hz, 1H), 3.09 (dd, $J = 9.2, 5.1$ Hz, 1H). ^{13}C NMR (126 MHz, acetone) δ 162.17, 155.42, 150.66, 144.24, 142.70, 141.95, 141.77, 135.47, 133.85, 131.82, 129.81, 127.96, 126.40, 122.84, 118.89, 109.17, 67.95, 56.99, 48.89. HRMS (ESI): calculated for ($\text{C}_{20}\text{H}_{16}\text{ClN}_5\text{O}_5\text{S}$) 472.043921, found 472.04752 ($\text{M}-\text{H}$)⁻.

4-(3-Chlorophenyl)-3-(4-methoxyphenyl)-N-(5-nitrothiazol-2-yl)-2-oxoimidazolidine-1-carboxamide(F15)

The title compound was synthesized according to the procedure F using **E15** and 2-amino-5-nitrothiazole, yield: 89%, yellowish white solid. ^1H NMR (500 MHz, DMSO) δ 12.05 (s, 1H), 8.65 (s, 1H), 7.63 (s, 1H), 7.45 (d, $J = 6.7$ Hz, 1H), 7.39 – 7.31 (m, 4H), 6.96 – 6.84 (m, 2H), 5.61 (dd, $J = 9.6, 6.5$ Hz, 1H), 4.46 (t, $J = 10.1$ Hz, 1H), 3.74 – 3.70 (m, 4H). ^{13}C NMR (126 MHz, DMSO) δ 160.15, 159.09, 155.65, 149.18, 147.81, 145.35, 139.89, 137.26, 135.82, 133.48, 129.02, 128.34, 125.27, 120.11, 115.08, 55.89, 55.01, 48.19. HRMS (ESI): calculated for ($\text{C}_{20}\text{H}_{16}\text{ClN}_5\text{O}_5\text{S}$) 474.06389, found 474.06265 ($\text{M}+\text{H}$)⁺

4-(3-Chlorophenyl)-3-(4-cyanophenyl)-N-(5-nitrothiazol-2-yl)-2-oxoimidazolidine-1-carboxamide(F16)

The title compound was synthesized according to the procedure F using **E16** and 2-amino-5-nitrothiazole, yield: 81%, yellowish white solid. ^1H NMR (500 MHz, acetone) δ 11.89 (s, 1H), 8.45 (s, 1H), 7.83 – 7.73 (m, 4H), 7.66 (t, $J = 1.9$ Hz, 1H), 7.54 (dt, $J = 7.6, 1.5$ Hz, 1H), 7.41 (t, $J = 7.8$ Hz, 1H), 7.37 (dt, $J = 8.2, 1.5$ Hz, 1H), 5.94 (dd, $J = 9.7, 5.8$ Hz, 1H), 4.69 (t, $J = 10.2$ Hz, 1H), 3.94 (dd, $J = 10.6, 5.8$ Hz, 1H). ^{13}C NMR (126 MHz, acetone) δ 162.17, 155.42,

150.66, 144.24, 142.70, 141.95, 141.77, 135.47, 133.85, 131.82, 129.81, 127.96, 126.40, 122.84, 118.89, 109.17, 56.99, 48.89. HRMS (ESI): calculated for (C₂₀H₁₃ClN₆O₄S) 469.04858, found 469.04678 (M+H)⁺

4-(3-Chlorophenyl)-3-(4-morpholinophenyl)-N-(5-nitrothiazol-2-yl)-2-oxoimidazolidine-1-carboxamide(F17)

The title compound was synthesized according to the procedure F using **E17** and 2-amino-5-nitrothiazole, yield: 83%, yellowish white solid. ¹H NMR (500 MHz, DMSO) δ 12.05 (s, 1H), 8.64 (s, 1H), 7.61 (s, 1H), 7.42 (dd, *J* = 12.0, 4.9 Hz, 1H), 7.38 – 7.32 (m, 2H), 7.24 (d, *J* = 9.0 Hz, 2H), 6.88 (d, *J* = 9.1 Hz, 2H), 5.59 (dd, *J* = 9.7, 6.3 Hz, 1H), 4.44 (t, *J* = 10.2 Hz, 1H), 3.70 (dd, *J* = 8.6, 4.3 Hz, 1H), 3.70 – 3.66 (m, 4H), 3.07 – 3.03 (m, 4H). ¹³C NMR (126 MHz, DMSO) δ 161.37, 154.16, 149.79, 148.97, 142.98, 142.35, 141.65, 133.49, 130.72, 128.54, 127.43, 127.22, 126.25, 124.40, 114.89, 66.04, 56.33, 47.98, 47.62. HRMS (ESI): calculated for (C₂₃H₂₁ClN₆O₅S) 529.10609, found 529.10486 (M+H)⁺

4-(3-Chlorophenyl)-3-(3-fluoro-4-morpholinophenyl)-N-(5-nitrothiazol-2-yl)-2-oxoimidazolidine-1-carboxamide(F18)

The title compound was synthesized according to the procedure F using **E18** and 2-amino-5-nitrothiazole, yield: 82%, yellowish white solid. ¹H NMR (500 MHz, acetone) δ 12.00 (s, 1H), 8.46 (s, 1H), 7.63 (t, *J* = 1.9 Hz, 1H), 7.53 (dt, *J* = 7.7, 1.5 Hz, 1H), 7.44 – 7.33 (m, 3H), 7.23 – 7.15 (m, 1H), 6.99 (t, *J* = 9.2 Hz, 1H), 5.76 (dd, *J* = 9.8, 6.0 Hz, 1H), 4.62 (t, *J* = 10.2 Hz, 1H), 3.90 (dd, *J* = 10.7, 6.0 Hz, 1H), 3.79 – 3.70 (m, 4H), 3.03 – 2.99 (m, 4H). ¹³C NMR (126 MHz, acetone) δ 155.71 (d, *J* = 245.4 Hz), 155.41, 154.74, 150.75, 150.66, 142.68, 142.37, 138.61 (d, *J* = 8.5 Hz), 135.32, 131.91 (d, *J* = 10.2 Hz), 131.69, 129.70, 128.12, 126.60, 119.78 (d, *J* = 3.2 Hz), 119.66 (d, *J* = 4.1 Hz), 112.07 (d, *J* = 25.0 Hz), 67.27, 57.60, 51.58, 48.77. HRMS (ESI): calculated for (C₂₃H₂₀ClFN₆O₅S) 547.09667, found 547.09473 (M+H)⁺

4-(3-Chlorophenyl)-3-(4-fluoro-3-(morpholinosulfonyl)phenyl)-N-(5-nitrothiazol-2-yl)-2-oxoimidazolidine-1-carboxamide(F19)

The title compound was synthesized according to the procedure F using **E19** and 2-amino-5-nitrothiazole, yield: 84%, yellowish white solid. ¹H NMR (500 MHz, acetone) δ 11.91 (s, 1H), 8.44 (s, 1H), 7.95 (ddd, *J* = 9.0, 4.0, 2.9 Hz, 1H), 7.80 (dd, *J* = 5.8, 2.8 Hz, 1H), 7.70 (t, *J* = 1.9 Hz, 1H), 7.58 (dt, *J* = 7.6, 1.6 Hz, 1H), 7.46 – 7.37 (m, 3H), 5.90 (dd, *J* = 9.7, 6.8 Hz, 1H), 4.70 (t, *J* = 10.2 Hz, 1H), 3.97 (dd, *J* = 10.7, 6.8 Hz, 1H), 3.68 – 3.56 (m, 4H), 2.98 – 2.85 (m, 4H).

^{13}C NMR (126 MHz, acetone) δ 162.20, 156.87 (d, $J = 254.6$ Hz), 155.52, 150.67, 144.18, 142.71, 141.54, 135.42, 133.98 (d, $J = 3.0$ Hz), 131.85, 130.57 (d, $J = 8.5$ Hz), 129.97, 128.50, 127.01, 125.90, 125.05 (d, $J = 16.3$ Hz), 119.17 (d, $J = 23.9$ Hz), 66.62, 57.78, 48.80, 46.63. HRMS (ESI): calculated for ($\text{C}_{23}\text{H}_{20}\text{ClFN}_6\text{O}_7\text{S}_2$) 611.05857, found 611.05646 ($\text{M}+\text{H}$) $^+$

4-(3-Chlorophenyl)-N-(5-nitrothiazol-2-yl)-2-oxo-3-(pyridin-3-yl)imidazolidine-1-carboxamide(F20)

The title compound was synthesized according to the procedure F using **E20** and 2-amino-5-nitrothiazole, yield: 85%, yellowish white solid. ^1H NMR (500 MHz, acetone) δ ^1H NMR (500 MHz, DMSO) δ 11.83 (s, 1H), 8.61 (d, $J = 2.2$ Hz, 1H), 8.55 (s, 1H), 8.43 (dd, $J = 4.8, 1.6$ Hz, 1H), 7.91 (dt, $J = 7.9, 2.1$ Hz, 1H), 7.57 (d, $J = 2.3$ Hz, 1H), 7.38 – 7.27 (m, 3H), 7.21 (dt, $J = 6.6, 2.2$ Hz, 1H), 5.84 (dd, $J = 9.7, 6.2$ Hz, 1H), 4.39 (t, $J = 10.1$ Hz, 1H), 3.71 (dd, $J = 10.5, 6.2$ Hz, 1H). ^{13}C NMR (126 MHz, DMSO) δ 163.58, 161.84, 155.88, 149.35, 147.24, 145.95, 144.81, 139.28, 137.22, 133.12, 133.25, 130.87, 125.64, 124.09, 122.32, 121.65, 54.21, 47.63. HRMS (ESI): calculated for ($\text{C}_{18}\text{H}_{13}\text{ClN}_6\text{O}_4\text{S}$) 445.04858, found 445.04700 ($\text{M}+\text{H}$) $^+$

4-(3-Chlorophenyl)-3-(6-fluoropyridin-3-yl)-N-(5-nitrothiazol-2-yl)-2-oxoimidazolidine-1-carboxamide(F21)

The title compound was synthesized according to the procedure F using **E21** and 2-amino-5-nitrothiazole, yield: 82%, yellowish white solid. ^1H NMR (500 MHz, acetone) δ 11.88 (s, 1H), 8.42 (d, $J = 1.2$ Hz, 1H), 8.37 – 8.30 (m, 1H), 8.14 (ddd, $J = 9.2, 6.9, 2.9$ Hz, 1H), 7.67 (d, $J = 2.0$ Hz, 1H), 7.57 (dt, $J = 7.4, 1.5$ Hz, 1H), 7.45 – 7.29 (m, 2H), 7.10 (dd, $J = 8.9, 3.3$ Hz, 1H), 5.86 (dd, $J = 9.7, 6.5$ Hz, 1H), 4.70 (t, $J = 10.2$ Hz, 1H), 3.99 (dd, $J = 10.7, 6.5$ Hz, 1H). ^{13}C NMR (126 MHz, acetone) δ 162.55, 161.61 (d, $J = 236.2$ Hz), 155.71, 150.74, 144.28, 143.00, 142.93 (d, $J = 16.0$ Hz), 141.55, 137.15 (d, $J = 8.3$ Hz), 135.59, 132.53 (d, $J = 4.7$ Hz), 131.90, 130.07, 128.49, 126.97, 110.61 (d, $J = 39.5$ Hz), 57.75, 49.11. HRMS (ESI): calculated for ($\text{C}_{18}\text{H}_{12}\text{ClFN}_6\text{O}_4\text{S}$) 463.03915, found 463.03757 ($\text{M}+\text{H}$) $^+$

4-(3-Chlorophenyl)-3-(6-chloropyridin-3-yl)-N-(5-nitrothiazol-2-yl)-2-oxoimidazolidine-1-carboxamide(F22)

The title compound was synthesized according to the procedure F using **E22** and 2-amino-5-nitrothiazole, yield: 91%, yellowish white solid. ^1H NMR (500 MHz, acetone) δ 11.87 (s, 1H), 8.56 (d, $J = 2.9$ Hz, 1H), 8.45 (s, 1H), 8.04 (dd, $J = 8.7, 2.9$ Hz, 1H), 7.69 (d, $J = 1.9$ Hz, 1H), 7.60 – 7.55 (m, 1H), 7.47 – 7.37 (m, 3H), 5.91 (dd, $J = 9.8, 6.3$ Hz, 1H), 4.71 (t, $J = 10.2$ Hz,

1H), 3.98 (dd, $J = 10.7, 6.4$ Hz, 1H). ^{13}C NMR (126 MHz, acetone) δ 162.17, 155.53, 150.62, 147.87, 144.35, 144.22, 142.70, 141.46, 135.49, 133.86, 133.65, 131.84, 129.97, 128.31, 126.79, 125.16, 57.17, 49.04. HRMS (ESI): calculated for ($\text{C}_{18}\text{H}_{12}\text{Cl}_2\text{N}_6\text{O}_4\text{S}$) 479.00960, found 479.00830 (M+H)⁺

4-(3-Chlorophenyl)-3-(5-chloropyridin-3-yl)-N-(5-nitrothiazol-2-yl)-2-oxoimidazolidine-1-carboxamide(F23)

The title compound was synthesized according to the procedure F using **E23** and 2-amino-5-nitrothiazole, yield: 81%, yellowish white solid. ^1H NMR (500 MHz, acetone) δ 11.84 (s, 1H), 8.66 (d, $J = 2.2$ Hz, 1H), 8.45 (s, 1H), 8.35 (d, $J = 2.1$ Hz, 1H), 8.14 (d, $J = 2.3$ Hz, 1H), 7.71 (d, $J = 2.0$ Hz, 1H), 7.59 (d, $J = 7.6$ Hz, 1H), 7.46 – 7.32 (m, 2H), 5.95 (dd, $J = 9.8, 6.2$ Hz, 1H), 4.72 (t, $J = 10.2$ Hz, 1H), 3.98 (dd, $J = 10.7, 6.2$ Hz, 1H). ^{13}C NMR (126 MHz, acetone) δ 162.13, 155.53, 150.56, 145.70, 144.23, 142.69, 142.26, 141.44, 135.52, 135.17, 132.07, 131.86, 129.99, 129.69, 128.22, 126.70, 57.01, 49.07. HRMS (ESI): calculated for ($\text{C}_{18}\text{H}_{12}\text{Cl}_2\text{N}_6\text{O}_4\text{S}$) 479.00960, found 479.00818 (M+H)⁺

3-(6-Bromopyridin-3-yl)-4-(3-chlorophenyl)-N-(5-nitrothiazol-2-yl)-2-oxoimidazolidine-1-carboxamide(F24)

The title compound was synthesized according to the procedure F using **E24** and 2-amino-5-nitrothiazole, yield: 84%, yellowish white solid. ^1H NMR (500 MHz, acetone) δ 11.87 (s, 1H), 8.55 (d, $J = 2.9$ Hz, 1H), 8.45 (s, 1H), 7.94 (dd, $J = 8.7, 3.0$ Hz, 1H), 7.69 (t, $J = 1.9$ Hz, 1H), 7.64 – 7.51 (m, 2H), 7.46 – 7.33 (m, 2H), 5.90 (dd, $J = 9.7, 6.3$ Hz, 1H), 4.71 (t, $J = 10.2$ Hz, 1H), 3.97 (dd, $J = 10.7, 6.3$ Hz, 1H). ^{13}C NMR (126 MHz, acetone) δ 162.17, 155.49, 150.61, 144.78, 142.70, 141.45, 138.06, 135.50, 134.33, 133.33, 131.85, 129.98, 128.96, 128.30, 126.78, 57.09, 49.05. HRMS (ESI): calculated for ($\text{C}_{18}\text{H}_{12}\text{BrClN}_6\text{O}_4\text{S}$) 524.95909, found 524.95526 (M+H)⁺

4-(3-Chlorophenyl)-N-(5-nitrothiazol-2-yl)-2-oxo-3-(quinolin-3-yl)imidazolidine-1-carboxamide(F25)

The title compound was synthesized according to the procedure F using **E25** and 2-amino-5-nitrothiazole, yield: 82%, yellowish white solid. ^1H NMR (500 MHz, acetone) δ 11.99 (s, 1H), 9.14 (d, $J = 2.6$ Hz, 1H), 8.45 (s, 1H), 8.38 (d, $J = 2.6$ Hz, 1H), 7.99 (d, $J = 8.4$ Hz, 1H), 7.89 (dd, $J = 8.3, 1.4$ Hz, 1H), 7.75 (d, $J = 2.0$ Hz, 1H), 7.71 (ddd, $J = 8.4, 6.7, 1.5$ Hz, 1H), 7.64 (dt, $J = 7.7, 1.4$ Hz, 1H), 7.59 (ddd, $J = 8.2, 6.8, 1.2$ Hz, 1H), 7.39 (t, $J = 7.9$ Hz, 1H), 7.32 (dt,

$J = 8.0, 1.5$ Hz, 1H), 6.06 (dd, $J = 9.7, 6.5$ Hz, 1H), 4.77 (t, $J = 10.2$ Hz, 1H), 4.04 (dd, $J = 10.7, 6.5$ Hz, 1H). ^{13}C NMR (126 MHz, acetone) δ 162.27, 155.84, 150.76, 146.91, 146.65, 144.19, 142.75, 141.81, 135.41, 131.76, 131.36, 130.12, 129.97, 129.88, 128.65, 128.46, 128.43, 128.33, 128.25, 126.93, 57.49, 49.11. HRMS (ESI): calculated for ($\text{C}_{22}\text{H}_{15}\text{ClN}_6\text{O}_4\text{S}$) 495.06423, found 495.06272 (M+H)⁺

4-(3-Chlorophenyl)-3-(naphthalen-2-yl)-N-(5-nitrothiazol-2-yl)-2-oxoimidazolidine-1-carboxamide(F26)

The title compound was synthesized according to the procedure F using **E26** and 2-amino-5-nitrothiazole, yield: 92%, yellowish white solid. ^1H NMR (500 MHz, DMSO) δ 12.04 (s, 1H), 8.66 (s, 1H), 7.94 (d, $J = 2.2$ Hz, 1H), 7.89 (d, $J = 8.9$ Hz, 1H), 7.84 (t, $J = 7.5$ Hz, 2H), 7.72 – 7.65 (m, 2H), 7.55 – 7.44 (m, 3H), 7.37 – 7.28 (m, 2H), 5.86 (dd, $J = 9.7, 6.1$ Hz, 1H), 4.53 (t, $J = 10.1$ Hz, 1H), 3.84 – 3.67 (m, 1H). ^{13}C NMR (126 MHz, DMSO) δ 161.52, 158.15, 154.12, 149.19, 146.09, 145.55, 143.08, 141.45, 133.47, 132.73, 130.71, 130.61, 128.59, 128.52, 127.51, 127.36, 126.77, 126.17, 125.99, 121.59, 120.34, 55.81, 47.78. HRMS (ESI): calculated for ($\text{C}_{23}\text{H}_{16}\text{ClN}_5\text{O}_4\text{S}$) 494.06898, found 494.06699 (M+H)⁺

3-(3-Chlorophenyl)-N-(5-nitrothiazol-2-yl)-2-oxo-4-phenylimidazolidine-1-carboxamide(F27)

The title compound was synthesized according to the procedure F using **E27** and 2-amino-5-nitrothiazole, yield: 85%, yellowish white solid. ^1H NMR (500 MHz, acetone) δ 12.00 (s, 1H), 8.44 (s, 1H), 7.67 (t, $J = 2.2$ Hz, 1H), 7.58 – 7.53 (m, 2H), 7.48 – 7.27 (m, 5H), 7.18 (dd, $J = 8.0, 2.0$ Hz, 1H), 5.82 (dd, $J = 9.7, 5.9$ Hz, 1H), 4.64 (t, $J = 10.1$ Hz, 1H), 3.90 (dd, $J = 10.6, 5.9$ Hz, 1H). ^{13}C NMR (126 MHz, acetone) δ 162.48, 155.62, 150.95, 144.19, 142.85, 139.78, 139.31, 134.84, 131.20, 130.13, 129.73, 127.99, 126.35, 123.45, 121.69, 58.06, 49.24. HRMS (ESI): calculated for ($\text{C}_{19}\text{H}_{14}\text{ClN}_5\text{O}_4\text{S}$) 444.05333, found 444.05175 (M+H)⁺

3-(3-Chlorophenyl)-4-(3-methoxyphenyl)-N-(5-nitrothiazol-2-yl)-2-oxoimidazolidine-1-carboxamide(F28)

The title compound was synthesized according to the procedure F using **E28** and 2-amino-5-nitrothiazole, yield: 88%, yellowish white solid. ^1H NMR (500 MHz, DMSO) δ 11.94 (s, 1H), 8.66 (s, 1H), 7.62 (t, $J = 2.0$ Hz, 1H), 7.39 – 7.33 (m, 2H), 7.26 (t, $J = 7.9$ Hz, 1H), 7.20 (dt, $J = 6.9, 2.0$ Hz, 1H), 7.08 (t, $J = 2.1$ Hz, 1H), 7.03 (d, $J = 7.5$ Hz, 1H), 6.85 (dd, $J = 8.3, 2.6$ Hz, 1H), 5.68 (dd, $J = 9.6, 6.1$ Hz, 1H), 4.45 (t, $J = 10.0$ Hz, 1H), 3.73 – 3.67 (m, 4H). ^{13}C NMR

(126 MHz, DMSO) δ 161.24, 159.62, 153.99, 149.67, 142.90, 142.45, 140.13, 137.86, 133.09, 130.48, 130.12, 125.33, 122.20, 120.84, 119.17, 113.87, 112.93, 56.08, 55.13, 47.90. HRMS (ESI): calculated for (C₂₀H₁₆ClN₅O₅S) 474.06389, found 474.06256 (M+H)⁺

3-(3-Chlorophenyl)-4-(4-methoxyphenyl)-N-(5-nitrothiazol-2-yl)-2-oxoimidazolidine-1-carboxamide(F29)

The title compound was synthesized according to the procedure F using **E29** and 2-amino-5-nitrothiazole, yield: 85%, yellowish white solid. ¹H NMR (500 MHz, DMSO) δ 12.15 – 11.59 (m, 1H), 8.65 (d, *J* = 2.0 Hz, 1H), 7.58 (s, 1H), 7.46 – 7.30 (m, 4H), 7.19 (dt, *J* = 4.8, 2.2 Hz, 1H), 6.89 (dd, *J* = 8.8, 2.0 Hz, 2H), 5.66 (dd, *J* = 9.5, 6.4 Hz, 1H), 4.43 (t, *J* = 9.9 Hz, 1H), 3.70 (d, *J* = 1.9 Hz, 4H). ¹³C NMR (126 MHz, DMSO) δ 161.25, 159.29, 153.95, 149.68, 142.91, 142.45, 137.79, 133.06, 130.42, 130.18, 128.62, 125.34, 122.47, 121.11, 114.28, 55.82, 55.06, 48.11. HRMS (ESI): calculated for (C₂₀H₁₆ClN₅O₅S) 474.06389, found 474.06271 (M+H)⁺

3-(3-Chlorophenyl)-4-(4-cyanophenyl)-N-(5-nitrothiazol-2-yl)-2-oxoimidazolidine-1-carboxamide(F30)

The title compound was synthesized according to the procedure F using **E30** and 2-amino-5-nitrothiazole, yield: 84%, yellowish white solid. ¹H NMR (500 MHz, DMSO) δ 11.88 (s, 1H), 8.66 (s, 1H), 7.84 (d, *J* = 8.0 Hz, 2H), 7.72 (d, *J* = 8.0 Hz, 2H), 7.64 (s, 1H), 7.35 (d, *J* = 4.7 Hz, 2H), 7.21 (h, *J* = 4.8 Hz, 1H), 5.84 (dd, *J* = 9.8, 5.9 Hz, 1H), 4.48 (t, *J* = 10.1 Hz, 1H), 3.70 (dd, *J* = 10.6, 5.8 Hz, 1H). ¹³C NMR (126 MHz, DMSO) δ 161.31, 153.92, 152.47, 144.10, 143.04, 142.42, 137.66, 133.26, 132.95, 130.64, 128.35, 125.49, 122.13, 120.70, 118.42, 111.46, 55.61, 47.55. HRMS (ESI): calculated for (C₂₀H₁₃ClN₆O₄S) 469.04858, found 469.04733 (M+H)⁺

3-(3-chlorophenyl)-N-(5-nitrothiazol-2-yl)-2-oxo-4-(pyridin-3-yl)imidazolidine-1-carboxamide(F31)

The title compound was synthesized according to the procedure F using **E31** and 2-amino-5-nitrothiazole, yield: 88%, yellowish white solid. ¹H NMR (500 MHz, DMSO) δ 11.97 (s, 1H), 8.71 (d, *J* = 2.2 Hz, 1H), 8.66 (s, 1H), 8.49 (dd, *J* = 4.8, 1.6 Hz, 1H), 7.96 (dt, *J* = 7.9, 2.1 Hz, 1H), 7.62 (d, *J* = 2.3 Hz, 1H), 7.41 – 7.30 (m, 3H), 7.21 (dt, *J* = 6.6, 2.2 Hz, 1H), 5.80 (dd, *J* = 9.7, 6.2 Hz, 1H), 4.50 (t, *J* = 10.1 Hz, 1H), 3.78 (dd, *J* = 10.5, 6.2 Hz, 1H). ¹³C NMR (126 MHz, DMSO) δ 163.09, 161.29, 153.96, 149.87, 149.05, 142.94, 142.49, 137.46, 135.10,

134.12, 133.25, 130.63, 125.64, 124.09, 122.59, 121.17, 54.16, 47.62. HRMS (ESI): calculated for (C₁₈H₁₃ClN₆O₄S) 445.04858, found 445.04711 (M+H)⁺

3-(3-chlorophenyl)-4-(6-chloropyridin-3-yl)-N-(5-nitrothiazol-2-yl)-2-oxoimidazolidine-1-carboxamide(F32)

The title compound was synthesized according to the procedure F using **E32** and 2-amino-5-nitrothiazole, yield: 80%, yellowish white solid. ¹H NMR (500 MHz, DMSO) δ 8.65 (s, 1H), 8.57 (d, *J* = 2.5 Hz, 1H), 8.05 (dd, *J* = 8.4, 2.6 Hz, 1H), 7.63 (d, *J* = 2.3 Hz, 1H), 7.52 (d, *J* = 8.4 Hz, 1H), 7.36 (d, *J* = 5.4 Hz, 2H), 7.22 (dq, *J* = 6.1, 3.4 Hz, 1H), 5.82 (dd, *J* = 9.8, 6.2 Hz, 1H), 4.48 (t, *J* = 10.2 Hz, 1H), 3.78 (dd, *J* = 10.6, 6.3 Hz, 1H). ¹³C NMR (126 MHz, DMSO) δ 161.22, 153.90, 150.54, 149.65, 149.58, 142.91, 142.53, 138.84, 137.28, 133.74, 133.33, 130.69, 125.76, 124.77, 122.64, 121.18, 53.43, 47.36. HRMS (ESI): calculated for (C₁₈H₁₂Cl₂N₆O₄S) 479.00960, found 479.00815 (M+H)⁺

3-(3-Chlorophenyl)-4-(2-chloropyrimidin-5-yl)-N-(5-nitrothiazol-2-yl)-2-oxoimidazolidine-1-carboxamide (F33)

The title compound was synthesized according to the procedure F using **E33** and 2-amino-5-nitrothiazole, yield: 80%, yellowish white solid. ¹H NMR (500 MHz, acetone) δ 11.87 (s, 1H), 9.00 (s, 2H), 8.45 (s, 1H), 7.75 – 7.70 (m, 1H), 7.48 (dd, *J* = 8.2, 2.0 Hz, 1H), 7.40 (t, *J* = 8.1 Hz, 1H), 7.24 (dd, *J* = 7.9, 2.0 Hz, 1H), 6.09 (dd, *J* = 9.9, 6.1 Hz, 1H), 4.74 (t, *J* = 10.4 Hz, 1H), 4.14 (dd, *J* = 10.8, 6.1 Hz, 1H). ¹³C NMR (126 MHz, acetone) δ 162.16, 161.94, 160.51, 157.56, 155.30, 150.65, 144.20, 142.72, 138.31, 135.13, 132.44, 131.51, 126.97, 123.86, 122.02, 53.48, 48.11. HRMS (ESI): calculated for (C₁₇H₁₁Cl₂N₇O₄S) 480.00485, found 480.00354 (M+H)⁺

4-(5-Bromopyridin-2-yl)-3-(3-chlorophenyl)-N-(5-nitrothiazol-2-yl)-2-oxoimidazolidine-1-carboxamide(F34)

The title compound was synthesized according to the procedure F using **E34** and 2-amino-5-nitrothiazole, yield: 84%, yellowish white solid. ¹H NMR (500 MHz, DMSO) δ 11.87 (s, 1H), 8.69 (d, *J* = 2.3 Hz, 1H), 8.65 (s, 1H), 8.08 (dd, *J* = 8.3, 2.4 Hz, 1H), 7.67 (d, *J* = 2.1 Hz, 1H), 7.58 (d, *J* = 8.3 Hz, 1H), 7.42 – 7.31 (m, 2H), 7.23 – 7.18 (m, 1H), 5.84 (dd, *J* = 9.7, 4.2 Hz, 1H), 4.41 (t, *J* = 10.1 Hz, 1H), 3.89 (dd, *J* = 10.5, 4.2 Hz, 1H). ¹³C NMR (126 MHz, DMSO) δ 161.22, 156.08, 154.00, 150.84, 149.58, 142.88, 142.55, 140.09, 137.97, 133.34, 130.71,

125.34, 124.58, 121.45, 120.28, 120.09, 56.48, 46.03. HRMS (ESI): calculated for (C₁₈H₁₂BrClN₆O₄S) 524.95909, found 524.95508 (M+H)⁺

3-(3-Chlorophenyl)-N-(5-nitrothiazol-2-yl)-2-oxo-4-(quinolin-2-yl)imidazolidine-1-carboxamide(F35)

The title compound was synthesized according to the procedure F using **E35** and 2-amino-5-nitrothiazole, yield: 89%, yellowish white solid. ¹H NMR (500 MHz, acetone) δ 12.01 (s, 1H), 8.45 (s, 1H), 8.39 (d, *J* = 8.5 Hz, 1H), 8.02 (d, *J* = 8.5 Hz, 1H), 7.95 (dd, *J* = 8.3, 1.4 Hz, 1H), 7.82 – 7.72 (m, 3H), 7.61 (ddd, *J* = 8.1, 6.7, 1.2 Hz, 1H), 7.50 (dd, *J* = 8.3, 2.2 Hz, 1H), 7.31 (t, *J* = 8.2 Hz, 1H), 7.14 (dd, *J* = 8.1, 2.0 Hz, 1H), 6.05 (dd, *J* = 9.8, 4.7 Hz, 1H), 4.77 – 4.60 (m, 1H), 4.18 (dd, *J* = 10.7, 4.7 Hz, 1H). ¹³C NMR (126 MHz, DMSO) δ 161.25, 158.03, 154.13, 149.71, 146.95, 142.92, 142.47, 138.24, 138.05, 133.20, 130.61, 130.24, 128.71, 128.00, 127.41, 127.14, 125.23, 121.60, 120.17, 119.47, 58.00, 46.16. HRMS (ESI): calculated for (C₂₂H₁₅ClN₆O₄S) 495.06423, found 495.06268 (M+H)⁺

3-(3-Chlorophenyl)-N-(5-nitrothiazol-2-yl)-2-oxo-4-(quinolin-3-yl)imidazolidine-1-carboxamide(F36)

The title compound was synthesized according to the procedure F using **E36** and 2-amino-5-nitrothiazole, yield: 94%, yellowish white solid. ¹H NMR (500 MHz, acetone) δ 11.98 (s, 1H), 9.13 (d, *J* = 2.3 Hz, 1H), 8.52 (d, *J* = 2.4 Hz, 1H), 8.45 (s, 1H), 8.02 (d, *J* = 8.5 Hz, 1H), 7.91 (d, *J* = 8.3 Hz, 1H), 7.81 – 7.69 (m, 2H), 7.59 (t, *J* = 7.5 Hz, 1H), 7.50 (dd, *J* = 8.3, 2.1 Hz, 1H), 7.32 (t, *J* = 8.1 Hz, 1H), 7.14 (dd, *J* = 8.1, 2.0 Hz, 1H), 6.14 (dd, *J* = 9.8, 6.1 Hz, 1H), 4.77 (t, *J* = 10.3 Hz, 1H), 4.13 (dd, *J* = 10.8, 6.1 Hz, 1H). ¹³C NMR (126 MHz, acetone) δ 162.33, 155.57, 150.84, 150.54, 149.21, 144.25, 142.82, 138.92, 135.65, 134.98, 132.47, 131.35, 130.96, 130.19, 129.05, 128.52, 128.15, 126.64, 123.71, 121.92, 56.28, 48.86. HRMS (ESI): calculated for (C₂₂H₁₅ClN₆O₄S) 495.06423, found 495.06284 (M+H)⁺

3-(3-Chlorophenyl)-N-(5-nitrothiazol-2-yl)-2-oxo-4-(quinolin-4-yl)imidazolidine-1-carboxamide(F37)

The title compound was synthesized according to the procedure F using **E37** and 2-amino-5-nitrothiazole, yield: 87%, yellowish white solid. ¹H NMR (500 MHz, acetone) δ 11.92 (s, 1H), 8.85 (d, *J* = 4.5 Hz, 1H), 8.45 (s, 1H), 8.38 (dd, *J* = 8.4, 1.2 Hz, 1H), 8.15 (d, *J* = 8.5 Hz, 1H), 7.89 – 7.84 (m, 2H), 7.81 – 7.73 (m, 1H), 7.53 – 7.43 (m, 2H), 7.33 (t, *J* = 8.2 Hz, 1H), 7.19 (dd, *J* = 8.0, 2.1 Hz, 1H), 6.73 (s, 1H), 4.92 (t, *J* = 10.2 Hz, 1H), 3.99 (dd, *J* = 10.5, 4.9 Hz,

1H). ¹³C NMR (126 MHz, acetone) δ 162.17, 155.58, 151.26, 150.70, 149.74, 144.24, 142.70, 139.38, 135.05, 131.54, 131.39, 130.63, 128.44, 126.25, 126.13, 123.71, 122.23, 122.09, 121.66, 120.32, 53.59, 47.95. HRMS (ESI): calculated for (C₂₂H₁₅ClN₆O₄S) 495.06423, found 495.06268 (M+H)⁺

3-(3-Chlorophenyl)-N-(5-nitrothiazol-2-yl)-2-oxo-4-(quinolin-6-yl)imidazolidine-1-carboxamide(F38)

The title compound was synthesized according to the procedure F using **E38** and 2-amino-5-nitrothiazole, yield: 84%, yellowish white solid. ¹H NMR (500 MHz, acetone) δ 12.00 (s, 1H), 8.90 (dd, *J* = 4.3, 1.7 Hz, 1H), 8.45 (s, 1H), 8.30 (dd, *J* = 8.3, 1.7 Hz, 1H), 8.17 – 8.09 (m, 1H), 8.07 (d, *J* = 8.8 Hz, 1H), 7.98 (dd, *J* = 8.8, 2.1 Hz, 1H), 7.74 (t, *J* = 2.1 Hz, 1H), 7.50 (ddd, *J* = 13.5, 8.3, 3.2 Hz, 2H), 7.31 (t, *J* = 8.2 Hz, 1H), 7.14 (dd, *J* = 8.1, 2.0 Hz, 1H), 6.06 (dd, *J* = 9.8, 5.9 Hz, 1H), 4.73 (t, *J* = 10.2 Hz, 1H), 4.04 (dd, *J* = 10.7, 5.9 Hz, 1H). ¹³C NMR (126 MHz, acetone) δ 162.28, 155.57, 152.05, 150.80, 149.14, 144.17, 142.74, 139.11, 137.66, 136.81, 134.80, 131.68, 131.17, 128.99, 128.34, 127.97, 126.40, 123.48, 122.85, 121.71, 57.93, 48.86. HRMS (ESI): calculated for (C₂₂H₁₅ClN₆O₄S) 495.06423, found 495.06293 (M+H)⁺

N-(5-Nitrothiazol-2-yl)-2-oxo-4-(quinolin-2-yl)-3-(quinolin-3-yl)imidazolidine-1-carboxamide(F39)

The title compound was synthesized according to the procedure F using **E39** and 2-amino-5-nitrothiazole, yield: 92%, yellowish white solid. ¹H NMR (500 MHz, DMSO) δ 11.99 (s, 1H), 9.15 (d, *J* = 2.5 Hz, 1H), 8.65 (s, 1H), 8.44 (d, *J* = 2.6 Hz, 1H), 8.39 (d, *J* = 8.6 Hz, 1H), 7.98 (d, *J* = 8.5 Hz, 1H), 7.94 – 7.86 (m, 3H), 7.80 (d, *J* = 8.5 Hz, 1H), 7.74 (ddd, *J* = 8.4, 6.7, 1.4 Hz, 1H), 7.67 (ddd, *J* = 8.5, 6.7, 1.5 Hz, 1H), 7.57 (dt, *J* = 12.0, 7.5 Hz, 2H), 6.15 (dd, *J* = 9.8, 5.1 Hz, 1H), 4.63 (t, *J* = 10.2 Hz, 1H), 4.09 (dd, *J* = 10.6, 5.1 Hz, 1H). ¹³C NMR (126 MHz, DMSO) δ 163.19, 157.96, 154.38, 146.99, 145.74, 144.79, 138.09, 130.93, 130.50, 130.30, 129.33, 128.74, 128.60, 128.04, 127.88, 127.50, 127.43, 126.90, 125.88, 119.79, 115.43, 111.48, 111.05, 57.93, 45.66. HRMS (ESI): calculated for (C₂₅H₁₇N₇O₄S) 512.11410, found 512.11554 (M+H)⁺

4-(3-Methoxyphenyl)-N-(5-nitrothiazol-2-yl)-2-oxo-3-(quinolin-3-yl)imidazolidine-1-carboxamide(F40)

The title compound was synthesized according to the procedure F using **E40** and 2-amino-5-nitrothiazole, yield: 92%, yellowish white solid. ¹H NMR (500 MHz, DMSO) δ 11.98 (s, 1H),

9.04 (d, $J = 2.5$ Hz, 1H), 8.67 (s, 1H), 8.37 (t, $J = 3.4$ Hz, 1H), 7.94 (dd, $J = 13.0, 8.3$ Hz, 2H), 7.74 – 7.67 (m, 1H), 7.62 – 7.57 (m, 1H), 7.23 (q, $J = 7.9$ Hz, 1H), 7.17 (s, 1H), 7.13 (d, $J = 7.7$ Hz, 1H), 6.81 (dd, $J = 8.2, 2.5$ Hz, 1H), 5.84 (dd, $J = 9.5, 6.7$ Hz, 1H), 4.56 (t, $J = 10.0$ Hz, 1H), 3.82 (dd, $J = 10.3, 6.6$ Hz, 1H), 3.69 (s, 3H). ^{13}C NMR (126 MHz, DMSO) δ 161.37, 159.62, 154.31, 149.71, 146.06, 144.89, 142.96, 142.41, 139.78, 130.22, 130.11, 129.37, 128.60, 127.84, 127.60, 127.44, 127.14, 119.56, 114.05, 113.20, 56.21, 55.14, 48.13. HRMS (ESI): calculated for ($\text{C}_{23}\text{H}_{18}\text{N}_6\text{O}_5\text{S}$) 491.11376, found 491.11215 (M+H)⁺

4-(4-Bromophenyl)-N-(5-nitrothiazol-2-yl)-2-oxo-3-(quinolin-3-yl)imidazolidine-1-carboxamide(F41)

The title compound was synthesized according to the procedure F using **E41** and 2-amino-5-nitrothiazole, yield: 87%, yellowish white solid. ^1H NMR (500 MHz, DMSO) δ 11.96 (s, 1H), 9.04 (d, $J = 2.5$ Hz, 1H), 8.65 (s, 1H), 8.35 (d, $J = 2.5$ Hz, 1H), 7.94 (dd, $J = 17.9, 8.3$ Hz, 2H), 7.71 (t, $J = 7.7$ Hz, 1H), 7.60 (t, $J = 7.5$ Hz, 1H), 7.53 (t, $J = 7.1$ Hz, 4H), 5.88 (dd, $J = 9.6, 6.4$ Hz, 1H), 4.57 (t, $J = 10.1$ Hz, 1H), 3.81 (dd, $J = 10.5, 6.4$ Hz, 1H). ^{13}C NMR (126 MHz, acetone) δ 162.40, 155.69, 142.78, 142.48, 138.73, 135.09, 134.25, 131.61, 129.61, 128.48, 128.24, 127.59, 126.90, 126.76, 126.01, 122.53, 121.55, 114.97, 57.71, 48.89. HRMS (ESI): calculated for ($\text{C}_{22}\text{H}_{15}\text{BrN}_6\text{O}_4\text{S}$) 539.01371, found 541.01244 (M+H)⁺

4-([1,1'-Biphenyl]-4-yl)-N-(5-nitrothiazol-2-yl)-2-oxo-3-(quinolin-3-yl)imidazolidine-1-carboxamide(F42)

The title compound was synthesized according to the procedure F using **E42** and 2-amino-5-nitrothiazole, yield: 96%, yellowish white solid. ^1H NMR (500 MHz, DMSO) δ 11.99 (s, 1H), 9.09 (d, $J = 2.5$ Hz, 1H), 8.67 (s, 1H), 8.42 (d, $J = 2.5$ Hz, 1H), 7.97 – 7.91 (m, 2H), 7.73 – 7.56 (m, 8H), 7.40 (t, $J = 7.6$ Hz, 2H), 7.32 (t, $J = 7.3$ Hz, 1H), 5.96 (dd, $J = 9.6, 6.4$ Hz, 1H), 4.60 (t, $J = 10.0$ Hz, 1H), 3.87 (dd, $J = 10.4, 6.4$ Hz, 1H). ^{13}C NMR (126 MHz, DMSO) δ 161.32, 154.36, 149.72, 145.99, 144.91, 142.93, 142.47, 140.43, 139.23, 137.35, 130.23, 129.40, 128.89, 128.61, 128.14, 127.85, 127.67, 127.61, 127.47, 127.24, 127.17, 126.68, 55.96, 48.19. HRMS (ESI): calculated for ($\text{C}_{28}\text{H}_{20}\text{N}_6\text{O}_4\text{S}$) 537.13450, found 537.13361 (M+H)⁺

4-(4-(1H-1,2,4-Triazol-1-yl)phenyl)-N-(5-nitrothiazol-2-yl)-2-oxo-3-(quinolin-3-yl)imidazolidine-1-carboxamide(F43)

The title compound was synthesized according to the procedure F using **E43** and 2-amino-5-nitrothiazole, yield: 96%, yellowish white solid. ^1H NMR (500 MHz, DMSO) δ 12.32 (s, 1H),

9.55 (s, 1H), 9.41 (d, $J = 2.5$ Hz, 1H), 9.01 (s, 1H), 8.73 (d, $J = 2.4$ Hz, 1H), 8.52 (s, 1H), 8.31 – 8.24 (m, 2H), 8.18 – 8.12 (m, 4H), 8.06 – 8.01 (m, 1H), 7.97 – 7.90 (m, 1H), 6.31 (dd, $J = 9.6, 6.7$ Hz, 1H), 4.96 (t, $J = 10.1$ Hz, 1H), 4.21 (dt, $J = 19.4, 9.7$ Hz, 1H). ^{13}C NMR (126 MHz, DMSO) δ 153.39, 151.64, 144.64, 142.78, 140.06, 136.47, 135.28, 133.27, 132.75, 127.98, 127.12, 120.38, 119.79, 119.54, 118.94, 118.17, 118.15, 117.81, 117.47, 110.17, 46.10, 38.37.

HRMS (ESI): calculated for ($\text{C}_{24}\text{H}_{17}\text{N}_9\text{O}_4\text{S}$) 528.12025, found 528.11877 ($\text{M}+\text{H}$)⁺

***N*-(5-Nitrothiazol-2-yl)-2-oxo-4-(6-phenylpyridin-3-yl)-3-(quinolin-3-yl)imidazolidine-1-carboxamide(F44)**

The title compound was synthesized according to the procedure F using **E44** and 2-amino-5-nitrothiazole, yield: 80%, yellowish white solid. ^1H NMR (500 MHz, acetone) δ 12.00 (s, 1H), 9.18 (d, $J = 2.6$ Hz, 1H), 8.93 (d, $J = 2.3$ Hz, 1H), 8.46 (s, 1H), 8.42 (d, $J = 2.5$ Hz, 1H), 8.18 (dd, $J = 8.4, 2.4$ Hz, 1H), 8.06 – 8.01 (m, 2H), 7.97 (d, $J = 8.5$ Hz, 1H), 7.91 (dd, $J = 10.9, 8.3$ Hz, 2H), 7.69 (t, $J = 7.6$ Hz, 1H), 7.57 (t, $J = 7.5$ Hz, 1H), 7.45 – 7.38 (m, 3H), 6.18 (dd, $J = 9.7, 6.6$ Hz, 1H), 4.82 (t, $J = 10.2$ Hz, 1H), 4.14 (dd, $J = 10.8, 6.6$ Hz, 1H). ^{13}C NMR (126 MHz, acetone) δ 162.27, 158.17, 155.87, 150.77, 150.22, 147.12, 146.70, 144.20, 142.75, 139.26, 136.82, 133.37, 131.24, 130.17, 130.14, 129.96, 129.52, 128.73, 128.66, 128.46, 128.25, 127.57, 121.23, 55.86, 49.01. HRMS (ESI): calculated for ($\text{C}_{27}\text{H}_{19}\text{N}_7\text{O}_4\text{S}$) 538.12975, found 538.12830 ($\text{M}+\text{H}$)⁺

***N*-(5-Nitrothiazol-2-yl)-2-oxo-4-(5-phenylfuran-2-yl)-3-(quinolin-3-yl)imidazolidine-1-carboxamide(F45)**

The title compound was synthesized according to the procedure F using **E45** and 2-amino-5-nitrothiazole, yield: 87%, yellowish white solid. ^1H NMR (500 MHz, acetone) δ 11.99 (s, 1H), 9.12 (d, $J = 2.5$ Hz, 1H), 8.41 (s, 2H), 7.48 (d, $J = 7.5$ Hz, 4H), 7.32 (s, 5H), 6.77 (dd, $J = 19.3, 3.4$ Hz, 2H), 6.13 (dd, $J = 9.7, 6.2$ Hz, 1H), 4.70 (t, $J = 10.2$ Hz, 1H), 4.43 (dd, $J = 10.6, 6.2$ Hz, 1H). ^{13}C NMR (126 MHz, acetone) δ 161.07, 159.12, 157.27, 155.17, 154.22, 149.02, 148.10, 145.23, 143.35, 138.06, 137.83, 135.27, 133.94, 131.19, 130.04, 129.99, 129.02, 128.73, 128.56, 128.31, 128.05, 127.17, 124.01, 57.88, 48.91. HRMS (ESI): calculated for ($\text{C}_{22}\text{H}_{15}\text{BrN}_6\text{O}_4\text{S}$) 527.11376, found 527.11230 ($\text{M}+\text{H}$)⁺

4-(4-(Furan-2-yl)phenyl)-*N*-(5-nitrothiazol-2-yl)-2-oxo-3-(quinolin-3-yl)imidazolidine-1-carboxamide(F46)

The title compound was synthesized according to the procedure F using **E46** and 2-amino-5-nitrothiazole, yield: 87%, yellowish white solid. ¹H NMR (500 MHz, acetone) δ 12.10 (s, 1H), 8.43 (s, 1H), 7.92 (dd, *J* = 45.3, 8.4 Hz, 2H), 7.70 (s, 1H), 7.65 – 7.46 (m, 4H), 7.43 – 7.32 (m, 4H), 6.95 – 6.83 (m, 2H), 5.71 (dd, *J* = 9.8, 6.4 Hz, 1H), 4.62 (t, *J* = 10.2 Hz, 1H), 3.91 (dd, *J* = 10.7, 6.3 Hz, 1H). ¹³C NMR (126 MHz, acetone) δ 162.20, 159.99, 158.07, 156.33, 154.20, 148.02, 147.00, 146.11, 145.95, 141.26, 139.82, 137.37, 135.04, 134.17, 132.14, 131.96, 130.52, 129.73, 129.66, 128.06, 127.85, 127.57, 125.93, 55.16, 49.31. HRMS (ESI): calculated for (C₂₂H₁₅BrN₆O₄S) 527.11376, found 527.11230 (M+H)⁺

3-(3,4-Bis(3-chlorophenyl)-2-oxoimidazolidine-1-carboxamido)benzoic acid(F47)

The title compound was synthesized according to the procedure F using **E5** and 3-aminobenzoic acid, yield: 76%, white solid. ¹H NMR (500 MHz, acetone) δ 10.69 – 10.19 (m, 1H), 8.33 (dt, *J* = 4.0, 2.0 Hz, 1H), 7.83 (td, *J* = 5.7, 2.9 Hz, 1H), 7.80 – 7.69 (m, 3H), 7.63 (dt, *J* = 3.9, 2.0 Hz, 1H), 7.54 – 7.44 (m, 2H), 7.44 – 7.38 (m, 2H), 7.37 – 7.28 (m, 2H), 7.19 – 7.09 (m, 1H), 5.77 (dt, *J* = 9.7, 5.7 Hz, 1H), 4.55 (td, *J* = 10.6, 4.6 Hz, 1H), 3.84 – 3.76 (m, 1H). ¹³C NMR (126 MHz, acetone) δ 167.41, 156.08, 150.99, 142.81, 139.77, 139.50, 135.35, 134.74, 132.53, 131.74, 130.01, 129.52, 127.93, 126.32, 125.67, 125.38, 124.31, 122.85, 121.10, 120.89, 56.79, 49.12. HRMS (ESI): calculated for (C₂₃H₁₇Cl₂N₃O₄) 470.06774 found 470.06570 (M+H)⁺

4-([1,1'-Biphenyl]-4-yl)-N-(3-(N,N'-dihydroxycarbamimidoyl)phenyl)-2-oxo-3-(quinolin-3-yl)imidazolidine-1-carboxamide(48)

The title compound was synthesized according to the procedure F using **E42** and 3-amino-*N,N'*-dihydroxybenzimidamide, yield: 69%, white solid. ¹H NMR (500 MHz, DMSO) δ 10.33 (s, 1H), 9.10 (d, *J* = 2.6 Hz, 1H), 8.96 (s, 1H), 8.86 (s, 1H), 8.82 (s, 1H), 8.42 (d, *J* = 2.6 Hz, 1H), 7.93 (t, *J* = 7.8 Hz, 2H), 7.84 (t, *J* = 2.1 Hz, 1H), 7.71 – 7.62 (m, 6H), 7.61 – 7.55 (m, 3H), 7.41 (t, *J* = 7.6 Hz, 2H), 7.31 (ddd, *J* = 13.2, 7.1, 2.8 Hz, 3H), 7.22 (t, *J* = 8.1 Hz, 1H), 5.91 (dd, *J* = 9.6, 6.4 Hz, 1H), 4.53 (t, *J* = 10.0 Hz, 1H), 3.78 (dd, *J* = 10.3, 6.4 Hz, 1H). ¹³C NMR (126 MHz, DMSO) δ 162.61, 159.44, 158.50, 155.10, 149.73, 147.67, 145.83, 144.59, 140.24, 140.12, 139.32, 137.97, 137.83, 134.83, 130.95, 129.03, 128.89, 128.56, 127.83, 127.76, 127.62, 127.28, 126.67, 114.45, 113.00, 109.93, 55.35, 45.70. HRMS (ESI): calculated for (C₃₂H₂₆N₆O₄) 559.20938 found 559.20770 (M+H)⁺

4-([1,1'-Biphenyl]-4-yl)-N-(5-(methylthio)-1,3,4-thiadiazol-2-yl)-2-oxo-3-(quinolin-3-yl)imidazolidine-1-carboxamide(F49)

The title compound was synthesized according to the procedure F using **E42** and 5-(methylthio)-1,3,4-thiadiazol-2-amine, yield: 75%, white solid. ¹H NMR (500 MHz, DMSO) δ 11.72 (s, 1H), 9.09 (d, *J* = 2.5 Hz, 1H), 8.42 (d, *J* = 2.5 Hz, 1H), 7.97 – 7.90 (m, 2H), 7.73 – 7.65 (m, 3H), 7.64 – 7.55 (m, 5H), 7.40 (t, *J* = 7.6 Hz, 2H), 7.32 (t, *J* = 7.3 Hz, 1H), 5.94 (dd, *J* = 9.6, 6.5 Hz, 1H), 4.57 (t, *J* = 10.0 Hz, 1H), 3.83 (dd, *J* = 10.4, 6.5 Hz, 1H), 2.73 (s, 3H). ¹³C NMR (126 MHz, DMSO) δ 163.05, 160.83, 158.10, 154.63, 149.64, 145.96, 144.82, 140.37, 139.25, 137.50, 130.41, 129.29, 128.88, 128.60, 128.08, 127.82, 127.65, 127.43, 127.36, 127.23, 126.67, 55.84, 48.34, 15.98. HRMS (ESI): calculated for (C₂₈H₂₂N₆O₂S₂) 539.13239 found 539.13055 (M+H)⁺

4-([1,1'-Biphenyl]-4-yl)-N-morpholino-2-oxo-3-(quinolin-3-yl)imidazolidine-1-carboxamide(F50)

The title compound was synthesized according to the procedure F using **E42** and morpholin-4-amine, yield: 79%, white solid. ¹H NMR (500 MHz, DMSO) δ 9.18 – 9.05 (m, 2H), 8.41 (q, *J* = 2.9 Hz, 1H), 7.93 (dt, *J* = 12.0, 6.1 Hz, 2H), 7.70 (t, *J* = 7.5 Hz, 1H), 7.64 – 7.55 (m, 7H), 7.40 (t, *J* = 7.5 Hz, 2H), 7.32 (t, *J* = 7.3 Hz, 1H), 5.87 (dd, *J* = 9.6, 6.5 Hz, 1H), 4.42 (t, *J* = 9.9 Hz, 1H), 3.70 – 3.66 (m, 4H), 3.09 (td, *J* = 7.3, 5.0 Hz, 1H), 2.88 (t, *J* = 4.5 Hz, 4H). ¹³C NMR (126 MHz, DMSO) δ 154.64, 150.91, 145.24, 143.57, 140.22, 139.30, 137.90, 131.24, 129.36, 128.91, 127.83, 127.78, 127.67, 127.64, 127.59, 127.37, 127.28, 127.09, 126.66, 65.93, 55.65, 55.29, 48.40. HRMS (ESI): calculated for (C₂₉H₂₇N₅O₃) 494.21921 found 494.21713 (M+H)⁺

4-([1,1'-Biphenyl]-4-yl)-N-(1-methylpyrrolidin-3-yl)-2-oxo-3-(quinolin-3-yl)imidazolidine-1-carboxamide(F51)

The title compound was synthesized according to the procedure F using **E42** and 1-methylpyrrolidin-3-amine, yield: 82%, white solid. ¹H NMR (500 MHz, DMSO) δ 9.07 (d, *J* = 2.6 Hz, 1H), 8.36 (d, *J* = 2.5 Hz, 1H), 8.31 (dd, *J* = 7.8, 1.6 Hz, 1H), 8.24 (s, 1H), 7.95 – 7.84 (m, 2H), 7.66 (ddd, *J* = 8.4, 6.8, 1.5 Hz, 1H), 7.62 (d, *J* = 8.4 Hz, 2H), 7.59 – 7.56 (m, 4H), 7.40 (t, *J* = 7.7 Hz, 2H), 7.35 – 7.28 (m, 1H), 5.84 (dd, *J* = 9.6, 6.2 Hz, 1H), 4.42 (td, *J* = 10.0, 1.7 Hz, 1H), 4.34 – 4.22 (m, 1H), 3.67 (d, *J* = 1.8 Hz, 1H), 2.77 (tt, *J* = 7.8, 4.3 Hz, 1H), 2.61 – 2.54 (m, 2H), 2.33 – 2.19 (m, 5H), 1.69 – 1.56 (m, 1H). ¹³C NMR (126 MHz, DMSO) δ 164.03, 159.42, 155.02, 152.59, 151.67, 145.66, 144.46, 140.19, 139.33, 138.15, 131.21,

128.91, 128.55, 127.70, 127.60, 127.45, 127.30, 126.67, 126.15, 62.26, 55.30, 54.31, 49.33, 48.43, 41.59, 32.71. HRMS (ESI): calculated for (C₃₀H₂₉N₅O₂) 492.23995 found 492.23804 (M+H)⁺

3.1.7.2 Biology

Determination of Minimal Inhibitory Concentration (MIC)

MIC method applied for *E. coli* TolC, *S. aureus* (strain Newman), and *E. coli* DH5alpha.

MIC values for *E. coli* TolC, *S. aureus* (strain Newman), and *E. coli* DH5alpha were determined for all compounds with a maximal DMSO concentration of 1% as previously described²⁵. Final compound concentrations prepared from serial dilutions ranged from 1.25 to 40 μM and were adapted for each compound depending on their antibacterial activity and the observation of compound precipitation in the growth medium. The ODs were determined after addition of the compounds and again after incubation for 16 h at 37 °C and 50 rpm in 96-well plates using a POLARstar Omega Microplate Reader (BMG LABTECH). Given MIC values are means of two independent determinations. They are defined as the lowest concentration of compounds that reduced OD₆₀₀ by ≥ 95 % and were read off the inhibition curves. Experiments were performed at least two times and standard deviation was less than 20 % (most cases: < 15 %). LB broth was used for *E. coli* and *B. subtilis*, and Müller Hinton medium was used for *S. aureus*.

MIC method applied against clinical staphylococcal strains.

The minimum inhibitory concentrations (MICs) of the selected compounds of the first series and control drugs were determined using the broth microdilution method, according to guidelines outlined by the Clinical and Laboratory Standards Institute CLSI²⁶, against clinical staphylococcal strains. Bacterial isolates were grown aerobically overnight on tryptic soy agar (TSA) plates at 37° C. Afterwards, a bacterial solution equivalent to 0.5 McFarland standard was prepared and diluted in cation-adjusted Mueller-Hinton broth (CAMHB) to achieve a bacterial concentration of about 5 × 10⁵ CFU/mL. Compounds and control drugs were added in the first row of the 96-well plates and serially diluted along the plates. Plates were then, incubated aerobically at 37° C for 18 – 20 h before recording MICs. MICs reported are the minimum concentration of the compounds and control drugs completely inhibited the bacterial growth as observed visually.

MIC method applied against several clinically relevant bacterial strains.

The MICs of the tested compounds and control drugs; linezolid, vancomycin, metronidazole (antibiotics), and fluconazole (antifungal drug) were determined using the broth microdilution method, according to guidelines outlined by the CLSI²⁷⁻²⁹ or as described in previous reports^{26,30,31}, against clinically-relevant bacterial (*Streptococcus pneumoniae*, *Clostridioides difficile*, vancomycin-resistant *Enterococcus faecalis*, and *Neisseria gonorrhoea* strains) and fungal (*Candida albicans*) strains. *S. pneumoniae* was grown overnight on TSA plate at 37° C, in presence of 5% carbon dioxide. *C. difficile* was grown anaerobically on brain heart infusion supplemented (BHIS) agar at 37° C for 48 h. *E. faecalis* was grown aerobically overnight on TSA at 37° C. *N. gonorrhoeae* was grown on BGC chocolate agar at 37° C for 24 h in presence of 5% CO₂. *C. albicans* was grown aerobically overnight on yeast peptone dextrose (YPD) agar plate at 35° C. Afterwards, a bacterial solution equivalent to 0.5 McFarland standard was prepared and diluted in TSB (for *S. pneumoniae* and *E. faecalis*) to achieve a bacterial concentration of about 5×10^5 CFU/mL. *C. difficile* was diluted in brain heart infusion supplemented (BHIS) broth, supplemented with yeast extract, hemin and vitamin K to achieve a bacterial concentration of about 5×10^5 CFU/mL. A 1.0 McFarland standard solution of *N. gonorrhoeae* was diluted in Brucella broth supplemented with yeast extract, neopeptone, hematin, pyridoxal and NAD to achieve a bacterial concentration of about 1×10^6 CFU/mL. *C. albicans* was diluted in Roswell Park Memorial Institute (RPMI 1640) medium with glutamine and without bicarbonate (GIBCO by Life Technologies, Green Island, NY, USA) which was buffered to pH 7.0 with 0.165 M of 3-(N-morpholino) propanesulfonic acid (MOPS) to achieve a fungal concentration of about 1.5×10^3 CFU/mL. Compounds and control drugs were added in the first row of the 96-well plates and serially diluted along the plates. Plates were then, incubated as previously described. MICs reported are the minimum concentration of the compounds and control drugs that could completely inhibit the visual growth of bacteria/fungi.

Expression of MurA

MurA enzyme from *E. coli* K12 were overexpressed as His-tag fusion proteins in *E. coli* BL21. The expression plasmids pAB3 (MurA) was a kind gift from Prof. Christian Klein, Universität Heidelberg.^{12,32} The transformed *E. coli* cells were grown in LB broth (containing 50 µg/mL kanamycin for MurA) on a shaker at 37 °C until a cell density (OD_{600 nm}) of 0.8 was reached, then 1 mM isopropyl-D-thiogalactopyranoside was added and shaking continued for 2 h at

37 °C. The cells were harvested by centrifugation at 4000 rpm for 30 min. The cell pellets were suspended in lysis buffer containing 20 mM Tris-HCl (pH 7.5), 250 mM NaCl, 5 mM imidazole and a protease inhibitor cocktail (cOmplete™, Roche), followed by sonication on ice for 10 min. The lysate was centrifuged at 4000 rpm for 30 min at 4 °C, and the obtained supernatant was loaded on a Ni²⁺-NTA agarose column (Qiagen) equilibrated with lysis buffer. The column was washed several times using lysis buffer, and the His-tagged proteins were eluted using lysis buffer also containing 750 mM imidazole. The protein fractions were dialyzed to remove the excess imidazole in a dialysis buffer containing 20 mM Tris-HCl (pH 8.0), 150 mM NaCl, 1mM DTT, protease inhibitor cocktail (cOmplete™, Roche) and 10% glycerol. The resulting protein concentrations were 5 µg/µL for MurA as determined by the NanoDrop 2000 (Thermo Scientific). The aliquoted proteins were snap frozen in liquid nitrogen and stored at -80 °C until needed²².

MurA assay

The assay was performed in 96-well plates in a final volume of 100 µL. MurA (27 pmoles) was pre incubated with inhibitors (or DMSO as a control) for 10 min at room temperature prior to addition of the substrates. A master mix consisting of 150 µM *UDP-N-acetylglucosamine* (UNAG), 150 µM PEP, 2 mM DTT and 25 mM Tris-HCl (pH 7.5) (final concentrations) was then added, and the mixture incubated at 37 °C for 30 min. The reaction was stopped by addition of 100 µL of a solution containing malachite green solution (0.045% (w/v) in a 1% PVA solution) and sodium molybdate (4.8% (w/v) in 5 N HCl) at a ratio of 3:1. After 5 min, the absorbance at 625 nm was measured using a POLARstar Omega Microplate Reader (BMG LABTECH). The background absorbance (same reaction without addition of MurA) was subtracted from the measured absorbances²².

3.1.7.3 Molecular Docking

All procedures were performed using the Molecular Operating Environment (MOE) software package (version 2019, Chemical Computing Group). For the docking simulations, PDB entry 1UAE (MurA co-crystallized with UDP-N-acetylglucosamine and fosfomycin) was used. The proteins were first prepared for docking using MOE software where the proteins were protonated and saved for docking. The binding site was identified by the site finder mode. Molecular docking simulations with F42 as a ligand were performed using the MMFF94x and

OPLS-AA force fields and the “triangle matcher” method and “Force field” as refinement. Using these settings, docking runs were performed.

3.1.8 References

- (1) Ventola, C. L. The Antibiotic Resistance Crisis: Part 1: Causes and Threats. *P T* **2015**, *40* (4), 277–283.
- (2) Gould, I. M.; Bal, A. M. New Antibiotic Agents in the Pipeline and How They Can Help Overcome Microbial Resistance. *Virulence* **2013**, *4* (2), 185–191. <https://doi.org/10.4161/viru.22507>.
- (3) Cascioferro, S.; Parrino, B.; Carbone, D.; Pecoraro, C.; Diana, P. Novel Strategies in the War against Antibiotic Resistance. *Future Med Chem* **2021**, *13* (6), 529–531. <https://doi.org/10.4155/fmc-2021-0009>.
- (4) Sapkota, M.; Marreddy, R. K. R.; Wu, X.; Kumar, M.; Hurdle, J. G. The Early Stage Peptidoglycan Biosynthesis Mur Enzymes Are Antibacterial and Antisporulation Drug Targets for Recurrent Clostridioides Difficile Infection. *Anaerobe* **2020**, *61*, 102129. <https://doi.org/10.1016/j.anaerobe.2019.102129>.
- (5) Bugg, T. D. H.; Braddick, D.; Dowson, C. G.; Roper, D. I. Bacterial Cell Wall Assembly: Still an Attractive Antibacterial Target. *Trends in Biotechnology* **2011**, *29* (4), 167–173. <https://doi.org/10.1016/j.tibtech.2010.12.006>.
- (6) Reddy, S. G.; Waddell, S. T.; Kuo, D. W.; Wong, K. K.; Pompliano, D. L. Preparative Enzymatic Synthesis and Characterization of the Cytoplasmic Intermediates of Murein Biosynthesis. *J. Am. Chem. Soc.* **1999**, *121* (6), 1175–1178. <https://doi.org/10.1021/ja983850b>.
- (7) Kahan, F. M.; Kahan, J. S.; Cassidy, P. J.; Kropp, H. The Mechanism of Action of Fosfomycin (Phosphonomycin). *Annals of the New York Academy of Sciences* **1974**, *235* (1), 364–386. <https://doi.org/10.1111/j.1749-6632.1974.tb43277.x>.
- (8) Docobo-Pérez, F.; Drusano, G. L.; Johnson, A.; Goodwin, J.; Whalley, S.; Ramos-Martín, V.; Ballesterot-Tellez, M.; Rodriguez-Martinez, J. M.; Conejo, M. C.; van Guilder, M.; Rodríguez-Baño, J.; Pascual, A.; Hope, W. W. Pharmacodynamics of Fosfomycin: Insights into Clinical Use for Antimicrobial Resistance. *Antimicrob Agents Chemother* **2015**, *59* (9), 5602–5610. <https://doi.org/10.1128/AAC.00752-15>.
- (9) Falagas, M. E.; Vouloumanou, E. K.; Samonis, G.; Vardakas, K. Z. Fosfomycin. *Clin Microbiol Rev* **2016**, *29* (2), 321–347. <https://doi.org/10.1128/CMR.00068-15>.
- (10) Guo, Y.; Tomich, A. D.; McElheny, C. L.; Cooper, V. S.; Tait-Kamradt, A.; Wang, M.; Hu, F.; Rice, L. B.; Sluis-Cremer, N.; Doi, Y. High-Level Fosfomycin Resistance in Vancomycin-Resistant Enterococcus Faecium. *Emerg Infect Dis* **2017**, *23* (11), 1902–1904. <https://doi.org/10.3201/eid2311.171130>.
- (11) Baum, E. Z.; Montenegro, D. A.; Licata, L.; Turchi, I.; Webb, G. C.; Foleno, B. D.; Bush, K. Identification and Characterization of New Inhibitors of the Escherichia Coli MurA Enzyme. *Antimicrobial Agents and Chemotherapy* **2001**, *45* (11), 3182–3188. <https://doi.org/10.1128/AAC.45.11.3182-3188.2001>.
- (12) Steinbach, A.; Scheidig, A. J.; Klein, C. D. The Unusual Binding Mode of Cnicin to the Antibacterial Target Enzyme MurA Revealed by X-Ray Crystallography. *Journal of Medicinal Chemistry* **2008**, *51* (16), 5143–5147. <https://doi.org/10.1021/jm800609p>.
- (13) Bachelier, A.; Mayer, R.; Klein, C. D. Sesquiterpene Lactones Are Potent and Irreversible Inhibitors of the Antibacterial Target Enzyme MurA. *Bioorganic & Medicinal Chemistry Letters* **2006**, *16* (21), 5605–5609. <https://doi.org/10.1016/j.bmcl.2006.08.021>.
- (14) Chang, C.-M.; Chem, J.; Chen, M.-Y.; Huang, K.-F.; Chen, C.-H.; Yang, Y.-L.; Wu, S.-H. Avenaciolides: Potential MurA-Targeted Inhibitors Against Peptidoglycan Biosynthesis in Methicillin-Resistant Staphylococcus Aureus (MRSA). *J. Am. Chem. Soc.* **2015**, *137* (1), 267–275. <https://doi.org/10.1021/ja510375f>.
- (15) Mendgen, T.; Scholz, T.; Klein, C. D. Structure–Activity Relationships of Tulipalines, Tuliposides, and Related Compounds as Inhibitors of MurA. *Bioorganic & Medicinal Chemistry Letters* **2010**, *20* (19), 5757–5762. <https://doi.org/10.1016/j.bmcl.2010.07.139>.
- (16) Miller, K.; Dunsmore, C. J.; Leeds, J. A.; Patching, S. G.; Sachdeva, M.; Blake, K. L.; Stubbings, W. J.; Simmons, K. J.; Henderson, P. J. F.; De Los Angeles, J.; Fishwick, C. W. G.; Chopra, I. Benzothioxalone Derivatives as Novel Inhibitors of UDP-N-Acetylglucosamine Enolpyruvyl Transferases (MurA and MurZ). *J Antimicrob Chemother* **2010**, *65* (12), 2566–2573. <https://doi.org/10.1093/jac/dkq349>.
- (17) Olesen, S. H.; Ingles, D. J.; Yang, Y.; Schönbrunn, E. Differential Antibacterial Properties of the MurA Inhibitors Terreic Acid and Fosfomycin. *J Basic Microbiol* **2014**, *54* (4), 322–326. <https://doi.org/10.1002/jobm.201200617>.
- (18) Jin, B.-S.; Han, S.-G.; Lee, W.-K.; Ryoo, S. W.; Lee, S. J.; Suh, S.-W.; Yu, Y. G. Inhibitory Mechanism of Novel Inhibitors of UDP-N-Acetylglucosamine Enolpyruvyl Transferase from Haemophilus Influenzae. **2009**, *19* (12), 1582–1589. <https://doi.org/10.4014/jmb.0905.05036>.

- (19) *Pharmaceuticals | Free Full-Text | Bromo-Cyclobutenaminones as New Covalent UDP-N-Acetylglucosamine Enolpyruvyl Transferase (MurA) Inhibitors.* <https://www.mdpi.com/1424-8247/13/11/362#> (accessed 2023-02-14).
- (20) Gilbert, A. M.; Failli, A.; Shumsky, J.; Yang, Y.; Severin, A.; Singh, G.; Hu, W.; Keeney, D.; Petersen, P. J.; Katz, A. H. Pyrazolidine-3,5-Diones and 5-Hydroxy-1H-Pyrazol-3(2H)-Ones, Inhibitors of UDP-N-Acetylenolpyruvyl Glucosamine Reductase. *J. Med. Chem.* **2006**, *49* (20), 6027–6036. <https://doi.org/10.1021/jm060499t>.
- (21) Kutterer, K. M. K.; Davis, J. M.; Singh, G.; Yang, Y.; Hu, W.; Severin, A.; Rasmussen, B. A.; Krishnamurthy, G.; Failli, A.; Katz, A. H. 4-Alkyl and 4,4'-Dialkyl 1,2-Bis(4-Chlorophenyl)Pyrazolidine-3,5-Dione Derivatives as New Inhibitors of Bacterial Cell Wall Biosynthesis. *Bioorganic & Medicinal Chemistry Letters* **2005**, *15* (10), 2527–2531. <https://doi.org/10.1016/j.bmcl.2005.03.058>.
- (22) Mokbel, S. A.; Fathalla, R. K.; El-Sharkawy, L. Y.; Abadi, A. H.; Engel, M.; Abdel-Halim, M. Synthesis of Novel 1,2-Diarylpyrazolidin-3-One-Based Compounds and Their Evaluation as Broad Spectrum Antibacterial Agents. *Bioorganic Chemistry* **2020**, *99*, 103759. <https://doi.org/10.1016/j.bioorg.2020.103759>.
- (23) *Strecker Synthesis - an overview | ScienceDirect Topics.* <https://www.sciencedirect.com/topics/biochemistry-genetics-and-molecular-biology/strecker-synthesis> (accessed 2023-03-20).
- (24) *The role of ligand efficiency metrics in drug discovery | Nature Reviews Drug Discovery.* <https://www.nature.com/articles/nrd4163> (accessed 2023-04-24).
- (25) Skarzynski, T.; Mistry, A.; Wonacott, A.; Hutchinson, S. E.; Kelly, V. A.; Duncan, K. Structure of UDP-N-Acetylglucosamine Enolpyruvyl Transferase, an Enzyme Essential for the Synthesis of Bacterial Peptidoglycan, Complexed with Substrate UDP-N-Acetylglucosamine and the Drug Fosfomycin. *Structure* **1996**, *4* (12), 1465–1474. [https://doi.org/10.1016/s0969-2126\(96\)00153-0](https://doi.org/10.1016/s0969-2126(96)00153-0).
- (26) *Lead structures for new antibacterials: stereocontrolled synthesis of a bioactive muraymycin analogue - PubMed.* <https://pubmed.ncbi.nlm.nih.gov/25318977/> (accessed 2023-01-10).
- (27) Seong, Y. J.; Alhashimi, M.; Mayhoub, A.; Mohammad, H.; Seleem, M. N. Repurposing Fenamic Acid Drugs To Combat Multidrug-Resistant Neisseria Gonorrhoeae. *Antimicrobial Agents and Chemotherapy* **2020**, *64* (7), e02206–e02219. <https://doi.org/10.1128/AAC.02206-19>.
- (28) Clinical and Laboratory Standards Institute. *Methods for Dilution Antimicrobial Susceptibility Tests for Bacteria That Grow Aerobically.*, 9th ed.; 2012.
- (29) Clinical and Laboratory Standards Institute. *Methods for Antimicrobial Susceptibility Testing of Anaerobic Bacteria.*; CLSI Wayne; PA., 2007.
- (30) Clinical and Laboratory Standards Institute. *Reference Method for Broth Dilution Antifungal Susceptibility Testing of Yeasts.*, Third Edit.; Wayne, PA, 2008.
- (31) Alhashimi M, M. A. & S. MN. Repurposing Salicylamide for Combating Multidrug-Resistant Neisseria Gonorrhoeae. *Antimicrobial Agents and Chemotherapy, AAC* **2019**, 01225–01219.
- (32) Elkashif, A.; Seleem, M. N. Investigation of Auranofin and Gold-Containing Analogues Antibacterial Activity against Multidrug-Resistant Neisseria Gonorrhoeae. *Scientific Reports* **2020**, *10* (1), 5602. <https://doi.org/10.1038/s41598-020-62696-3>.
- (33) Jöst, C.; Nitsche, C.; Scholz, T.; Roux, L.; Klein, C. D. Promiscuity and Selectivity in Covalent Enzyme Inhibition: A Systematic Study of Electrophilic Fragments. *Journal of Medicinal Chemistry* **2014**, *57* (18), 7590–7599. <https://doi.org/10.1021/jm5006918>.

3.2 Chapter 2

Discovery of Triaryl Malonamides as a Novel Class of MurA Inhibitors with Potential Antibacterial Activity

Abstract

The emergence of antimicrobial-resistant bacteria has highlighted the urgent need for the discovery and development of new antibacterial agents with novel or less explored mechanisms of action. The enzymes involved in the early steps of peptidoglycan biosynthesis, such as MurA, are crucial targets for antibacterial drug discovery. However, resistance to current MurA inhibitors, such as fosfomycin, has become a significant issue. In this study, we report the identification of a triaryl malonamide scaffold that inhibits MurA. These inhibitors were developed based on our exploration of imidazolidinone derivatives as MurA inhibitors (Chapter 1). The advantage of this triaryl malonamide scaffold lies in its shorter synthesis pathway and enhanced flexibility for modifications. The scaffold shows identical inhibitory activities towards the MurA C115D mutant and the wild-type MurA enzymes, resulting in compounds **4c** and **2d** ($IC_{50} = 4.32 \mu\text{M}$ and $4.67 \mu\text{M}$, respectively).

3.2.1 Introduction

Since the discovery of sulfonamides and β -lactams in the first half of the 20th century, antimicrobial agents have played a crucial role in saving countless lives and improving quality of life¹. However, their extensive use, along with frequent misuse and abuse, have led to the emergence of antimicrobial-resistant pathogenic bacteria, posing a serious threat to public health^{2,3}. As a result, there is an urgent need to discover and develop new antibacterial agents.

The structural integrity of bacteria is maintained by the cell wall, which protects them from the osmotic pressure of the cell exterior⁴. Peptidoglycan is a vital constituent of the bacterial cell wall that provides mechanical strength and resistance to environmental stress. The MurA enzyme catalyzes the first step of this process and thus, it becomes an attractive target for antibacterial therapy. MurA transfers enolpyruvate from phosphoenolpyruvate to UDP-N-acetylglucosamine (Figure 1)^{8,9}. The resulting product, UDP-GlcNAc-enolpyruvate, is then converted to UDP-acetylmuramic acid by the MurB enzyme⁵. The MurC-F enzymes sequentially add amino acids to form UDP-MurNAc-pentapeptide, which is an essential component of the peptidoglycan cell wall⁶⁻⁸. Mur enzymes are essential and highly conserved in both Gram-negative and Gram-positive bacteria, but eukaryotic cells do not have them,

making inhibitors of these enzymes selective for bacteria⁹. The deletion or deactivation of the MurA gene results in the death of bacteria due to loss of cell integrity and makes them more vulnerable to osmotic lysis^{10,11}. Hence, MurA is a promising candidate for the development of antibiotics since it plays an essential role in microbial survival.

Fosfomycin is an antibiotic that is derived from a natural source. It is primarily used as an early treatment for paediatric gastrointestinal infections caused by Shiga-like toxin-producing *E. coli* (STEC)¹² and is also considered a first-line agent for treating bacterial urinary tract infections¹³.

However, resistance to fosfomycin arises and has received significant attention. Reports show that bacteria, including *Escherichia coli*, *Mycobacterium tuberculosis*, *Chlamydia trachomatis*, and *Borrelia burgdorferi*^{14–18}, have developed resistance to fosfomycin through various methods, such as mutations or encoding proteins that neutralize or inactivate fosfomycin^{19–22}.

The molecular target of fosfomycin has been determined to be MurA²³. Fosfomycin works by blocking the activity of MurA through covalent alkylation of its catalytic Cys115^{24–26}. Fosfomycin's effectiveness and potency depend on the cysteine's sulfhydryl interaction with the epoxide of fosfomycin. Therefore, the mutation of Cys-to-Asp in some organisms confers resistance to fosfomycin.

Other factors such as *fosA* gene²⁷ in Gram-negative bacteria and *fosB* gene in Gram-positive bacteria, have been found to contribute to fosfomycin resistance^{28–30}. They encode fosfomycin-modifying enzymes (FMEs) that chemically modify fosfomycin, rendering it ineffective against the bacteria. FosA enzymes transfer a glutathione molecule to fosfomycin, while FosB enzymes add bacillithiol, thereby modifying the fosfomycin and preventing its binding to MurA^{28,31}.

Therefore, it is of critical importance to identify new scaffolds that can inhibit MurA and overcome resistance while demonstrating safety on mammalian cells. Despite the discovery of numerous inhibitors in recent years through high-throughput screening campaigns or classical medicinal chemistry approaches, none of them have advanced to clinical trials or been developed for therapeutic use^{32–37}.

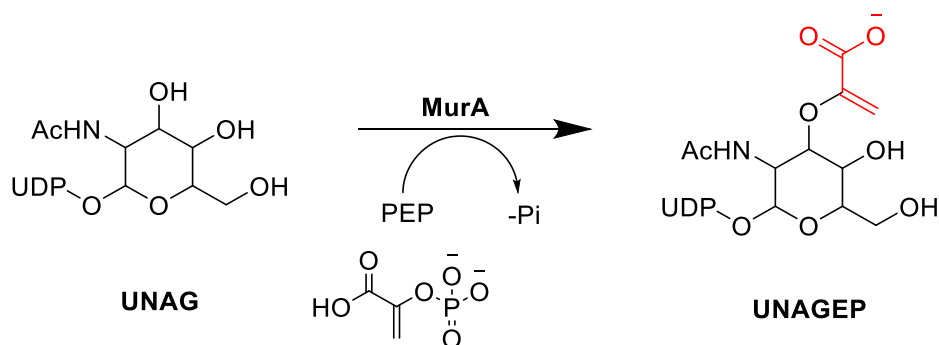


Figure 1: MurA catalyzed reaction

In this study, we report the identification of a triaryl malonamide scaffold that inhibits MurA, resulting in identical inhibitory activities towards the *E. coli* MurA C115D mutant and the wild type MurA enzyme.

3.2.2 Results and Discussion

3.2.2.1 Compound design

During our exploration of potential MurA inhibitors to combat bacterial infections, we discovered and developed several imidazolidinone derivatives as promising inhibitors of MurA presented by compound **1** and **2** (Figure 2). This series of imidazolidinone derivatives could inhibit both wild type MurA and the C115D mutant developed by fosfomycin-resistant *E. coli*. However, the lengthy six-step synthesis scheme required for these derivatives (Chapter 1) prompted us to explore the possibility of simplifying the scaffold to the respective open analogues to get a shorter synthetic pathway with higher synthetic feasibility and accelerate the optimization while maintaining its bioactivity. As shown in Figure 2, we were able to simplify the scaffold and synthesize the triaryl malonamide derivatives **1c** and **1d**, which differ from **1** and **2** (imidazolidinone derivatives from chapter 1) in two key ways: the methylene bridge connecting the two nitrogens of the imidazolidinone in **1** and **2** was removed, and the N atom between two carbonyl groups was replaced with a CH₂ group. Despite these changes, the triaryl malonamide derivatives maintained its activity against MurA comparable to that of imidazolidinone derivatives, demonstrating the potential of the simplified scaffold for further optimization. Moreover, the new scaffold can be synthesized in just three steps as shown in Scheme 1, which is more efficient than the 6-step synthesis required for the imidazolidinone derivatives (Chapter 1). This change still offers great synthetic flexibility for modifying rings A, B, and C independently, providing the opportunity to install polar hetero-aryls and alicyclic rings simultaneously, aiding in the structure optimization process.

Results and Discussion

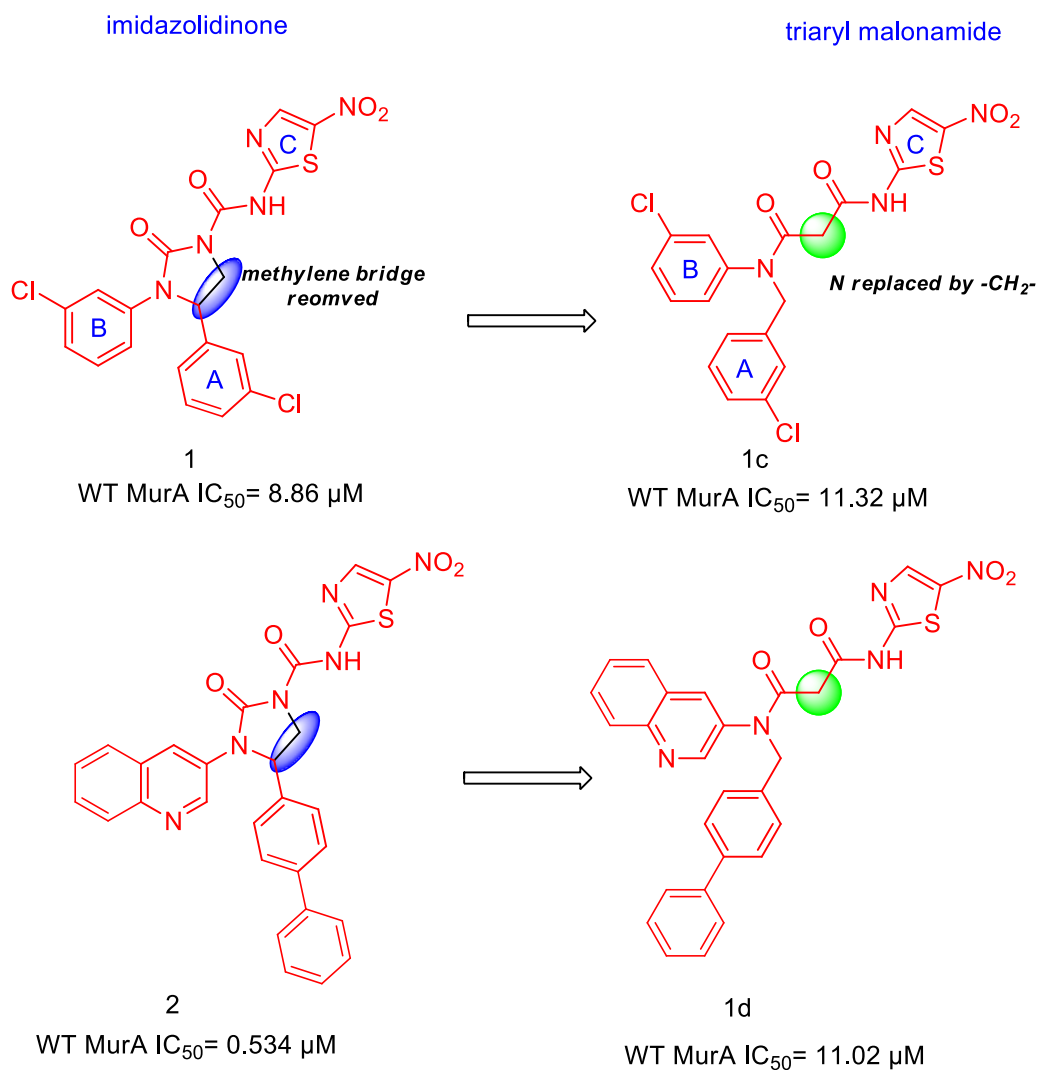


Figure 2: Previously synthesized imidazolidinone inhibitors (**1** and **2**) and malonamide scaffold (**1c** and **1d**).

In this study, we chose **1c** and **1d** scaffolds for further exploration, since they are analogues of compounds **1** and **2**, the two key compounds in Chapter 1. We fixed ring A as a 3-chloro benzyl group and ring B as a 3-chloro phenyl group during the modification of **1c**, while modifications were made to ring C. Similarly, for **1d**, we fixed ring A as a [1,1'-biphenyl]-4-yl methyl group and ring B as a quinolin-3-yl group while modifying ring C (Figure 3).

Similar to our previous findings in Chapter 1 with compounds **1** and **2**, the introduction of a 5-nitrothiazol-2-yl group at the N³ position (referred to as R in Table 1) in compound **1c** and **1d** showed moderate inhibition of MurA, with an IC_{50} value of 11.32 μ M and 11.02 μ M, respectively.

We further optimized the structure of our lead compounds **1c** and **1d** by exploring the use of various substituents on the malonamide core to improve the clogP of the compounds.

Additionally, we investigated the SAR of the scaffold by synthesizing and testing a range of polar hetero-aryls and alicyclic rings, as shown in Figure 3.

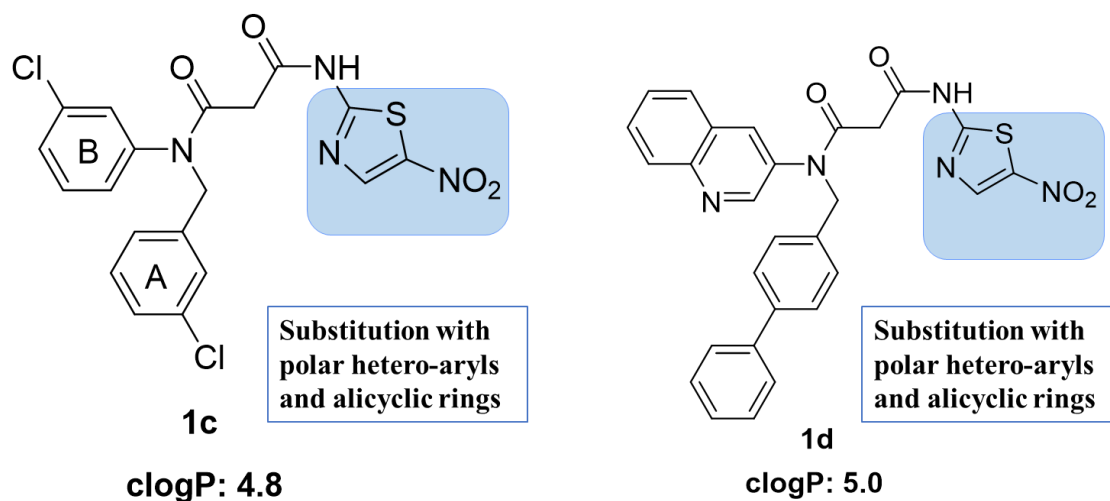
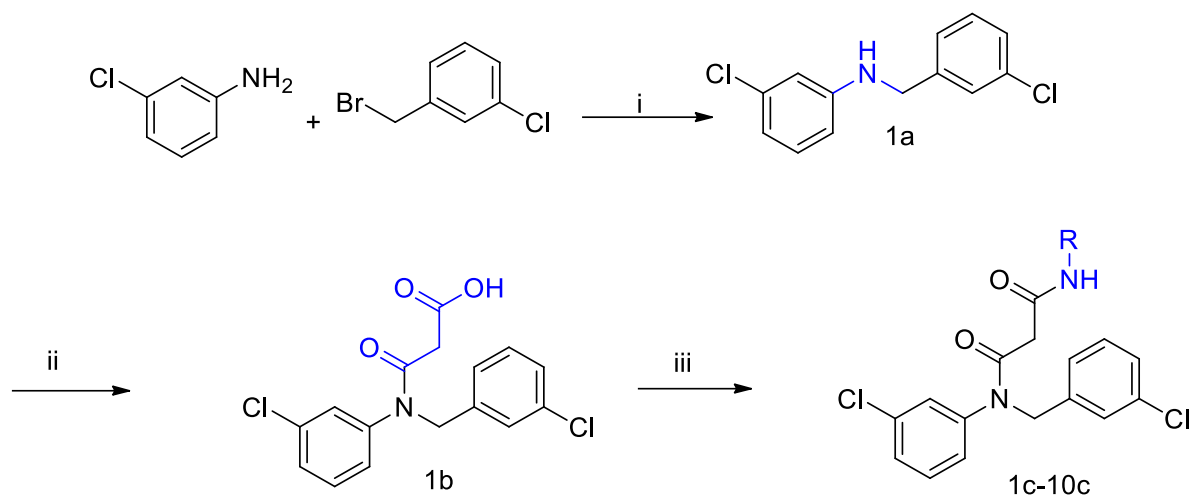


Figure 3: Modifications followed in optimization.

3.2.3 Chemistry

The synthesis of the malonamide derivatives (**1c–10c** and **1d–7d**) involved a concise three-step sequence that is utilized in both Scheme 1 and Scheme 2, respectively. First, *m*-chloro aniline was reacted with *m*-chloro benzyl bromide in Scheme 1 to give the *N*-benzylaniline **1a**. Subsequently, an amide coupling reaction was performed on **1a** using malonic acid, HBTU as a coupling agent, and triethylamine as a base, yielding the malonic acid monoamide derivative **1b**. Finally, in the last step, different amines were used to perform another amide coupling reaction on **1b** to generate the desired malonamide derivatives (**1c–10c**). In Scheme 2, a similar reaction was performed by reacting 3-aminoquinoline and 4-bromomethylbiphenyl to yield **2a**, followed by an amide coupling reaction using malonic acid and HBTU to yield the malonic acid monoamide derivative **2b**. Finally, in the last step, different amines were used to perform another amide coupling reaction on **2b** to generate the desired malonamide derivatives (**1d–7d**).

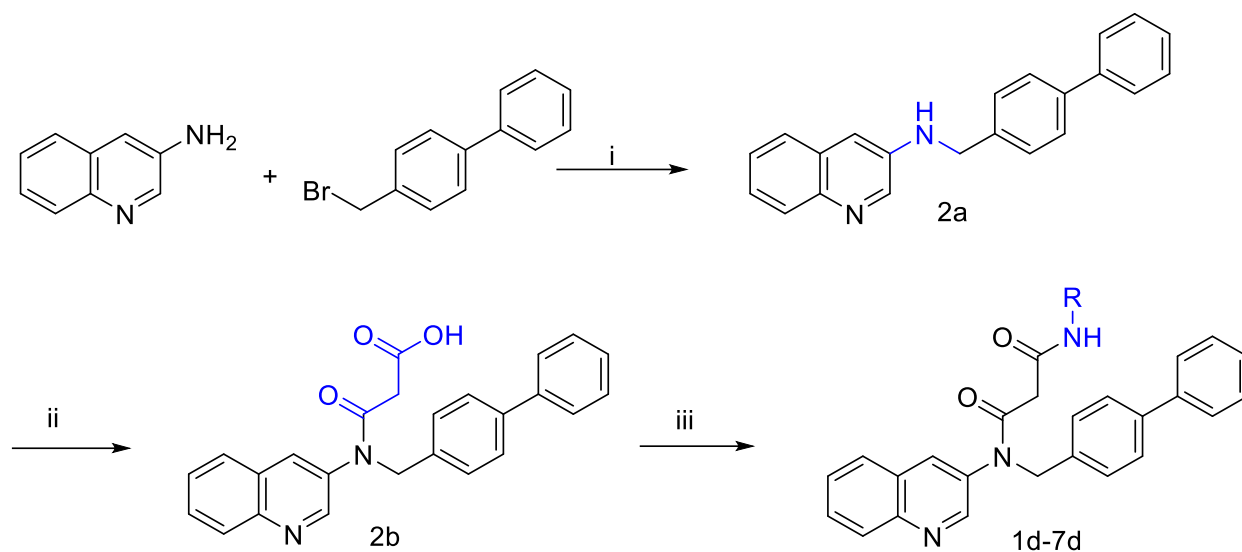
Scheme 1



Reagents and conditions i) DMF, 2 eq Cs₂CO₃ at RT for 24 h. ii) DCM, 10 drops TEA, 2 eq HBTU, 1.5 eq malonic acid at RT, overnight. iii) DCM, 10 drops TEA, 2 eq HBTU, 1.5 eq amine derivative at RT, overnight.

No.	R	No.	R	No.	R	No.	R
1c		2c		3c		4c	
5c		6c		7c		8c	
9c		10c					

Scheme 2



Reagents and conditions i) DMF, 2 eq Cs₂CO₃ at RT for 24 h. ii) DCM, 10 drops TEA, 2 eq HBTU, 1.5 eq malonic acid at RT, overnight. iii) DCM, 10 drops TEA, 2 eq HBTU, 1.5 eq amine derivative at RT, overnight.

No.	R	No.	R	No.	R	No.	R
1d		2d		3d		4d	
5d		6d		7d			

3.2.4 Biological Evaluation

The activity of MurA was evaluated using a standard malachite green assay, measuring the amount of released inorganic phosphate using malachite green and sodium molybdate. The reaction mixture was incubated for 30 min at 37 °C. Together, the phosphate released and these reagents form a green complex that is quantified spectrophotometrically.

Compounds were tested for their *in vitro* ability to inhibit MurA *E. coli* enzyme, by first testing the inhibition of the compounds at a screening dose of 20 μM. Fosfomycin was used as positive control. The percentage inhibition recorded for each compound is an average of at least two

independent experiments (Table 1). The IC₅₀ values were determined for compounds displaying more than 60% inhibition (Table 1). IC₅₀ determination was done through testing a range of 5 concentrations with three replicates per concentration; the IC₅₀ value recorded for each compound is an average of at least two independent experiments. The assay was repeated with an adapted concentration range to allow a more precise evaluation of the IC₅₀ values.

3.2.4.1.1 Analogues of compound 1c

In this study, we examined the impact of altering one specific structural feature of the scaffold while keeping the others unchanged. This allowed us to establish structure-activity relationships (SAR) for each modified feature. By evaluating the impact of substituents on inhibitory activity, we aim to elucidate the key structural features and binding interactions influencing MurA inhibition.

Further 5-membered motifs other than 5-nitrothiazol-2-yl were explored in the next round of screening. The presence of 1-methyl-1H-pyrazole-4-yl showed promising activity, with an IC₅₀ of 8.20 μM (Compound **2c**, Table 1). The pyrazole may contribute to favorable binding interactions with MurA, potentially through hydrogen bonding. Additionally, compared to the hit compound (**1c**), **2c** exhibited a significant decrease in its clogP value (from 4.8 in the lead compound **1c** to 3.5 in **2c**, Table 1). On the other hand, the 2-(methylthio)-1,3,4-thiadiazol-2-yl was detrimental to the activity as demonstrated by compound **3c**.

A fused heterocycle, specifically indole-5-yl, enhanced the inhibitory activity against MurA (compound **4c** IC₅₀ =4.32 μM), while compound **5c** with a benzothiazol-2-yl showed no inhibitory activity towards MurA. The difference in activity between compound **4c** and **5c** can be attributed to the different attachment site. In **4c**, the indole-5-yl -group is positioned with the pyrrole facing outward, while in **5c**, the benzothiazol-2-yl-group is positioned with the thiazole facing inward. This difference in orientation may affect the ability of the groups to interact with MurA.

Next, phenyl derivatives were evaluated. Compound **6c**, featuring 4-nitrophenol-2-yl, did not exhibit inhibitory activity towards MurA. In contrast, compound **7c** contains a phenol-2-yl and showed an IC₅₀ value of 10.69 μM. The difference in the activity of **7c** and **6c** (4-nitrophenol-2-yl) can be attributed to the nitro group's electron-withdrawing nature in **6c**, which can disrupt interactions, leading to decreased binding affinity to the active site of MurA and lower

inhibitory activity compared to **7c**. Furthermore, **8c** featuring 6-chlorobenzonitrile-2-yl showed no activity towards MurA.

Compounds **9c** and **10c** exhibited no activity against MurA. It is speculated that the nature of the ring like the more polar and electron deficient pyridine and morpholine analogues **9c** and **10c** respectively may be the reason for their inactivity, possibly indicating the correlation of potency with the degree of lipophilicity.

3.2.4.1.2 Analogues of compound 1d

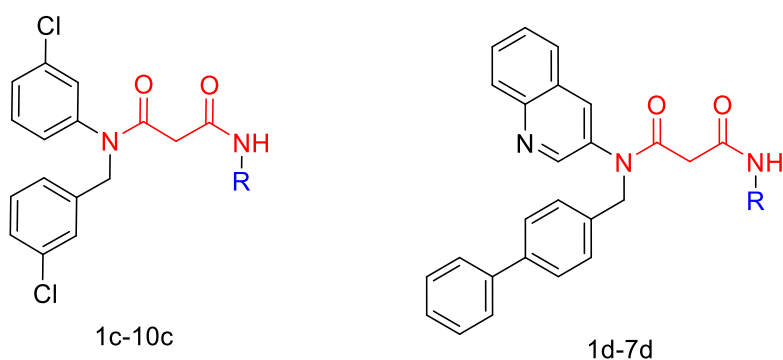
Following a similar approach as with the first series, we began exploring the second series. We proceeded to investigate fused bicycles, 6-membered motifs such as substituted phenyl and substituted pyridine in the subsequent screening phase.

Similar to the observations made with first series, the screening of the second series reaffirmed that the presence of a fused heterocycle, specifically benzimidazole-2-yl (**2d**), resulted in the highest inhibitory activity towards MurA in both series with an IC_{50} value of 4.67 μ M. Conversely, **3d**, featuring a [1,2,4]triazolo[4,3-a]pyridin-3-yl substituent, showed no inhibitory activity towards MurA.

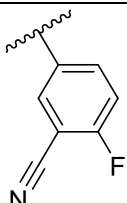
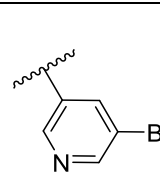
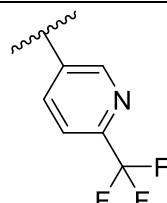
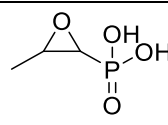
Additionally, **4d** containing a 4-nitrophenol-2-yl substituent, displayed moderate inhibitory activity towards MurA, with an IC_{50} value of 18.20 μ M. Notably, **6c** with the same substituent was inactive. Therefore, it is expected that **4d** is more active, possibly due to a different binding mode adopted by this group. On the other hand, **5d**, featuring 2-fluorobenzonitrile-5-yl showed no activity towards MurA.

Furthermore, **6d** and **7d** featuring a 5-bromopyridin-3-yl substituent and 6-(trifluoromethyl)pyridin-3-yl respectively showed low inhibitory activity towards MurA. This could be attributed to the polarity of the pyridine moiety in **6d** and **7d**.

Table 2: MurA Inhibition of Malonamides 1d–7d and 1c–10c



No.	R	%inh @20μM	IC ₅₀ (μM)	clogP	No.	R	%inh @20μM	IC ₅₀ (μM)	clogP
1c		71.34 ±4.83	11.32 ±1.71	4.8	2c		74.01 ±6.91	8.20 ±1.14	3.5
3c		n.i	n.d.	4.6	4c		81.39 ±3.79	4.32 ±0.98	4.9
5c		n.i	n.d.	5.4	6c		n.i	n.d.	4.3
7c		79.46 ±6.31	10.69 ±1.34	4.6	8c		38.13 ±8.11	n.d.	5.5
9c		n.i	n.d.	4.8	10c		n.i	n.d.	3.0
1d		79.03 ±2.71	11.02 ±1.44	5.0	2d		87.09 ±3.15	4.67 ±0.44	5.0
3d		n.i	n.d.	4.4	4d		64.51 ±2.36	18.2 ±2.05	5.0

5d		29.66 ±6.81	n.d.	5.4		6d		56.32 ±4.32	n.d.	5.8
7d		48.89 ±6.37	n.d.	5.3	fosfomycin		n.d.	6.13	n.d.	

^aData shown are the mean of at least two independent experiments, SD ≤ 10%. ni, no inhibition, n.d., not determined.

3.2.5 Molecular Docking

In an attempt to get a better insight about the binding mode of our most potent inhibitor from the nitrothiazole series, **4c** (IC₅₀ = 4.32 μM), molecular docking was performed at MurA binding pocket (PDB code: 1UAE)³⁸ using MOE. As depicted in Figure 4, the hypothetical binding model revealed anchoring of compound 4c between N23 and L124 with the asparagine 23 residue benefitting from halogen bonding interactions with the chloro of (3-chlorophenyl) and leucine 124 performing two CH-π interactions with both the phenyl and the pyrrole (of indole). In addition, three CH-π interactions were found with P121, S162 and V327. Two additional important hydrogen-bond interactions are also observed between the carbonyl (of malonamide) and R120, and CH-N interactions between the H of the phenyl(of indole) with H125, which can explain the improved potency of 4c.

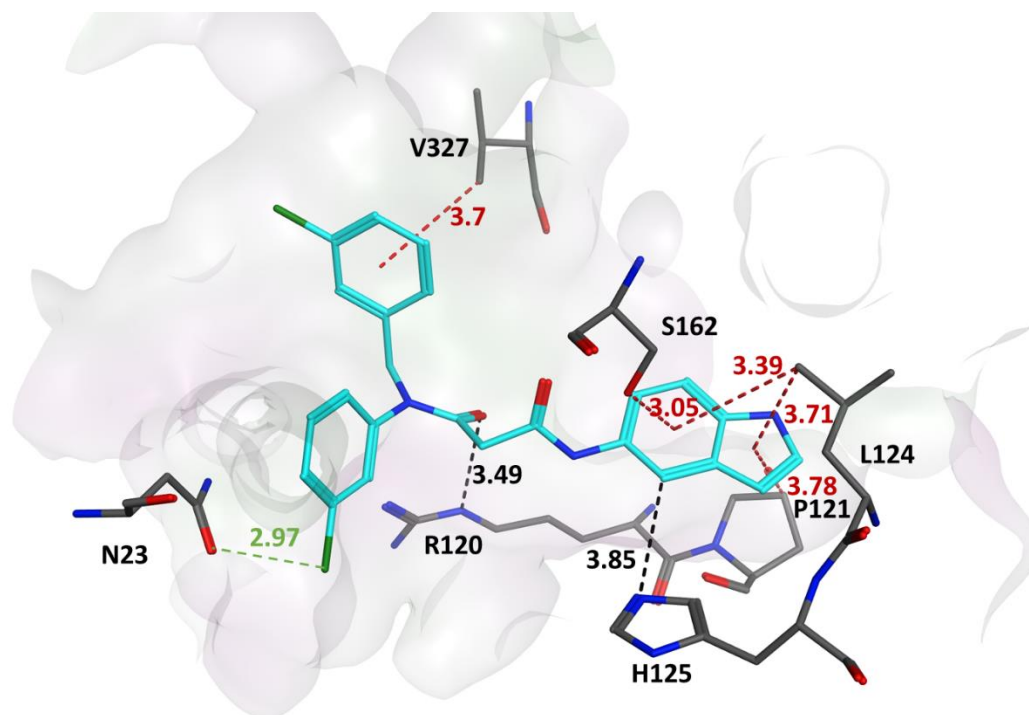


Figure 4: Predicted binding mode (by molecular docking) of 4c in the X-ray cocrystal structure of UNAG and fosfomycin with MurA from *E. coli* (PDB code: 1UAE)³⁸. Inhibitor 4c (cyan sticks) was predicted to fill the UNAG binding pocket completely. Amino acid residues (gray) involved in direct interactions are labelled. Distances (Dark red numbers for π interactions and black numbers for hydrogen-bonding interactions) are given in Å; black, dashed lines: H bonds; Dark red dashed lines: CH- π and CH-N interactions; green, dashed lines: Halogen bonds.

3.2.6 Conclusions

The SAR analysis of the triaryl malonamide derivatives **1b** and **2b** coupled with amines revealed that certain functional groups in the R-group can have a significant impact on the inhibitory activity towards the MurA enzyme.

For the first series, compounds **1c** and **7c**, which contain 5-nitrothiazol-2-yl and phenol-2-yl groups respectively, showed IC_{50} values of 11.32 μ M and 10.69 μ M respectively. The presence of some heterocyclic rings, such as indole and 1-methyl-1H-pyrazole, also had a positive effect on inhibition as seen in compounds **4c** and **2c** with IC_{50} values of 4.32 μ M and 8.20 μ M respectively with the latter demonstrating a significant advantage in terms of logP, boasting a value of 3.5 compared to the lead compound **1c** with a value of 4.8.

For the second series, the most effective substituent for enhancing the inhibitory activity was found to be the benzimidazole group, as seen in compound **2d**, which had an IC₅₀ value of 4.67 μM. The presence of 5-nitrothiazol-2-yl in **1d** and 4-nitrophenol-2-yl in **4d** groups also had a positive effect on inhibitory activity with IC₅₀ values of 11.02 μM and 18.20 μM respectively.

3.2.7 Experimental

3.2.7.1 Chemistry

All air- or moisture-sensitive reactions were carried out in dried glassware (>100 °C) under an atmosphere of nitrogen or argon. Dried solvents were distilled before use. Analytical TLC was performed on precoated silica gel plates (Macherey-Nagel, Polygram SIL G/UV254). Visualization was accomplished with UV-light, KMnO₄, or a ceric ammonium molybdate chamber. The products were purified by flash chromatography on silica gel columns (Macherey-Nagel 60, 0.04–0.063 mm). Preparative high-performance liquid chromatography (HPLC) was performed on a Waters Autopurifier System (APS) with a Phenomenex Gemini C18 column (250 × 4.6 mm, particle size 5 μm) as an analytical column for method development and a Phenomenex Gemini C18 column (250 × 19 mm, particle size 5 μm) for preparative separation. Detection was performed using a mass trigger. ¹H and ¹³C spectra were recorded with a Bruker Fourier Spectrometer [300 MHz (¹H), 75 MHz (¹³C)] or a Bruker AV 500 [500 MHz (¹H), 126 MHz (¹³C)] spectrometer in CDCl₃, acetone-d₆, DMSO-d₆, or MeOH-d₄ unless otherwise specified. Chemical shifts are given in parts per million (ppm) and referenced against the residual proton or carbon resonances of the >99% deuterated solvents as internal standard. Coupling constants (*J*) are given in hertz (Hz). Data are reported as follows: chemical shift, multiplicity (s = singlet, d = doublet, t = triplet, q = quartet, m = multiplet, dd = doublet of doublets, dt = doublet of triplets, br = broad, and combinations of these) coupling constants, and integration. NMR spectra were evaluated using Mnova. Liquid chromatography–mass spectrometry (LC–MS) was performed on a LC–MS system consisting of a Dionex UltiMate 3000 pump, autosampler, column compartment, detector (Thermo Fisher Scientific, Dreieich, Germany), and ESI quadrupole MS (MSQ Plus or ISQ EC, Thermo Fisher Scientific, Dreieich, Germany). High-resolution mass was determined by LC–MS/MS using the Thermo Scientific Q Exactive Focus Orbitrap LC–MS/MS system. The purity of the final compounds was determined by LC–MS using a gradient with (A) H₂O + 0.1% FA to (B) ACN + 0.1% FA at a flow rate of 600 μL/min and 45 °C. The gradient was initiated by a 1 min

isocratic step at 5% B followed by an increase to 99% B in 15 min to end up with a 5 min step at 99% B before re-equilibration under the initial conditions. The purity of the final compounds was determined by using the area percentage method on the UV trace recorded at a wavelength of 254 nm and found to be >95%.

3.2.7.1.1 General procedure for the synthesis of 3-chloro-*N*-(3-chlorobenzyl) aniline(1a) and *N*-([1,1'-biphenyl]-4-ylmethyl) quinolin-3-amine (2a). General Procedure A

In a 250 mL round-bottomed flask, for **1a** synthesis, 3-chlorobenzyl bromide (2g, 10 mmol, 1 equiv) and 3-chloroaniline (1.28g, 10 mmol, 1 equiv) and for **2a** synthesis, 4-bromomethylbiphenyl (2.47g, 10 mmol, 1 equiv) and 3-quinolineamine (1.44g, 10 mmol, 1 equiv), was dissolved in dimethylformamide(30 mL) in the presence of K₂CO₃ (4.1g, 30 mmol, 3 equiv). The reaction mixture was left to stir at room temperature for 24 h. After completion of the reaction (monitored by TLC), the mixture was the mixture was evaporated till complete dryness under vacuum. The residue was partitioned between dichloromethane (150 mL) and H₂O (50 mL), and then the aqueous layer was re-extracted using 3 portions of dichloromethane (150 mL). Organic layers were then collected and dried over anhydrous magnesium sulfate and evaporated under vacuum. The residue was then purified using preparative high-performance liquid chromatography.

3-Chloro-*N*-(3-chlorobenzyl) aniline (1a): The title compound was synthesized according to the procedure A using 3-chlorobenzyl bromide and 3-chloroaniline, yield: 83%, colorless liquid. ¹H NMR (500 MHz, acetone) δ 7.34 (ddd, *J* = 7.9, 2.2, 1.5 Hz, 1H), 7.31 – 7.20 (m, 3H), 7.16 (t, *J* = 7.9 Hz, 1H), 6.84 (ddd, *J* = 7.9, 2.2, 1.2 Hz, 1H), 6.72 (t, *J* = 2.2 Hz, 1H), 6.64 (ddd, *J* = 7.9, 2.1, 1.2 Hz, 1H), 5.21 (t, *J* = 5.3 Hz, 1H), 4.45 (dt, *J* = 5.4, 0.9 Hz, 2H). *m/z*: (*M+H*)⁺: 252.03.

***N*-([1,1'-Biphenyl]-4-ylmethyl) quinolin-3-amine (2a):** The title compound was synthesized according to the procedure A using biphenyl benzyl bromide and quinoline-3-amine, yield: 81%, colorless liquid. ¹H NMR (500 MHz, acetone) δ 8.18 (d, *J* = 1.6 Hz, 1H), 8.00 (dd, *J* = 7.4, 1.3 Hz, 1H), 7.63 – 7.53 (m, 5H), 7.48 – 7.33 (m, 5H), 6.69 (t, *J* = 5.8 Hz, 1H), 4.58 (dt, *J* = 5.7, 0.8 Hz, 2H). *m/z*: (*M+H*)⁺: 311.15.

3.2.7.1.2 General procedure for the synthesis of 3-((3-chlorobenzyl)(3-chlorophenyl)amino)-3-oxopropanoic acid (1b) and 3-(([1,1'-biphenyl]-4-ylmethyl)(quinolin-3-yl)amino)-3-oxopropanoic-acid (2b). General Procedure B.

In a 100 mL round-bottomed flask, malonic acid (0.52g, 5 mmol, 1 equiv) was dissolved in dimethylformamide (20 mL). Afterwards, the appropriate amine **1a** or **2a** (6 mmol, 1.2 equiv) and TEA (10 drops) were added, and the reaction mixture was left to stir for 15 min at room temperature. Afterwards, HBTU (2.8g, 7.5 mmol, 1.5 equiv) was added, then the reaction mixture was stirred at room temperature overnight. After completion of the reaction (monitored by TLC), the mixture was evaporated till complete dryness under vacuum. The residue was partitioned between dichloromethane (150 mL) and brine (50 mL), and then the aqueous layer was re-extracted using 3 portions of dichloromethane (150 mL). Organic layers were then collected and dried over anhydrous magnesium sulfate and evaporated under vacuum. The residue was then purified using preparative high-performance liquid chromatography to give the carboxylic acid amide derivatives in different yields.

3-((3-Chlorobenzyl)(3-chlorophenyl)amino)-3-oxopropanoic acid (2a): The title compound was synthesized according to the procedure B using **1a**, yield: 91%, white solid. ¹H NMR (500 MHz, acetone) δ 11.94 (s, 1H), 7.37 – 7.16 (m, 8H), 5.16 (s, 1H), 3.52 (s, 1H). *m/z*: (*M+H*)⁺: 338.03.

3-(((1,1'-Biphenyl)-4-ylmethyl)(quinolin-3-yl)amino)-3-oxopropanoic acid (2b): The title compound was synthesized according to the procedure B using **2a**, yield: 88%, white solid. ¹H NMR (500 MHz, acetone) δ 11.92 (s, 1H), 8.52 (d, *J* = 1.6 Hz, 1H), 8.14 – 8.09 (m, 2H), 8.07 (dd, *J* = 2.3, 1.6 Hz, 1H), 7.77 – 7.71 (m, 1H), 7.65 (td, *J* = 7.6, 1.2 Hz, 1H), 7.62 – 7.50 (m, 5H), 7.48 – 7.41 (m, 2H), 7.41 – 7.33 (m, 3H), 5.30 (s, 2H), 3.51 (s, 2H). *m/z*: (*M+H*)⁺: 397.15.

3.2.7.1.3 General procedure for the synthesis of malonamide derivatives (1c–10c and 1d–7d). General Procedure C.

In a 100 mL round-bottomed flask, 3 mmol of the malonic acid derivative **1b/2b** was dissolved in 10 mL dimethylformamide. Afterwards, the appropriate amine (1.2 equiv) and TEA (3 equiv) were added, and the reaction mixture was left to stir for 15 min at room temperature. Afterwards, HBTU (1.5 equiv) was added, then the reaction mixture was stirred at room temperature overnight. The flask content was then evaporated under vacuum till dryness. The residue was partitioned between 100 mL of dichloromethane and 100 mL of brine, and then the aqueous layer was extracted with three 50 mL portions of dichloromethane. The combined organic extracts were filtered over anhydrous MgSO₄, filtered, the solvent was removed under reduced pressure, and the product was purified by preparative HPLC to give the malonamide derivatives in different yields.

***N*¹-(3-Chlorobenzyl)-*N*¹-(3-chlorophenyl)-*N*³-(5-nitrothiazol-2-yl) malonamide(1c)**

The title compound was synthesized according to the procedure C using **1b** and 2-amino-5-nitrothiazole, yield: 71%, yellowish white solid. ¹H NMR (500 MHz, acetone) δ 12.01 (s, 1H), 8.39 (s, 1H), 7.71 – 6.87 (m, 8H), 5.00 (s, 2H), 3.66 (s, 2H). ¹³C NMR (126 MHz, acetone) δ 167.38, 167.16, 161.73, 143.75, 143.39, 142.24, 140.17, 135.37, 134.58, 131.99, 130.89, 129.58, 129.53, 129.22, 128.37, 128.16, 127.80, 52.87, 42.71. HRMS (ESI): calculated for (C₁₉H₁₄Cl₂N₄O₄S) 465.01911, found 465.01785 (M+H)⁺

***N*¹-(3-Chlorobenzyl)-*N*¹-(3-chlorophenyl)-*N*³-(1-methyl-1*H*-pyrazol-4-yl) malonamide(2c)**

The title compound was synthesized according to the procedure C using **1b** and 1-methyl-1*H*-pyrazol-4-amine, yield: 78%, white solid. ¹H NMR (500 MHz, DMSO) δ 9.97 (s, 1H), 7.85 (s, 1H), 7.44 – 7.34 (m, 4H), 7.34 – 7.28 (m, 3H), 7.26 – 7.19 (m, 2H), 4.92 (s, 2H), 3.78 (s, 3H), 3.22 (s, 2H). ¹³C NMR (126 MHz, DMSO) δ 166.93, 163.50, 143.01, 139.61, 133.51, 133.07, 130.98, 130.22, 129.55, 128.19, 128.14, 127.65, 127.22, 127.07, 126.45, 121.32, 121.21, 51.41, 42.43, 38.62. HRMS (ESI): calculated for (C₂₀H₁₈Cl₂N₄O₂) 417.08851, found 417.08649 (M+H)⁺

***N*¹-(3-Chlorobenzyl)-*N*¹-(3-chlorophenyl)-*N*³-(5-(methylthio)-1,3,4-thiadiazol-2-yl) malonamide(3c)**

The title compound was synthesized according to the procedure C using **1b** and 5-(methylthio)-1,3,4-thiadiazol-2-amine, yield: 74%, white solid. ¹H NMR (500 MHz, DMSO) δ 12.56 (s, 1H), 7.41 (d, *J* = 6.0 Hz, 3H), 7.37 – 7.30 (m, 3H), 7.21 (td, *J* = 6.1, 3.3 Hz, 2H), 4.89 (s, 2H), 3.45 (s, 2H), 2.71 (s, 3H). ¹³C NMR (126 MHz, DMSO) δ 166.16, 165.85, 160.39, 158.19, 142.56, 139.46, 133.56, 133.08, 131.16, 130.30, 128.40, 128.36, 127.76, 127.34, 127.26, 126.62, 51.46, 42.61, 15.98. HRMS (ESI): calculated for (C₁₉H₁₆Cl₂N₄O₂S₂) 467.01700, found 467.01559 (M+H)⁺

***N*¹-(3-Chlorobenzyl)-*N*¹-(3-chlorophenyl)-*N*³-(1*H*-indol-5-yl) malonamide(4c)**

The title compound was synthesized according to the procedure C using **1b** and 5-aminoindole, yield: 76%, white solid. ¹H NMR (500 MHz, DMSO) δ 11.02 (s, 1H), 9.78 (s, 1H), 7.83 (s, 1H), 7.46 (s, 1H), 7.42 – 7.31 (m, 6H), 7.31 – 7.22 (m, 3H), 7.14 (d, *J* = 8.7 Hz, 1H), 6.40 (t, *J* = 2.3 Hz, 1H), 4.94 (s, 2H), 3.42 (s, 2H). ¹³C NMR (126 MHz, DMSO) δ 167.25, 164.74,

143.16, 139.71, 133.60, 133.17, 132.91, 131.05, 130.74, 130.29, 128.27, 128.20, 127.69, 127.51, 127.27, 127.14, 126.48, 126.00, 115.00, 111.25, 111.09, 101.21, 51.52, 43.37. HRMS (ESI): calculated for (C₂₄H₁₉Cl₂N₃O₂) 452.09326, found 452.09164 (M+H)⁺

***N*¹-(Benzo[d]thiazol-2-yl)-*N*³-(3-chlorobenzyl)-*N*³-(3-chlorophenyl) malonamide(5c)**

The title compound was synthesized according to the procedure C using **1b** and 2-amino-benzothiazole, yield: 78%, white solid. ¹H NMR (500 MHz, acetone) δ 8.13 (s, 1H), 7.93 (d, *J* = 7.9 Hz, 1H), 7.72 (d, *J* = 8.1 Hz, 1H), 7.48 – 7.40 (m, 4H), 7.39 (d, *J* = 2.4 Hz, 1H), 7.35 – 7.24 (m, 5H), 5.02 (s, 2H), 3.60 (s, 2H). ¹³C NMR (126 MHz, acetone) δ 167.65, 166.60, 162.58, 158.20, 149.92, 143.75, 140.48, 135.38, 134.64, 133.08, 132.00, 130.96, 129.68, 129.54, 129.30, 128.39, 127.89, 126.90, 124.55, 122.27, 121.78, 52.86, 42.75. HRMS (ESI): calculated for (C₂₃H₁₈Cl₂N₃O₂S) 470.04968, found 470.04800 (M+H)⁺

***N*¹-(3-Chlorobenzyl)-*N*¹-(3-chlorophenyl)-*N*³-(2-hydroxy-5-nitrophenyl) malonamide(6c)**

The title compound was synthesized according to the procedure C using **1b** and 2-amino-4-nitrophenol, yield: 81%, white solid. ¹H NMR (500 MHz, acetone) δ 10.14 (s, 1H), 9.14 (d, *J* = 2.7 Hz, 1H), 7.90 (dd, *J* = 8.9, 2.8 Hz, 1H), 7.49 – 7.37 (m, 4H), 7.36 – 7.24 (m, 5H), 7.10 (d, *J* = 8.9 Hz, 1H), 5.03 (s, 2H), 3.50 (s, 2H). ¹³C NMR (126 MHz, acetone) δ 168.81, 166.28, 153.35, 143.73, 141.40, 140.43, 135.39, 134.64, 131.99, 130.95, 129.54, 129.23, 128.37, 128.19, 128.05, 127.81, 121.05, 116.61, 116.54, 115.46, 52.82, 42.86. HRMS (ESI): calculated for (C₂₂H₁₇Cl₂N₃O₅) 474.06235, found 474.06350 (M+H)⁺

***N*¹-(3-Chlorobenzyl)-*N*¹-(3-chlorophenyl)-*N*³-(2-hydroxyphenyl) malonamide(7c)**

The title compound was synthesized according to the procedure C using **1b** and 2-aminophenol, yield: 78%, white solid. ¹H NMR (500 MHz, acetone) δ 9.81 (s, 1H), 7.77 (dd, *J* = 8.0, 1.6 Hz, 1H), 7.47 – 7.40 (m, 3H), 7.39 – 7.24 (m, 6H), 6.98 (td, *J* = 7.7, 1.6 Hz, 1H), 6.91 (dd, *J* = 8.0, 1.5 Hz, 1H), 6.81 (td, *J* = 7.7, 1.5 Hz, 1H), 5.02 (s, 2H), 3.46 (s, 2H). ¹³C NMR (126 MHz, acetone) δ 168.62, 166.36, 148.47, 143.85, 140.50, 135.33, 134.62, 131.93, 130.92, 129.52, 129.41, 129.19, 128.31, 128.15, 127.76, 127.46, 125.88, 122.36, 120.49, 117.25, 52.78, 42.89. HRMS (ESI): calculated for (C₂₂H₁₈Cl₂N₂O₃) 429.07727, found 429.07654 (M+H)⁺

***N*¹-(3-Chloro-2-cyanophenyl)-*N*³-(3-chlorobenzyl)-*N*³-(3-chlorophenyl) malonamide(8c)**

The title compound was synthesized according to the procedure C using **1b** and 2-amino-6-chlorobenzonitrile, yield: 72%, white solid. ¹H NMR (500 MHz, DMSO) δ 10.44 (s, 1H), 7.70

(t, $J = 8.2$ Hz, 1H), 7.62 (d, $J = 8.3$ Hz, 1H), 7.53 (d, $J = 8.0$ Hz, 1H), 7.42 (d, $J = 5.3$ Hz, 3H), 7.36 – 7.28 (m, 3H), 7.27 – 7.21 (m, 2H), 4.93 (s, 2H), 3.42 (s, 2H). ^{13}C NMR (126 MHz, DMSO) δ 166.57, 166.02, 165.39, 142.72, 141.96, 139.52, 135.84, 134.84, 133.60, 133.07, 131.18, 130.29, 128.39, 128.20, 127.71, 127.29, 126.55, 126.07, 123.28, 113.83, 106.84, 51.41, 42.79. HRMS (ESI): calculated for ($\text{C}_{23}\text{H}_{16}\text{Cl}_3\text{N}_3\text{O}_2$) 472.03863, found 472.03699 ($\text{M}+\text{H}$)⁺

***N*¹-(3-Chlorobenzyl)-*N*¹-(3-chlorophenyl)-*N*³-(4-chloropyridin-3-yl) malonamide(9c)**

The title compound was synthesized according to the procedure C using **1b** and 4-chloropyridin-3-amine, yield: 71%, white solid. ^1H NMR (500 MHz, DMSO) δ 10.03 (s, 1H), 8.84 (s, 1H), 8.32 (d, $J = 5.3$ Hz, 1H), 7.59 (d, $J = 5.3$ Hz, 1H), 7.47 (t, $J = 7.8$ Hz, 1H), 7.43 (d, $J = 4.8$ Hz, 2H), 7.37 (d, $J = 8.0$ Hz, 1H), 7.34 (d, $J = 3.2$ Hz, 1H), 7.31 (s, 1H), 7.23 (t, $J = 7.5$ Hz, 2H), 4.93 (s, 2H), 3.52 (s, 2H). ^{13}C NMR (126 MHz, DMSO) δ 166.92, 166.00, 150.73, 146.71, 146.59, 142.81, 139.55, 135.54, 133.62, 133.13, 131.88, 131.22, 130.32, 129.80, 127.72, 127.33, 126.58, 124.64, 121.32, 51.51, 42.58. HRMS (ESI): calculated for ($\text{C}_{21}\text{H}_{16}\text{Cl}_3\text{N}_3\text{O}_2$) 448.03863, found 448.03705 ($\text{M}+\text{H}$)⁺

***N*¹-(3-Chlorobenzyl)-*N*¹-(3-chlorophenyl)-*N*³-morpholinomalonamide(10c)**

The title compound was synthesized according to the procedure C using **1b** and morpholin-4-amine, yield: 71%, white solid. ^1H NMR (500 MHz, DMSO) δ 8.65 (s, 1H), 7.45 – 7.14 (m, 8H), 4.90 (d, $J = 7.9$ Hz, 2H), 3.80 – 3.55 (m, 4H), 3.30 (s, 2H), 2.75 – 2.48 (m, 4H). ^{13}C NMR (126 MHz, DMSO) δ 169.40, 167.41, 163.94, 163.11, 143.26, 139.79, 133.70, 133.23, 131.12, 130.24, 128.13, 127.92, 127.32, 126.70, 66.03, 55.49, 51.24, 40.66. HRMS (ESI): calculated for ($\text{C}_{20}\text{H}_{21}\text{Cl}_2\text{N}_3\text{O}_3$) 422.10382, found 422.10202 ($\text{M}+\text{H}$)⁺

***N*¹-([1,1'-Biphenyl]-4-ylmethyl)-*N*³-(5-nitrothiazol-2-yl)-*N*¹-(quinolin-3-yl) malonamide(1d)**

The title compound was synthesized according to the procedure C using **2b** and 2-amino-5-nitrothiazole, yield: 88%, yellowish white solid. ^1H NMR (500 MHz, acetone) δ 11.97 (s, 1H), 8.79 (q, $J = 2.9$ Hz, 1H), 8.37 (d, $J = 7.1$ Hz, 1H), 8.28 (q, $J = 2.6$ Hz, 1H), 8.05 (t, $J = 7.9$ Hz, 1H), 7.90 (t, $J = 7.7$ Hz, 1H), 7.80 (q, $J = 7.5$ Hz, 1H), 7.62 (dt, $J = 14.3, 7.3$ Hz, 6H), 7.46 – 7.41 (m, 4H), 5.17 (d, $J = 6.5$ Hz, 2H), 3.71 (d, $J = 7.1$ Hz, 2H). ^{13}C NMR (126 MHz, acetone) δ 168.39, 165.06, 163.54, 144.08, 142.61, 142.12, 140.94, 137.69, 137.21, 136.87, 135.38, 130.38, 129.73, 129.12, 128.98, 128.71, 127.91, 127.74, 127.15, 126.86, 124.47, 120.76, 48.29, 43.05. HRMS (ESI): calculated for ($\text{C}_{28}\text{H}_{21}\text{N}_5\text{O}_4\text{S}$) 524.13925, found 524.13689 ($\text{M}+\text{H}$)⁺

***N*¹-([1,1'-Biphenyl]-4-ylmethyl)-*N*³-(1H-benzo[d]imidazol-2-yl)-*N*¹-(quinolin-3-yl) malonamide(2d)**

The title compound was synthesized according to the procedure C using **2b** and 2-amino-benzimidazole, yield: 76%, white solid. ¹H NMR (500 MHz, DMSO) δ 9.89 (s, 1H), 8.53 (d, *J* = 1.6 Hz, 1H), 8.14 – 8.09 (m, 1H), 8.07 (dd, *J* = 2.3, 1.6 Hz, 1H), 7.77 – 7.71 (m, 1H), 7.65 (td, *J* = 7.6, 1.2 Hz, 1H), 7.62 – 7.50 (m, 5H), 7.48 – 7.41 (m, 2H), 7.41 – 7.33 (m, 3H), 7.27 – 7.20 (m, 1H), 7.23 – 7.12 (m, 3H), 5.30 (s, 2H), 3.77 (s, 2H). ¹³C NMR (126 MHz, DMSO) δ 168.52, 164.29, 148.46, 142.61, 142.12, 140.94, 137.69, 137.54, 137.21, 135.87, 135.39, 130.38, 129.73, 129.12, 128.98, 128.71, 127.91, 127.74, 127.15, 126.86, 124.47, 121.76, 121.44, 120.76, 113.43, 113.34, 48.29, 43.26. HRMS (ESI): calculated for (C₃₂H₂₅N₅O₂) 512.20865, found 512.20669 (M+H)⁺

***N*¹-([1,1'-Biphenyl]-4-ylmethyl)-*N*³-([1,2,4]triazolo[4,3-*a*]pyridin-3-yl)-*N*¹-(quinolin-3-yl) malonamide(3d)**

The title compound was synthesized according to the procedure C using **2b** and [1,2,4]triazolo[4,3-*a*]pyridin-3-amine, yield: 79%, white solid. ¹H NMR (500 MHz, DMSO) δ 11.01 (s, 1H), 8.83 (d, *J* = 2.5 Hz, 1H), 8.39 (d, *J* = 2.5 Hz, 1H), 8.04 (dd, *J* = 17.5, 7.7 Hz, 2H), 7.98 (d, *J* = 8.2 Hz, 1H), 7.82 (t, *J* = 7.7 Hz, 1H), 7.75 (d, *J* = 9.3 Hz, 1H), 7.64 (ddd, *J* = 19.2, 13.2, 7.5 Hz, 6H), 7.45 – 7.34 (m, 6H), 7.01 (t, *J* = 6.8 Hz, 1H), 5.14 (s, 2H), 3.55 (s, 2H). ¹³C NMR (126 MHz, DMSO) δ 167.01, 163.05, 150.54, 148.72, 146.49, 139.62, 139.15, 137.82, 136.31, 135.95, 134.84, 134.71, 130.38, 128.92, 128.75, 128.41, 128.02, 127.84, 127.46, 127.03, 126.72, 126.57, 123.77, 115.57, 113.41, 51.90, 42.77. HRMS (ESI): calculated for (C₃₁H₂₄N₆O₂) 513.20390, found 513.20108 (M+H)⁺

***N*¹-([1,1'-Biphenyl]-4-ylmethyl)-*N*³-(2-hydroxy-5-nitrophenyl)-*N*¹-(quinolin-3-yl) malonamide(4d)**

The title compound was synthesized according to the procedure C using **2b** and 2-amino-4-nitrophenol, yield: 88%, white solid. ¹H NMR (500 MHz, acetone) δ 10.02 (s, 1H), 9.11 (s, 1H), 8.78 (dd, *J* = 31.8, 2.5 Hz, 1H), 8.26 (dd, *J* = 35.2, 2.5 Hz, 1H), 8.05 (d, *J* = 8.5 Hz, 1H), 7.95 – 7.85 (m, 2H), 7.80 (ddd, *J* = 7.7, 4.9, 2.7 Hz, 1H), 7.65 – 7.57 (m, 6H), 7.43 (ddd, *J* = 14.2, 10.0, 6.1 Hz, 5H), 7.34 (tdd, *J* = 5.3, 3.4, 2.0 Hz, 1H), 5.14 (s, 2H), 3.57 (s, 2H). ¹³C NMR (126 MHz, acetone) δ 168.44, 164.80, 154.71, 142.61, 142.12, 140.94, 139.96, 137.69, 137.21, 135.37, 130.38, 129.73, 129.12, 128.98, 128.71, 127.91, 127.74, 127.15, 126.86, 126.68,

124.47, 120.76, 119.57, 116.19, 115.51, 48.29, 43.21. HRMS (ESI): calculated for (C₃₁H₂₄N₄O₅) 533.18249, found 533.18091 (M+H)⁺

***N*¹-([1,1'-Biphenyl]-4-ylmethyl)-*N*³-(3-cyano-4-fluorophenyl)-*N*¹-(quinolin-3-yl) malonamide(5d)**

The title compound was synthesized according to the procedure C using **2b** and 5-amino-2-fluorobenzonitrile, yield: 72%, white solid. ¹H NMR (500 MHz, DMSO) δ 10.22 (s, 1H), 8.79 (d, *J* = 2.5 Hz, 1H), 8.32 (d, *J* = 2.5 Hz, 1H), 7.98 (d, *J* = 8.4 Hz, 1H), 7.91 – 7.84 (m, 2H), 7.76 (t, *J* = 7.7 Hz, 1H), 7.64 – 7.58 (m, 6H), 7.45 – 7.40 (m, 3H), 7.37 (d, *J* = 8.0 Hz, 2H), 7.33 (t, *J* = 7.3 Hz, 1H), 5.10 (s, 2H), 3.42 (s, 2H). ¹³C NMR (126 MHz, DMSO) δ 166.74, 165.72, 163.11, 158.16 (d, *J* = 252.3 Hz), 150.60, 146.41, 139.65, 139.14, 136.05, 135.65, 134.85 (d, *J* = 6.0 Hz), 130.27, 128.91, 128.75, 128.50 (d, *J* = 38.6 Hz), 127.44, 127.35 (d, *J* = 12.0 Hz), 126.72, 126.57, 126.37, 126.30, 122.82, 117.01 (d, *J* = 20.2 Hz), 116.93, 113.86, 99.85 (d, *J* = 16.1 Hz), 51.92, 44.01. HRMS (ESI): calculated for (C₃₂H₂₃FN₄O₂) 515.18833, found 515.18701 (M+H)⁺

***N*¹-([1,1'-Biphenyl]-4-ylmethyl)-*N*³-(5-bromopyridin-3-yl)-*N*¹-(quinolin-3-yl) malonamide(6d)**

The title compound was synthesized according to the procedure C using **2b** and 5-bromopyridin-3-amine, yield: 81%, white solid. ¹H NMR (500 MHz, DMSO) δ 10.67 (s, 1H), 8.69 – 8.67 (m, 2H), 8.45 (d, *J* = 1.8 Hz, 1H), 8.36 (t, *J* = 2.2 Hz, 1H), 8.29 (d, *J* = 8.6 Hz, 1H), 8.03 (dd, *J* = 8.6, 1.8 Hz, 1H), 7.75 – 7.73 (m, 2H), 7.71 (d, *J* = 8.1 Hz, 2H), 7.68 – 7.66 (m, 3H), 7.60 (d, *J* = 8.0 Hz, 2H), 7.48 (d, *J* = 7.8 Hz, 2H), 7.37 (t, *J* = 7.4 Hz, 1H), 5.22 (s, 2H), 3.61 (s, 2H). ¹³C NMR (126 MHz, DMSO) δ 168.83, 167.15, 165.06, 153.09, 150.37, 146.49, 144.84, 139.50, 139.06, 136.45, 134.95, 132.79, 130.73, 128.97, 128.65, 128.04, 127.59, 126.75, 126.71, 125.06, 121.12, 119.70, 119.46, 115.56, 65.97, 43.53. HRMS (ESI): calculated for (C₃₀H₂₃BrN₄O₂) 551.10826, found 551.10790 (M+H)⁺

***N*¹-([1,1'-Biphenyl]-4-ylmethyl)-*N*¹-(quinolin-3-yl)-*N*³-(6-(trifluoromethyl)pyridin-3-yl) malonamide(7d)**

The title compound was synthesized according to the procedure C using **2b** and 6-(trifluoromethyl)pyridin-3-amine, yield: 83%, white solid. ¹H NMR (500 MHz, DMSO) δ 10.48 (s, 1H), 8.79 (d, *J* = 2.5 Hz, 1H), 8.64 (d, *J* = 2.5 Hz, 1H), 8.33 (d, *J* = 2.4 Hz, 1H), 8.17 (dd, *J* = 8.6, 2.5 Hz, 1H), 7.98 (d, *J* = 8.4 Hz, 1H), 7.89 (d, *J* = 8.2 Hz, 1H), 7.80 (d, *J* = 8.6

Hz, 1H), 7.75 (t, $J = 7.7$ Hz, 1H), 7.61 (td, $J = 11.7, 7.5$ Hz, 5H), 7.43 (t, $J = 7.6$ Hz, 2H), 7.39 – 7.31 (m, 3H), 5.10 (s, 2H), 3.47 (s, 2H). ^{13}C NMR (126 MHz, DMSO) δ 166.65, 166.40, 150.57, 146.40, 140.66, 140.42, 139.64, 139.14, 138.12, 136.02, 134.80, 130.29, 128.91, 128.77, 128.64, 128.31, 127.45, 127.37, 127.31, 126.72, 126.57, 126.43, 121.70, (q, $J = 273.2$ Hz), 121.20, 51.90, 44.09. HRMS (ESI): calculated for $(\text{C}_{31}\text{H}_{23}\text{F}_3\text{N}_4\text{O}_2)$ 541.18514, found 541.18395 (M+H)⁺

3.2.7.2 Biology

Expression of MurA

In Chapter 1, section 3.1.7.2, a detailed description of the protocol can be found.

MurA assay

In Chapter 1, section 3.1.7.2, a detailed description of the protocol can be found.

3.2.7.3 Molecular Docking

All procedures were performed using the Molecular Operating Environment (MOE) software package (version 2019, Chemical Computing Group). For the docking simulations, PDB entry 1UAE (MurA co-crystallized with UDP-N-acetylglucosamine and fosfomycin) was used. The proteins were first prepared for docking using MOE software where the proteins were protonated and saved for docking. The binding site was identified by the site finder mode. Molecular docking simulations with **4c** as a ligand were performed using the MMFF94x and OPLS-AA force fields and the “triangle matcher” method and “Force field” as refinement. Using these settings, docking runs were performed.

3.2.8 References

- (1) Ligon, B. L. Penicillin: Its Discovery and Early Development. *Seminars in Pediatric Infectious Diseases* **2004**, *15* (1), 52–57. <https://doi.org/10.1053/j.spid.2004.02.001>.
- (2) Fair, R. J.; Tor, Y. Antibiotics and Bacterial Resistance in the 21st Century. *Perspect Medicin Chem* **2014**, *6*, 25–64. <https://doi.org/10.4137/PMC.S14459>.
- (3) Ventola, C. L. The Antibiotic Resistance Crisis: Part 1: Causes and Threats. *P T* **2015**, *40* (4), 277–283.
- (4) Anderson, J. S.; Matsushashi, M.; Haskin, M. A.; Strominger, J. L. Biosynthesis of the Peptidoglycan of Bacterial Cell Walls. II. Phospholipid Carriers in the Reaction Sequence. *J Biol Chem* **1967**, *242* (13), 3180–3190.
- (5) Eniyan, K.; Dharavath, S.; Vijayan, R.; Bajpai, U.; Gourinath, S. Crystal Structure of UDP-N-Acetylglucosamine-Enolpyruvate Reductase (MurB) from Mycobacterium Tuberculosis. *Biochimica et Biophysica Acta (BBA) - Proteins and Proteomics* **2018**, *1866* (3), 397–406. <https://doi.org/10.1016/j.bbapap.2017.11.013>.
- (6) Mol, C. D.; Brooun, A.; Dougan, D. R.; Hilgers, M. T.; Tari, L. W.; Wijnands, R. A.; Knuth, M. W.; McRee, D. E.; Swanson, R. V. Crystal Structures of Active Fully Assembled Substrate- and Product-Bound Complexes of UDP-N-Acetylmuramic Acid:L-Alanine Ligase (MurC) from Haemophilus Influenzae. *J Bacteriol* **2003**, *185* (14), 4152–4162. <https://doi.org/10.1128/JB.185.14.4152-4162.2003>.

- (7) Bertrand, J. A.; Auger, G.; Martin, L.; Fanchon, E.; Blanot, D.; Le Beller, D.; van Heijenoort, J.; Dideberg, O. Determination of the MurD Mechanism through Crystallographic Analysis of Enzyme Complexes. *J Mol Biol* **1999**, *289* (3), 579–590. <https://doi.org/10.1006/jmbi.1999.2800>.
- (8) Basavannacharya, C.; Robertson, G.; Munshi, T.; Keep, N. H.; Bhakta, S. ATP-Dependent MurE Ligase in Mycobacterium Tuberculosis: Biochemical and Structural Characterisation. *Tuberculosis* **2010**, *90* (1), 16–24. <https://doi.org/10.1016/j.tube.2009.10.007>.
- (9) Eschenburg, S.; Priestman, M. A.; Abdul-Latif, F. A.; Delachaume, C.; Fassy, F.; Schönbrunn, E. A Novel Inhibitor That Suspends the Induced Fit Mechanism of UDP-N-Acetylglucosamine Enolpyruvyl Transferase (MurA) *. *Journal of Biological Chemistry* **2005**, *280* (14), 14070–14075. <https://doi.org/10.1074/jbc.M414412200>.
- (10) Blake, K. L.; O'Neill, A. J.; Mengin-Lecreulx, D.; Henderson, P. J. F.; Bostock, J. M.; Dunsmore, C. J.; Simmons, K. J.; Fishwick, C. W. G.; Leeds, J. A.; Chopra, I. The Nature of Staphylococcus Aureus MurA and MurZ and Approaches for Detection of Peptidoglycan Biosynthesis Inhibitors. *Mol Microbiol* **2009**, *72* (2), 335–343. <https://doi.org/10.1111/j.1365-2958.2009.06648.x>.
- (11) MurA (MurZ), the enzyme that catalyzes the first committed step in peptidoglycan biosynthesis, is essential in Escherichia coli | *Journal of Bacteriology*. <https://journals.asm.org/doi/10.1128/jb.177.14.4194-4197.1995> (accessed 2023-04-14).
- (12) Emergence of Fosfomycin-Resistant Isolates of Shiga-Like Toxin-Producing Escherichia coli O26 - PMC. <https://www.ncbi.nlm.nih.gov/pmc/articles/PMC89208/> (accessed 2023-04-14).
- (13) Nicolle, L. E. Urinary Tract Infection: Traditional Pharmacologic Therapies. *Am J Med* **2002**, *113 Suppl 1A*, 35S-44S. [https://doi.org/10.1016/s0002-9343\(02\)01058-6](https://doi.org/10.1016/s0002-9343(02)01058-6).
- (14) De Smet, K. A. L.; Kempell, K. E.; Gallagher, A.; Duncan, K.; Young, D. B. Alteration of a Single Amino Acid Residue Reverses Fosfomycin Resistance of Recombinant MurA from Mycobacterium Tuberculosis. *Microbiology (Reading)* **1999**, *145* (Pt 11), 3177–3184. <https://doi.org/10.1099/00221287-145-11-3177>.
- (15) Jiang, S.; Gilpin, M. E.; Attia, M.; Ting, Y.-L.; Berti, P. J. Lyme Disease Enolpyruvyl-UDP-GlcNAc Synthase: Fosfomycin-Resistant MurA from Borrelia Burgdorferi, a Fosfomycin-Sensitive Mutant, and the Catalytic Role of the Active Site Asp. *Biochemistry* **2011**, *50* (12), 2205–2212. <https://doi.org/10.1021/bi1017842>.
- (16) Nikolaidis, I.; Favini-Stabile, S.; Dessen, A. Resistance to Antibiotics Targeted to the Bacterial Cell Wall. *Protein Sci* **2014**, *23* (3), 243–259. <https://doi.org/10.1002/pro.2414>.
- (17) McCoy, A. J.; Sandlin, R. C.; Maurelli, A. T. In Vitro and In Vivo Functional Activity of Chlamydia MurA, a UDP-N-Acetylglucosamine Enolpyruvyl Transferase Involved in Peptidoglycan Synthesis and Fosfomycin Resistance. *Journal of Bacteriology* **2003**, *185* (4), 1218–1228. <https://doi.org/10.1128/JB.185.4.1218-1228.2003>.
- (18) Alrowais, H.; McElheny, C. L.; Sychala, C. N.; Sastry, S.; Guo, Q.; Butt, A. A.; Doi, Y. Fosfomycin Resistance in Escherichia Coli, Pennsylvania, USA. *Emerg Infect Dis* **2015**, *21* (11), 2045–2047. <https://doi.org/10.3201/eid2111.150750>.
- (19) Arca, P.; Rico, M.; Braña, A. F.; Villar, C. J.; Hardisson, C.; Suárez, J. E. Formation of an Adduct between Fosfomycin and Glutathione: A New Mechanism of Antibiotic Resistance in Bacteria. *Antimicrob Agents Chemother* **1988**, *32* (10), 1552–1556. <https://doi.org/10.1128/AAC.32.10.1552>.
- (20) Horii, T.; Kimura, T.; Sato, K.; Shibayama, K.; Ohta, M. Emergence of Fosfomycin-Resistant Isolates of Shiga-like Toxin-Producing Escherichia Coli O26. *Antimicrob Agents Chemother* **1999**, *43* (4), 789–793. <https://doi.org/10.1128/AAC.43.4.789>.
- (21) Venkateswaran, P. S.; Wu, H. C. Isolation and Characterization of a Phosphonomycin-Resistant Mutant of Escherichia Coli K-12. *J Bacteriol* **1972**, *110* (3), 935–944. <https://doi.org/10.1128/jb.110.3.935-944.1972>.
- (22) Qu, T.; Shi, K.; Ji, J.; Yang, Q.; Du, X.; Wei, Z.; Yu, Y. Fosfomycin Resistance among Vancomycin-Resistant Enterococci Owing to Transfer of a Plasmid Harboring the FosB Gene. *Int J Antimicrob Agents* **2014**, *43* (4), 361–365. <https://doi.org/10.1016/j.ijantimicag.2013.11.003>.
- (23) Hendlin, D.; Stapley, E. O.; Jackson, M.; Wallick, H.; Miller, A. K.; Wolf, F. J.; Miller, T. W.; Chalet, L.; Kahan, F. M.; Foltz, E. L.; Woodruff, H. B.; Mata, J. M.; Hernandez, S.; Mochales, S. Phosphonomycin, a New Antibiotic Produced by Strains of Streptomyces. *Science* **1969**, *166* (3901), 122–123. <https://doi.org/10.1126/science.166.3901.122>.
- (24) Marquardt, J. L.; Brown, E. D.; Lane, W. S.; Haley, T. M.; Ichikawa, Y.; Wong, C. H.; Walsh, C. T. Kinetics, Stoichiometry, and Identification of the Reactive Thiolate in the Inactivation of UDP-GlcNAc Enolpyruvyl Transferase by the Antibiotic Fosfomycin. *Biochemistry* **1994**, *33* (35), 10646–10651. <https://doi.org/10.1021/bi00201a011>.
- (25) Wanke, C.; Amrhein, N. Evidence That the Reaction of the UDP-N-Acetylglucosamine 1-Carboxyvinyltransferase Proceeds through the O-Phosphothioketal of Pyruvic Acid Bound to Cys115 of the Enzyme. *Eur J Biochem* **1993**, *218* (3), 861–870. <https://doi.org/10.1111/j.1432-1033.1993.tb18442.x>.

- (26) Kahan, F. M.; Kahan, J. S.; Cassidy, P. J.; Kropp, H. The Mechanism of Action of Fosfomycin (Phosphonomycin). *Ann N Y Acad Sci* **1974**, *235* (0), 364–386. <https://doi.org/10.1111/j.1749-6632.1974.tb43277.x>.
- (27) *Structure and Dynamics of FosA-Mediated Fosfomycin Resistance in Klebsiella pneumoniae and Escherichia coli / Antimicrobial Agents and Chemotherapy*. <https://journals.asm.org/doi/10.1128/AAC.01572-17> (accessed 2022-10-16).
- (28) Cao, M.; Bernat, B. A.; Wang, Z.; Armstrong, R. N.; Helmann, J. D. FosB, a Cysteine-Dependent Fosfomycin Resistance Protein under the Control of Sigma(W), an Extracytoplasmic-Function Sigma Factor in Bacillus Subtilis. *J Bacteriol* **2001**, *183* (7), 2380–2383. <https://doi.org/10.1128/JB.183.7.2380-2383.2001>.
- (29) Etienne, J.; Gerbaud, G.; Fleurette, J.; Courvalin, P. Characterization of Staphylococcal Plasmids Hybridizing with the Fosfomycin Resistance Gene FosB. *FEMS Microbiology Letters* **1991**, *84* (1), 119–122. <https://doi.org/10.1111/j.1574-6968.1991.tb04580.x>.
- (30) *Mechanistic studies of FosB: a divalent-metal-dependent bacillithiol-S-transferase that mediates fosfomycin resistance in Staphylococcus aureus - PMC*. <https://www.ncbi.nlm.nih.gov/pmc/articles/PMC3960972/> (accessed 2023-04-14).
- (31) Pakhomova, S.; Rife, C. L.; Armstrong, R. N.; Newcomer, M. E. Structure of Fosfomycin Resistance Protein FosA from Transposon Tn2921. *Protein Sci* **2004**, *13* (5), 1260–1265. <https://doi.org/10.1110/ps.03585004>.
- (32) *Covalent inhibitors of bacterial peptidoglycan biosynthesis enzyme MurA with chloroacetamide warhead - ScienceDirect*. <https://www.sciencedirect.com/science/article/pii/S0223523422006547> (accessed 2023-02-14).
- (33) Bachelier, A.; Mayer, R.; Klein, C. D. Sesquiterpene Lactones Are Potent and Irreversible Inhibitors of the Antibacterial Target Enzyme MurA. *Bioorganic & Medicinal Chemistry Letters* **2006**, *16* (21), 5605–5609. <https://doi.org/10.1016/j.bmcl.2006.08.021>.
- (34) Chang, C.-M.; Chem, J.; Chen, M.-Y.; Huang, K.-F.; Chen, C.-H.; Yang, Y.-L.; Wu, S.-H. Avenaciolides: Potential MurA-Targeted Inhibitors Against Peptidoglycan Biosynthesis in Methicillin-Resistant Staphylococcus Aureus (MRSA). *J. Am. Chem. Soc.* **2015**, *137* (1), 267–275. <https://doi.org/10.1021/ja510375f>.
- (35) Dunsmore, C. J.; Miller, K.; Blake, K. L.; Patching, S. G.; Henderson, P. J. F.; Garnett, J. A.; Stubbings, W. J.; Phillips, S. E. V.; Palestrant, D. J.; Angeles, J. D. L.; Leeds, J. A.; Chopra, I.; Fishwick, C. W. G. 2-Aminotetralones: Novel Inhibitors of MurA and MurZ. *Bioorg Med Chem Lett* **2008**, *18* (5), 1730–1734. <https://doi.org/10.1016/j.bmcl.2008.01.089>.
- (36) *Benzoethoxalone derivatives as novel inhibitors of UDP-N-acetylglucosamine enolpyruvyl transferases (MurA and MurZ) - PubMed*. <https://pubmed.ncbi.nlm.nih.gov/20861142/> (accessed 2023-01-04).
- (37) Olesen, S. H.; Ingles, D. J.; Yang, Y.; Schönbrunn, E. Differential Antibacterial Properties of the MurA Inhibitors Terreic Acid and Fosfomycin. *J Basic Microbiol* **2014**, *54* (4), 322–326. <https://doi.org/10.1002/jobm.201200617>.
- (38) Skarzynski, T.; Mistry, A.; Wonacott, A.; Hutchinson, S. E.; Kelly, V. A.; Duncan, K. Structure of UDP-N-Acetylglucosamine Enolpyruvyl Transferase, an Enzyme Essential for the Synthesis of Bacterial Peptidoglycan, Complexed with Substrate UDP-N-Acetylglucosamine and the Drug Fosfomycin. *Structure* **1996**, *4* (12), 1465–1474. [https://doi.org/10.1016/s0969-2126\(96\)00153-0](https://doi.org/10.1016/s0969-2126(96)00153-0).

3.3 Chapter 3

"Discovery of MurA Inhibitors through screening of the HIPS Library "

Abstract

The discovery of new antibiotics is crucial in the fight against antibiotic resistance. In this study, we used a combination of computational and *in vitro* screening approaches to identify potential inhibitors of the bacterial enzyme MurA, which is involved in cell-wall biosynthesis and is a promising target for antibacterial drug development. We categorized a library of 7,000 compounds using SwissSimilarity into 50 compound families based on their chemical structures. We selected a group of 168 representatives and evaluated them for their drug-likeness and physicochemical properties using SwissADME, a comprehensive *in silico* tool, that incorporates Lipinski's rule. Moreover, PAINS filter in SwissADME was also utilized for removing any compounds that were likely to interfere with the assay. This finally led to the selection of 152 compounds for the MurA inhibition enzyme assay. Of the 152 compounds screened, 38 demonstrated significant inhibitory activity against MurA at 50 μM (>80% inhibition) and were classified as actives. Eight families were identified after a second round of screening at a lower concentration of 20 μM . Further analysis of a potent hit, **HIPS843**, which is a derivative of 2-methylsulfonyl-4-pyrimidinyl tetrazoles revealed that it had favorable properties for drug development, including a low molecular weight and logP value, as well as high Ligand Efficiency and Ligand Lipophilicity Efficiency (LLE) values. This suggests that **HIPS843** may be a promising lead compound for further development. Our findings demonstrate the importance of using a combination of computational and *in vitro* approaches to identify potential drug candidates with desired pharmacological properties and pave the way for the development of new antibiotics to combat antibiotic resistance.

3.3.1 Screening for Hits

3.3.1.1 Introduction

Although the element of chance is inherent in the screening process, it remains the primary method utilized by the pharmaceutical industry for drug discovery. Through the screening of a diverse array of molecules against targeted proteins, pharmacophores can be identified and modified by medicinal chemists to generate potential drug candidates for clinical development.¹

3.3.1.2 Terminology

- **Active.**

During the initial stage of screening, a molecule may be deemed "active" if it demonstrates efficacy against the designated target. However, it is possible for molecules to affect targets in a non-specific manner, leading to false positives. This phenomenon is often observed when molecules behave like detergents or non-specifically adhere to proteins.^{2,3}
- **Hit.**

A molecule can only be considered a "hit" if its active effect is reproducible. In many cases, a screening collection will contain several related compounds that are evaluated concurrently to inform the development of a structure-activity relationship (SAR). For a hit to progress to the status of a lead, it is essential to establish a well-defined SAR and selectivity against the target.^{2,3}
- **Lead.**

The identification of a lead compound is the ultimate goal of a screening procedure. Leads are hits that have undergone chemical modification in the laboratory to optimize their biological properties.^{2,3}
- **Primary and secondary screening**

The primary screen involves the initial evaluation of molecules using the drug target alone. Actives that are identified in this stage are then subjected to secondary screening to assess their selectivity using a variety of protein targets. This secondary screening is crucial to confirm that the actives are specifically acting on the target, rather than through non-specific binding, and to eliminate false positives. Additionally, it is important to test the actives on whole cells during secondary screening as some molecules may be toxic.⁴
- **Phenotypic screening**

Phenotypic screens are typically employed to identify molecules that alter the overall characteristics of a cell, rather than targeting a specific, purified molecular target. One advantage of phenotypic screening over target-based approaches is the ability to evaluate one or more targets in their natural cellular environment. Additionally, this method can eliminate molecules that are unable to cross the cell membrane and bind to the target. However, it can be challenging to determine the molecular target once molecules have been selected through phenotypic screening, requiring a process of

"deconvolution" to interpret the data. This process is further complicated if there are multiple targets involved, which is often the case with small molecules.⁵

3.3.1.3 Primary Screening of HIPS Compounds Against MurA: Identification of Hits.

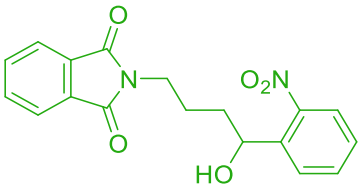
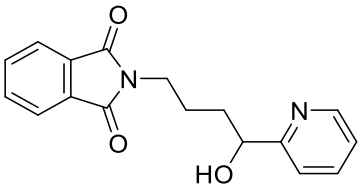
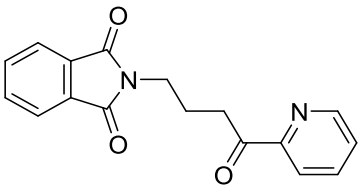
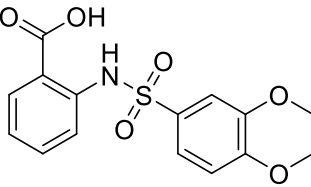
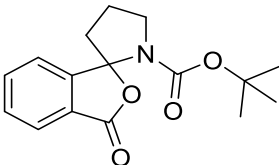
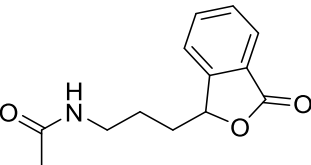
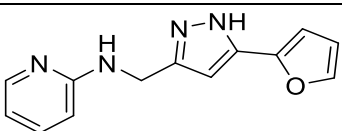
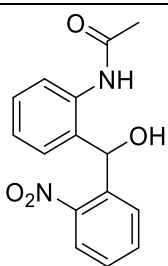
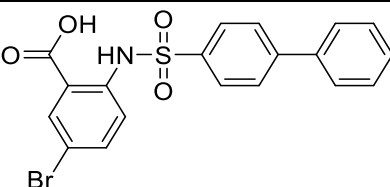
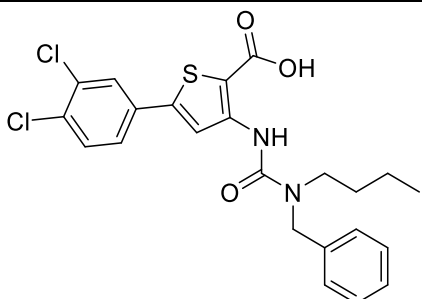
In this study, we used the HIPS library, which comprises a total of 7,000 compounds. We employed SwissSimilarity to classify the compounds into 50 families based on their chemical structure. From these families, we selected 168 compounds for primary screening to evaluate their activity against MurA at a concentration of 50 μ M. Furthermore, as part of the selection process, we utilized SwissADME to assess the drug likeness of the 168 compounds planned for primary screening against MurA. We applied Lipinski's rule to evaluate the properties of the molecules, including molecular weight, lipophilicity, and the number of hydrogen bond donors/acceptors, in order to determine their suitability as drug candidates. This additional step ensured that the compounds selected for screening possessed the necessary properties to have a chance of becoming successful drugs. In addition to applying Lipinski's rule, we also considered PAINS (Pan-Assay Interference Compounds) in our compound-selection process. PAINS are compounds that tend to interfere with various assays, leading to false-positive results, and they have been identified and classified in the PAINS database. This helped to ensure that the compounds selected for screening were less likely to interfere with the assay and lead to false-positive results providing a more accurate assessment of their activity against MurA. Although the aminothiazole moiety in **HIPS5346** is known as a PAINS (Pan-Assay Interference Compounds), we decided to keep it in our compound selection process due to the numerous antibacterial agents containing aminothiazole moieties that have been developed and are currently used in clinical practice⁶⁻⁸. Following the application of Lipinski's rule of five and PAINS filtering, 152 compounds were retained out of an initial set of 168 compounds intended for primary screening, as 16 molecules were deemed unsuitable due to their failure to comply with Lipinski's rule or the presence of PAINS alerts.

Among the 152 compounds evaluated in the primary screening, 38 compounds demonstrated significant inhibitory activity (>80%) against MurA at 50 μ M and were classified as actives. To further prioritize these compounds, a second round of screening was performed at a lower concentration of 20 μ M. Out of the 38 actives re-screened, ten compounds (**HIPS015**, **HIPS428**, **HIPS844**, **HIPS1269**, **HIPS1298**, **HIPS1396**, **HIPS1500**, **HIPS5346**, **HIPS6864**,

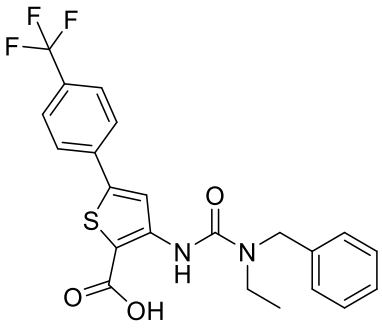
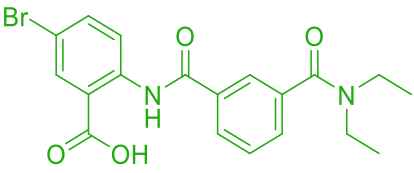
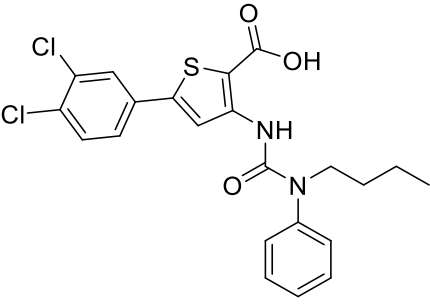
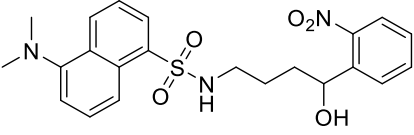
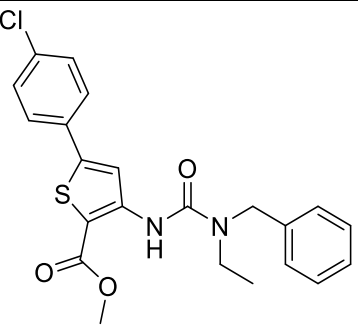
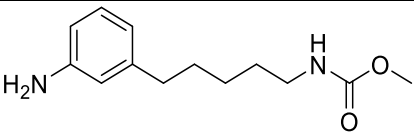
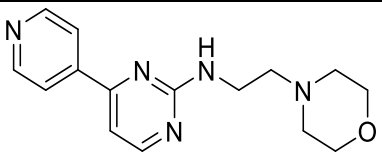
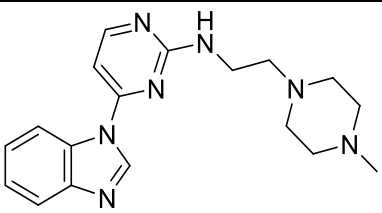
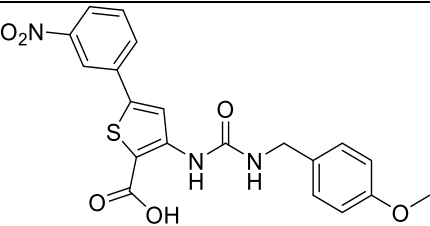
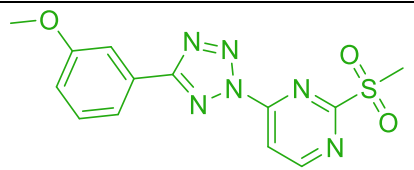
Results and Discussion

and HIPS6888) showed strong inhibition (>70%) at 20 μ M and were identified as hits as shown in Table 1.

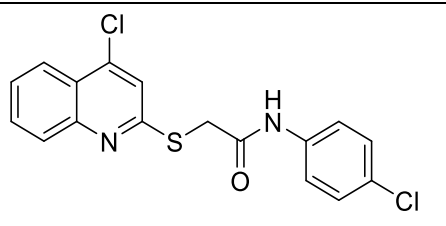
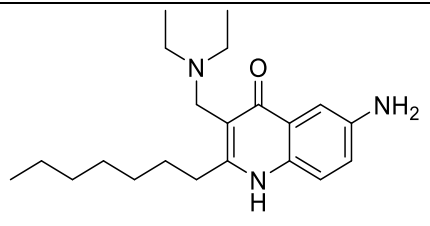
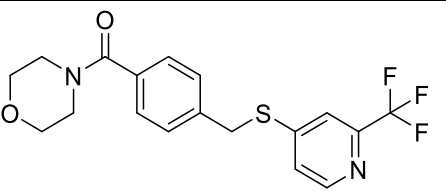
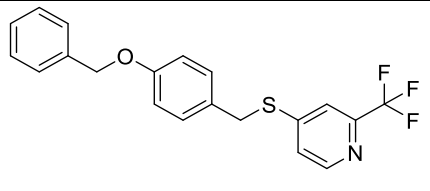
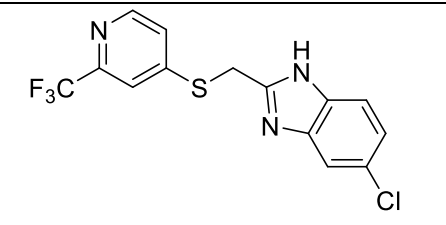
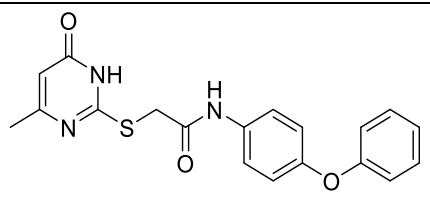
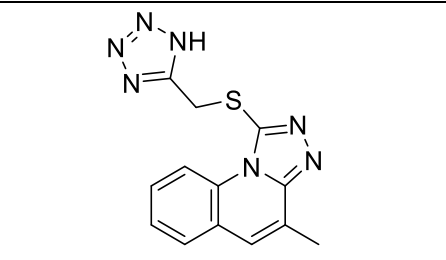
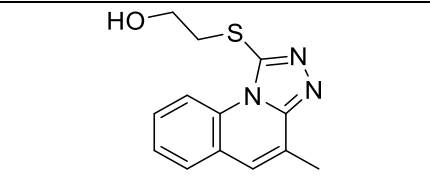
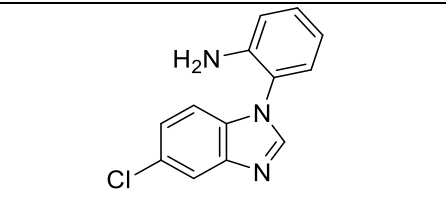
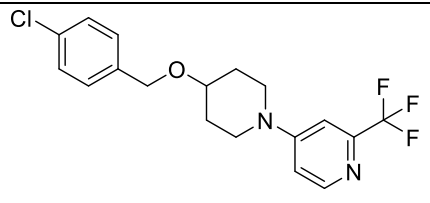
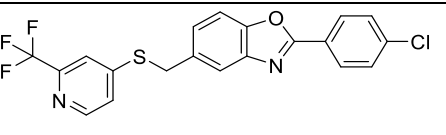
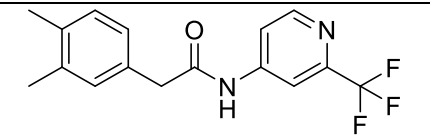
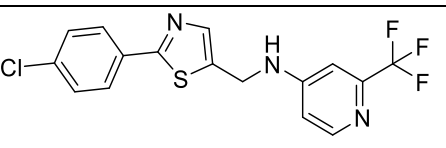
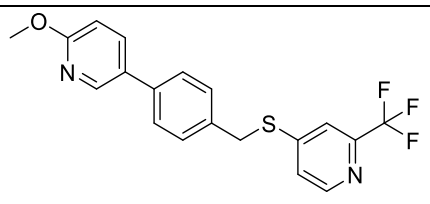
Table 1: Screening of 152 HIPS compounds at 50 and 20 μ M

HIPS code	Structure	%inh @50	%inh @20	HIPS code	Structure	%inh @50	%inh @20
015		103	100	040		4	n.d.
041		18	n.d.	061		50	n.d.
065		14	n.d.	079		14	n.d.
082		23	n.d.	206		28	n.d.
335		15	n.d.	422		101	11

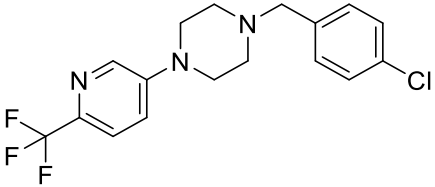
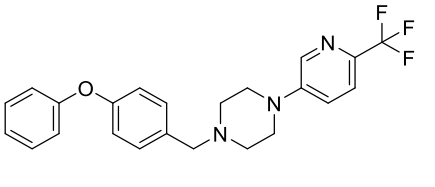
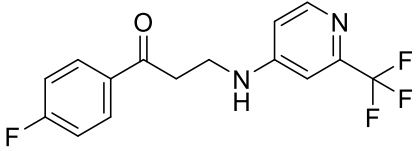
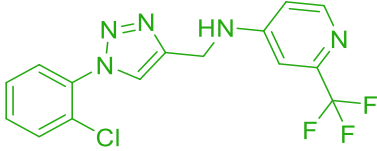
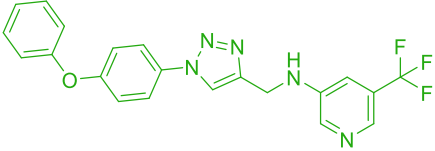
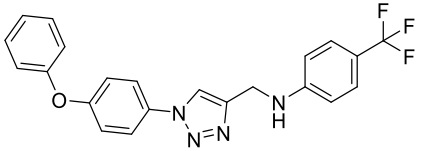
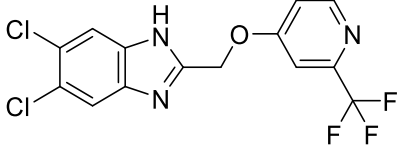
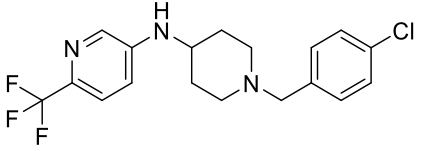
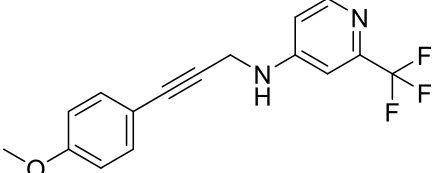
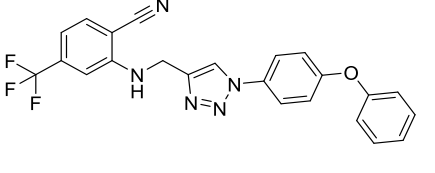
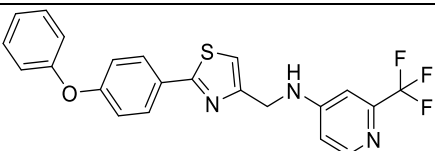
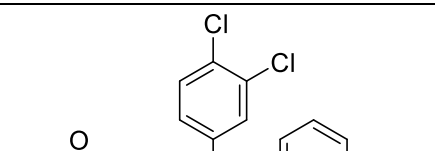
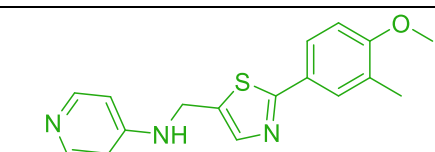
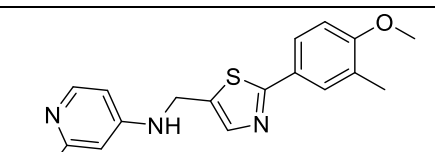
Results and Discussion

423		0	n.d.	428		100	71
440		90	n.d.	535		88	34
575		79	n.d.	629		36	n.d.
651		0	n.d.	699		0	n.d.
807		36	n.d.	844		93	92

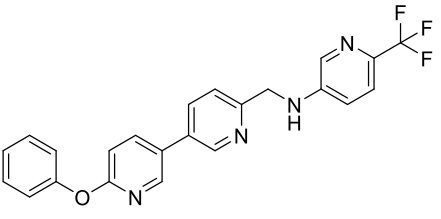
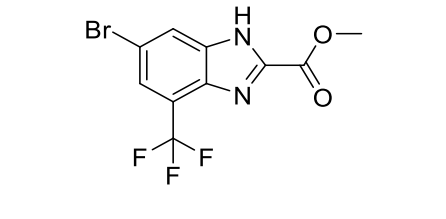
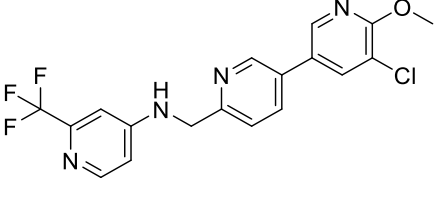
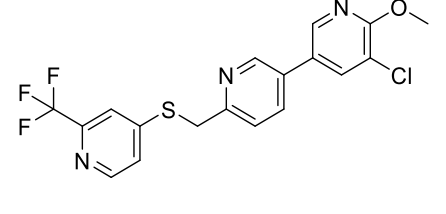
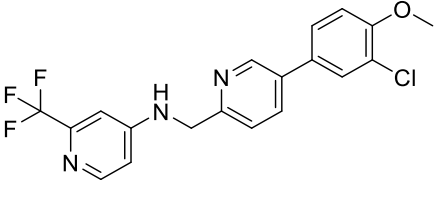
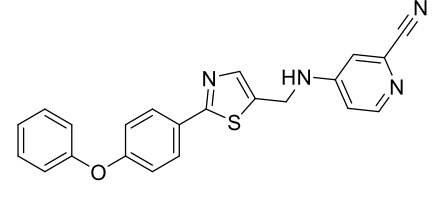
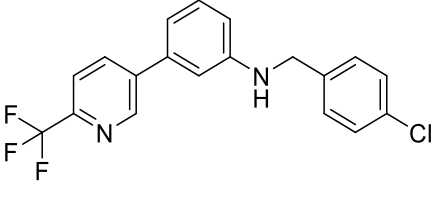
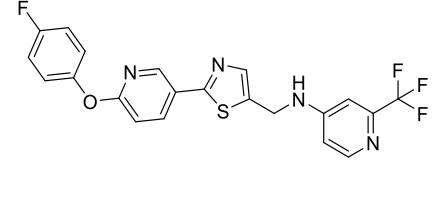
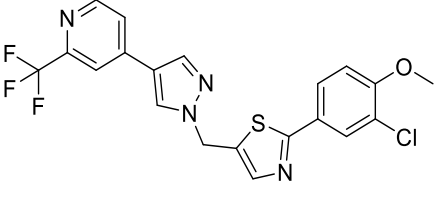
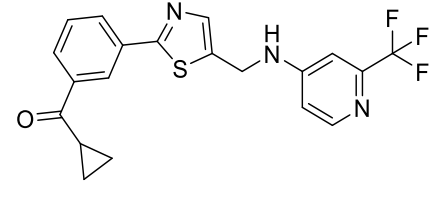
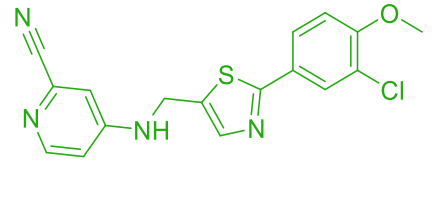
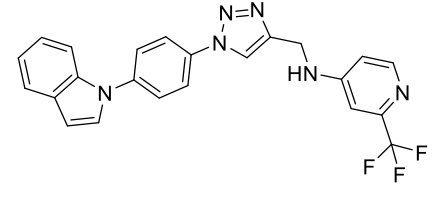
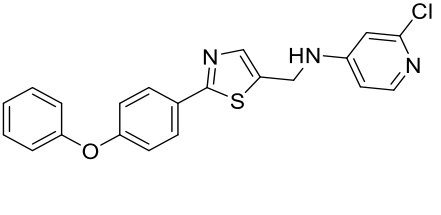
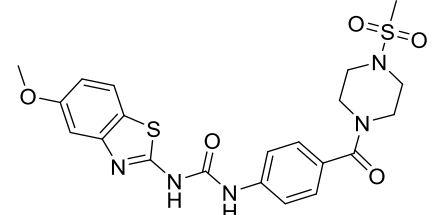
Results and Discussion

995		71	n.d.	1002		0	n.d.
1047		84	15	1049		86	n.i
1091		84	27	1092		12	n.d.
1096		82	n.d.	1097		81	47
1103		22	n.d.	1118		50	n.d.
1129		77	n.d.	1172		74	n.d.
1195		47	n.d.	1200		61	n.d.

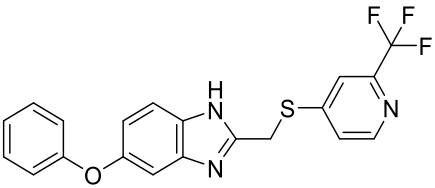
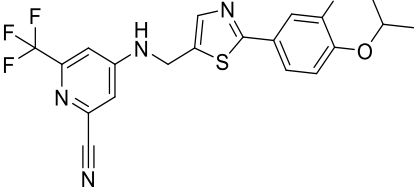
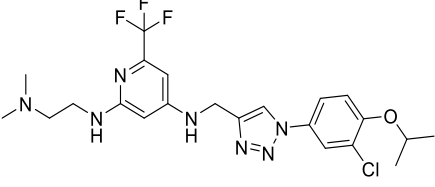
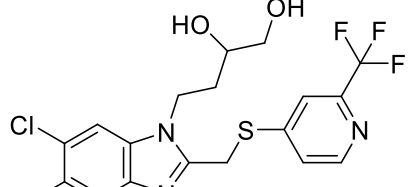
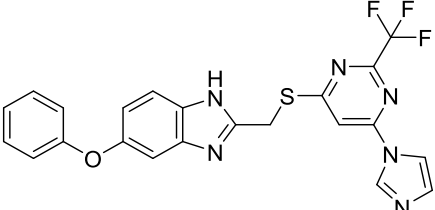
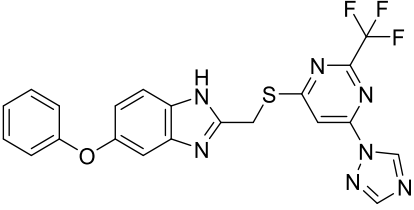
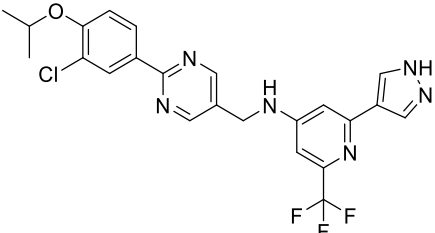
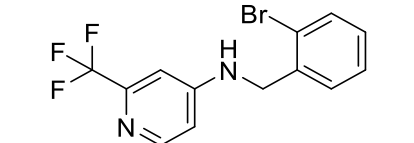
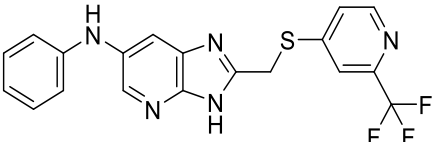
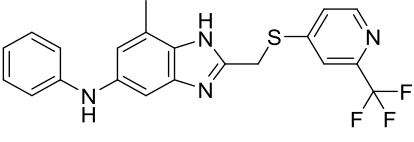
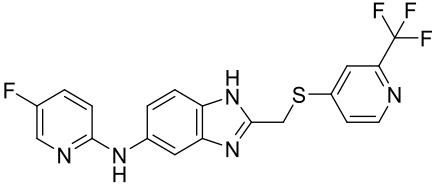
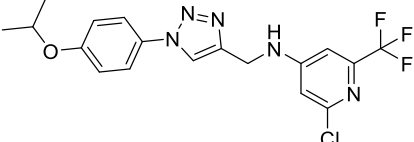
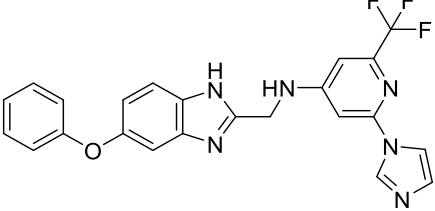
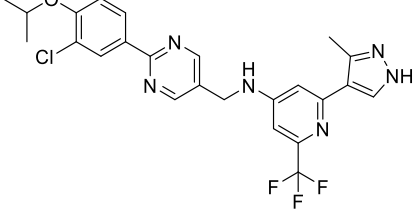
Results and Discussion

1226		28	n.d.	1248		7	n.d.
1259		34	n.d.	1269		95	100
1298		92	92	1308		69	n.d.
1312		34	n.d.	1339		38	n.d.
1345		10	n.d.	1351		56	n.d.
1358		36	n.d.	1389		0	n.d.
1396		98	101	1401		78	n.d.

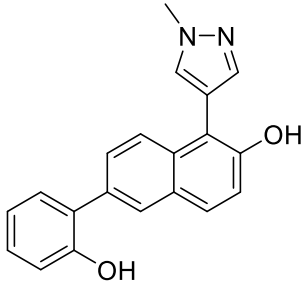
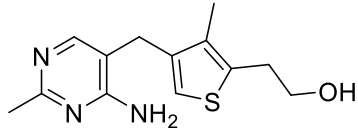
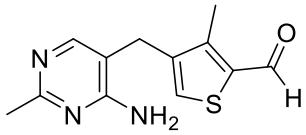
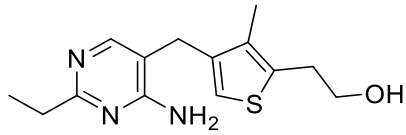
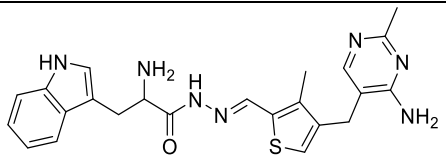
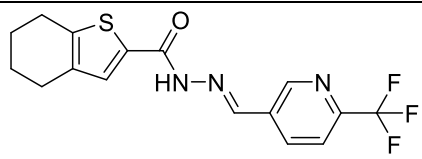
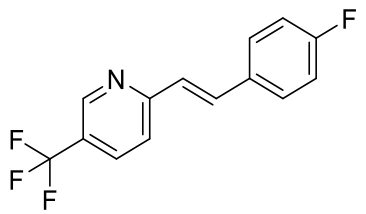
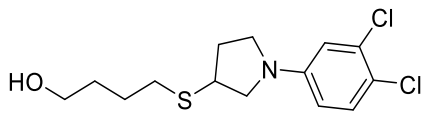
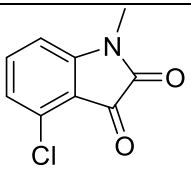
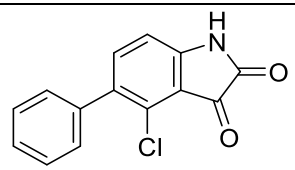
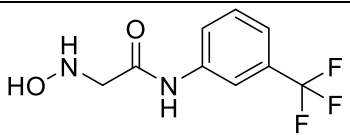
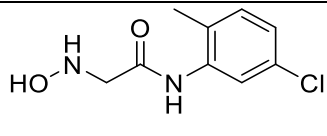
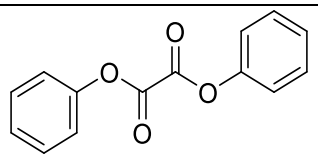
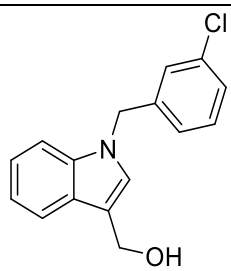
Results and Discussion

1426		72	n.d.	1427		44	n.d.
1429		60	n.d.	1438		44	n.d.
1439		24	n.d.	1440		70	n.d.
1451		90	21	1454		0	n.d.
1463		70	n.d.	1475		25	n.d.
1500		100	88	1629		70	n.d.
1661		31	n.d.	1741		15	n.d.

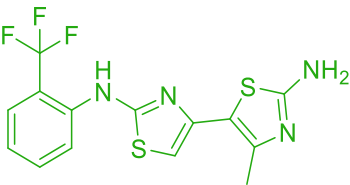
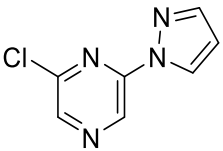
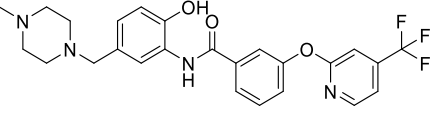
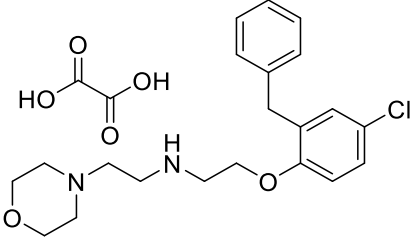
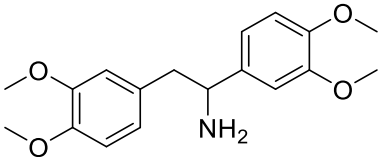
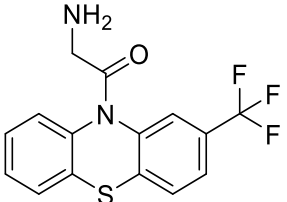
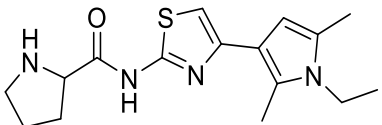
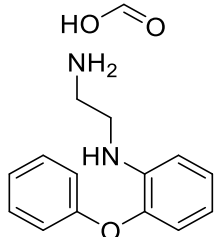
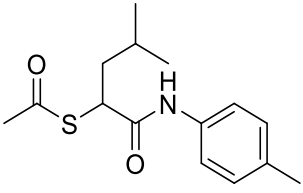
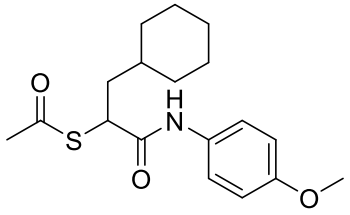
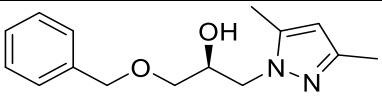
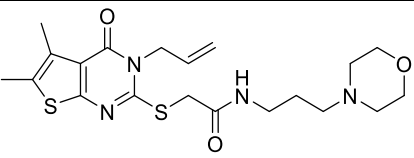
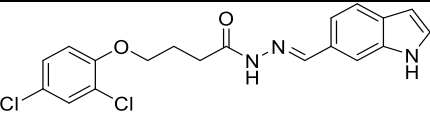
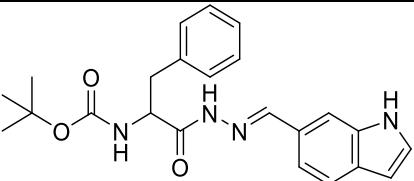
Results and Discussion

1774		25	n.d.	1808		75	n.d.
1824		0	n.d.	1969		72	n.d.
2029		19	n.d.	2030		42	n.d.
2050		52	n.d.	2052		0	n.d.
2060		86	60	2064		51	n.d.
2080		62	n.d.	2083		24	n.d.
2153		0	n.d.	2220		52	n.d.

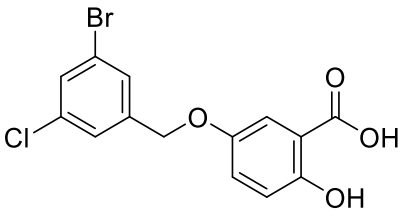
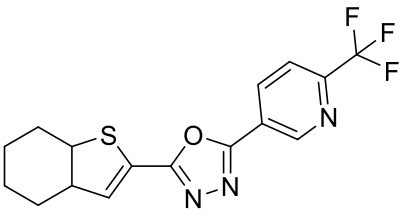
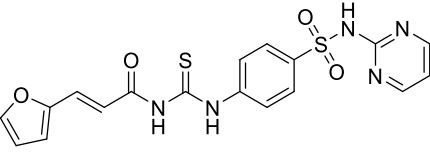
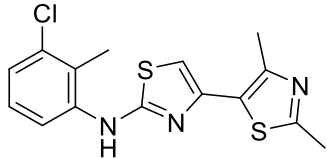
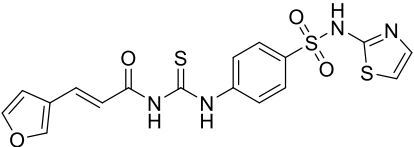
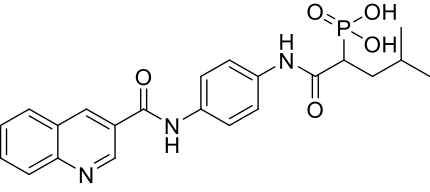
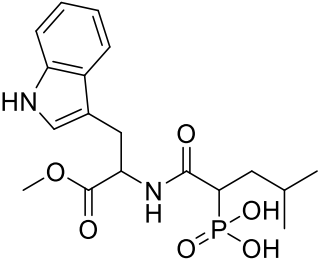
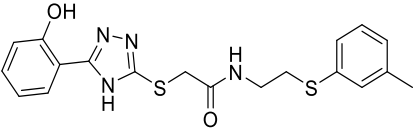
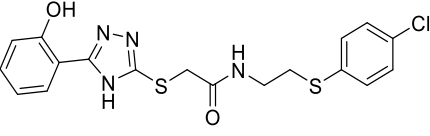
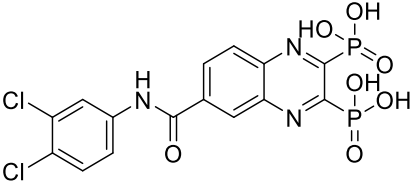
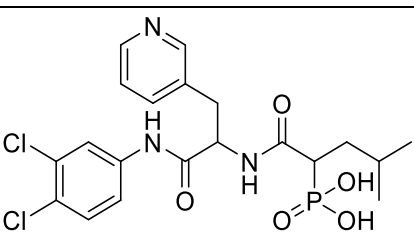
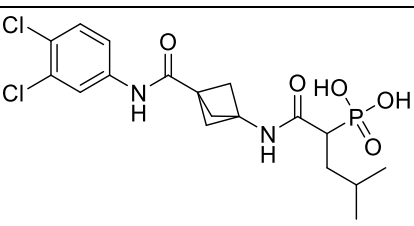
Results and Discussion

2426		54	n.d.	5052		98	ni
5054		100	ni	5056		100	ni
5075		100	51	5196		n.i	n.d.
5203		n.i	n.d.	5208		ni	n.d.
5212		ni	n.d.	5231		86	18
5273		90	ni	5283		94	ni
5314		94	17	5320		92	ni

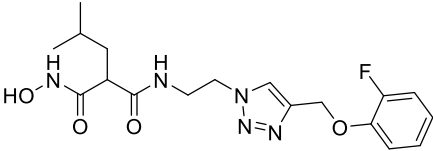
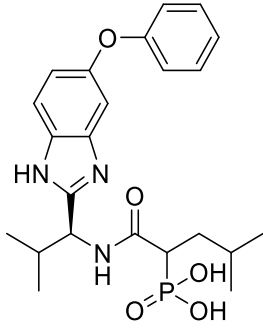
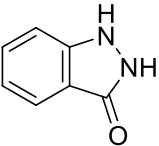
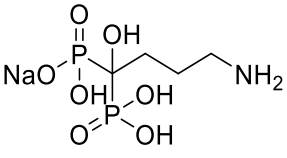
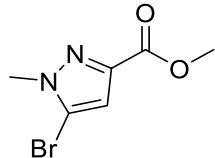
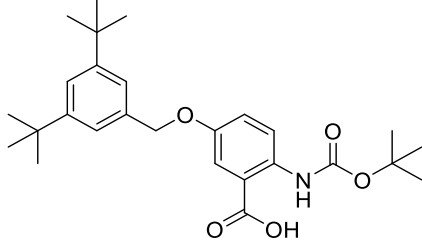
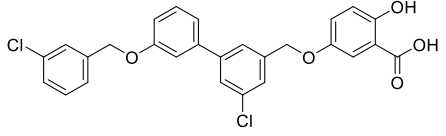
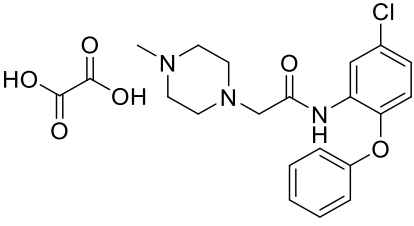
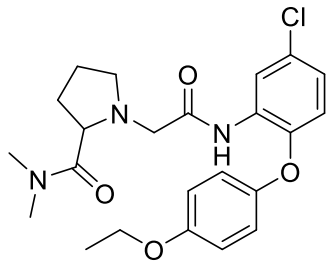
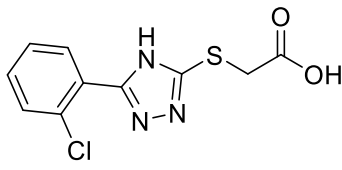
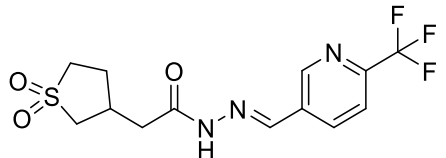
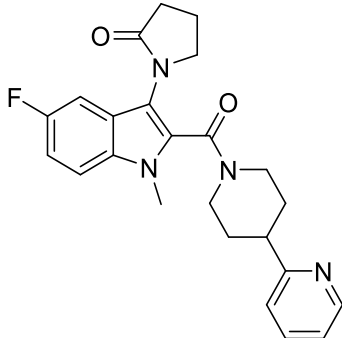
Results and Discussion

5346		97	94	5355		ni	n.d.
5367		ni	n.d.	5383		ni	n.d.
5408		ni	n.d.	5420		89	ni
5501		100	13	5504		94	ni
5510		99	35	5518		90	14
5565		ni	n.d.	5572		ni	n.d.
5595		ni	n.d.	5598		ni	n.d.

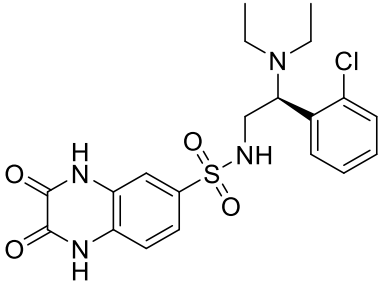
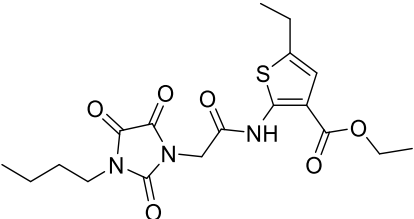
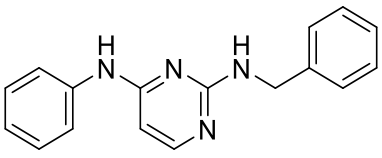
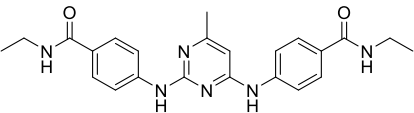
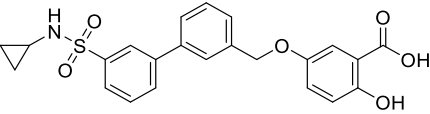
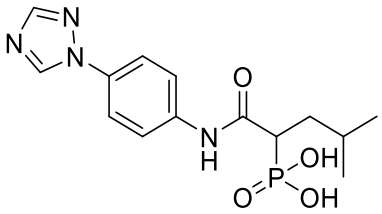
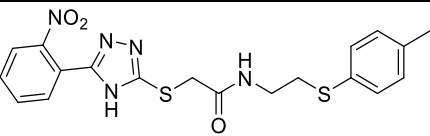
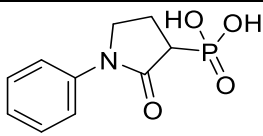
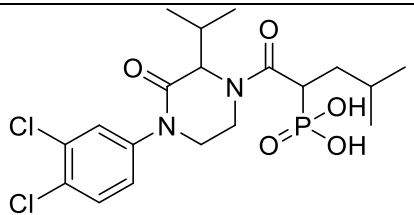
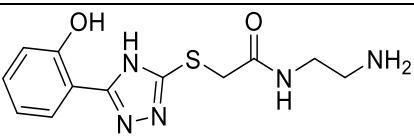
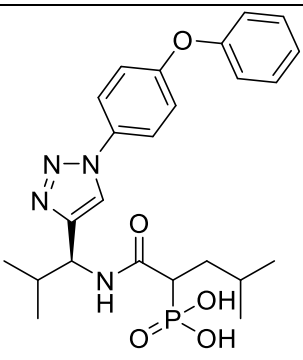
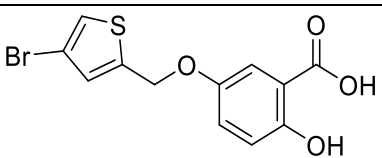
Results and Discussion

6091		ni	n.d.	6115		65	n.d.
6120		57	n.d.	6145		ni	n.d.
6147		87	63	6154		-57	n.d.
6157		36	n.d.	6160		43	n.d.
6163		ni	n.d.	6179		-36	n.d.
6182		-172	n.d.	6184		-400	n.d.

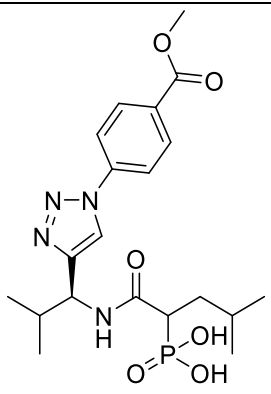
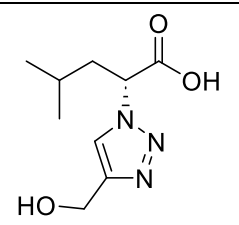
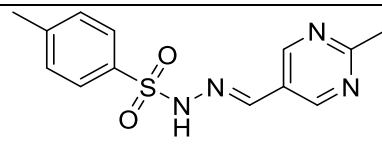
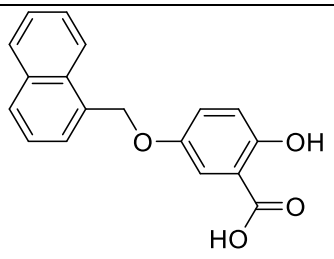
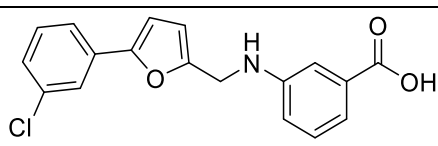
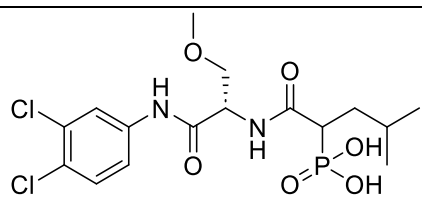
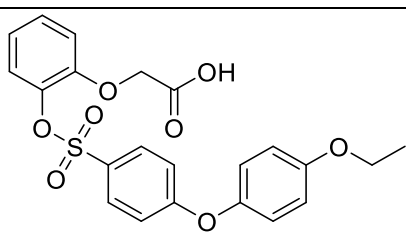
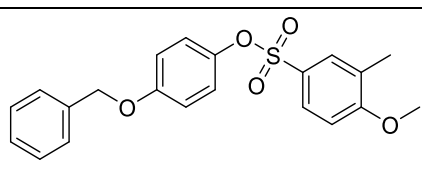
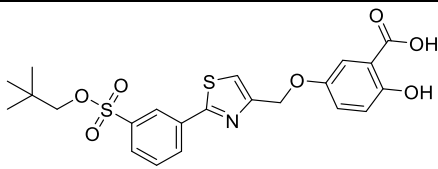
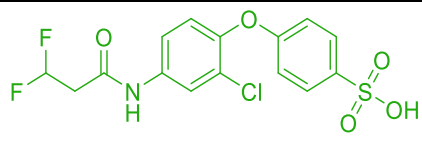
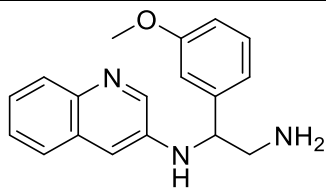
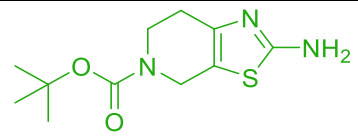
Results and Discussion

6191		77	n.d.	6204		ni	n.d.
6220		86	ni	6254		ni	n.d.
6264		ni	n.d.	6277		54	n.d.
6295		66	n.d.	6318		ni	n.d.
6326		ni	n.d.	6373		14	n.d.
6380		ni	n.d.	6397		ni	n.d.

Results and Discussion

6422		22	n.d.	6433		28	n.d.
6444		ni	n.d.	6452		ni	n.d.
6457		20	n.d.	6461		ni	n.d.
6463		ni	n.d.	6477		ni	n.d.
6484		ni	n.d.	6491		ni	n.d.
6545		ni	n.d.	6569		54	n.d.

Results and Discussion

6589		ni	n.d.	6623		75	n.d.
6787		n.d.	n.i	6790		n.d.	36
6795		n.d.	67	6797		n.d.	n.i
6800		86	56	6804		n.d.	n.i
6840		39	n.d.	6864		93	79
6868		ni	n.d.	6888		100	89

^aData shown are the mean of at least two independent experiments, SD \leq 10%. ni, no inhibition, n.d., not determined.

3.3.1.4 IC₅₀ determination for hits

The subsequent step involved determination of the half-maximal inhibitory concentration (IC₅₀) values for the ten hits identified in the previous screening that showed strong inhibition (>70%) at 20 μM. The resulting IC₅₀ are shown in Table 2.

Table 2: IC₅₀ for hits

HIPS code	Structure	IC ₅₀ (μM)	HIPS code	Structure	IC ₅₀ (μM)
015		1.32	428		17.64
844		13.71	1269		18.93
1298		3.34	1396		0.20
1500		0.96	5346		2.70
6864		10.32	6888		0.84

^aData shown are the mean of at least two independent experiments, SD ≤ 10%.

3.3.1.5 Similarity search of hits.

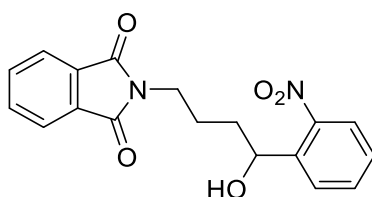
Then, a similarity search of the hits was done through the entire HIPS library using SwissSimilarity adjusted to 70% similarity and the result were as follows:

- 5 compounds similar to **HIPS015** "nitrophenylbutylisoindolinediones",
- 6 compounds similar to **HIPS428** "Benzamidobenzoic acids",
- 3 compounds similar to **HIPS844** "2-Methylsulfonyl-4-pyrimidinyl tetrazoles",
- 60 compounds similar to **HIPS1298** "Triazolymethylpyridine amines",
- 4 compounds similar to **HIPS1396** "Thiazolymethylpyridine amines",
- 63 compounds similar to **HIPS1500** "Thiazolymethylamino picolinonitriles",
- 5 compounds similar to **HIPS5346** "Bithiazole diamines",
- 3 compounds similar to **HIPS6888** "Thiazolopyridine carboxylates" and they were all tested for their inhibitory action on MurA at 10 μ M.

3.3.1.5.1 HIPS015 similarities (Nitrophenylbutylisoindolinediones)

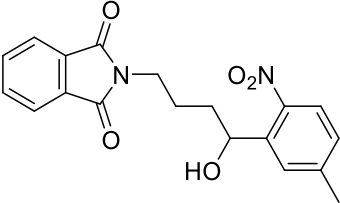
Out of the five tested compounds, two completely lost activity, two showed around 70% inhibition while **HIPS536** showed total inhibition (Table 3).

Table 3: HIPS015 similarities



%inh@10 μ M:100, IC₅₀: 1.32 μ M

HIPS code	Structure	%inh@10 μ M	HIPS code	Structure	%inh@10 μ M
38		1	536		105
537		13	644		69

654		64		
-----	---	----	--	--

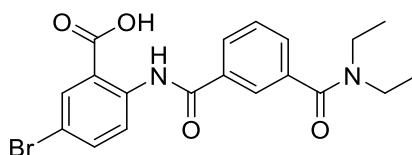
^aData shown are the mean of at least two independent experiments, SD \leq 10%.

The SAR analysis conducted on the "nitrophenylbutylisoindolinediones" yielded some intriguing results. Notably, **HIPS038**, which contained an oxo instead of a hydroxy group, demonstrated a complete loss of activity. Conversely, **HIPS536** exhibited 100% activity, indicating that a butyl or propyl group can serve as an appropriate spacer. However, when the spacer was increased to five carbons in **HIPS537**, the activity was entirely lost, underscoring the crucial role of spacer length in maintaining activity. Additionally, the introduction of a *para*-methyl group to the nitro group on either a 3-carbon spacer in **HIPS644** or a four-carbon spacer in **HIPS654** resulted in a decrease in activity.

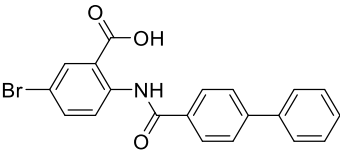
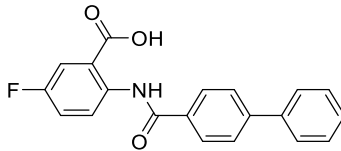
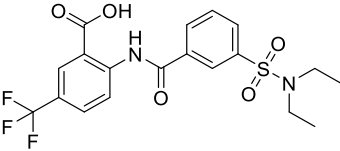
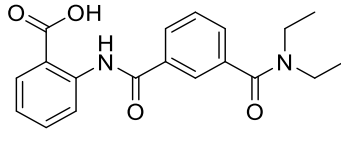
3.3.1.5.2 HIPS428 similarities (Benzamidobenzoic acids)

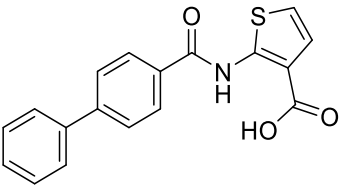
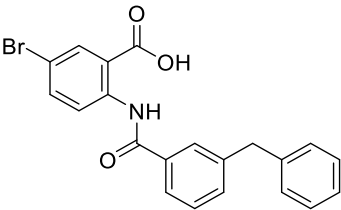
All of the six tested compounds showed no activity at 10 μ M except HIPS337 showing 58% inhibition (Table 4).

Table 4: HIPS428 similarities



%inh@10 μ M:61, IC₅₀: 17.64 μ M

HIPS code	Structure	%inh@10 μ M	HIPS code	Structure	%inh@10 μ M
189		n.i	190		n.i
337		58	427		n.i

437		n.i	569		n.i
-----	---	-----	-----	--	-----

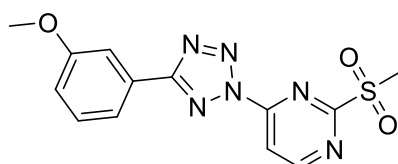
^aData shown are the mean of at least two independent experiments, SD \leq 10%. ni, no inhibition.

The SAR analysis of the benzamidobenzoic acid family revealed that replacement of diethylcarbamoyl with 1,1'-biphenyl-4-carboxamido in compounds **HIPS189**, **HIPS190**, and **HIPS437** resulted in complete loss of activity. Only when diethylcarbamoyl was replaced with diethyl sulfamoyl, compound **HIPS337** showed activity.

It is important to note that the SAR analysis of the benzamidobenzoic acids family may not be conclusive due to the concentration used for measuring inhibitory activity. The IC₅₀ value of **HIPS428** was found to be 17.28 μ M, while the % inhibition was measured at 10 μ M. Therefore, to draw more accurate SAR conclusions, it is planned to repeat the screening at a concentration closer to the IC₅₀ value (20 μ M).

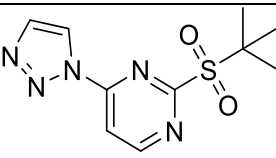
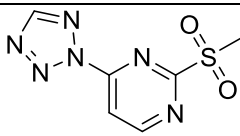
3.3.1.5.3 HIPS844 similarities (2-Methylsulfonyl-4-pyrimidinyl tetrazoles)

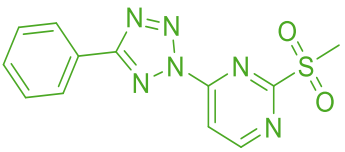
Both **HIPS843** and **HIPS862** kept activity with **HIPS862** completely inhibiting MurA at 10 μ M while **HIPS833** completely lost activity (Table 5).



%inh@10 μ M:79, IC₅₀: 13.71 μ M

Table 5: HIPS844 similarities

HIPS code	Structure	%inh@10 μ M	HIPS code	Structure	%inh@10 μ M
833		n.i	843		65

862		95			
-----	---	----	--	--	--

^aData shown are the mean of at least two independent experiments, SD \leq 10%. ni, no inhibition.

The SAR analysis of this family revealed that when the 3-methoxyphenyl group was replaced with a phenyl group in **HIPS862**, the compound still showed full activity, indicating that methoxy substitution at this position is not essential for activity but also this position can be used as a growing vector for further compound elongation. Removing the phenyl in **HIPS843** at the 5-position of the tetrazole ring reduced MurA inhibition.

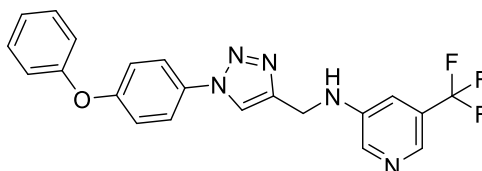
Notably, compound **HIPS843**, which retained inhibitory activity, is a small molecule with low molecular weight and logP. To further investigate the potential of this compound, we calculated the Ligand Efficiency (LE) and Ligand Lipophilicity Efficiency (LLE) values, which were found to be 0.48 and 4.1, respectively. These results indicate that **HIPS843** could be a promising fragment hit for further development in MurA drug discovery. Additionally, we also identified **HIPS862** as another potential fragment hit with an LE value of 0.38 and LLE of 3.7, both of which meet the Rule of Three for fragment-based lead discovery^{9,10}.

However, the substitution of methylsulfonyl with *tert*-butyl sulfonyl in **HIPS833** resulted in complete loss of activity. This suggests that the size of the alkyl attached to the sulfonyl group plays a crucial role in the binding to MurA.

3.3.1.5.4 HIPS1298 similarities (*N*-Triazolylmethylpyridine amines)

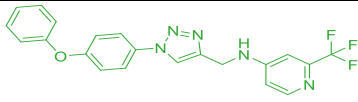
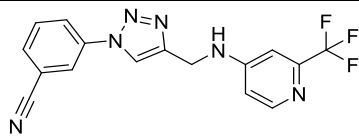
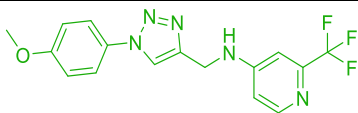
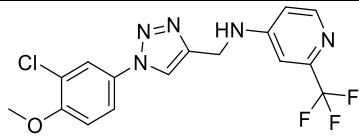
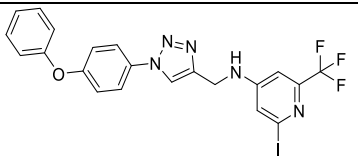
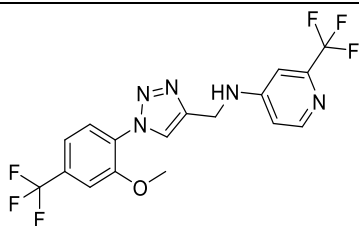
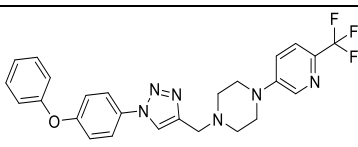
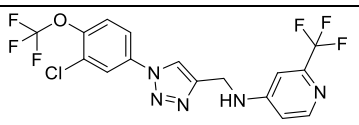
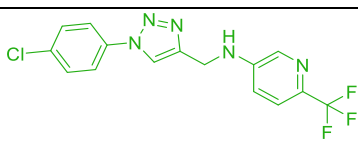
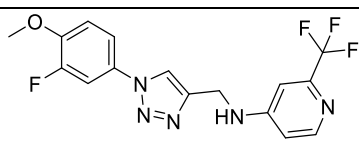
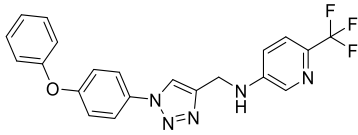
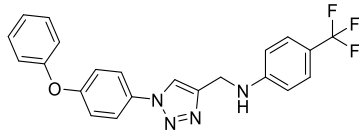
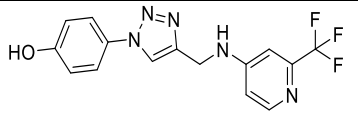
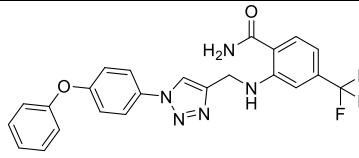
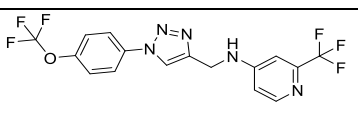
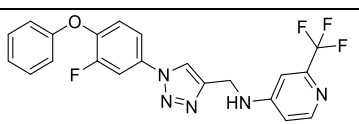
Out of 60 tested compounds, eleven showed >70% inhibition with **HIPS1611** completely inhibiting MurA at 10 μ M, 11 compounds showed %inhibition in the range of 50–69% and the rest showed less than 50% inhibition (Table 6).

Table 6: HIPS1298 similarities

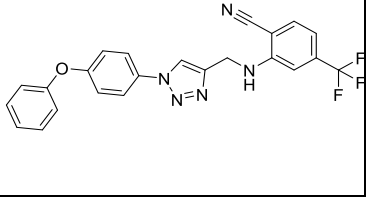
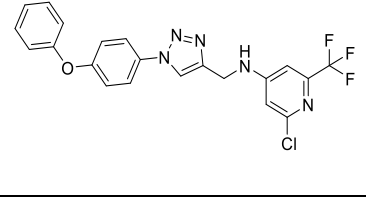
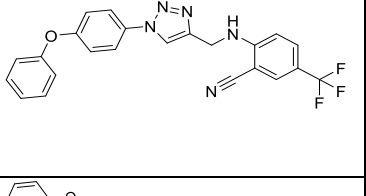
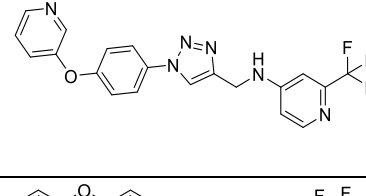
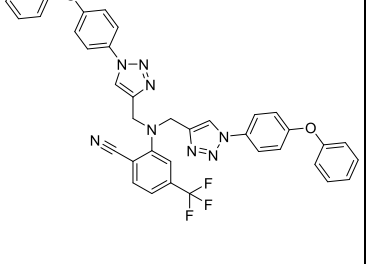
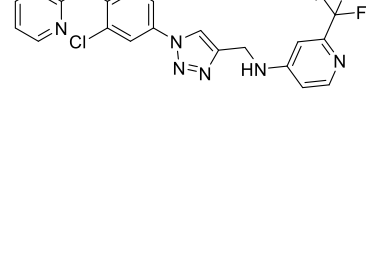
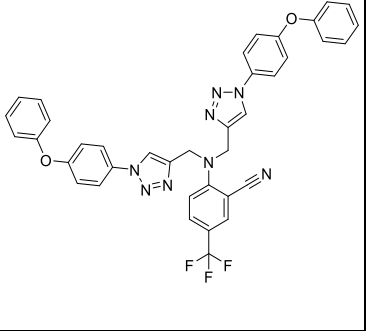
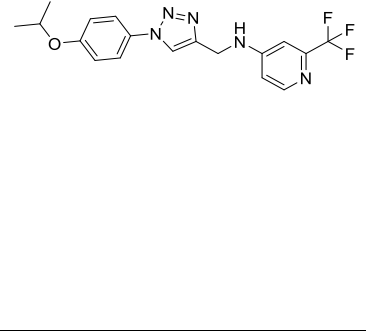
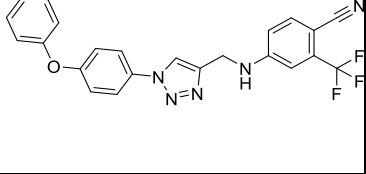
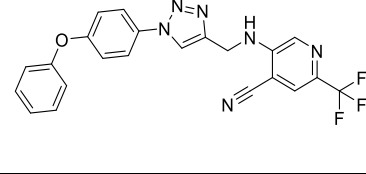
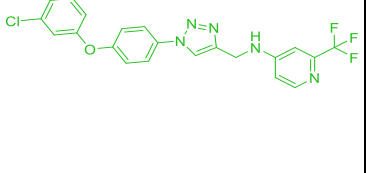
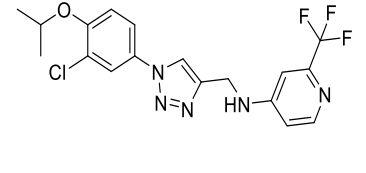
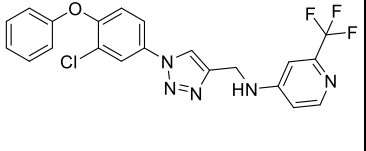
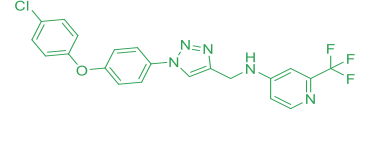
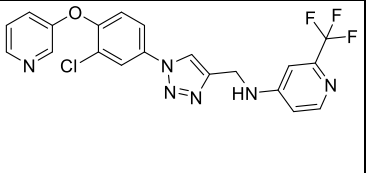
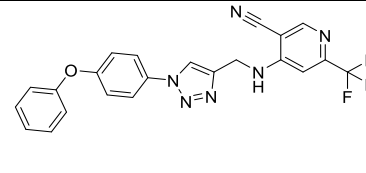


%inh@10 μ M: 92, IC₅₀: 3.34 μ M

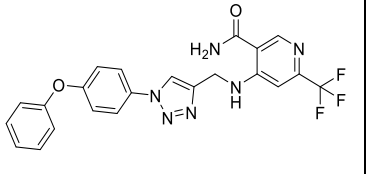
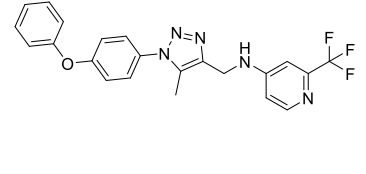
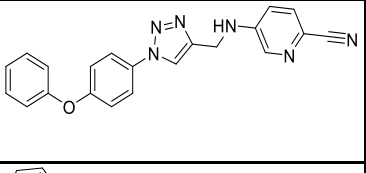
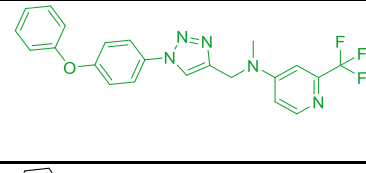
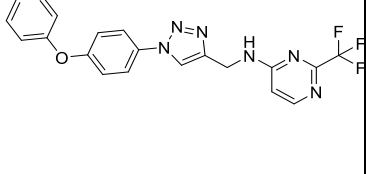
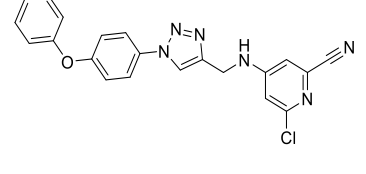
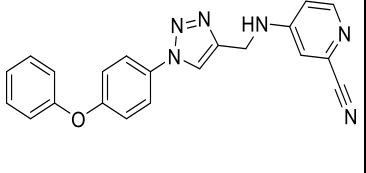
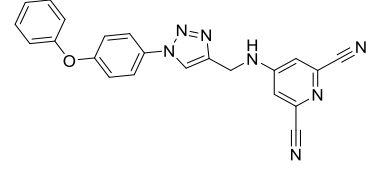
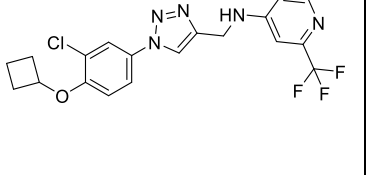
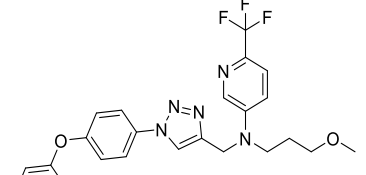
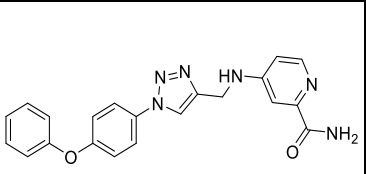
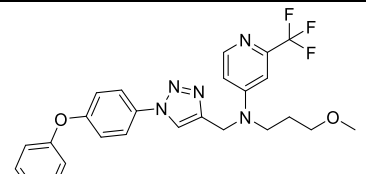
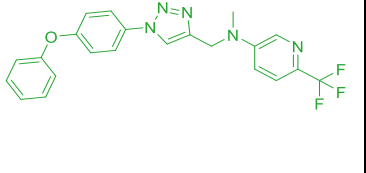
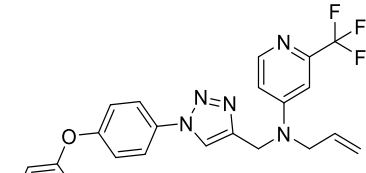
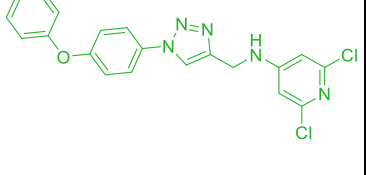
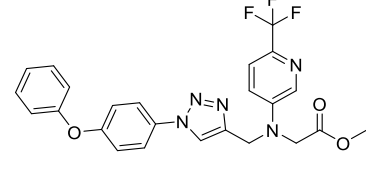
Results and Discussion

HIPS code	Structure	% inh @ 10 μ M	HIPS code	Structure	% inh @ 10 μ M
1121		88	1281		13
1211		74	1282		26
1229		23	1287		28
1243		41	1300		56
1249		81	1305		23
1250		56	1308		26
1266		32	1316		49
1275		66	1318		54

Results and Discussion

1351		45	1491		44
1352		49	1492		13
1354		18	1493		49
1355		11	1566		9
1402		39	1569		69
1437		76	1584		7
1448		52	1611		98
1453		39	1614		61

Results and Discussion

1615		48	1667		56
1617		41	1668		78
1630		12	1674		31
1631		38	1675		n.i
1641		41	1689		9
1654		41	1690		7
1656		81	1691		n.i
1658		94	1692		38

Results and Discussion

1659		76	1693		22
1662		12	1699		39
1706		56	1836		13
1708		61	1861		n.i
1826		43	1864		17
1827		64	1835		69

^aData shown are the mean of at least two independent experiments, SD \leq 10%. ni, no inhibition.

SAR analysis was performed to identify the key structural features that contribute to their activity against MurA. The first set of compounds tested were **HIPS1121** (pyridine-4-amine) and **HIPS1298** (pyridine-3-amine), which showed no significant difference in activity. Similarly, substituting trifluoromethyl with 3-chloro in **HIPS1659** maintained activity. However, adding another chloro group to the pyridine ring in **HIPS1658** enhanced activity.

Next, the 4-phenoxyphenyl group was substituted with 4-methoxyphenyl, 4-chlorophenyl and 4-hydroxyphenyl in **HIPS1211**, **HIPS1249** and **HIPS1266** respectively. While the 4-methoxy

and 4-chloro substitutions maintained the activity to some extent, the introduction of 4-hydroxy resulted in a complete loss of activity.

Furthermore, substituting the 4-phenoxyphenyl group with 3-chloro-phenoxyphenyl in **HIPS1437** maintained activity, while substituting the 4-phenoxyphenyl with 4-chloro-phenoxyphenyl group in **HIPS1611** highly increased activity.

Another observation was made when adding a methyl group to the amino group attached to the pyridine ring in **HIPS1656** and **HIPS1668**, which maintained activity.

To summarize (Figure 1), the SAR analysis revealed that the 4-phenoxyphenyl group attached to the triazole ring can be substituted with 4-methoxyphenyl or 4-chlorophenyl to maintain activity. While the addition of 4-chloro to the phenoxy phenyl enhanced the activity. The position of the N of pyridine was found to be non-critical as both pyridine-3-amine and pyridine-4-amine showed similar activity. Additionally, the position of the trifluoromethyl group in the pyridine ring was also found to be non-critical, as both 3-trifluoromethyl and 4-trifluoromethyl showed similar activity. Furthermore, trifluoromethyl can be substituted by a chloro and dichlorination enhances the activity. Finally, *N*-methylation maintained the activity.

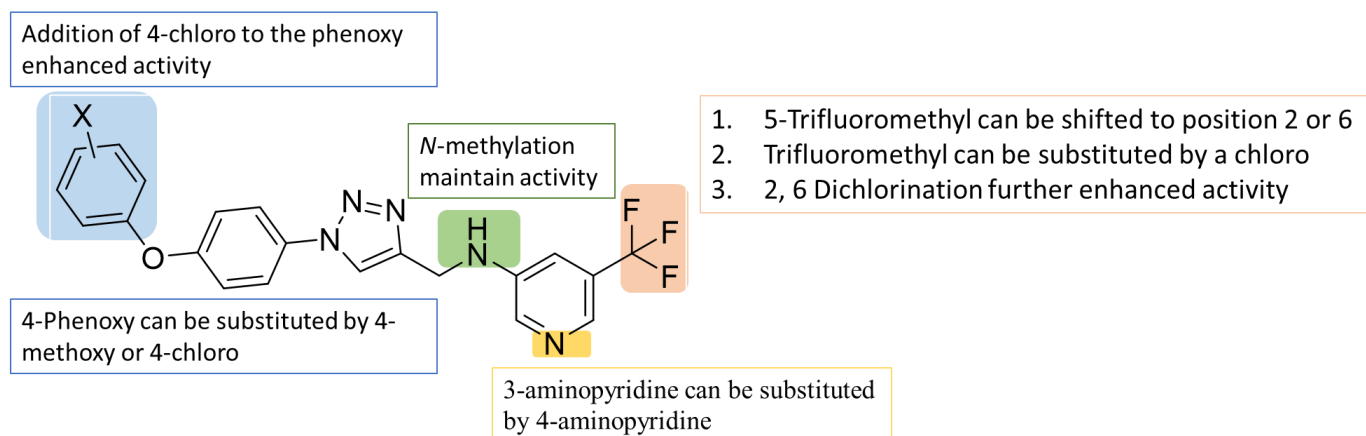
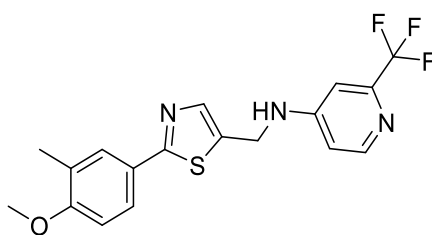


Figure 1: SAR summary of HIPS1298 similarities.

3.3.1.5.5 HIPS1396 similarities (*N*-Thiazolylmethylpyridine amines)

Out of the four tested compounds, two showed >50% inhibition, with **HIPS1333** showing 86% at 10 μ M. while the rest showed less than 30% inhibition (Table 7).

Table 7: HIPS1396 similarities



%inh@10 μ M:100, IC₅₀: 0.20 μ M

HIPS code	Structure	%inh@10 μ M	HIPS code	Structure	%inh@10 μ M
1333		86	1490		60.76
1336		12	1737		27.5

^aData shown are the mean of at least two independent experiments, SD \leq 10%.

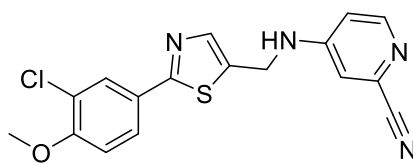
The SAR analysis of the screened compounds reveals key structural features that contribute to their activity against MurA. In this case, we are comparing the activity of compounds with different heterocyclic rings in place of the thiazole ring in the lead compound, **HIPS1396**.

The first heterocyclic ring to be evaluated was the pyridine ring in **HIPS1333**, which maintained the high level of activity seen in **HIPS1396**. Next, the isoxazole ring was evaluated as a replacement for the thiazole ring in **HIPS1490**. However, the resulting compound showed a decrease in activity. Finally, substituting the thiazole ring with benzoxazole in **HIPS1336** and oxadiazole in **HIPS1737** led to a huge loss of activity.

3.3.1.5.6 HIPS1500 similarities (Thiazolylmethylamino picolinonitriles)

Out of 63 tested compounds, no compound showed >70% inhibition with **HIPS1676** showed 68% MurA at 10 μ M, 18 compounds showed %inhibition in the range of 40–60% and the rest showed less than 40% inhibition (Table 8).

Table 8: HIPS1500 similarities



%inh@10 μ M: 95, IC₅₀: 0.96 μ M

HIPS code	Structure	%inh@10 μ M	HIPS code	Structure	%inh@10 μ M
1195		7	1487		19
1314		8	1488		22
1349		9	1489		14
1350		18	1495		11
1401		36	1496		n.i
1416		50	1505		12

Results and Discussion

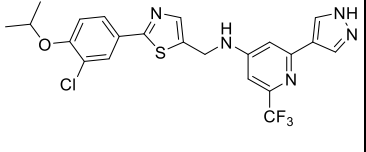
1419		41	1506		45
1420		14	1507		12
1421		23	1508		49
1440		13	1509		51
1454		9	1510		32
1455		22	1511		38
1456		36	1512		43

Results and Discussion

1457		24	1513		48
1458		27	1514		n.i
1459		25	1515		7
1460		31	1516		28
1461		39	1517		18
1462		49	1518		11
1475		50	1519		26
1476		38	1526		51
1477		33	1557		n.i

Results and Discussion

1478		21	1577		n.i
1479		54	1578		18
1480		39	1657		49
1481		44	1660		39
1482		42	1661		41
1483		37	1663		44
1484		35	1669		33
1485		29	1670		43
1486		13	1671		47

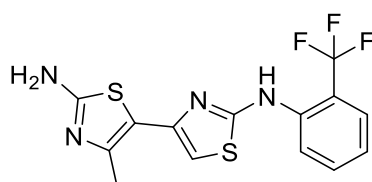
1676		68		
------	---	----	--	--

^aData shown are the mean of at least two independent experiments, SD ≤ 10%.

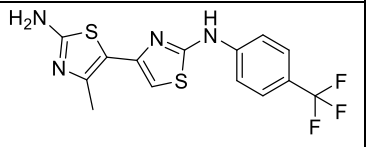
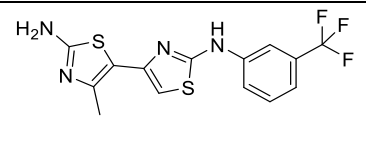
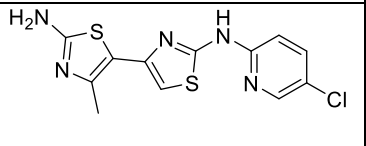
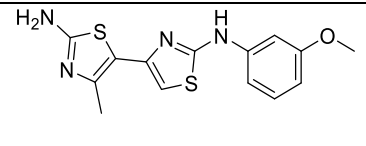
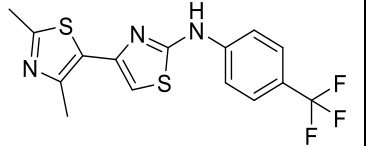
3.3.1.5.7 HIPS5346 similarities (Bithiazole diamines)

Out of 5 tested compounds, two showed >60% inhibition with **HIPS5349** showing 74% of MurA inhibition at 10 μM, two compounds showed around 50% inhibition and the last showed around 30% inhibition (Table 9).

Table 9: HIPS5346 similarities



%inh@10μM: 84, IC₅₀: 2.70 μM

HIPS code	Structure	%inh@10 μM	HIPS code	Structure	%inh@10 μM
5240		32	5348		62
5349		74	5352		50
5353		55			

^aData shown are the mean of at least two independent experiments, SD ≤ 10%.

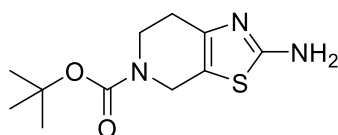
The SAR analysis of bithiazole diamine derivatives revealed the importance of the position and nature of the substituents on the phenyl ring. Comparison of **HIPS5346** with its analog **HIPS5348** showed that changing the position of the trifluoromethyl from *ortho* to *meta* maintained activity. However, changing the position of trifluoromethyl to *para* in **HIPS5240** led to a huge drop in activity. Substitution of the trifluoromethyl with a methoxy in **HIPS5352**

resulted in a slight decrease in activity, suggesting the importance of the electron-withdrawing character of the trifluoromethyl group. Replacement of the 2-amino group in **HIPS5240** with a 2-methyl group in **HIPS5353** led to an enhancement of activity. Finally, the replacement of the trifluoromethyl phenyl group with 5-chloropyridin-2-yl in **HIPS5349** showed an improvement in activity.

3.3.1.5.8 HIPS6888 similarities (Thiazolopyridine carboxylates)

Two out of the three tested compounds showed >80% inhibition with **HIPS6891** showing 94% of MurA inhibition at 10 μ M, one compound showed around 50% inhibition (Table 10).

Table 10: HIPS6888 similarities



%inh@10 μ M:87, IC₅₀: 0.84 μ M

HIPS code	Structure	%inh@10 μ M	HIPS code	Structure	%inh@10 μ M
6891		94	7020		79
7021		51			

^aData shown are the mean of at least two independent experiments, SD \leq 10%.

The SAR analysis of these compounds shows that removal of the *tert*-butyl carbonyl in (**HIPS6888**) to expose the ^{secondary} amine (**HIPS6891**) did not alter the activity. However, adding a 4-chlorobenzoyl (**HIPS7020**) or 4-methoxybenzoyl (**HIPS7021**), the activity decreased.

3.3.2 Conclusions and Future Prospects

In this study, we employed computational and *in vitro* methods to identify potential inhibitors of MurA and provide valuable insights into the SAR of several chemical families. The HIPS

library, consisting of 7000 compounds, was classified into 50 families using SwissSimilarity. From these families, 152 compounds were selected for primary screening to evaluate their activity against MurA. The compounds were filtered for their drug-likeness and physicochemical properties using SwissADME, which eliminated any compounds that deviated from Lipinski's rule and/or contained PAINS motifs to ensure that the compounds selected for screening were less likely to interfere with the assay and lead to false-positive results.

Out of the 152 compounds evaluated in the primary screening, 38 demonstrated significant inhibition activity (>80%) against MurA at 50 μ M and were classified as actives. 8 families were identified as hits after a second round of screening at a lower concentration of 20 μ M. The hits were further analyzed using SAR analysis, and their similarities were searched in the entire HIPS library using SwissSimilarity adjusted to 70% similarity.

A total of 149 molecules distributed over several families, such as "Nitrophenylbutylisindolinediones," "Benzamidobenzoic acids," "Thiazolymethylpyridine amines," and "Thiazolymethylamino picolinonitriles," were analyzed for their SAR.

Regarding the 2-methylsulfonyl-4-pyrimidinyl tetrazole family, SAR analysis revealed that compound **HIPS843**, which retained high inhibitory activity in the SAR analysis of Methylsulfonylpyrimidine tetrazoles, is a small molecule with low molecular weight and low logP. To further investigate the potential of this compound, we calculated the LE and LLE values, which were found to be 0.48 and 4.1, respectively.

Future Prospects

A priority for further research is to perform co-crystal analysis, which can provide valuable information for further medicinal chemistry efforts to improve the potency and selectivity of the compounds.

Additionally, evaluating the selectivity of the hits against other enzymes involved in bacterial cell wall biosynthesis, such as MurB, can determine their potential for dual action and improved antibacterial activity.

To ensure the safety of the compounds, *in vitro* studies should be carried out to assess their selectivity and toxicity before progressing to *in vivo* studies. This information can also provide

insights into the compounds' potency, which can be further evaluated by determining the IC₅₀ values for the hits.

Since **HIPS843** was identified as a promising lead compound with only two similar compounds in the HIPS library, further synthesis for this family could be beneficial for drug development.

Overall, the identification of potential inhibitors of MurA is an important step towards addressing the growing problem of antibiotic resistance. However, it will require continued research and development efforts, including co-crystal studies, selectivity evaluation, and toxicity assays, to optimize these compounds for clinical trials and the eventual development of new antibiotics.

3.3.3 Experimental

Expression of MurA

In Chapter 1, section 3.1.7.2, a detailed description of the protocol can be found.

MurA assay

In Chapter 1, section 3.1.7.2, a detailed description of the protocol can be found.

3.3.4 References

- (1) *Target 2035: probing the human proteome - PubMed*. <https://pubmed.ncbi.nlm.nih.gov/31278990/> (accessed 2023-01-07).
- (2) Guo, Z. [Strategy of molecular drug design: hits, leads and drug candidates]. *Yao Xue Xue Bao* **2008**, *43* (9), 898–904.
- (3) Kitchen, D. B.; Wolf, M. Hit-to-Lead in Drug Discovery. **2016**, *3* (3), 38–40.
- (4) Cotticelli, M. G.; Rasmussen, L.; Kushner, N. L.; McKellip, S.; Sosa, M. I.; Manouvakhova, A.; Feng, S.; White, E. L.; Maddry, J. A.; Heemskerk, J.; Oldt, R. J.; Surrey, L. F.; Ochs, R.; Wilson, R. B. Primary and Secondary Drug Screening Assays for Friedreich Ataxia. *J Biomol Screen* **2012**, *17* (3), 303–313. <https://doi.org/10.1177/1087057111427949>.
- (5) Swinney, D. C. Phenotypic vs. Target-Based Drug Discovery for First-in-Class Medicines. *Clin Pharmacol Ther* **2013**, *93* (4), 299–301. <https://doi.org/10.1038/clpt.2012.236>.
- (6) Brogard, J. M.; Jehl, F.; Willemin, B.; Lamalle, A. M.; Blickle, J. F.; Monteil, H. Clinical Pharmacokinetics of Cefotiam. *Clin Pharmacokinet* **1989**, *17* (3), 163–174. <https://doi.org/10.2165/00003088-198917030-00003>.
- (7) *Evaluation of Cefazolin, a New Cephalosporin Antibiotic | Antimicrobial Agents and Chemotherapy*. <https://journals.asm.org/doi/10.1128/AAC.3.4.488> (accessed 2023-04-16).
- (8) Das, D.; Sikdar, P.; Bairagi, M. Recent Developments of 2-Aminothiazoles in Medicinal Chemistry. *Eur J Med Chem* **2016**, *109*, 89–98. <https://doi.org/10.1016/j.ejmech.2015.12.022>.
- (9) Schultes, S.; de Graaf, C.; Haaksma, E. E. J.; de Esch, I. J. P.; Leurs, R.; Krämer, O. Ligand Efficiency as a Guide in Fragment Hit Selection and Optimization. *Drug Discovery Today: Technologies* **2010**, *7* (3), e157–e162. <https://doi.org/10.1016/j.ddtec.2010.11.003>.
- (10) Congreve, M.; Carr, R.; Murray, C.; Jhoti, H. A 'Rule of Three' for Fragment-Based Lead Discovery? *Drug Discovery Today* **2003**, *8* (19), 876–877. [https://doi.org/10.1016/S1359-6446\(03\)02831-9](https://doi.org/10.1016/S1359-6446(03)02831-9).

4. Summary and Future Outlook

This thesis focuses on the discovery and development of MurA inhibitors, which play a crucial role in antibacterial drug discovery. **Chapter 1** provides an overview of antibacterial drug discovery and highlights the MurA enzyme, with a particular emphasis on fosfomycin resistance. Recent developments in MurA inhibitors are also discussed.

Chapter 2 outlines the research objectives, including the scientific goal and the working strategy employed. The chapter describes the structural modification approach used for developing MurA inhibitors, as well as the utilization of computational and *in vitro* screening to identify potential inhibitors from the HIPS library.

Chapter 3 presents the results obtained from the research. In section **3.1**, the application of scaffold hopping from pyrazolidinone to imidazolidinone is described. A series of imidazolidinone-based MurA inhibitors is reported, which were developed through scaffold hopping. The optimized scaffold exhibited low logP values and potent inhibition of both wild-type MurA and the fosfomycin-resistant MurA C115D mutant. The newly developed compounds demonstrated promising IC₅₀ values, ranging from 0.534 to 0.881 μ M, for the most potent compounds. The scaffold-hopping approach allowed independent modifications of the rings, resulting in improved clogP values while maintaining high potency.

In section **3.2**, scaffold simplification of the imidazolidinone scaffold from section **3.1** is discussed. Triaryl malonamide derivatives were identified as open analogues of the imidazolidinone scaffold. The triaryl malonamide scaffold showed comparable inhibitory activities against both the MurA C115D mutant and the wild-type MurA enzymes. This simplified scaffold offered advantages in terms of synthesis scheme and clogP value.

Section **3.3** focuses on the application of computation and *in vitro* screening to identify potential MurA inhibitors. A total of 7000 compounds from the HIPS library were classified into 50 families using SwissSimilarity. Primary screening of 152 compounds resulted in 38 demonstrating significant inhibition activity against MurA. After a second round of screening, eight families were identified as hits. SAR analysis and similarity searching further characterized the hits. The potent hit, **HIPS843**, showed favorable properties for drug development and is considered a promising hit compound.

In conclusion, this thesis presents a comprehensive exploration of the discovery and development of MurA inhibitors. The research contributes to the understanding of MurA inhibition and offers potential candidates for further optimization and development of novel antibiotics to combat bacterial infections, including those caused by fosfomycin-resistant strains.

Future Outlook

1. Co-crystal Studies: Co-crystal studies can provide valuable information for further medicinal-chemistry efforts to improve the potency and selectivity of the MurA inhibitors. Understanding the structural details of the inhibitor–enzyme interaction can guide the design of more optimized compounds.
2. Toxicity and pharmacokinetic studies: To ensure the safety of the compounds, *in vitro* studies should be carried out to assess their selectivity and toxicity before progressing to *in vivo* studies. This information can also provide insights into the compounds' potency, which can be further evaluated by determining the IC₅₀ values. Additionally, conducting toxicity, pharmacokinetic, and pharmacodynamic studies will be crucial to assess the compounds' safety, absorption, distribution, metabolism, excretion, and efficacy *in vivo*.
3. *In vivo* evaluation and preclinical studies: To assess the therapeutic potential of MurA inhibitors, it is crucial to conduct *in vivo* evaluations and preclinical studies. Animal models can provide valuable insights into the efficacy, safety, and pharmacokinetics of the inhibitors. These studies can also help determine the optimal dosing regimens and evaluate the potential for toxicity or adverse effects, paving the way for future clinical trials.
4. Investigation of combination therapy and synergistic interactions: Investigating combination therapy with other antibiotics that have different modes of action can be an effective strategy for reducing the risk of resistance development. Exploring potential synergistic interactions between MurA inhibitors and other antibiotics could lead to the development of more effective treatments for bacterial infections. Studying the compounds in combination with other antibiotics against bacterial strains *in vitro* and *in vivo* can provide valuable insights into their synergistic effects and potential clinical applications.

Summary and Future Outlook

In conclusion, the outlook for MurA inhibitor research is promising, with opportunities for further optimization, mechanistic studies, *in vivo* evaluations. Co-crystal studies, toxicity assays, and pharmacokinetic studies are crucial for the development and optimization of MurA inhibitors. Additionally, investigating synergistic interactions, can enhance the effectiveness of these compounds in combating bacterial infections. Continued research efforts in these areas have the potential to advance antibacterial drug discovery and address the urgent need for new antibiotics.

5. References

- (1) Woese, C. R.; Kandler, O.; Wheelis, M. L. Towards a Natural System of Organisms: Proposal for the Domains Archaea, Bacteria, and Eucarya. *Proc Natl Acad Sci U S A* **1990**, *87* (12), 4576–4579. <https://doi.org/10.1073/pnas.87.12.4576>.
- (2) Sender, R.; Fuchs, S.; Milo, R. Revised Estimates for the Number of Human and Bacteria Cells in the Body. *PLOS Biology* **2016**, *14* (8), e1002533. <https://doi.org/10.1371/journal.pbio.1002533>.
- (3) Donia, M. S.; Fischbach, M. A. HUMAN MICROBIOTA. Small Molecules from the Human Microbiota. *Science* **2015**, *349* (6246), 1254766. <https://doi.org/10.1126/science.1254766>.
- (4) Cook, M.; Molto, E.; Anderson, C. Fluorochrome Labelling in Roman Period Skeletons from Dakhleh Oasis, Egypt. *Am J Phys Anthropol* **1989**, *80* (2), 137–143. <https://doi.org/10.1002/ajpa.1330800202>.
- (5) Aminov, R. A Brief History of the Antibiotic Era: Lessons Learned and Challenges for the Future. *Frontiers in Microbiology* **2010**, *1*.
- (6) Rachakonda, S.; Cartee, L. Challenges in Antimicrobial Drug Discovery and the Potential of Nucleoside Antibiotics. *Curr Med Chem* **2004**, *11* (6), 775–793. <https://doi.org/10.2174/0929867043455774>.
- (7) Schentag, J. J. Correlation of Pharmacokinetic Parameters to Efficacy of Antibiotics: Relationships between Serum Concentrations, MIC Values, and Bacterial Eradication in Patients with Gram-Negative Pneumonia. *Scand J Infect Dis Suppl* **1990**, *74*, 218–234.
- (8) Sefton, A. M. Mechanisms of Antimicrobial Resistance: Their Clinical Relevance in the New Millennium. *Drugs* **2002**, *62* (4), 557–566. <https://doi.org/10.2165/00003495-200262040-00001>.
- (9) Fleming, A. On the Antibacterial Action of Cultures of a Penicillium, with Special Reference to Their Use in the Isolation of B. Influenzæ. *Br J Exp Pathol* **1929**, *10* (3), 226–236.
- (10) Adedeji, W. A. THE TREASURE CALLED ANTIBIOTICS. *Ann Ib Postgrad Med* **2016**, *14* (2), 56–57.
- (11) Ligon, B. L. Penicillin: Its Discovery and Early Development. *Seminars in Pediatric Infectious Diseases* **2004**, *15* (1), 52–57. <https://doi.org/10.1053/j.spid.2004.02.001>.
- (12) Lewis, K. Platforms for Antibiotic Discovery. *Nat Rev Drug Discov* **2013**, *12* (5), 371–387. <https://doi.org/10.1038/nrd3975>.
- (13) Singh, V.; Haque, S.; Singh, H.; Verma, J.; Vibha, K.; Singh, R.; Jawed, A.; Tripathi, C. K. M. Isolation, Screening, and Identification of Novel Isolates of Actinomycetes from India for Antimicrobial Applications. *Front Microbiol* **2016**, *7*, 1921. <https://doi.org/10.3389/fmicb.2016.01921>.
- (14) National Nosocomial Infections Surveillance (NNIS) Report, Data Summary from October 1986-April 1996, Issued May 1996. A Report from the National Nosocomial Infections Surveillance (NNIS) System. *Am J Infect Control* **1996**, *24* (5), 380–388.
- (15) Dancer, S. J. The Problem with Cephalosporins. *J Antimicrob Chemother* **2001**, *48* (4), 463–478. <https://doi.org/10.1093/jac/48.4.463>.
- (16) Armstrong, G. L.; Conn, L. A.; Pinner, R. W. Trends in Infectious Disease Mortality in the United States during the 20th Century. *JAMA* **1999**, *281* (1), 61–66. <https://doi.org/10.1001/jama.281.1.61>.
- (17) Lobanovska, M.; Pilla, G. Penicillin's Discovery and Antibiotic Resistance: Lessons for the Future? *Yale J Biol Med* **2017**, *90* (1), 135–145.
- (18) Institute of Medicine (US) Committee on Emerging Microbial Threats to Health in the 21st Century. *Microbial Threats to Health: Emergence, Detection, and Response*; Smolinski, M. S., Hamburg, M. A., Lederberg, J., Eds.; National Academies Press (US): Washington (DC), 2003.
- (19) Walsh, C. T.; Wencewicz, T. A. Prospects for New Antibiotics: A Molecule-Centered Perspective. *J Antibiot (Tokyo)* **2014**, *67* (1), 7–22. <https://doi.org/10.1038/ja.2013.49>.
- (20) Abraham, E. P.; Chain, E. An Enzyme from Bacteria Able to Destroy Penicillin. *Nature* **1940**, *146* (3713), 837–837. <https://doi.org/10.1038/146837a0>.
- (21) *Mechanisms of Antibiotic Resistance - PubMed*. <https://pubmed.ncbi.nlm.nih.gov/27227291/> (accessed 2022-09-26).
- (22) *Addressing the Antibiotic Resistance Problem with Probiotics: Reducing the Risk of Its Double-Edged Sword Effect - PubMed*. <https://pubmed.ncbi.nlm.nih.gov/28018315/> (accessed 2022-09-26).
- (23) 2019 Summary Report On Antimicrobials Sold or Distributed for Use in Food-Producing Animals. 49.
- (24) Martin, M. J.; Thottathil, S. E.; Newman, T. B. Antibiotics Overuse in Animal Agriculture: A Call to Action for Health Care Providers. *Am J Public Health* **2015**, *105* (12), 2409–2410. <https://doi.org/10.2105/ajph.2015.302870>.
- (25) Theuretzbacher, U. Future Antibiotics Scenarios: Is the Tide Starting to Turn? *Int J Antimicrob Agents* **2009**, *34* (1), 15–20. <https://doi.org/10.1016/j.ijantimicag.2009.02.005>.
- (26) Theuretzbacher, U. Resistance Drives Antibacterial Drug Development. *Current Opinion in Pharmacology* **2011**, *11* (5), 433–438. <https://doi.org/10.1016/j.coph.2011.07.008>.

- (27) Piddock, L. J. V. The Crisis of No New Antibiotics--What Is the Way Forward? *Lancet Infect Dis* **2012**, *12* (3), 249–253. [https://doi.org/10.1016/S1473-3099\(11\)70316-4](https://doi.org/10.1016/S1473-3099(11)70316-4).
- (28) *The crisis of no new antibiotics--what is the way forward?* - PubMed. <https://pubmed.ncbi.nlm.nih.gov/22101066/> (accessed 2022-09-26).
- (29) Ventola, C. L. The Antibiotic Resistance Crisis: Part 1: Causes and Threats. *PT* **2015**, *40* (4), 277–283.
- (30) Yoneyama, H.; Katsumata, R. Antibiotic Resistance in Bacteria and Its Future for Novel Antibiotic Development. *Biosci Biotechnol Biochem* **2006**, *70* (5), 1060–1075. <https://doi.org/10.1271/bbb.70.1060>.
- (31) Nikaido, H. Molecular Basis of Bacterial Outer Membrane Permeability Revisited. *Microbiol Mol Biol Rev* **2003**, *67* (4), 593–656. <https://doi.org/10.1128/MMBR.67.4.593-656.2003>.
- (32) Blair, J. M. A.; Webber, M. A.; Baylay, A. J.; Ogbolu, D. O.; Piddock, L. J. V. Molecular Mechanisms of Antibiotic Resistance. *Nat Rev Microbiol* **2015**, *13* (1), 42–51. <https://doi.org/10.1038/nrmicro3380>.
- (33) Putman, M.; van Veen, H. W.; Konings, W. N. Molecular Properties of Bacterial Multidrug Transporters. *Microbiol Mol Biol Rev* **2000**, *64* (4), 672–693. <https://doi.org/10.1128/MMBR.64.4.672-693.2000>.
- (34) Nakashima, R.; Sakurai, K.; Yamasaki, S.; Nishino, K.; Yamaguchi, A. Structures of the Multidrug Exporter AcrB Reveal a Proximal Multisite Drug-Binding Pocket. *Nature* **2011**, *480* (7378), 565–569. <https://doi.org/10.1038/nature10641>.
- (35) Alekshun, M. N.; Levy, S. B. Regulation of Chromosomally Mediated Multiple Antibiotic Resistance: The Mar Regulon. *Antimicrob Agents Chemother* **1997**, *41* (10), 2067–2075. <https://doi.org/10.1128/AAC.41.10.2067>.
- (36) Pomposiello, P. J.; Bennik, M. H.; Demple, B. Genome-Wide Transcriptional Profiling of the Escherichia Coli Responses to Superoxide Stress and Sodium Salicylate. *J Bacteriol* **2001**, *183* (13), 3890–3902. <https://doi.org/10.1128/JB.183.13.3890-3902.2001>.
- (37) Walsh, C. Molecular Mechanisms That Confer Antibacterial Drug Resistance. *Nature* **2000**, *406* (6797), 775–781. <https://doi.org/10.1038/35021219>.
- (38) Spratt, B. G. Resistance to Antibiotics Mediated by Target Alterations. *Science* **1994**, *264* (5157), 388–393. <https://doi.org/10.1126/science.8153626>.
- (39) Weisblum, B. Erythromycin Resistance by Ribosome Modification. *Antimicrob Agents Chemother* **1995**, *39* (3), 577–585. <https://doi.org/10.1128/AAC.39.3.577>.
- (40) Vetting, M. W.; Hegde, S. S.; Wang, M.; Jacoby, G. A.; Hooper, D. C.; Blanchard, J. S. Structure of QnrB1, a Plasmid-Mediated Fluoroquinolone Resistance Factor. *J Biol Chem* **2011**, *286* (28), 25265–25273. <https://doi.org/10.1074/jbc.M111.226936>.
- (41) Chopra, I. Molecular Mechanisms Involved in the Transport of Antibiotics into Bacteria. *Parasitology* **1988**, *96 Suppl*, S25-44. <https://doi.org/10.1017/s0031182000085966>.
- (42) Smith, J. T.; Amyes, S. G. Bacterial Resistance to Antifolate Chemotherapeutic Agents Mediated by Plasmids. *Br Med Bull* **1984**, *40* (1), 42–46. <https://doi.org/10.1093/oxfordjournals.bmb.a071946>.
- (43) Spratt, B. G. Antibiotic Resistance: Counting the Cost. *Curr Biol* **1996**, *6* (10), 1219–1221. [https://doi.org/10.1016/s0960-9822\(96\)00700-2](https://doi.org/10.1016/s0960-9822(96)00700-2).
- (44) Lenski, R. E.; Nguyen, T. T. Stability of Recombinant DNA and Its Effects on Fitness. *Trends Ecol Evol* **1988**, *3* (4), S18-20. [https://doi.org/10.1016/0169-5347\(88\)90132-2](https://doi.org/10.1016/0169-5347(88)90132-2).
- (45) Andersson, D. I.; Hughes, D. Antibiotic Resistance and Its Cost: Is It Possible to Reverse Resistance? *Nat Rev Microbiol* **2010**, *8* (4), 260–271. <https://doi.org/10.1038/nrmicro2319>.
- (46) Melnyk, A. H.; Wong, A.; Kassen, R. The Fitness Costs of Antibiotic Resistance Mutations. *Evolutionary Applications* **2015**, *8* (3), 273–283. <https://doi.org/10.1111/eva.12196>.
- (47) *Compensatory evolution in rifampin-resistant Escherichia coli* - PubMed. <https://pubmed.ncbi.nlm.nih.gov/11102350/> (accessed 2023-04-14).
- (48) Andersson, D. I. The Biological Cost of Mutational Antibiotic Resistance: Any Practical Conclusions? *Curr Opin Microbiol* **2006**, *9* (5), 461–465. <https://doi.org/10.1016/j.mib.2006.07.002>.
- (49) Projan, S. J.; Shlaes, D. M. Antibacterial Drug Discovery: Is It All Downhill from Here? *Clin Microbiol Infect* **2004**, *10 Suppl 4*, 18–22. <https://doi.org/10.1111/j.1465-0691.2004.1006.x>.
- (50) Spellberg, B.; Powers, J. H.; Brass, E. P.; Miller, L. G.; Edwards, J. E. Trends in Antimicrobial Drug Development: Implications for the Future. *Clin Infect Dis* **2004**, *38* (9), 1279–1286. <https://doi.org/10.1086/420937>.
- (51) DiMasi, J. A.; Grabowski, H. G.; Hansen, R. W. Innovation in the Pharmaceutical Industry: New Estimates of R&D Costs. *J Health Econ* **2016**, *47*, 20–33. <https://doi.org/10.1016/j.jhealeco.2016.01.012>.
- (52) Mehl, B.; Santell, J. Projecting Future Drug Expenditures--2001. *Am J Health Syst Pharm* **2001**, *58* (2), 125–133. <https://doi.org/10.1093/ajhp/58.2.125>.
- (53) *A Comparative Study on the Cost of New Antibiotics and Drugs of Other Therapeutic Categories* | PLOS ONE. <https://journals.plos.org/plosone/article?id=10.1371/journal.pone.0000011> (accessed 2022-09-26).
- (54) *The price of innovation: new estimates of drug development costs* - PubMed. <https://pubmed.ncbi.nlm.nih.gov/12606142/> (accessed 2022-09-26).

- (55) Peck, C. C. Drug Development: Improving the Process. *Food & Drug L.J.* **1997**, *52*, 163.
- (56) Tipper, D. J.; Strominger, J. L. Mechanism of Action of Penicillins: A Proposal Based on Their Structural Similarity to Acyl-D-Alanyl-D-Alanine. *Proc Natl Acad Sci U S A* **1965**, *54* (4), 1133–1141.
- (57) *How antibiotics kill bacteria: from targets to networks* - PubMed. <https://pubmed.ncbi.nlm.nih.gov/20440275/> (accessed 2023-04-22).
- (58) Murakami, K. S.; Darst, S. A. Bacterial RNA Polymerases: The Whole Story. *Current Opinion in Structural Biology* **2003**, *13* (1), 31–39. [https://doi.org/10.1016/S0959-440X\(02\)00005-2](https://doi.org/10.1016/S0959-440X(02)00005-2).
- (59) Feklistov, A.; Mekler, V.; Jiang, Q.; Westblade, L. F.; Irschik, H.; Jansen, R.; Mustaev, A.; Darst, S. A.; Ebright, R. H. Rifamycins Do Not Function by Allosteric Modulation of Binding of Mg²⁺ to the RNA Polymerase Active Center. *Proc Natl Acad Sci U S A* **2008**, *105* (39), 14820–14825. <https://doi.org/10.1073/pnas.0802822105>.
- (60) Ward, J. B. Biosynthesis of Peptidoglycan: Points of Attack by Wall Inhibitors. *Pharmacol Ther* **1984**, *25* (3), 327–369. [https://doi.org/10.1016/0163-7258\(84\)90004-4](https://doi.org/10.1016/0163-7258(84)90004-4).
- (61) Schumann, P. 5 - Peptidoglycan Structure. In *Methods in Microbiology*; Rainey, F., Oren, A., Eds.; Taxonomy of Prokaryotes; Academic Press, 2011; Vol. 38, pp 101–129. <https://doi.org/10.1016/B978-0-12-387730-7.00005-X>.
- (62) Egan, A. J. F.; Biboy, J.; van't Veer, I.; Breukink, E.; Vollmer, W. Activities and Regulation of Peptidoglycan Synthases. *Philos Trans R Soc Lond B Biol Sci* **2015**, *370* (1679), 20150031. <https://doi.org/10.1098/rstb.2015.0031>.
- (63) Heijenoort, J. van. Recent Advances in the Formation of the Bacterial Peptidoglycan Monomer Unit. *Nat. Prod. Rep.* **2001**, *18* (5), 503–519. <https://doi.org/10.1039/A804532A>.
- (64) Bouhss, A.; Trunkfield, A. E.; Bugg, T. D. H.; Mengin-Lecreulx, D. The Biosynthesis of Peptidoglycan Lipid-Linked Intermediates. *FEMS Microbiol Rev* **2008**, *32* (2), 208–233. <https://doi.org/10.1111/j.1574-6976.2007.00089.x>.
- (65) Chattaway, F. W. Microbial Cell Walls and Membranes: By H J Rogers, H R Perkins and J B Ward. Pp 564. Chapman & Hall, London. 1980 £30. ISBN 0-412-12030-5. *Biochemical Education* **1982**, *10* (1), 33–33. [https://doi.org/10.1016/0307-4412\(82\)90023-1](https://doi.org/10.1016/0307-4412(82)90023-1).
- (66) Goodell, E. W.; Schwarz, U. Release of Cell Wall Peptides into Culture Medium by Exponentially Growing Escherichia Coli. *J Bacteriol* **1985**, *162* (1), 391–397. <https://doi.org/10.1128/jb.162.1.391-397.1985>.
- (67) Young, K. D. Bacterial Shape. *Mol Microbiol* **2003**, *49* (3), 571–580. <https://doi.org/10.1046/j.1365-2958.2003.03607.x>.
- (68) Schleifer, K. H.; Kandler, O. Peptidoglycan Types of Bacterial Cell Walls and Their Taxonomic Implications. *Bacteriol Rev* **1972**, *36* (4), 407–477. <https://doi.org/10.1128/br.36.4.407-477.1972>.
- (69) Hogan, D.; Kolter, R. Why Are Bacteria Refractory to Antimicrobials? *Curr Opin Microbiol* **2002**, *5* (5), 472–477. [https://doi.org/10.1016/s1369-5274\(02\)00357-0](https://doi.org/10.1016/s1369-5274(02)00357-0).
- (70) Shah, N. Reversing Resistance: The next Generation Antibacterials. *Indian Journal of Pharmacology* **2015**, *47*, 248. <https://doi.org/10.4103/0253-7613.157109>.
- (71) Fleming, A. Classics in Infectious Diseases: On the Antibacterial Action of Cultures of a Penicillium, with Special Reference to Their Use in the Isolation of B. Influenzae by Alexander Fleming, Reprinted from the British Journal of Experimental Pathology 10:226-236, 1929. *Rev Infect Dis* **1980**, *2* (1), 129–139.
- (72) Salton, M. R. J.; Horne, R. W. Studies of the Bacterial Cell Wall. II. Methods of Preparation and Some Properties of Cell Walls. *Biochim Biophys Acta* **1951**, *7* (2), 177–197. [https://doi.org/10.1016/0006-3002\(51\)90017-0](https://doi.org/10.1016/0006-3002(51)90017-0).
- (73) Anderson, J. S.; Matsushashi, M.; Haskin, M. A.; Strominger, J. L. Biosynthesis of the Peptidoglycan of Bacterial Cell Walls. II. Phospholipid Carriers in the Reaction Sequence. *J Biol Chem* **1967**, *242* (13), 3180–3190.
- (74) Izaki, K.; Matsushashi, M.; Strominger, J. L. Glycopeptide Transpeptidase and D-Alanine Carboxypeptidase: Penicillin-Sensitive Enzymatic Reactions. *Proc Natl Acad Sci USA* **1966**, *55* (3), 656–663. <https://doi.org/10.1073/pnas.55.3.656>.
- (75) Tiyanont, K.; Doan, T.; Lazarus, M. B.; Fang, X.; Rudner, D. Z.; Walker, S. Imaging Peptidoglycan Biosynthesis in Bacillus Subtilis with Fluorescent Antibiotics. *Proc Natl Acad Sci U S A* **2006**, *103* (29), 11033–11038. <https://doi.org/10.1073/pnas.0600829103>.
- (76) Bugg, T. D.; Walsh, C. T. Intracellular Steps of Bacterial Cell Wall Peptidoglycan Biosynthesis: Enzymology, Antibiotics, and Antibiotic Resistance. *Nat Prod Rep* **1992**, *9* (3), 199–215. <https://doi.org/10.1039/np9920900199>.
- (77) Mengin-Lecreulx, D.; Heijenoort, J. van. Characterization of the Essential Gene GlmM Encoding Phosphoglucosamine Mutase in Escherichia Coli(*). *Journal of Biological Chemistry* **1996**, *271* (1), 32–39. <https://doi.org/10.1074/jbc.271.1.32>.

- (78) Shinde, Y.; Ahmad, I.; Surana, S.; Patel, H. The Mur Enzymes Chink in the Armour of Mycobacterium Tuberculosis Cell Wall. *European Journal of Medicinal Chemistry* **2021**, *222*, 113568. <https://doi.org/10.1016/j.ejmech.2021.113568>.
- (79) Sidiq, K.; Sabir, D.; Salih, R.; Nasir, T. Insights into the Evolutionary Origin of Mycoplasma Species. **2020**, *4*, 68–85. <https://doi.org/10.22034/HBB.2020.06>.
- (80) Schneider, T.; Sahl, H.-G. An Oldie but a Goodie - Cell Wall Biosynthesis as Antibiotic Target Pathway. *Int J Med Microbiol* **2010**, *300* (2–3), 161–169. <https://doi.org/10.1016/j.ijmm.2009.10.005>.
- (81) Hrast, M.; Sosič, I.; Sink, R.; Gobec, S. Inhibitors of the Peptidoglycan Biosynthesis Enzymes MurA-F. *Bioorganic chemistry* **2014**, *55*. <https://doi.org/10.1016/j.bioorg.2014.03.008>.
- (82) Maitra, A.; Munshi, T.; Healy, J.; Martin, L. T.; Vollmer, W.; Keep, N. H.; Bhakta, S. Cell Wall Peptidoglycan in Mycobacterium Tuberculosis: An Achilles' Heel for the TB-Causing Pathogen. *FEMS Microbiol Rev* **2019**, *43* (5), 548–575. <https://doi.org/10.1093/femsre/fuz016>.
- (83) De Smet, K. A. L.; Kempell, K. E.; Gallagher, A.; Duncan, K.; Young, D. B. Alteration of a Single Amino Acid Residue Reverses Fosfomycin Resistance of Recombinant MurA from Mycobacterium Tuberculosis. *Microbiology (Reading)* **1999**, *145* (Pt 11), 3177–3184. <https://doi.org/10.1099/00221287-145-11-3177>.
- (84) Xu, L.; Wu, D.; Liu, L.; Zheng, Q.; Song, Y.; Ye, L.; Sha, S.; Kang, J.; Xin, Y.; Ma, Y. Characterization of Mycobacterial UDP-N-Acetylglucosamine Enolpyruvyle Transferase (MurA). *Res Microbiol* **2014**, *165* (2), 91–101. <https://doi.org/10.1016/j.resmic.2014.01.004>.
- (85) Kumar, P.; Saumya, K. U.; Giri, R. Identification of Peptidomimetic Compounds as Potential Inhibitors against MurA Enzyme of *Mycobacterium Tuberculosis*. *J Biomol Struct Dyn* **2020**, *38* (17), 4997–5013. <https://doi.org/10.1080/07391102.2019.1696231>.
- (86) Moraes, G. L.; Gomes, G. C.; Sousa, P. R. M. D.; Alves, C. N.; Govender, T.; Kruger, H. G.; Maguire, G. E. M.; Lamichhane, G.; Lameira, J. Structural and Functional Features of Enzymes of Mycobacterium Tuberculosis Peptidoglycan Biosynthesis as Targets for Drug Development. *Bulletin of the International Union Against Tuberculosis and Lung Disease* **2015**, *95* (2), 95–111. <https://doi.org/10.1016/j.tube.2015.01.006>.
- (87) *Structure of UDP-N-acetylglucosamine enolpyruvyl transferase, an enzyme essential for the synthesis of bacterial peptidoglycan, complexed with substrate UDP-N-acetylglucosamine and the drug fosfomycin - PubMed*. <https://pubmed.ncbi.nlm.nih.gov/8994972/> (accessed 2023-05-15).
- (88) Benson, T. E.; Marquardt, J. L.; Marquardt, A. C.; Etzkorn, F. A.; Walsh, C. T. Overexpression, Purification, and Mechanistic Study of UDP-N-Acetylenolpyruvylglucosamine Reductase. *Biochemistry* **1993**, *32* (8), 2024–2030. <https://doi.org/10.1021/bi00059a019>.
- (89) Benson, T. E.; Walsh, C. T.; Hogle, J. M. The Structure of the Substrate-Free Form of MurB, an Essential Enzyme for the Synthesis of Bacterial Cell Walls. *Structure* **1996**, *4* (1), 47–54. [https://doi.org/10.1016/S0969-2126\(96\)00008-1](https://doi.org/10.1016/S0969-2126(96)00008-1).
- (90) Mol, C. D.; Brooun, A.; Dougan, D. R.; Hilgers, M. T.; Tari, L. W.; Wijnands, R. A.; Knuth, M. W.; McRee, D. E.; Swanson, R. V. Crystal Structures of Active Fully Assembled Substrate- and Product-Bound Complexes of UDP-N-Acetylmuramic Acid:L-Alanine Ligase (MurC) from Haemophilus Influenzae. *J Bacteriol* **2003**, *185* (14), 4152–4162. <https://doi.org/10.1128/JB.185.14.4152-4162.2003>.
- (91) Bertrand, J. A.; Auger, G.; Fanchon, E.; Martin, L.; Blanot, D.; van Heijenoort, J.; Dideberg, O. Crystal Structure of UDP-N-Acetylmuramoyl-L-Alanine:D-Glutamate Ligase from Escherichia Coli. *EMBO J* **1997**, *16* (12), 3416–3425. <https://doi.org/10.1093/emboj/16.12.3416>.
- (92) Kouidmi, I.; Levesque, R. C.; Paradis-Bleau, C. The Biology of Mur Ligases as an Antibacterial Target. *Molecular Microbiology* **2014**, *94* (2), 242–253. <https://doi.org/10.1111/mmi.12758>.
- (93) Basavannacharya, C.; Robertson, G.; Munshi, T.; Keep, N. H.; Bhakta, S. ATP-Dependent MurE Ligase in Mycobacterium Tuberculosis: Biochemical and Structural Characterisation. *Tuberculosis* **2010**, *90* (1), 16–24. <https://doi.org/10.1016/j.tube.2009.10.007>.
- (94) Silhavy, T. J.; Kahne, D.; Walker, S. The Bacterial Cell Envelope. *Cold Spring Harb Perspect Biol* **2010**, *2* (5), a000414. <https://doi.org/10.1101/cshperspect.a000414>.
- (95) Healy, V. L.; Lessard, I. A.; Roper, D. I.; Knox, J. R.; Walsh, C. T. Vancomycin Resistance in Enterococci: Reprogramming of the d-Ala-d-Ala Ligases in Bacterial Peptidoglycan Biosynthesis. *Chemistry & Biology* **2000**, *7* (5), R109–R119. [https://doi.org/10.1016/S1074-5521\(00\)00116-2](https://doi.org/10.1016/S1074-5521(00)00116-2).
- (96) Lovering, A. L.; de Castro, L. H.; Lim, D.; Strynadka, N. C. J. Structural Insight into the Transglycosylation Step of Bacterial Cell-Wall Biosynthesis. *Science* **2007**, *315* (5817), 1402–1405. <https://doi.org/10.1126/science.1136611>.
- (97) Huang, C.-Y.; Shih, H.-W.; Lin, L.-Y.; Tien, Y.-W.; Cheng, T.-J. R.; Cheng, W.-C.; Wong, C.-H.; Ma, C. Crystal Structure of Staphylococcus Aureus Transglycosylase in Complex with a Lipid II Analog and Elucidation of Peptidoglycan Synthesis Mechanism. *Proc Natl Acad Sci U S A* **2012**, *109* (17), 6496–6501. <https://doi.org/10.1073/pnas.1203900109>.

- (98) Sobhanifar, S.; King, D. T.; Strynadka, N. C. J. Fortifying the Wall: Synthesis, Regulation and Degradation of Bacterial Peptidoglycan. *Curr Opin Struct Biol* **2013**, *23* (5), 695–703. <https://doi.org/10.1016/j.sbi.2013.07.008>.
- (99) Hendlin, D.; Stapley, E. O.; Jackson, M.; Wallick, H.; Miller, A. K.; Wolf, F. J.; Miller, T. W.; Chaiet, L.; Kahan, F. M.; Foltz, E. L.; Woodruff, H. B.; Mata, J. M.; Hernandez, S.; Mochales, S. Phosphonomycin, a New Antibiotic Produced by Strains of *Streptomyces*. *Science* **1969**, *166* (3901), 122–123. <https://doi.org/10.1126/science.166.3901.122>.
- (100) Docobo-Pérez, F.; Drusano, G. L.; Johnson, A.; Goodwin, J.; Whalley, S.; Ramos-Martín, V.; Ballesterotellez, M.; Rodríguez-Martínez, J. M.; Conejo, M. C.; van Guilder, M.; Rodríguez-Baño, J.; Pascual, A.; Hope, W. W. Pharmacodynamics of Fosfomycin: Insights into Clinical Use for Antimicrobial Resistance. *Antimicrob Agents Chemother* **2015**, *59* (9), 5602–5610. <https://doi.org/10.1128/AAC.00752-15>.
- (101) Picozzi, S. C. M.; Casellato, S.; Rossini, M.; Paola, G.; Tejada, M.; Costa, E.; Carmignani, L. Extended-Spectrum Beta-Lactamase-Positive *Escherichia Coli* Causing Complicated Upper Urinary Tract Infection: Urologist Should Act in Time. *Urology Annals* **2014**, *6* (2), 107–112. <https://doi.org/10.4103/0974-7796.130536>.
- (102) Dijkmans, A. C.; Zacarías, N. V. O.; Burggraaf, J.; Mouton, J. W.; Wilms, E. B.; van Nieuwkoop, C.; Touw, D. J.; Stevens, J.; Stevens, J.; Kamerling, I. M. C. Fosfomycin: Pharmacological, Clinical and Future Perspectives. *Antibiotics (Basel)* **2017**, *6* (4), E24. <https://doi.org/10.3390/antibiotics6040024>.
- (103) Guo, Y.; Tomich, A. D.; McElheny, C. L.; Cooper, V. S.; Tait-Kamradt, A.; Wang, M.; Hu, F.; Rice, L. B.; Sluis-Cremer, N.; Doi, Y. High-Level Fosfomycin Resistance in Vancomycin-Resistant *Enterococcus Faecium*. *Emerg Infect Dis* **2017**, *23* (11), 1902–1904. <https://doi.org/10.3201/eid2311.171130>.
- (104) Musmade, D.; Patil, P.; Aher, S.; Ware, A. INDO AMERICAN JOURNAL OF PHARMACEUTICAL RESEARCH MUR-A: A CRITICAL TARGET BEHIND NEW ANTIBACTERIAL DRUG DISCOVERY. *indoamerican journal of pharmaceutical research* **2013**.
- (105) *Intravenous fosfomycin for the treatment of nosocomial infections caused by carbapenem-resistant Klebsiella pneumoniae in critically ill patients: a prospective evaluation - ScienceDirect*. <https://www.sciencedirect.com/science/article/pii/S1198743X14615445> (accessed 2022-10-16).
- (106) Xu, Y. J.; Quan, J. J.; Shi, K. R.; Yu, Y. S. [Mechanisms of fosfomycin resistance of extended-spectrum β -lactamases-producing *Escherichia coli* and *Klebsiella pneumoniae*]. *Zhonghua Yi Xue Za Zhi* **2018**, *98* (2), 122–126. <https://doi.org/10.3760/cma.j.issn.0376-2491.2018.02.010>.
- (107) Patel, B.; Patel, K.; Shetty, A.; Soman, R.; Rodrigues, C. Fosfomycin Susceptibility in Urinary Tract Enterobacteriaceae. *J Assoc Physicians India* **2017**, *65* (9), 14–16.
- (108) Falagas, M. E.; Vouloumanou, E. K.; Samonis, G.; Vardakas, K. Z. Fosfomycin. *Clin Microbiol Rev* **2016**, *29* (2), 321–347. <https://doi.org/10.1128/CMR.00068-15>.
- (109) *Fosfomycin suppresses RS-virus-induced Streptococcus pneumoniae and Haemophilus influenzae adhesion to respiratory epithelial cells via the platelet-activating factor receptor - PMC*. <https://www.ncbi.nlm.nih.gov/pmc/articles/PMC7110074/> (accessed 2023-05-15).
- (110) Falagas, M. E.; Athanasaki, F.; Voulgaris, G. L.; Triarides, N. A.; Vardakas, K. Z. Resistance to Fosfomycin: Mechanisms, Frequency and Clinical Consequences. *Int J Antimicrob Agents* **2019**, *53* (1), 22–28. <https://doi.org/10.1016/j.ijantimicag.2018.09.013>.
- (111) Kumar, S.; Parvathi, A.; Hernandez, R. L.; Cadle, K. M.; Varela, M. F. Identification of a Novel UDP-N-Acetylglucosamine Enolpyruvyl Transferase (MurA) from *Vibrio Fischeri* That Confers High Fosfomycin Resistance in *Escherichia Coli*. *Arch Microbiol* **2009**, *191* (5), 425–429. <https://doi.org/10.1007/s00203-009-0468-9>.
- (112) Gisin, J.; Schneider, A.; Nägele, B.; Borisova, M.; Mayer, C. A Cell Wall Recycling Shortcut That Bypasses Peptidoglycan de Novo Biosynthesis. *Nat Chem Biol* **2013**, *9* (8), 491–493. <https://doi.org/10.1038/nchembio.1289>.
- (113) Borisova, M.; Gisin, J.; Mayer, C. Blocking Peptidoglycan Recycling in *Pseudomonas Aeruginosa* Attenuates Intrinsic Resistance to Fosfomycin. *Microb Drug Resist* **2014**, *20* (3), 231–237. <https://doi.org/10.1089/mdr.2014.0036>.
- (114) Scorti, M.; Lacharme-Lora, L.; Wagner, M.; Chico-Calero, I.; Losito, P.; Vázquez-Boland, J. A. Coexpression of Virulence and Fosfomycin Susceptibility in *Listeria*: Molecular Basis of an Antimicrobial in Vitro-in Vivo Paradox. *Nat Med* **2006**, *12* (5), 515–517. <https://doi.org/10.1038/nm1396>.
- (115) *Molecular mechanisms of fosfomycin resistance in clinical isolates of Escherichia coli - PubMed*. <https://pubmed.ncbi.nlm.nih.gov/20071153/> (accessed 2023-05-15).
- (116) Tsuruoka, T.; Miyata, A.; Yamada, Y. Two Kinds of Mutants Defective in Multiple Carbohydrate Utilization Isolated from in Vitro Fosfomycin-Resistant Strains of *Escherichia Coli* K-12. *J Antibiot (Tokyo)* **1978**, *31* (3), 192–201. <https://doi.org/10.7164/antibiotics.31.192>.

- (117) Karageorgopoulos, D. E.; Wang, R.; Yu, X.-H.; Falagas, M. E. Fosfomycin: Evaluation of the Published Evidence on the Emergence of Antimicrobial Resistance in Gram-Negative Pathogens. *J Antimicrob Chemother* **2012**, *67* (2), 255–268. <https://doi.org/10.1093/jac/dkr466>.
- (118) Marchese, A.; Gualco, L.; Debbia, E. A.; Schito, G. C.; Schito, A. M. In Vitro Activity of Fosfomycin against Gram-Negative Urinary Pathogens and the Biological Cost of Fosfomycin Resistance. *Int J Antimicrob Agents* **2003**, *22 Suppl 2*, 53–59. [https://doi.org/10.1016/s0924-8579\(03\)00230-9](https://doi.org/10.1016/s0924-8579(03)00230-9).
- (119) Tsuruoka, T.; Yamada, Y. Characterization of Spontaneous Fosfomycin (Phosphonomycin)-Resistant Cells of Escherichia Coli B in Vitro. *J Antibiot (Tokyo)* **1975**, *28* (11), 906–911. <https://doi.org/10.7164/antibiotics.28.906>.
- (120) Zhanel, G. G.; Walkty, A. J.; Karlowsky, J. A. Fosfomycin: A First-Line Oral Therapy for Acute Uncomplicated Cystitis. *Can J Infect Dis Med Microbiol* **2016**, *2016*, 2082693. <https://doi.org/10.1155/2016/2082693>.
- (121) Venkateswaran, P. S.; Wu, H. C. Isolation and Characterization of a Phosphonomycin-Resistant Mutant of Escherichia Coli K-12. *J Bacteriol* **1972**, *110* (3), 935–944. <https://doi.org/10.1128/jb.110.3.935-944.1972>.
- (122) Couce, A.; Briales, A.; Rodríguez-Rojas, A.; Costas, C.; Pascual, Á.; Blázquez, J. Genomewide Overexpression Screen for Fosfomycin Resistance in Escherichia Coli: MurA Confers Clinical Resistance at Low Fitness Cost. *Antimicrob Agents Chemother* **2012**, *56* (5), 2767–2769. <https://doi.org/10.1128/AAC.06122-11>.
- (123) Pakhomova, S.; Rife, C. L.; Armstrong, R. N.; Newcomer, M. E. Structure of Fosfomycin Resistance Protein FosA from Transposon Tn2921. *Protein Sci* **2004**, *13* (5), 1260–1265. <https://doi.org/10.1110/ps.03585004>.
- (124) Zhao, J.; Zhu, Y.; Li, Y.; Mu, X.; You, L.; Xu, C.; Qin, P.; Ma, J. Coexistence of SFO-1 and NDM-1 β -Lactamase Genes and Fosfomycin Resistance Gene FosA3 in an Escherichia Coli Clinical Isolate. *FEMS Microbiol Lett* **2015**, *362* (1), 1–7. <https://doi.org/10.1093/femsle/fnu018>.
- (125) Cao, M.; Bemat, B. A.; Wang, Z.; Armstrong, R. N.; Helmann, J. D. FosB, a Cysteine-Dependent Fosfomycin Resistance Protein under the Control of Sigma(W), an Extracytoplasmic-Function Sigma Factor in Bacillus Subtilis. *J Bacteriol* **2001**, *183* (7), 2380–2383. <https://doi.org/10.1128/JB.183.7.2380-2383.2001>.
- (126) Thompson, M. K.; Keithly, M. E.; Goodman, M. C.; Hammer, N. D.; Cook, P. D.; Jagessar, K. L.; Harp, J.; Skaar, E. P.; Armstrong, R. N. Structure and Function of the Genomically Encoded Fosfomycin Resistance Enzyme, FosB, from Staphylococcus Aureus. *Biochemistry* **2014**, *53* (4), 755–765. <https://doi.org/10.1021/bi4015852>.
- (127) Qu, T.; Shi, K.; Ji, J.; Yang, Q.; Du, X.; Wei, Z.; Yu, Y. Fosfomycin Resistance among Vancomycin-Resistant Enterococci Owing to Transfer of a Plasmid Harbouring the FosB Gene. *Int J Antimicrob Agents* **2014**, *43* (4), 361–365. <https://doi.org/10.1016/j.ijantimicag.2013.11.003>.
- (128) Etienne, J.; Gerbaud, G.; Fleurette, J.; Courvalin, P. Characterization of Staphylococcal Plasmids Hybridizing with the Fosfomycin Resistance Gene FosB. *FEMS Microbiology Letters* **1991**, *84* (1), 119–122. <https://doi.org/10.1111/j.1574-6968.1991.tb04580.x>.
- (129) Fillgrove, K. L.; Pakhomova, S.; Newcomer, M. E.; Armstrong, R. N. Mechanistic Diversity of Fosfomycin Resistance in Pathogenic Microorganisms. *J. Am. Chem. Soc.* **2003**, *125* (51), 15730–15731. <https://doi.org/10.1021/ja039307z>.
- (130) Castañeda-García, A.; Blázquez, J.; Rodríguez-Rojas, A. Molecular Mechanisms and Clinical Impact of Acquired and Intrinsic Fosfomycin Resistance. *Antibiotics* **2013**, *2* (2), 217–236. <https://doi.org/10.3390/antibiotics2020217>.
- (131) Fillgrove, K. L.; Pakhomova, S.; Schaab, M. R.; Newcomer, M. E.; Armstrong, R. N. Structure and Mechanism of the Genomically Encoded Fosfomycin Resistance Protein, FosX, from Listeria Monocytogenes. *Biochemistry* **2007**, *46* (27), 8110–8120. <https://doi.org/10.1021/bi700625p>.
- (132) Rodríguez-Rojas, A.; Blázquez, J.; Castañeda-García, A. Molecular Mechanisms and Clinical Impact of Acquired and Intrinsic Fosfomycin Resistance. *Antibiotics* **2013**, *2*. <https://doi.org/10.3390/antibiotics2020217>.
- (133) Nikolaidis, I.; Favini-Stabile, S.; Dessen, A. Resistance to Antibiotics Targeted to the Bacterial Cell Wall. *Protein Sci* **2014**, *23* (3), 243–259. <https://doi.org/10.1002/pro.2414>.
- (134) Miller, K.; Dunsmore, C. J.; Leeds, J. A.; Patching, S. G.; Sachdeva, M.; Blake, K. L.; Stubbings, W. J.; Simmons, K. J.; Henderson, P. J. F.; De Los Angeles, J.; Fishwick, C. W. G.; Chopra, I. Benzothioxalone Derivatives as Novel Inhibitors of UDP-N-Acetylglucosamine Enolpyruvyl Transferases (MurA and MurZ). *J Antimicrob Chemother* **2010**, *65* (12), 2566–2573. <https://doi.org/10.1093/jac/dkq349>.
- (135) Baum, E. Z.; Montenegro, D. A.; Licata, L.; Turchi, I.; Webb, G. C.; Foleno, B. D.; Bush, K. Identification and Characterization of New Inhibitors of the Escherichia Coli MurA Enzyme. *Antimicrobial Agents and Chemotherapy* **2001**, *45* (11), 3182–3188. <https://doi.org/10.1128/AAC.45.11.3182-3188.2001>.

- (136) Eschenburg, S.; Priestman, M. A.; Abdul-Latif, F. A.; Delachaux, C.; Fassy, F.; Schönbrunn, E. A Novel Inhibitor That Suspends the Induced Fit Mechanism of UDP-N-Acetylglucosamine Enolpyruvyl Transferase (MurA) *. *Journal of Biological Chemistry* **2005**, *280* (14), 14070–14075. <https://doi.org/10.1074/jbc.M414412200>.
- (137) Schönbrunn, E.; Eschenburg, S.; Krekel, F.; Luger, K.; Amrhein, N. Role of the Loop Containing Residue 115 in the Induced-Fit Mechanism of the Bacterial Cell Wall Biosynthetic Enzyme MurA. *Biochemistry* **2000**, *39* (9), 2164–2173. <https://doi.org/10.1021/bi991091j>.
- (138) El Zoeiby, A.; Sanschagrin, F.; Levesque, R. C. Structure and Function of the Mur Enzymes: Development of Novel Inhibitors. *Molecular Microbiology* **2003**, *47* (1), 1–12. <https://doi.org/10.1046/j.1365-2958.2003.03289.x>.
- (139) Barbosa, M. D. F. S.; Yang, G.; Fang, J.; Kurilla, M. G.; Pompliano, D. L. Development of a Whole-Cell Assay for Peptidoglycan Biosynthesis Inhibitors. *Antimicrob Agents Chemother* **2002**, *46* (4), 943–946. <https://doi.org/10.1128/AAC.46.4.943-946.2002>.
- (140) Dunsmore, C. J.; Miller, K.; Blake, K. L.; Patching, S. G.; Henderson, P. J. F.; Garnett, J. A.; Stubbings, W. J.; Phillips, S. E. V.; Palestrant, D. J.; Angeles, J. D. L.; Leeds, J. A.; Chopra, I.; Fishwick, C. W. G. 2-Aminotetralones: Novel Inhibitors of MurA and MurZ. *Bioorg Med Chem Lett* **2008**, *18* (5), 1730–1734. <https://doi.org/10.1016/j.bmcl.2008.01.089>.
- (141) Ramaswamy, S.; Musser, J. M. Molecular Genetic Basis of Antimicrobial Agent Resistance in Mycobacterium Tuberculosis: 1998 Update. *Tuber Lung Dis* **1998**, *79* (1), 3–29. <https://doi.org/10.1054/tuld.1998.0002>.
- (142) Cm, C.; J, C.; My, C.; Kf, H.; Ch, C.; Yl, Y.; Sh, W. Avenaciolides: Potential MurA-Targeted Inhibitors against Peptidoglycan Biosynthesis in Methicillin-Resistant Staphylococcus Aureus (MRSA). *Journal of the American Chemical Society* **2015**, *137* (1). <https://doi.org/10.1021/ja510375f>.
- (143) Isa, M. A. Homology Modeling and Molecular Dynamic Simulation of UDP-N-Acetylmuramoyl-l-Alanine-d-Glutamate Ligase (MurD) from Mycobacterium Tuberculosis H37Rv Using in Silico Approach. *Computational Biology and Chemistry* **2019**, *78*, 116–126. <https://doi.org/10.1016/j.compbiolchem.2018.11.002>.
- (144) *Pharmaceuticals | Free Full-Text | Bromo-Cyclobutenaminones as New Covalent UDP-N-Acetylglucosamine Enolpyruvyl Transferase (MurA) Inhibitors*. <https://www.mdpi.com/1424-8247/13/11/362#> (accessed 2023-02-14).
- (145) Zhang, F.; Graham, J.; Zhai, T.; Liu, Y.; Huang, Z. Discovery of MurA Inhibitors as Novel Antimicrobials through an Integrated Computational and Experimental Approach. *Antibiotics (Basel)* **2022**, *11* (4), 528. <https://doi.org/10.3390/antibiotics11040528>.
- (146) *Pharmaceuticals | Free Full-Text | Next-Generation Heterocyclic Electrophiles as Small-Molecule Covalent MurA Inhibitors*. <https://www.mdpi.com/1424-8247/15/12/1484> (accessed 2023-02-14).
- (147) *Identification and Biochemical Characterization of Pyrrolidinediones as Novel Inhibitors of the Bacterial Enzyme MurA* / *Journal of Medicinal Chemistry*. <https://pubs.acs.org/doi/abs/10.1021/acs.jmedchem.2c01275> (accessed 2023-02-14).
- (148) *Covalent inhibitors of bacterial peptidoglycan biosynthesis enzyme MurA with chloroacetamide warhead* - *ScienceDirect*. <https://www.sciencedirect.com/science/article/pii/S0223523422006547> (accessed 2023-02-14).
- (149) Neuhaus, F. C.; Hammes, W. P. Inhibition of Cell Wall Biosynthesis by Analogues and Alanine. *Pharmacol Ther* **1981**, *14* (3), 265–319. [https://doi.org/10.1016/0163-7258\(81\)90030-9](https://doi.org/10.1016/0163-7258(81)90030-9).

Youssef Aboushady

01119110913

yousefshady@gmail.com

Objective

As a lecturer assistant with over 6 years experience at a highly reputable organisation, I am seeking an opportunity to be a senior lecturer in my local town. I am excited to use all the leadership skills, educational and research knowledge I have gained to continue upholding the town's commitment to quality education.

Education

Master's in Medicinal Chemistry 11/2017 - 08/2019
German University in Cairo

A+

Bachelor of Pharmacy 09/2012 - 06/2017
German University in Cairo

GPA: 0.7 equivalent to A+(Excellent with Highest Honors) and equivalent to 4.0 using the US Scale

Work Experience

German University in Cairo 09/2017 - Nowadays

Lecturer assistant

I work as a chemistry tutor where I learned to integrate multimedia approaches to teaching literature using instructional technology. I taught Organic chemistry, Medicinal chemistry, Drug design and Analytical chemistry.

Achievements and Awards

Class Ranking: ranked 5th out of 500 students and honored by the Egyptian Pharmacists Syndicate.

Skill

Presentational and communicational skills ■ ■ ■ ■ ■

Work under stress and Time management ■ ■ ■ ■ ■

Critical thinking and Problem solving ■ ■ ■ ■ ■

MS Office ■ ■ ■ ■ ■

Reference

Prof. Ashraf. Abadi
Head of department in Pharmaceutical chemistry
· German University in Cairo

Tel: 01001588454

Email: Ashraf.abadi@guc.edu.eg

الملخص العربي

مقاومة المضادات الحيوية (AMR) هي قضية صحية عامة عالمية متنامية، حيث تصبح البكتيريا مقاومة بشكل متزايد للأدوية المستخدمة في علاج العدوى. إحدى النهج الواعدة لمكافحة مقاومة المضادات الحيوية هي استهداف الإنزيمات المحددة ضمن الكائنات الدقيقة التي تعتبر أساسية لبقاءها. أحد هذه الإنزيمات هو ميور أ، الذي يلعب دوراً رئيسياً في تصنيع جدران الخلايا البكتيرية باستهدافه الخطوة السيتوبلازمية الأولى لتخليق البيبتيدوجليكان. تناولت الرسالة البحثية الحالية تشييد وتقييم مائة و سبع وستون من المشتقات المستحدثة كمضادات للبكتيريا وتقييم هذه المركبات كمثبطات محتملة لانزيم ميور - أ. من هذه المركبات، ١٤٨ كانت من مشتقات اميدازوليدينون و ١٩ كانت من مشتقات تريارايل مالونامايد. بالإضافة إلى ذلك، من خلال فحص و فرز مكتبة هيبس، تم الوصول لعدة نتائج إيجابية لمركبات اظهرت نشاطا مثبطا لانزيم ميور - أ. نتائجا تشير الى إمكانية اعتبار هذه المركبات كمرشحين واعدين لتطوير مشتقات جديدة للمضادات الحيوية لمكافحة مقاومة المضادات الحيوية من خلال استهداف إنزيم ميور - أ على وجه التحديد.

كلية الدراسات العليا
الجامعة الألمانية بالقاهرة

تصميم وتشبيد مشتقات جديدة من مثبطات انزيمات الميور – أ و تقيمها البيولوجي كمضادات للبكتيريا

رسالة تم تقديمها لاستكمال متطلبات الحصول على درجة الدكتوراه في الكيمياء الصيدلانية في الجامعة الألمانية بالقاهرة و للحصول على درجة الدكتوراه في العلوم الطبيعية (دكتوراه الفلسفة في العلوم الطبيعية) من كلية العلوم الطبيعية والتكنولوجيا في جامعة سارلاند

درجة دكتوراه مزدوجة

رسالة مقدمة من

يوسف محمد احمد ابوشادي

تحت إشراف

أستاذ دكتور/ أنا هيرش

رئيس قسم تصميم العقاقير وتحسينها
معهد هلمهولتز لأبحاث الصيدلة
جامعة سارلاند، ألمانيا

أستاذ دكتور/ أشرف مصطفى كمال عبادي

أستاذ الكيمياء الصيدلانية
رئيس قسم الكيمياء الصيدلانية
كلية الصيدلة والتكنولوجيا الحيوية
الجامعة الألمانية بالقاهرة

دكتور/ محمد عبد الحليم

أستاذ مساعد الكيمياء الصيدلانية
كلية الصيدلة و التكنولوجيا الحيوية
الجامعة الألمانية بالقاهرة